The American Mineralogist

Journal of the Mineralogical Society of America

VOL. 46 MAY-JUNE, 1961 Nos. 5 and 6

Contents

(Continued on Cover 2)

Published bi-monthly by the Society

Mineralogical Society of America

ASSOCIATED WITH THE GEOLOGICAL SOCIETY OF AMERICA

The enlarged issues of this journal for 1961 are made possible by a grant from the Penrose Fund of the Geological Society of America.

The American Mineralogist—Journal of the Mineralogical Society of America

The journal, containing articles on mineralogy, crystallography, and allied sciences, is issued every two months. Contributions are invited.

The general conduct of the journal is in the hands of the editor, Lewis S. Ramsdell, Department of Mineralogy, University of Michigan, to whom all manuscripts should be submitted.

Second class postage paid at Menasha, Wis., under Act of March 3, 1879. Acceptance for mailing at the special rate of postage provided for in section 1103, Act of Oct 3, 1917, paragraph 4 section 429 P. L. & R. authorized March 13, 1922. Application pending to mail second class at Silver Spring, Md.

Notice of change of address, orders, and remittances should be sent to Marjorie Hooker, c/o U. S. Geological Survey, Washington 25, D. C.

Printed by George Banta Company, Inc., Menasha, Wisconsin
Printed in the United States of America

FIRST: LOOK AT UNITRON'S NEW POLARIZING MICROSCOPE

Here is a precision measuring instrument for both orthoscopic and conoscopic observations, designed to meet the exacting requirements of science, education, and industry. Its many features make it ideal for work in chemistry, crystallography, mineralogy and biology as well as in the technology of paper, glass, textiles and petroleum.

CHECK THESE OPTICAL & MECHANICAL FEATURES

Note that UNITRON'S new Model MPS comes complete with optics and accessories and includes features usually associated only with much more costly models.

- **EYEPIECES:** Micro 5X providing measurements to 0.0025mm. and cross-hair 10X. The eye lenses focus to produce sharp reticle images and are keyed to prevent rotation.
- **OBJECTIVES:** 4X(N.A.0.1), 10X(N.A.0.25), 40X(N.A.0.65), achromatic, strain-free, each with centerable mount.
- **NOSEPIECE:** quick-change type for critical centering.
- **CONDENSER and POLARIZER:** three-lens condenser with upper elements on a swing-out mounting, provides either parallel or convergent light. A dovetail-slide focusing mount and iris diaphragm insure optimum illumination and resolution.
- **POLAROID POLARIZER:** rotatable through 360° and graduated every 45°. Plano-concave mirror.
- **ANALYZER:** Polaroid, in sliding metal mount.
- **BERTRAND LENS:** for the study of interference figures, fixed-focus lens is centerable and mounted in a slideway.
- **STAGE:** diameter 115mm., revolves through 360°, graduated in degrees and reads to 6′ with vernier. The top is calibrated in mms. in two directions and is drilled and tapped for an accessory mechanical stage. Stage clips.
- **COMPENSATORS:** two compensators are included; a quarter-wave plate and first order red plate. These fit into a slot above the objective lens.
- **FOCUSING:** coarse and micrometric fine adjustments.
- **STAND:** heavy stand, arm inclines to horizontal position.

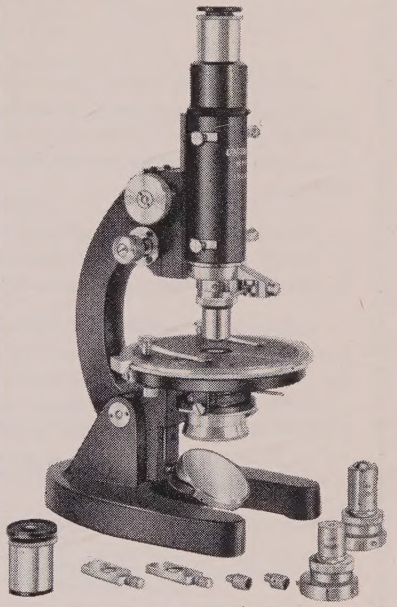

1 Iris diaphragm
2 Polarizer
3 Swing-out lever
4 Focusing lock
5 Focusing slide

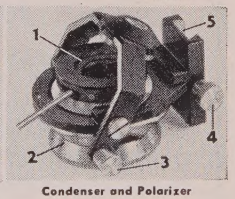

Condenser and Polarizer

THEN: LOOK AT THE PRICE!

Model MPS complete as described, in fitted cabinet . . . . . **$269** FOB BOSTON

Quantity prices on three or more.

Accessory mechanical stage . . . **$14.75**

AVAILABLE ON FREE 10 DAY TRIAL

Send for complete catalog on UNITRON Microscopes.

UNITRON

Instrument Company, Microscope Sales Division
66 Needham St., Newton Highlands 61, Mass.

Please rush UNITRON Catalog on Microscopes. 41

Name_____

Company_____

Address_____

City_____ State_____

THE TREND IS TO UNITRON

RHOANGLO MINE SERVICES LIMITED

Kitwe, Northern Rhodesia

SENIOR MINERALOGIST
MINERALOGIST

Applications are invited from qualified mineralogists for posts in the Mineralogical Section of the Research and Development Division, Kitwe, which undertakes a wide range of projects in extraction metallurgy for the Rhodesian Companies of the Anglo American Corporation of South Africa Limited. These vacancies are the result of promotions and expansion.

Facilities in the Mineralogical Section include X-Ray diffraction equipment, projection microscope and infrasizing and superpanning equipment as well as the usual microscopes, photographic facilities and sample preparation equipment. Analytical services are available.

Applicants for the post of Mineralogist should have had some experience in determinative mineralogy and in petrology. The Senior Mineralogist, who would report directly to the Assistant Superintendent of the Division, should have sound experience in the above fields and the ability to co-ordinate and supervise the work of a team of three mineralogists. He would also be required to liaise with geologists and research and plant personnel on mineralogical problems. A knowledge of mineral concentration techniques would be an advantage.

The commencing basic salaries for these positions will be determined by qualifications and experience but will not be less than:--

Senior Mineralogist	£1,587 (Stg) per annum
Mineralogist	£1,191 (Stg) per annum

In addition to the basic salary, both positions carry a bonus varying with the prosperity of the copper-mining industry (at present about 40% of basic salary) and a variable cost of living allowance (currently about £62 per annum). There are also generous pension, life assurance and medical benefits and a low rate of income tax. Air or sea passage for the successful candidates would be paid by the Company and, dependent upon the point of entry into the salary range, assistance would be provided towards importation expenses.

Kitwe in Northern Rhodesia is situated on the Central African Plateau at an altitude of 4,100 feet above sea level and consequently enjoys an equable healthy climate of dry winters with a rainy season moderating summer temperatures.

Ample all the year round facilities for all the usual sports are available and the generous leave allowance together with excellent rail, road and air communications permits long leaves to be spent at either various coastal resorts or abroad. Leave may be accumulated for up to three years and varies between 48 and 51 days per annum depending on salary.

Housing provided complete with basic furniture, refrigerator etc. is of excellent standard and provided with all modern amenities at a nominal rental and African domestic labour is readily available.

Replies, stating age, marital status, qualifications, experience record, and availability, together with names of two referees, and a recent photograph, should be addressed by airmail to the Secretaries, P.O. Box 172 Kitwe, Northern Rhodesia.

ANALYTICAL CHEMIST:

Experienced in analysis of rocks, minerals and ores. Good background in classical methods and knowledge of some instrumental techniques such as emission spectrography, X-ray spectrochemistry, and flame spectrophotometry, and interested in geochemistry. Knowledge of ion exchange techniques preferable.

MINIMUM REQUIREMENTS:

Masters degree in inorganic chemistry or equivalent experience in actual analytical work. Demanding routine work and opportunity for independent research as a member of a research team working presently on geochemistry and mineralogy of Nevada rocks and minerals. Move to new, modern, well-equipped laboratory in a year.

SALARY:

Salary depending on experience and educational background.

WRITE:

Dr. A. Volborth
Nevada Mining Analytical Laboratory
University of Nevada
Reno, Nevada

BIG SAVINGS NOW

up to 33% off

Terrific Values on JEWELRY CRAFT and ROCKHOUNDING Supplies!

ROCKHOUNDER'S KNAPSACK

The buy of the year

Tremendous value – this is army surplus material at a low, low price. Made of a sturdy, waterproof khaki canvas, very well stitched—well made. Perfect to carry rocks, equipment, books, maps, everything you might tote on a Rockhounding trip. Sportsmen, fishermen, hunters – everybody likes them. They sling easily over your shoulder to carry any kind of load. 7½" x 5" wide x 12" deep—with shoulder strap

H115-1 J . . . . . *each only* $1.50

NEW epoxy ADHESIVE

So good it's replacing rivets

MIRACLE ADHESIVE — you've seen it on T-V and in LIFE — *it bonds materials* stronger than anything else. Aircraft industry using it instead of Rivets—replaces nails and screws. Perfect for jewelry making — *Unconditionally guaranteed!* Kit of 2 jars with complete instructions.

Order as: Z1-J . . . . . only $1.50

This "15X Ruper" Magnifier with any magnifier you now use. Full ⅓ diameter corrected lens! Nickel plated metal folding frame. Equivalent to other $6 magnifiers.

Order as: T130-25J $1.00

WE DARE YOU TO COMPARE

FLASHLIGHT MAGNIFIER

Enlarges Objects 7X

Place "Flash Magnifier" ON object under scrutiny – snap on flashlight — and get 7 times magnification exactly where you need it. Gem stones and minerals look more beautiful... markings, flaws, defects are easily spotted. 7" long. Metal and plastic case. Colossal value.

Z-179 J only $1.95

Complete including 2 batteries . . .

Z-180 J . only $2.15

49¢ GOLD PANNING OUTFIT

GOLD PANNING KIT

exciting fun for the entire family

Everything you need to pan for gold — including directions. 12" gold pan, sample pouch of ore and an alnico magnet. Shows you how to go about it . . . just like the old 49'ers did. It's a real thrill . . . and many streams in all parts of the country have gold in them. Get a kit and head for the open country. Excellent gift item too. Start panning for gold now. Order —

Z-72 J - 49'er Gold Panning Outfit . . 1 for $2.95

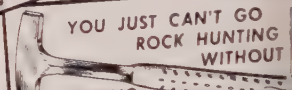

YOU JUST CAN'T GO ROCK HUNTING WITHOUT

ESTWING PROSPECTOR PICK

Forged all-steel one piece h handle prospecting pick with new blue everlasting nylon cus handle grip — non slip 13 in long with 7 head which weig oz. Guaranteed unbreakable.

Order as Z-60-J . . . . . now only

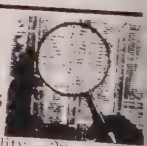

TERRIFIC VALUES IN READER MAGNIFIERS

Imported quality 2X magnific tion — optical lens. Ideal for jew elry making, rockhounding, stam collecting, etc. Fits easily i pocket. Black Ebonite handle— polished chrome frame.

Z-181 J 2" Magnifier . each $1.0

Z-182 J 3" Magnifier . each 1.9

SPARKLING — SUPERB SPECIMEN CARDS!

10 different specimens on card — all tumbled and polished — many of gem quality!

Wonderful cards for everyone interested in rockhounding. Educational — instructive — good for class work — and an "absolute must" for the beginning collector.

Big value . . . terrific buy — order one or more now — you must see them to appreciate . . . we guarantee you'll be delighted!

Y Z-101 J Mexico and the Southwest"	only $1.00
Y Z-102 J "Brazilian Agates"	only $1.00
Y Z-103 J "Mother of Pearl"	only $1.00
Y Z-183 J "Brazilian Gem Materials" . .	only $1.00
Y Z-184 J "Gem Materials of the West" .	only $1.00
Y Z-185 J "World Wide Gem Materials"	only $1.00
Y Z-186 J "International Gem Stones" .	only $1.00
Y Z-187 J "Colorful Gem Stones"	only $1.00
Y Z-188 J "California Gem Materials" .	only $1.00

YOU DO BETTER WORK WHEN YOU SEE BETTER WITH MAGNI-FOCUSER

Binocular Magnifier

Leaves both hands free to work

MAGNI-FOCUSER

Designed for All Professions and Trades

Make all precision work easier work

T121-3 J MAGNI-FOCUSER, magnifies 1¾ times at 14"	$10.50	2 lbs.
T121-5 J MAGNI-FOCUSER magnifies 2¼ times at 10" . . .	$10.50	2 lbs.
T121-7 J MAGNI-FOCUSER, magnifies 2¾ times at 8" . . .	$10.50	2 lbs.
T121-10 J MAGNI-FOCUSER, magnifies 3½ times at 4" . . .	$12.50	2 lbs.
T121-13 J MAGNI-FOCUSER, magnifies 4¾ times at 3" . . .	$15.00	2 lbs.
T121-17 J MAGNI-FOCUSER, magnifies 5¼ times at 2½" . . .	$15.00	2 lbs.

Any work that requires **precision** can be done easier, and more accurately with a Magni-Focuser — the **binocular** magnifier.

Magni-Focuser shows an object in **third dimension** greatly magnified—with the depth and clarity of normal vision. It **reduces eye-strain** and **prevents squinting**—thus **saving time**, increasing accuracy, and minimizing the chance of errors and accidents.

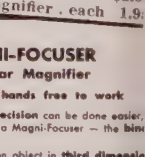

RELIEVE "EYE STRAIN" WITH A MAGNI-FOCUSER

All items sold on Money Back Guarantee!

GRIEGER'S 1633 E. WALNUT PASADENA, CALIF.

Prices include Taxes and Postage!

INTERNATIONAL MINERALOGICAL ASSOCIATION

Third General Meeting

April 1962 Washington, D.C.

TIME TABLE

April 11	MSA Charter plane departs London for New York.
12-13	Free time before Northern Field Trip.
14-16	Northern Field Trip, New York-Washington.
17	Commission meetings, Washington.
18-20	Scientific sessions, Washington.
	April 18 Symposium, Mineralogy of Sulfides.
	19 Open session.
	20 Symposium, Layered Intrusives.
21-23	Southern Field Trip, Virginia.
24-27	Museum Excursion, Washington-Boston.
28-30	Free time.
May 1	MSA Charter plane departs New York for London.

Northern Field Trip New York-Washington, April 14-16 Leader: Paul F. Kerr

Cost: $50.00 includes lodging, food, transportation, and guidebook.

April 14: New York City. Visits to American Museum of Natural History, Columbia University, Department of Geology, and Lamont Geological Observatory.
15: Paterson, New Jersey (zeolite); Franklin, New Jersey.
16: Cornwall, Pennsylvania (magnetite, hematite).

Southern Field Trip Virginia, April 21-23 Leader: Richard V. Dietrich

Cost: $50.00 includes lodging, food, transportation, and guidebook.

April 21: Amelia Court House (pegmatite), Willis Mtn. (kyanite), Roseland (rutile).
22-23: Virginia mineral localities, and Luray limestone caverns.

Museum Excursion Washington-Boston, April 24-27 Leader: Clifford Frondel

An excursion in private cars to visit museums in Philadelphia, New York, New Haven, and Boston is being scheduled. This trip will probably depart from Washington late on April 23rd, spend the first night between Washington and Philadelphia, the second night in New York, and the third night in or near Boston. The cost will be about $10-$15 per day for food and lodging; there will be no charge for transportation.

Scientific sessions Washington, April 18-20

Two one-day symposia are planned. One on the Mineralogy of Sulfides will be held on April 18 under the chairmanship of Prof. Alfred J. Frueh (Dept. Geological Sciences, McGill University, Montreal, 2, Canada). The other, on Layered Intrusives, will be held on April 20 under the chairmanship of Prof. C. E. Tilley (Department of Mineralogy, Cambridge, England).

(Continued on next page)

1962 International Mineralogical Association Meeting

(Continued from previous page)

Papers presenting new material on varied aspects of either of these topics are invited. Titles should be submitted as soon as possible to the Chairmen, and abstracts should be submitted not later than November 1, 1961. To allow time for discussion, the number of papers will be limited and selections will be made after receipt of abstracts. April 19 will be devoted to the presentation of papers on any topic of interest to mineralogists. Titles, abstracts, and the amount of time estimated for presentation should be submitted as soon as possible to Prof. D. J. Fisher (Rosenwald Hall, University of Chicago, Chicago 37, Illinois). Selections for the program will be made by the Executive Committee, on the basis of what it regards as those of greatest interest.

Commission meetings — Washington, April 17

Information on subjects to be considered at the various Commission meetings will be supplied to registrants in advance of the meeting.

Registration: A fee of $15.00 will be asked of each person attending. This fee will cover registration, a welcome reception on April 17, a dinner on April 19, and admissions to several places of interest in Washington.

Housing: Housing will be available for North American registrants at the Marriott Motor Hotel at the following daily room rates: $18.00 (single occupant), $20.00 (double occupancy), $22.00 (three occupants), $24.00 (four occupants). There are no extra charges for parking and other services. The Local Committee is planning to provide accommodations for the majority of visitors from overseas who may desire them through the personal hospitality of scientists residing in the Washington area. Those sending in provisional registration will receive further information.

Travel: The Mineralogical Society of America has been assured of a certain amount of funds that can be used toward the travel expense of foreign participants if needed. Allocation of these funds will depend on the number of IMA member societies to be represented and the number of registrants. The MSA is planning a round-trip flight, London-New York, by charter plane, for the period April 11-May 1, 1962, at a cost of $100.00 per person, to facilitate attendance. International airline regulations require that participants in such a flight be MSA members in good standing for at least six months prior to the time of the flight. The flight will accommodate 118 people and immediate family members are eligible if space is available. The cost may be slightly higher per person if not all seats are occupied. It is very important that you indicate your intention to use this flight as soon as possible.

Registration forms are being mailed to all members of the Mineralogical Society of America. Others who wish registration forms or information concerning this meeting may write to Miss Marjorie Hooker, U. S. Geological Survey, Washington 25, D.C.

D. Jerome Fisher, *President*
Rosenwald Hall
University of Chicago
Chicago 37, Illinois, U.S.A.

Alvin Van Valkenburg, *Chairman*
IMA Local Committee
National Bureau of Standards
Washington 25, D.C., U.S.A.

THE AMERICAN MINERALOGIST

JOURNAL OF THE MINERALOGICAL SOCIETY OF AMERICA

Vol. 46 MAY–JUNE, 1961 Nos. 5 and 6

KIMZEYITE, A ZIRCONIUM GARNET FROM MAGNET COVE, ARKANSAS*

CHARLES MILTON, BLANCHE L. INGRAM, AND LAWRENCE V. BLADE,
U. S. Geological Survey, Washington, D. C.

ABSTRACT

Kimzeyite, $Ca_3(Zr, Ti, Mg, Fe'', Nb)_2(Al, Fe''', Si)_3O_{12}$, is a new type of garnet occurring as dodecahedrons modified by trapezohedron at Magnet Cove, Arkansas, in a carbonatite with abundant apatite, monticellite, calcite, perovskite (dysanalyte), magnetite, and minor biotite, pyrite, and vesuvianite. It is dark brown, H about 7, isotropic, insoluble in acids, infusible before the blowpipe, D = 4.0, $n = 1.94$. The three strongest x-ray powder pattern lines with intensities as measured are 1.667 (10), 2.539 (9), 2.79 (8); the unit cell constant is 12.46 Å. Microchemical analysis gave CaO 29.8, ZrO_2 29.9, TiO_2 5.0, MgO 0.5, FeO 0.8, Nb_2O_5 1.0, Al_2O_3 11.0, Fe_2O_3 13.4, SiO_2 9.6, sum 101.0 which computes to $Ca_{3.11}(Zr_{1.42}{}^{+4}Ti_{0.40}{}^{+3}Mg_{0.07}{}^{+2}Fe_{0.07}{}^{+2}Nb_{0.05}{}^{+5})(Al_{1.26}{}^{+3}Fe_{0.98}{}^{+3}Si_{0.91}{}^{+4})O_{12.00}$. Basically, this is $Ca_3Zr_2(Al_2Si)O_{12}$ with Ti replacing Zr and Fe replacing Al. Zirconium has been found in other garnets (schorlomite from Magnet Cove, melanite from Kaiserstuhl, Germany, and titanian andradite from Oka, Quebec) in quantity up to several per cent, but in none of these is it a major constituent. Kimzeyite is named in honor of the Kimzey family, long known in connection with Magnet Cove mineralogy.

INTRODUCTION

During geological study of the Magnet Cove, Arkansas, carbonatite by Erickson and Blade (1956), their attention was directed by Mr. Joe Kimzey of Malvern, Arkansas, to small dark brown garnets about 1 mm. diameter in the Kimzey calcite quarry. Because garnet of various types, including titanian andradite (melanite) and schorlomite with up to 16.9% TiO_2, have long been known from Magnet Cove, the unusual character of the garnets from this limestone quarry was not realized until a spectrographic analysis (by A. T. Myers of the U. S. Geological Survey) indicated zirconium as a major constituent. A second spectrographic analysis of especially cleaned material (by H. Bastron of the U. S. Geological Survey) confirmed the major zirconium content of the garnet. A preliminary note on kimzeyite was published in Science (Milton and Blade, 1958), giving Bastron's spectrographic data which shows more than 20% ZrO_2 to be present.

* Publication authorized by the Director, U. S. Geological Survey.

Kimzeyite, although certainly a garnet, as will be shown, differs greatly in its composition from all garnets previously known. It appears that two-thirds of the normal tetrahedral silicon positions are occupied by aluminum and iron atoms, and of the normal octahedral aluminum-iron positions, almost all are occupied by zirconium and titanium. Correspondingly, the SiO_2 content is only 9.6%; most garnets contain 30 to 40%, and even the least siliceous types (titanian) contain over 25% SiO_2.

Kimzeyite is of further interest in being the first known zirconium silicate containing substantial aluminum, contrary to Frondel's observation (1957) "The (zirconium) silicates without exception lack aluminum. . . ." However, with a bare third of the normal silicon positions of garnet occupied by this element, the question may be raised as to kimzeyite being a silicate even though a garnet, since such compounds as $Gd_3Fe_2Fe_3O_{12}$ or $Y_3Al_2Al_3O_{12}$ are considered garnets, even though not silicates.

Occurrence

Kimzeyite occurs in a light colored phase of carbonatite (Fig. 1) which is associated with ijolite in the Kimzey calcite quarry. With the dominant white coarsely crystallized calcite are scattered irregular zones enriched in white to pale greenish finely prismatic apatite, massive light brown monticellite, and smaller but conspicuous black magnetite and perovskite, and in minor amount some yellow vesuvianite, green mica, and pyrite. The garnet in this rock forms small and far from abundant dark brown crystals, with prominent dodecahedron and almost equally developed trapezohedron (Fig. 2). All so far found are small, usually under 1 mm. diameter. Larger garnets also occur in weathered apatite rock coated with buff clay, in the same quarry; these contain no zirconium.

Kimzeyite is easily differentiated from perovskite with a hand lens in being brown with subrounded crystals (dodecahedron-trapezohedron), whereas perovskite is almost black and sharply angular (octahedron with minor cube). In thin section, the two minerals are easily distinguished by the pale brown of kimzeyite with its subrounded outlines, contrasted with the dark brown sharply angular perovskite. Perovskite also shows the usual segmented anisotropy, whereas kimzeyite is isotropic. Magnetite is easily distinguished by its magnetism, and in section by its opacity.

A typical thin section of the carbonatite showing kimzeyite and some of its associated minerals is shown in Fig. 3.

The crystals as shown in Fig. 3 contain considerable visible inclusions,

FIG. 1. Kimzeyite-bearing limestone, Magnet Cove, Ark. Two crystals of kimzeyite are present, indicated by circles. These are about average size. The white areas are fibrous apatite and calcite, the slightly darker glossy pale brownish monticellite. Rather coarse black magnetite (lower left) and disseminated black perovskite (dysanalyte) can also be seen.

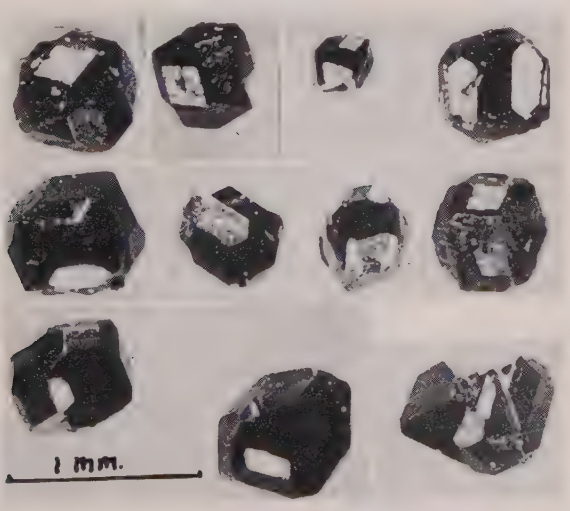

FIG. 2. Kimzeyite crystals isolated from carbonatite matrix. At the lower right is a kimzeyite crystal intergrown with a perovskite crystal.

mainly of apatite, calcite, and monticellite. Only the very smallest appear to be fairly free from such inclusions. In preparing the sample for chemical analysis, single crystals were crushed, and many were found to contain microscopic clear euhedral (?) crystals of anhydrite, confirmed microchemically, optically, and by *x*-ray powder pattern (by E. C. T. Chao, U. S. Geological Survey). Whether or not equally minute anhydrite exists dispersed in the rock matrix of the kimzeyite would be difficult to determine.

Because of these inclusions, which could not be dissolved out com-

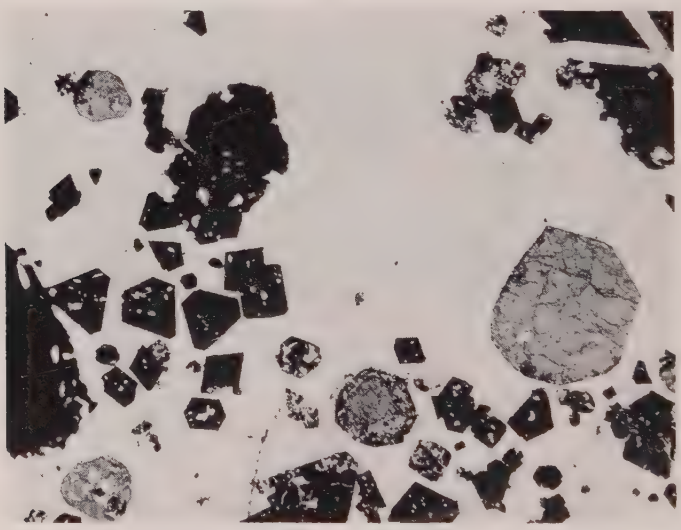

FIG. 3. Thin section of carbonatite, showing four rounded kimzeyite crystals (gray), and numerous smaller angular perovskite crystals (black) in calcitic matrix. The large black masses are magnetite; at the upper right two apatite crystals cut the magnetite.

pletely by acids or otherwise removed except by tedious hand picking under the microscope, preparation of sufficiently clean material for analysis was a long drawn-out task, extending over available time for some years.

DENSITY, INDEX OF REFRACTION, AND OTHER PHYSICAL PROPERTIES

The approximate density of whole kimzeyite crystals showing few or no visible inclusions was determined by finding the density of a diluted Clerici solution in which they barely floated or sank, namely 3.94. Because of the impossibility of verifying complete purity of any particle of kimzeyite, only an approximation to a true density is possible. Actually, as explained below, this is low, and a better value would be nearer 4.0.

The index of refraction determined by the immersion method was found to be $1.94 \pm .01$, using liquids prepared and standardized by Robert L. Meyrowitz of the U. S. Geological Survey.

Using Gladstone and Dale's equation relating composition, index of refraction, and density (Larsen and Berman, 1934), with specific refractivities given by these authors (except for substitution of $k_{Fe_2O_3} = 0.290$ instead of 0.308, as suggested by Jaffe (1946)), it is found that $n = 1.92$ (against measured 1.94) if the measured density is assumed correct, or $d = 4.00$ gm. cm.$^{-3}$ (against measured 3.94) if the measured index of refraction is assumed correct.*

The discrepancy between observed and calculated density is not large and it is more likely that the measured refractive index is nearer the true value than is the measured density. Therefore, it may be inferred that the whole garnet crystals used in the density determinations contained substantial inclusions of lower density, *i.e.*, apatite 3.2, monticellite, 3.2, calcite 2.7, or anhydrite 2.9 gm. cm.$^{-3}$. For example, a crystal of density 4 with 10% (by volume) of admixture with density 3 would have a net density of 3.9, and from the illustration (Fig. 3) showing the heterogeneity of kimzeyite this degree of admixture is quite possible. Accordingly the density of kimzeyite is most probably greater than the measured 3.94.

However, we can also calculate the density, using the formula for kimzeyite developed in Table 3, the cell edge constant measured by Axelrod, and the value 8 for Z (moles per unit cell) for the garnet structure: resulting in $d = 4.03$. Using this value for d in Gladstone and Dale's equation gives $n = 1.946$ in fair agreement with the measured 1.94.

The streak of kimzeyite or the color of its powder is light brown; and the hardness is about that of quartz—7. It is almost if not entirely insoluble in hot concentrated HCl or HNO_3 or $HF + H_2SO_4$, and is infusible before the blowpipe. Here again the highly poikilitic character of the kimzeyite necessitated a special procedure—it was impossible to find a homogeneous fragment large enough to hold in a platinum forceps in a blowpipe flame. Therefore reasonably clean microscopic fragments were wrapped in platinum foil, and the packet heated in an air-gas blast to bright red heat for fifteen minutes. The kimzeyite showed no sign of fusion.

Kimzeyite is heavier than most other garnets, only those with 8-coordinated iron or manganese being heavier (almandite and calderite); only some strongly titanian garnets have higher index of refraction;

* The value of $k_{TiO_2} = .397$ given by Jaffe is used also for $k_{Ti_2O_3}$ for which he gives no data. The error thus introduced is unknown but probably small.

and the cell constant a_0 appears to be larger than that of any known natural garnet.

Marie L. Lindberg of the U. S. Geological Survey has kindly measured the film (11944) of the sample whose analysis is given in Table 2. Her data are given in Table 1.

TABLE 1. POWDER PATTERN DATA OF KIMZEYITE

Intensity	d(Å) meas.	hkl	d(Å) calc.
4	4.42	220	4.406
6	3.12	400	3.115
8	2.79	420	2.786
1	2.656	332	2.657
9	2.539	422	2.543
1	2.439	510, 431	2.444
1	2.273	521	2.275
2	2.019	532, 611	2.021
3	1.969	620	1.970
4	1.728	640	1.728
10	1.667	642	1.675
2	1.558	800	1.558
1	1.469	660	1.468
4	1.395	840	1.393
2	1.360	842	1.360
3	1.328	664	1.328
2	1.157		
4	1.137		
1	1.110		
2	1.011		
1 Broad	0.930		
2	0.848		
2	0.791		

The lower cut off is at 10 Å. The film was corrected for shrinkage; the radiation nickel-filtered copper with $K_\alpha = 1.5418$ Å. The published lattice constant $a_0 = 12.46$ Å obtained by J. M. Axelrod (Milton and Blade, 1958) was used to index the pattern; the agreement of measured and calculated d-spacings is good.

COMPOSITION

Table 2 gives the chemical and spectrographic (of trace elements) analyses of kimzeyite. (Spectrographic analyses for major constituents were also made by the same analysts, with results concordant with Ingram's quantitative analysis.)

CHEMICAL ANALYSIS (METHODS)

One portion (50 mg.) of sample was used for $H_2O(-)$, SiO_2, Fe_2O_3, Al_2O_3, ZrO_2, Nb_2O_5, TiO_2, CaO, MgO, and MnO determinations. An-

other portion (13 mg.) was used to determine the total reducing capacity, and a third portion (25 mg.) was used to determine total H_2O.

The 50-mg. sample was dried to constant weight at 110° C. to determine $H_2O(-)$. It was then sintered with Na_2O_2 at 460° C. The sinter was dissolved in HCl. SiO_2 was determined gravimetrically by double dehydration of the solution and volatilization of the SiO_2 with HF and excess H_2SO_4.

The filtrate from the SiO_2 determination was treated with NH_4OH to precipitate the R_2O_3 group. The precipitate was ignited and weighed, and the filtrate was reserved for Ca, Mg, and Mn determinations. The R_2O_3 was fused with $K_2S_2O_7$ and dissolved in HCl and tartaric acid. Iron was separated from the group by making the solution ammoniacal and gassing with H_2S. FeS was dissolved and, after oxidation, the Fe was precipitated with NH_4OH. The precipitate was ignited and weighed as Fe_2O_3.

The solution remaining after H_2S precipitation of Fe contained Al, Zr, Nb, and Ti. Zr, Nb, and Ti were removed from solution by precipita-

Table 2. Chemical Analysis of Kimzeyite, Magnet Cove, Arkansas
Analyst, Blanche L. Ingram

SiO_2	9.6	*alternate values * used in Table 3*
FeO	5.8	0.8
Fe_2O_3	7.8	13.4
TiO_2	5.6	Ti_2O_3 5.0
ZrO_2	29.9	
Nb_2O_5	1.0	
Al_2O_3	11.0	
CaO	29.8	
MgO	0.5	
	101.0	

also MnO<0.1
H_2O^-<0.1
total H_2O<0.1
also Na 0.1–0.5 (spectrographic on 1 milligram; Helen Worthing and Katherine Hazel, U. S. Geol. Survey, analysts).
On a different but equally purified sample, Harry Bastron, U. S. Geol. Survey, found spectrographically Mn 0.1, Sn 0.07, Sc 0.06, Cu, Ba, and Sr, traces; and looked for but not found, Ag, Au, Hg, Ru, Rh, Pd, Ce, Ir, Pt, Mo, W, Re, Ge, Pb, As, Sb, Bi, Zn, Cd, Te, In, Co, Ni, Ga, Cr, V, Y, La, Hf, Th, Ta, Be, Li, Na, K, B. High Fe precludes determination of low P.

* No differentiation of Fe^{+2} and Ti^{+3} can be made in the chemical analysis. Values for FeO and Fe_2O_3 are therefore given with all of the Ti as Ti^{+4}, and, alternately, with all the Ti as Ti^{+3}.

tion with cupferron. This precipitate was ignited and weighed. The oxides were dissolved and Ti was determined colorimetrically with "Tiron"; Nb was determined colorimetrically using thiocyanate and Zr was determined gravimetrically as the oxide after precipitation with mandelic acid. Corrections were applied for the effect of Ti on the Nb determination and of Nb on the Zr determination. Al_2O_3 was considered the difference between the total R_2O_3 and the sum of Fe_2O_3, ZrO_2, TiO_2 and Nb_2O_5.

Calcium was precipitated with $(NH_4)_2C_2O_4$ from the reserved filtrate. The precipitate was ignited and weighed as CaO. Ammonium salts were destroyed in the filtrate from the calcium determination and Mg and Mn were precipitated with 8-hydroxyquinoline in an ammoniacal medium. The precipitate was dried at 110° C. and weighed. It was then ignited at 800° C. and the oxides dissolved. Mn was determined colorimetrically by oxidation to permanganate.

Total reducing capacity was determined by fusing the sample with sodium fluoborate in a tube furnace at approximately 900° C. in an atmosphere of N_2. The fused sample was dissolved in an atmosphere of N_2 with 10% H_2SO_4 containing H_3BO_3, and titrated with standard $K_2Cr_2O_7$ using sodium diphenylamine sulfonate as indicator. A fusion technique was necessary; the mineral is insoluble in the usual HF-H_2SO_4 mixture.

Total H_2O was determined by the Penfield method.

Comments on Analysis

Because of the abundant perovskite, containing 5.6 ± 0.3% Nb, associated with kimzeyite in the Kimzey calcite quarry, and as much as 8.8% Nb in perovskite from the adjoining "perovskite hill" (Fryklund, Harner, and Kaiser, 1954), the possibility that the analyzed kimzeyite was contaminated with perovskite must be considered. However, because of the care used in selecting the particles for analysis, serious contamination is unlikely. Further if the Nb were indeed present in perovskite containing as much Nb as 8.8%, then there should have been about 11% of this mineral in the sample but no lines of perovskite appeared on the *x*-ray powder pattern of the analyzed sample. With reference to perovskite with *less* Nb as possible contaminant (Fryklund et al., also cite 3.1% Nb in perovskite from Magnet Cove) the argument is even stronger: there would be correspondingly more perovskite to show up on the powder pattern if it were present. It may therefore be accepted that the Nb found in the kimzeyite is in the structure. Finally, as noted by Rankama and Sahama (1950), Nb is commonly associated with both Zr and Ti, both major elements in kimzeyite.

Bastron did not find Hf, which because of the high Zr could be ex-

pected in detectable amount. In zirconium silicates of alkalic rocks and carbonatites, the Hf/Zr ratio varies from 0.007 (in catapleite) to 0.069 (in eudialyte) as listed by Fleischer (1955). These values would correspond to 0.15% and 1.5% respectively of Hf. It is probable that any hafnium in kimzeyite is less than 0.1% (Bastron, oral communication).

Bastron also reports Sn 0.07% with a trace of Cu. Conceivably these may represent contamination from the brass sieves used in processing the sample. On the other hand, Ramdohr (1936) has found Sn replacing Ti, to the extent of 10% Sn in sphene.

The 0.06% Sc reported by Bastron is noteworthy.

Rankama and Sahama (1950) observe that scandium is virtually absent in calcium garnets (page 513) and likewise in zirconium minerals, notwithstanding the similar ionic radii of scandium and zirconium (page 515).

Computation of Formula

Anticipating what follows, the formula proposed for kimzeyite, as a garnet, derived from the normal garnet type formula $R_3^{+2}R_2^{+3}Si_3O_{12}$, is $Ca_3(Zr,^{+4}, Ti^{+3}, Mg^{+2}, Fe^{+2}, Nb^{+5})_2(Al^{+3}Fe^{+3}Si^{+4})_3O_{12}$ or basically $Ca_3Zr_2(Al_2Si)O_{12}$. Essentially, the normal two trivalent ions (i.e., Al and Fe) in common garnet are here replaced by two zirconiums, with a minor further replacement of the latter by titanium, etc; and two of the normal three silicons are replaced by aluminum and iron.

The basic data for establishing the formula of kimzeyite are presented in Table 3, with the simple calculations leading to the formula.

A recent paper by Geller, Miller, and Treuting (1960) describes a remarkably extensive series of synthetic garnets, among them, garnets containing much zirconium (and also, niobium), but with germanium instead of silicon in tetrahedral position. The compound $Ca_3ZrFe^{+2.9}Ge_{2.8}O_{12}$ (defect structure) was made, whose similarity to kimzeyite $Ca_3(Zr, Ti^{+3})_2(Al, Fe, Si)O_{12}$ is apparent. They were unable to substitute Zr^4 for Ge^4 (*i.e.*, in tetrahedral co-ordination) observing that it is "very probable that the Zr^{4+} ion would go only into octahedral sites." As is well known, Ge^4 (ionic radius 0.50 Å) and Si^4 (ionic radius 0.40 Å) are generally replaceable for each other in silicate structures, so their work with germanium garnets may reasonably be extrapolated to silicon garnets. Because in kimzeyite zirconium with titanium virtually fills all the octahedral (6-co-ordinated) positions (calcium similarly pre-occupying all the 8-co-ordinated locations), ferric iron and aluminum have only the tetrahedral silicon positions available. As is well known, such tetrahedrally co-ordinated ferric iron exists in biotite (Eitel, 1954) and cronstedtite (Hendricks, 1939). Even more to the point, tetrahedral iron

TABLE 3. COMPUTATION OF FORMULA OF KIMZEYITE

Analysis		Cation%	Oxygen%	Cation% At. Wt.	Equiv. Oxygen	Cation% At. Wt.×171
CaO	29.8	21.3	8.5	.532	.532	3.11 ($\times 10^{-3}$)
MgO	0.5	0.3	0.2	.012	.012	.07 ($\times 10^{-3}$)
FeO	0.8	0.6	0.2	.011	.011	.07 ($\times 10^{-3}$)
Fe_2O_3	13.4	9.4	4.0	.168	.252	.98 ($\times 10^{-3}$)
Ti_2O_3	5.0	3.3	1.7	.069	.104	.40 ($\times 10^{-3}$)
Al_2O_3	11.0	5.8	5.2	.215	.322	1.26 ($\times 10^{-3}$)
ZrO_2	29.9	22.1	7.8	.242	.484	1.42 ($\times 10^{-3}$)
Nb_2O_5	1.0	0.7	0.3	.008	.020	.05 ($\times 10^{-3}$)
SiO_2	9.6	4.5	5.1	.160	.320	.94 ($\times 10^{-3}$)
	101.0%	68.0%	33.0%		2057 (=12×171.4)	

Assuming the general garnet structural formula $A_3^{VIII}B_2^{VI}X_3^{IV}O_{12}$, the cations may be grouped as follows according to their respective co-ordinations, 8, 6, and 4, which corresponds well with their ionic radii.

	Co-ordination	Ionic radius	Electrostatic charge
$A = Ca^{+2}_{3.11}$	8	1.03 Å	6.22
$B = Mg^{+2}_{.07}$	6	.66	.14
$Nb^{+5}_{.05}$	6	.69	.25
$Ti^{+3}_{.40}$	6	.76	1.20
$Fe^{+2}_{.07}$	6	.74	.14
$Zr^{+4}_{1.42}$ 2.01	6	.79	5.68
$X = Si^{+4}_{.94}$	4	.40	3.76
$Fe^{+3}_{.98}$	4	<.64	2.94
$Al^{+3}_{1.26}$ 3.18	4	.49	3.78
			24.11 (cationic)
O^{-2}_{12}			24.00 (anionic)

must exist in the garnet $Gd_3Fe_5O_{12}$ ($Gd_3Fe_2Fe_3O_{12}$) synthesized by Bertaut and Forrat (1956); and tetrahedral aluminum in the yttro-garnet $Y_3Al_5O_{12}$ ($Y_3Al_2Al_3O_{12}$) synthesized by Yoder and Keith (1951). In many silicates, such as feldspars and zeolites, aluminum replaces silicon in

tetrahedral co-ordination. As to the ionic radius of such tetrahedrally co-ordinated iron, Green (1959) lists no value; but from geometrical considerations it must be less than the ionic radius he does list for octahedral trivalent iron, 0.64.

The slight excess of cationic over anionic charge, 0.11 (0.5%) must be considered a numerical error arising from rounding off decimals, and may be disregarded.

The formula of kimzeyite is therefore

$$Ca_{3.11}(Zr^{+4}_{1.42}Ti^{+3}_{0.40}Mg^{+2}_{0.07}Fe^{+2}_{0.07}Nb^{+5}_{0.05})(Al^{+3}_{1.26}Fe^{+3}_{0.98}Si^{+4}_{0.94})O_{12.00}$$

with

$$A_{3.11}B_{2.01}X_{3.18}O_{12.00}$$

or, more simply

$$Ca_3(Zr, Ti''', Mg, Fe'', Nb)_2(Al, Fe''', Si)_3O_{12}$$

and derives from a basic formula $Ca_3Zr_2(Al_2Si)O_{12}$ by substitution of Ti, etc. for Zr and Fe for Al.

It is evident from co-ordination and ionic radius considerations, that zirconium can not occupy a Si position in the structure, but only that of a trivalent octahedrally co-ordinated ion; and that titanium must be similarly located—together with the magnesium, ferrous iron, and niobium. The assignment of Ti in the garnet structure—whether octahedrally replacing trivalent iron or aluminum, or tetrahedrally replacing silicon, has long been an open question. Fleischer (1937) stated the problem concisely as follows: "There is considerable uncertainty at present as to the role of titanium in garnets. The problem has been discussed by Kunitz, who came to the conclusion that Ti replaces Si in these garnets. In nearly all the recent analyses, however, the molecular ratios are high for RO_2 and RO, and low for R_2O_3, which makes plausible the suggestion of Zedlitz that part of the titanium is present in the trivalent state. (Any Ti_2O_3 present would cause a corresponding amount of Fe_2O_3 to be reported as FeO.)"

Zedlitz (1933, 1935) analysed three titanium garnets, melanite from Kaiserstuhl, melanite from Magnet Cove, and a garnet from Ivaara, Finland, with 12.10%, 4.60% and $17.3 \pm 0.5\%$ TiO_2, respectively. In computing their formulas he assigned in each case sufficient TiO_2 to SiO_2 to arrive at a close approximation to the type garnet ionic ratios of $3R^{VIII}2R^{VI}3R^{IV}$, grouping with the SiO_2 the Al_2O_3, but not the equally available Fe_2O_3. His justification for grouping TiO_2 with SiO_2, with the implication that Ti ions replace Si ions in the structure, is a hypothetical isomorphous replacement of Si by Ti at high temperatures (he admits that at ordinary temperatures no stable 4-co-ordinated structures are

known) and that this replacement is somehow preserved through rapid cooling ("rasche Abkuhlung des Oberflachenmuttergesteins"). We think his disregarding the possibility (if not probability) of Fe, as well as Al, ions replacing silicon is unjustified. It may also be noted that although Zedlitz's analysis of the Finnish garnet shows neither FeO nor Ti_2O_3, in computing the formula he assigns the bulk of the titanium to R^{VI} as TiO_2 *or* Ti_2O_3 ("TiO_2 oder Ti_2O_3 Rest"). In so doing he may have been influenced by the work of Gossner and Reindl (1934) who, discussing their analysis of a melanite from Magnet Cove (TiO_2 4.39%), observed that it was unlikely that titanium and silicon were isomorphously replaceable to any significant degree. These same authors, further in the same publication, discussing their analysis of astrophylite, have Ti (TiO_2 8.02%) and Zr (ZrO_2 5.34%) grouped isomorphously, but do not have silicon replaced by Ti.

Zedlitz (1935) attempted synthesis of $Ca_3Fe_2(SiO_4)_3$, $Ca_3Fe_2[(Si, Ti)O_4]_3$ with Si, Ti = 1:1, and $Ca_3Fe_2(TiO_4)_3$ in order to elucidate silicon-titanium replacement; but could not make these garnets. Recently Christophe-Michel-Levy (1956) has made both $Ca_3Fe_2(SiO_4)_3$ with $a_0 = 12.014 \pm .005$ and a titanium melanite $a_0 = 12.064 \pm .005$ but did not study these further.

P. Tarte (written communication, 1959) has recently investigated the co-ordination of titanium in garnets by their infrared absorption spectra, and kindly permitted us to mention here some of his unpublished results. He finds evidence that tetrahedrally co-ordinated titanium does replace silicon at least in part; and that whereas all common garnets have a consistent absorption spectrum, the presence of titanium causes marked divergence; and the spectrum of kimzeyite is even more markedly different from that of common garnets.

In summary, then, while we have considered the titanium in kimzeyite to be present as Ti_2O_3 and the titanium ions to be in octahedral co-ordination in the normal trivalent ionic position, other workers view at least part of the titanium (in titanium garnets) as TiO_2 and in tetrahedral co-ordination in the normal silicon position. The general question, whether Ti replaces Si, or octahedral Al, or both, is still open; but in kimzeyite, the weight of evidence favors replacement of aluminum in octahedral co-ordination.

Zirconium in Other Garnets

A crystal of Magnet Cove schorlomite from the Harvard Holden collection (85491) was reported to show appreciable (3.5–4%) zirconia by *x*-ray fluorescence (Milton, D. J., personal communication, 1958). A

spectrographic determination by N. Sheffey of the U. S. Geological Survey on the same material gave 2.7% ZrO_2.

Titanian andradite from the Oka, Quebec, carbonatite, found associated with niocalite, perovskite, and pyrochlore, contains 3.7% ZrO_2 (Nickel, 1960). Through the courtesy of Dr. J. A. Gower, the following data may be quoted from a report by E. H. Nickel (1956).

"*Andradite garnet*, a calcium-iron silicate, was found as a minor constituent. A spectrographic analysis of the andradite reveals that in addition to the iron and calcium, it contains 3% titanium and 2% manganese. The andradite varies in color from clear yellow, through brown, to black. The yellow garnet has a normal cell edge for andradite (12.03 Å) as determined by *x*-ray diffraction analysis, while the cell edge of the black garnet is abnormally high (12.15 Å). The only significant chemical difference between the two garnets is in zirconium content. The yellow garnet contains no appreciable zirconium . . ."

Dr. Gower (1959) further notes that the black garnet contains 0.25% Nb_2O_5, at least, and probably somewhat more.

It is of interest to note that at Oka, as in the Magnet Cove carbonatite, two garnets occur closely associated in similar paragenesis but only one contains zirconium.

Zedlitz, as already mentioned, found 0.19% ZrO_2 in the Kaiserstuhl melanite (TiO_2 12.10%). He cites an earlier analysis by R. Soltmann in 1890 who found 1.28% ZrO_2 in Kaiserstuhl melanite.

Because of these three instances of melanite (or andradite, schorlomite) containing substantial zirconia, it would be desirable to ascertain its presence or absence in all such analyzed garnets. Harry J. Rose, Jr., of the U. S. Geological Survey examined a small collection of schorlomites from the Yale University Brush collection, with the following results:

Specimen	Source	Zirconium found by *x*-ray fluorescence
2599	Magnet Cove	>1%
2596	Magnet Cove	>1%
2598	Magnet Cove	>1%
2597	Magnet Cove	.5–1%
907	Magnet Cove	.05–.1%
4333	Magnet Cove	<.05%
2600	Magnet Cove	<.05%
2591	Kaiserstuhl	.05–0.1%

Kimzeyite run at the same time showed far greater zirconia than any of these.

The four schorlomites containing more than a tenth of a per cent zir-

conia are coarsely crystallized (a centimeter or more across) and do not differ noticeably from those with least zirconia.

It follows that many though not all schorlomites from carbonatites contain zirconia from traces up to several per cent, and the presence or absence of this element should be established spectrographically or by *x*-ray fluoresence in analyses of such garnets; and if zirconia is present in more than tenths of a per cent it should be determined chemically.

The Name Kimzeyite

Kimzeyite has been named to honor the members of the Kimzey family who for almost a century have been instrumental in obtaining and preserving many of the remarkable mineral specimens for which the Magnet Cove area is famous. Williams (1891) refers to William T. Kimzey repeatedly, and the family since have continued to play an active part in the economic and mineralogical development of the Magnet Cove area. Mr. Joe W. Kimzey has kindly given us the following information concerning the Kimzey family (personal letter, October 16, 1958). "Wm. J. Kimzey came to the Magnet Cove area during the early 1870's and engaged in prospecting the area and collecting fine specimens of the numerous rare minerals for the leading dealers and some English, French, and German scientists, some of whom visited the 'Cove' from time to time. After the death of Wm. J. in 1906, his sons, John, Lawton, and Joe W., have spent much time seeking out specimens of the unusual and rare minerals of the area, that now enrich the finer mineral collections throughout the world. It was Joe W. who called the new zirconium garnet to the attention of Mr. Blade and Mr. Erickson in 1953 and who served as State Geologist for Arkansas during 1943 to 1945."

Acknowledgments

Many people have materially assisted in this study, and we cannot name them all. Besides our numerous colleagues of the U. S. Geological Survey, and Michael Fleischer in particular, we are largely indebted to Mr. Norman T. Williams, State Geologist of Arkansas and to Mr. Joe W. Kimzey of Malvern, Arkansas, former State Geologist of Arkansas, for many kindnesses extended in a field study of the occurrence; we are also grateful to Professor Rustum Roy, of Pennsylvania State University, to Dr. Hatten S. Yoder, Jr. of the Geophysical Laboratory, to Professor Clifford Frondel, of Harvard University, and to Dr. P. Tarte, of the University of Liege, Belgium for their friendly interest and most helpful discussions of the problems encountered in this investigation; needless to say they are not responsible for any erroneous statements or conclusions of this report. Dr. J. A. Gower of the Northwestern Explorations,

Ltd., Vancouver, B. C., and Dr. E. H. Nickel, of the Mines Branch, Department of Mines and Technical Survey, Ottawa, Canada, have furnished us specimens and data of the Oka, Quebec, zirconium garnet. Mr. Daniel J. Milton called our attention to the previously unrecognized considerable zirconium content of Magnet Cove schorlomite. Professor Horace Winchell of Yale University generously placed at our disposal the small reference collection of titanian garnets from the Brush collection.

References

Bertaut, Felix, and Forrat, Francis (1956), Structure des ferrites ferrimagnetiques des terres rares: *Acad. Sci. Paris comptes rendus*, **242,** 382–384.

Christophe-Michel-Levy, M. (1956), Reproduction artificielle des grenats calciques: grossulaire et andradite: *Bull. Soc. francaise Mineral. Crist.*, **70,** 124–128.

Eitel, Wilhelm (1954), The Physical Chemistry of the Silicates: University of Chicago Press, p. 20.

Erickson, R. L., and Blade, L. V. (1956), Map of bedrock geology of Magnet Cove igneous area, Hot Spring County, Arkansas: *U. S. Geol. Survey Mineral Inv. Field Studies Map MF* **53.**

Fleischer, M. (1937), Relation between chemical composition and physical properties in the garnet group: *Am. Mineral.*, **22,** 751–759.

Fleischer, M. (1955), Hafnium content and hafnium-zirconium ratio in minerals and rocks: *U. S. Geol. Survey Bull.*, **1021-A,** 9.

Frondel, Clifford (1957), Zirconium: Mineralogy and Geochemistry: *2d Nuclear Engineering and Science Conference Paper No.* **57-NESC-32** *Am. Soc. Mech. Engineers.*

Fryklund, V. C., Jr., Harner, R. S., and Kaiser, E. P. (1954), Niobium (columbium) and titanium at Magnet Cove and Potash Sulphur Springs, Arkansas: *U. S. Geol. Survey Bull.*, **1015 B.,** 48.

Geller, S., and Miller, C. E. with an appendix by Trueting, R. G. (1960), New synthetic garnets: *Acta Cryst.*, **13,** 179–186.

Gossner, B., and Reindl, E. (1934), Über die chemische Zusammensetzung titanhaltiger Silikate, insbesondere von Astrophyllite: *Centralblatt f. Mineralogie., etc. Abt.* **A** 161–167.

Gower, J. A. (1959), personal communication to L. G. Berry.

Green, Jack (1959), Geochemical Table of the elements for 1959: *Geol. Soc. America Bull.*, **70,** 1127–1184.

Hendricks, Sterling B. (1939), Random structures of layer minerals as illustrated by cronstedite ($2FeO \cdot Fe_2O_3 \cdot SiO_2 \cdot 2H_2O$). Possible iron content of kaolin: *Am. Mineral.*, **24,** 529–539.

Jaffe, Howard W. (1956), Application of the rule of Gladstone and Dale to minerals: *Am. Mineral.*, **41,** 757–777.

Larsen, Esper S., and Berman, Harry (1934), The microscopic determination of the nonopaque minerals, 2d ed: *U. S. Geol. Survey Bull.*, **848,** 30–31.

Milton, Charles, and Blade, Lawrence V. (1958), Preliminary note on kimzeyite, a new zirconium garnet: *Science*, **127,** 1343.

Nickel, E. H. (1956), A mineralogical study of diamond drill core NX-6 from the Oka. P. Q. property of the Molybdenum Corporation of America: *Investigation No.* **MD-3116** *Canada Dept. of Mines and Technical Surveys, Mines Branch.*

NICKEL, E. H. (1960), A zirconium-bearing garnet from Oka, Quebec: *Canadian Mineral.*, **6,** 549–550.

RAMDOHR, R. (1936), Ein Zinnvorkommen im Marmor bei Arandis, Deutsch Sudwestafrika: *Neues Jahrb. Min. Geol. B.B.*, **70, A,** 1 (cited in Rankama and Sahama, 1950 p. 732).

RANKAMA, KALERVO AND SAHAMA, TH. G. (1950), Geochemistry: The University of Chicago Press.

WILLIAMS, J. FRANCIS (1891), The igneous rock of Arkansas: Vol. II, Annual Report, Geological Survey of Arkansas.

YODER, H. S., AND KEITH, M. C. (1951), Complete substitution of aluminum for silicon—the system $3MnO \cdot Al_2O_3 \cdot 3SiO_2$-$3Y_2O_3$-$5Al_2O_3$: *Am. Mineral.*, **36,** 519–533.

ZEDLITZ, OTTO (1933), Über titanreichen Kalkeisengranat I: *Centralblatt f. Mineralogie, etc., Abt.* **A** 225–239.

ZEDLITZ, OTTO (1935), Über titanreichen Kalkeisengranat II: *Centralblatt f. Mineralogie, etc., Abt.* **A** 68–78.

Manuscript received July 11, 1960.

THE AMERICAN MINERALOGIST, VOL. 46, MAY–JUNE, 1961

TEPHROITE FROM FRANKLIN, NEW JERSEY*

CORNELIUS S. HURLBUT, JR., *Department of Mineralogy, Harvard University.*

ABSTRACT

A study of tephroite specimens from Franklin and Sterling Hill, New Jersey showed in all of them the presence of thin sheets of willemite believed to be a product of exsolution. These sheets are oriented parallel to the {100} and {010} planes of tephroite with the *a* and *c* axes of tephroite and willemite parallel. It is believed that little zinc remains in the tephroite structure and that much of it reported in chemical analyses has been contributed by intergrown willemite. This conclusion is supported by experiments synthesizing tephroite. The indices of refraction and *d* spacing of {130} vary as would be expected with changes in amounts of MgO, FeO and CaO.

INTRODUCTION

Tephroite, Mn_2SiO_4, a member of the olivine group, was described as a new mineral from Sterling Hill by Breithaupt in 1823. A chemical analysis of the original material was published by Brush (1864) together with several additional chemical analyses of tephroite made by others. These analyses report ZnO in varying amounts which Brush attributed to invariably associated zincite. Palache (1937) did not agree with Brush and stated " . . . that the molecular ratios in some analyses more nearly satisfy the orthosilicate formula when zinc is regarded as essentially a part of the mineral rather than as a constituent of mechanical inclusions." The present study was undertaken for the purpose of investigating the variations in the properties of tephroite with changes in chemical composition, particularly the effect of zinc. Relationships were not expected to be simple for analyses show, in addition to ZnO, variable amounts of MgO, FeO, and CaO.

DESCRIPTION OF THE SPECIMENS

For this study 27 specimens in the Harvard collection labelled *tephroite* and *roepperite* were assembled. Several additional specimens were kindly made available by Mr. John L. Baum of the New Jersey Zinc Company and Mr. John Albanese of Union, New Jersey.

The name *tephroite* was given to the original material because of its gray color (from the Greek—*ash-colored*) but only six of the specimens studied were gray; thirteen were reddish brown; four rose-red. Roepperite is black. It was also considered for it has been described as a variety of tephroite containing notably high amounts of FeO and ZnO. Of

* Contribution No. 395 from the Department of Mineralogy and Petrology, Harvard University.

the four roepperite specimens available, three proved to be black willemite.

When examined microscopically, most tephroite is seen to contain minute inclusions. These inclusions have been studied by Metsger, Tennant and Rodda (1958) who conclude they are franklinite and are responsible for the color variation. Black franklinite is present in roepperite and red franklinite (spinel) is present in the red tephroite. " . . . paler shades of gray and flesh pink . . . are due to the sparse scattering of inclusions." It has previously been thought that zincite inclusions were responsible for the red coloring. However, in some tephroite specimens flakes of both red zincite and black franklinite are present associated with willemite sheets and elongated parallel to the *c* axis of the tephroite.

Portions of all the specimens gave under ultra violet light the characteristic greenish luminescence of willemite. Some of this fluorescence resulted from massive willemite intergrown with the tephroite but much of it seemed to be coming from the tephroite itself. Closer examination showed thin fluorescing sheets of colorless willemite lying along the {100} and {010} planes of the tephroite. Sections normal to these two directions, {001}, show the traces of the sheets intersecting at right angles (Fig. 1). Under magnification more and thinner sheets become visible forming a minute crosshatched pattern. This is best observed in thin section where it is seen that the willemite sheets although discontinuous are all crystallographically oriented with the *c* axis of willemite parallel to the *c* axis of the tephroite host, Fig. 2. The major and most continuous willemite sheets are irregularly spaced and may have a thickness as great as 0.10 mm. The lesser sheets are much less continuous with thickness ranging from 0.05 mm. to less than 0.005 mm. A similar intimate intergrowth of willemite with glaucochroite was reported by O'Daniel and Tscheischwili (1944).

The cleavage of tephroite is given as {100} and {010}, the directions of the interlayered sheets of willemite. On most of the Franklin tephroite when examined in detail these directions of breaking do not yield plane surfaces but are striated in a direction parallel to the *c* axis; an observation early made by Brush (1864). They appear to be more a parting than a cleavage, separating easily along the planes of the major willemite sheets. On most specimens it is impossible to develop a cleavage between these parting planes and in thin section no cleavage cracks are visible between the willemite layers. Small transparent crystals of Franklin tephroite show no cleavage parallel to {100} or {010} but a good {001} cleavage.

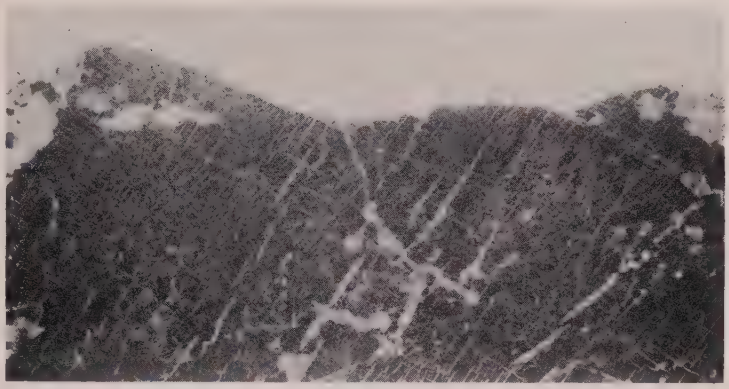

FIG. 1. Polished surface of tephroite crystal cut nearly normal to the c axis. Photographed under ultraviolet light with fluorescing willemite recorded as light lines and areas. Full scale.

In addition to the parallelism of the c axes of the tephroite and the included willemite there is a parallelism of other axial directions. X-ray rotation photographs were taken of the willemite with the rotation axes perpendicular to the sheets. One set of sheets, parallel to {100} of tephroite, yields 13.97 Å as the identity period (a_0 of willemite); the other set of sheets at right angles and parallel to {010} of tephroite

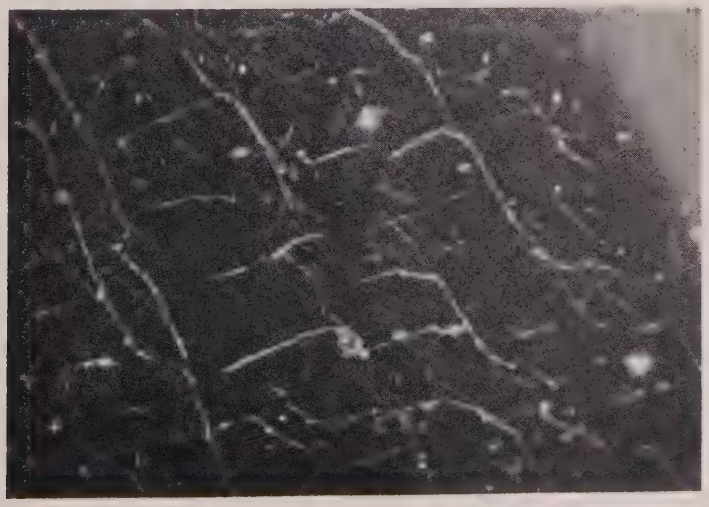

FIG. 2. Photomicrograph of tephroite thin section cut nearly normal to the c axis. Crossed nicols. Light lines are willemite. Area: 2×1.7 millimeters.

yields 24.20 Å as the identity period. For the willemite $c_0 = 9.35$ Å. The axial dimensions of the willemite and tephroite thus compare as follows:

Tephroite	$a_0 = 4.87$ Å	$b_0 = 10.64$	$c_0 = 6.23$
Willemite	$a_0 = 13.97$ Å	$\perp(10\bar{1}0) = 24.20$	$c_0 = 9.35$

For willemite Bragg and Zachariasen (1930) give $a_0 = 13.96$ Å, $c_0 = 9.34$. The closest structural correspondence of the two sets of dimensions is found in the values for c_0, for $3 \times c_0$ of tephroite is 18.69 Å, nearly equal to $2 \times c_0$ of willemite, 18.70 Å.

The constant orientation of the willemite with respect to the tephroite host as well as the intimate intergrowth strongly suggest that the willemite is a product of exsolution. Moreover, it is almost certain that much of the zinc reported in chemical analyses was contributed by willemite.

Chemical Composition

Palache (1937) lists 13 chemical analyses of tephroite from Franklin and Sterling Hill. All of these show the presence of FeO (3.33% max.), and all but the earliest two MgO (15.9% max.) and ZnO (18.90% max.). CaO (2.70% max.) is present in six analyses. With the possibility of so many elements substituting for manganese in the tephroite structure, it at first appeared a hopeless task to correlate in any significant manner the physical constants with chemical composition.

Of the 13 specimens represented by the analyses given by Palache (1937, p. 77) only one (number 11) was available for study. This is a reddish-brown tephroite with abundant interlaminated sheets of willemite. The analysis made by L. H. Bauer (No. 1, Table 1) gives ZnO = 12.15%. With the thought that willemite may have contributed much of the zinc to the analysis, a magnetic separation was made on minus 325 mesh material. Tephroite is slightly magnetic, willemite non-magnetic. After many passes through the Frantz isodynamic separator, even the most magnetic material was far from being free of willemite as shown by inspection under the microscope and ultra-violet light, and the presence of willemite lines in an *x*-ray powder photograph. An analysis of this admittedly contaminated sample by Mr. Jun Ito gave 6.1% ZnO, approximately one half of that reported in the earlier analysis. With zinc present in the unseparated willemite as well as in the franklinite of the coloring inclusions, the amount in the tephroite structure must be considerably less. Could this mean that zinc is a negligible variant in the composition of tephroite?

Of the 27 specimens studied, one was selected for a complete analysis. This was of a large reddish brown tephroite crystal from which only the coarse associated willemite had been separated. The analysis, No. 2,

Table 1, compares very favorably with several earlier analyses reported by Palache (1937). Partial analyses were made of seven other tephroite specimens from Franklin and Sterling Hill and one of roepperite. In these zinc is not reported since willemite and probably franklinite was present in all and its determination would not have been significant. For comparison a partial analysis of tephroite from Långban containing no zinc was also made. In most of these analyses the chief oxide other than MnO is MgO and thus most of the specimens belong essentially to the series Mg_2SiO_4-Mn_2SiO_4. Glasser and Osborn (1960) point out that a continuous solid solution series exists between Mg_2SiO_4 and Mn_2SiO_4.

TABLE 1. ANALYSES OF TEPHROITE*

	1	2	3	4	5	6	7	8	9	10
SiO_2	29.53	30.17								
ZnO	12.15	10.22								none
MnO	43.64	49.57	36.09	32.82	58.42	53.18	46.19	51.31	28.68	55.65
MgO	9.64	4.92	15.28	15.76	2.40	1.07	8.72	2.66	5.65	10.75
FeO	4.41	3.94	1.26	1.40	0.79	0.78	1.90	0.29	24.28	0.09
CaO	–	0.05	0.63	0.10	0.05	4.40	tr	2.81	tr	1.10
Ig. loss	—	1.00								
	99.37	99.87								
					Molecular ratio MnO:MgO					
MnO	72.02	85.13	57.29	55.92	93.26	96.58	75.29	91.64	74.27	74.64
MgO	27.98	14.87	42.71	44.08	6.74	3.42	24.71	8.36	26.73	25.36

* 1. Harvard No. 105489 Reddish-brown tephroite, Franklin, in Palache (1937) L. H. Bauer, analyst.
Analyses 2–10 Jun Ito, analyst.
2. Harvard No. 105617 Reddish-brown tephroite, Franklin
3. Hancock Coll. (Harvard) Pink tephroite crystals, Sterling Hill
4. Harvard No. 85551 Reddish brown crystals, Sterling Hill
5. Rowe Coll. (Harvard) Gray tephroite, Franklin
6. Harvard No. 33651 Gray tephroite, Franklin
7. Harvard No. 105490 Reddish brown tephroite, Franklin
8. Harvard No. 19574 Gray tephroite, Franklin
9. Bauer Coll. (Harvard) Black Roepperite, Franklin
10. Harvard No. 106580 Gray tephroite, Långban, Sweden

SYNTHESIS

In an effort to determine the extent of the solid solubility of zinc in tephroite a series of crystalline substances in the system $MnO \cdot MgO \cdot ZnO \cdot SiO_2$ were synthesized. The method of dry fusion following closely that used by Snow (1943) is briefly as follows: Reagent grade chemicals were used—silicic acid and the carbonates of the metals. Amounts of the

reagents proportional to the stoichometric mole per cents were ground together in an agate mortar. The mixture placed in a platinum crucible was then heated at 950° C. in a stream of nitrogen for 90 minutes. The sintered oxides were then removed from the furnace and reground to insure thorough mixing. This powdered material was divided into two halves, pressed into pellets and returned to the furnace in separate crucibles where it was heated at 1250° C. for 90 minutes in a stream of nitrogen. One portion was then removed and cooled quickly in air. The other portion remained in the furnace which was cooled at the rate of 20° C. per hour to 950° C. At this temperature the furnace was turned off and allowed to cool to room temperature.

The first synthesis was of Mn_2SiO_4. This was followed by other runs in which increasing amounts of ZnO were introduced with proportionally less MnO. MgO in varying amounts was introduced in several runs. Data obtained on the slowly cooled material are summarized in Table 4. The *x*-ray powder data obtained on the slowly cooled and rapidly cooled products were the same within the limits of error. However, the indices of refraction of the slowly cooled material containing zinc were all slightly higher than the corresponding rapidly cooled portion. The maximum difference in refractive index was 0.014.

X-Ray Investigation

X-ray Weissenberg photographs were taken on a crystal of tephroite supplied by Mr. Albanese. This crystal, transparent and nearly colorless, was one of five in a cavity in franklinite-willemite ore from Franklin. The largest of these crystals was 2 millimeters long. Spectroscopic analysis showed less than 1.0% ZnO and less than 0.5% MgO, FeO, CaO. It appeared to be very similar to crystals described by Gordon (1922) and others analysed by L. H. Bauer and reported by Palache (1928). In Bauer's analysis MgO = 0.46, ZnO = 1.53, FeO = 0.31%. The unit cell dimensions were determined as $a_0 = 4.871$ Å, $b_0 = 10.636$, $c_0 = 6.232$. These are all slightly larger than those given for tephroite from Franklin by O'Daniel and Tscheischwili (1944), which were $a_0 = 4.86$ Å, $b_0 = 10.62$, $c_0 = 6.22$, but almost identical with those reported by Strunz (1957). The axial ratios $a_0 : b_0 : c_0 = 0.458 : 1 : 0.586$. Palache (1937) gives the morphological axial ratios $a : b : c = 0.461 : 1 : 0.589$. The specific gravity of these crystals, the only tephroite studied which it is felt is sufficiently free of mechanical inclusions to give a significant determination, is 4.10 measured on the Berman balance. The calculated specific gravity of Mn_2SiO_4 for the measured cell dimensions is 4.15. It is also interesting to note that these crystals show a good {001} cleavage but no {100} or {010} cleavage.

TABLE 2. POWDER X-RAY DIFFRACTION DATA FOR SYNTHETIC TEPHROITE
Filtered copper radiation with quartz standard

hkl	*d* obs.	I	*hkl*	*d* obs.	I
020	5.301	15	131	2.611	70
110	4.431	5	112	2.572	90
021	4.044	20	041, 200	2.440	15
101	3.830	5			
111	3.624	6	210	2.307	15
002	3.116	14	140	2.335	20
130	2.867	100	211	2.200	18
022	2.688	10	132	2.101	5
040	2.660	30	113, 222	1.811	35

X-ray study of the other natural and synthetic tephroite was confined largely to recording of powder diffraction data. In Table 2 the *d* spacings of synthetic Mn_2SiO_4 are given. It will be noted in Table 2 that the line of greatest intensity ($d = 2.867$) is given by the plane (130). Yoder and Sahama (1957) presented a determinative curve for olivine (forsterite-fayalite) based on the position of this (130) reflection which is of high intensity and varies linearly throughout the series. Sahama and Hytönen (1958) also used this (130) *d* spacing to distinguish between members of the monticellite-kirschsteinite series. In all the manganese bearing olivines (130) is also a high intensity reflection and was thus chosen as the structural parameter to measure in the present study.

The data were recorded using a Norelco Geiger-counter diffractometer with a scan speed of $\frac{1}{4}°$ per minute and a chart speed equal to 2 inches per degree 2θ. Finely ground samples, mixed with quartz to about 20% of their volume, were made into pressed mounts. The position of the copper Kα ($10\bar{1}1$) reflection for quartz ($2\theta = 26.664°$) was used to correct the measurements of the (130) reflection of the tephroite.

The values of d_{130} for the analyzed tephroites are given in Table 3 and for the synthesized tephroite in Table 4. Both are plotted in Fig. 3 as a function of the MnO:MgO ratio.

REFRACTIVE INDICES

The indices of refraction of material labelled "tephroite" from Franklin and Sterling Hill show a considerable variation reflecting compositional difference. The β refractive indices of analyzed tephroites obtained using sodium light are given in Table 4 and are plotted in Fig. 3 as a function of the ratio of MnO:MgO. The β refractive indices of synthetic products containing MgO given in Table 4 are also plotted in Fig. 3.

TABLE 3. X-RAY MEASUREMENTS AND REFRACTIVE INDICES OF NATURAL TEPHROITE*

	MnO:MgO		β index	d_{130}
1	72.02	27.98	1.775±0.001	2.840±0.001
2	85.13	14.87	1.795	2.850
3	57.29	42.71	1.739	2.829
4	55.92	44.08	1.743	2.827
5	93.26	6.74	1.800	2.861
6	96.58	3.42	1.791	2.871
7	75.07	24.93	1.775	2.844
8	91.64	8.36	1.790	2.868
9	74.72	26.73	1.804	2.840
10	74.64	25.36	1.768	2.848
11	98.12	1.88	1.803	2.863

* Numbers 1–10 correspond to analyses of Table 1. Number 11 is tephroite from Antarctica described by Mason (1959) and loaned by him for this study.

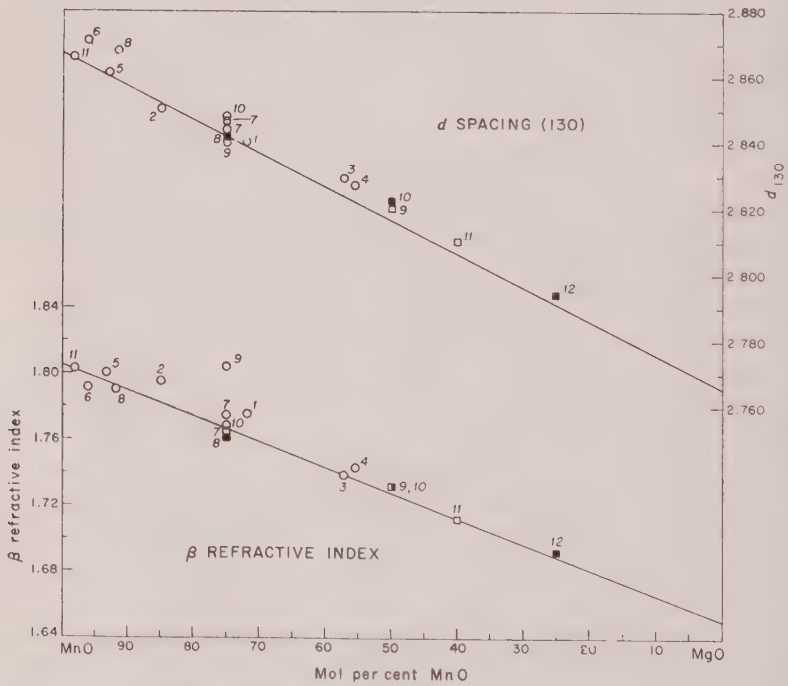

FIG. 3. Plot of d_{130} spacing and refractive index of tephroite plotted against mol per cent MnO. Circles represent natural tephroite; squares represent synthetic tephroite. Open squares—no zinc in starting material; solid squares—zinc present in starting material. Curves are drawn assuming a linear variation between Mn_2SiO_4 and Mg_2SiO_4 for d_{130}, and refractive indices.

Discussion of Results

In Fig. 3 are plotted the d_{130} spacings and β refractive indices of synthetic and analysed natural tephroite against mol per cent of MnO. The curves are drawn as straight lines assuming linear variations between the fictive end points. For tephroite $d_{130}=2.867$ Å, $\beta=1.805$; forsterite $d_{130}=2.766$ Å (Yoder and Sahama, 1957), $\beta=1.651$ (Larsen and Berman, 1934).

The departure of the plotted points from both curves is believed due largely to the presence of cations other than Mn^{++} and Mg in the A position of A_2SiO_4. For Fe_2SiO_4 (fayolite) $d_{130}=2.833$ Å (Yoder and Sahama, 1957) and $\beta=1.886$ (Larsen and Berman, 1934). Thus Fe^{++}, when substituting for Mn^{++}, tends to slightly lower the d_{130} spacing and to raise the refractive index. For $CaMgSiO_4$ (monticellite) $d_{130}=2.934$ Å (Sahama and Hytönen, 1958) and $\beta=1.651$. Calcium has the effect when substituting for Mn^{++} of increasing the d_{130} spacing and decreasing the refractive index. The effect of the presence of Fe^{++} is shown most strikingly in specimen No. 9 (roepperite) with 24.28 wt. per cent FeO, and to a lesser extent in Nos. 1 and 2. Specimen No. 6 (4.40 wt. per CaO) shows the increase of d_{130} and decrease of β index with appreciable calcium.

Table 4. *X*-Ray Measurements and Refractive Indices of Synthetic Tephroite, A_2SiO_4

	Mol Per Cent of A Cation			β index	d_{130}
	Mn	Zn	Mg		
1	100			$1.805^{\pm 0.001}$	$2.867^{\pm 0.001}$
2	95	5		1.803	2.863
3	90	10		1.804	2.861
4	85	15		1.803	2.860
5	80	20		1.802	2.860
6	75	25		1.802	2.860
7	75		25	1.764	2.847
8	60	20	20	1.760	2.842
9	50		50	1.732	2.820
10	45	10	45	1.731	2.822
11	40		60	1.712	2.810
12	20	20	60	1.693	2.794

The position of the plotted points in Fig. 3 for both refractive index and d_{130} for natural tephroite are essentially what would be expected from the compositions without consideration of zinc. One can thus conclude that zinc, if at all significant, plays a very minor role.

Consideration of the data given in Table 4 indicates that the solid solubility of zinc in tephroite is limited. The zinc that enters the lattice has little or no effect on the refractive index, but appears to have a slight effect on the structure as shown by the reduction of the d spacing of (130). Additions of 5, 10, and 15 mol per cent of ZnO to the starting mixture show a progressive, though slight, decrease in this spacing of the crystalline products. Greater amounts of ZnO show no effect. Unfortunately it is impossible to tell how much of the available zinc substituted for manganese in the tephroite and how much formed the separate phase, Zn_2SiO_4. Willemite lines were detectable on all diffractometer recordings in which the starting material for the synthesis contained more than 5 mol per cent ZnO. A separate phase of lower refractive index ($n = 1.69$) was also observed optically. It seems reasonable to conclude that up to a certain amount the more zinc available, the more will be taken into the tephroite structure though even at low concentrations all of it is not accommodated. The experiments indicate that certainly not more than 10% and probably less than 5% of zinc substitutes for manganese. The slight effect of the presence of zinc is shown in the two pairs of synthetic products 7-8 and 9-10. One member of each pair contained ZnO, the other none, the ratio of MnO:MgO remaining the same; yet the indices of refraction and the d_{130} spacings are closely similar.

Although it is possible to identify a tephroite and a willemite phase in the synthesized material, there was no indication in the fine grained crystalline aggregates of any ordered arrangement between them as in natural tephroite. It was thus impossible to tell by observation whether they formed simultaneously or that the willemite was exsolved on cooling. Although the d spacing of (130) was essentially the same in both quenched and slowly cooled samples, the index of refraction of the quenched material was consistently lower. For example for run No. 4, $\beta = 1.804$ slowly cooled and $\beta = 1.790$ on the quenched sample. There is thus indication that there has been unmixing on slow cooling.

The greatest amount of zinc reported in a tephroite analysis by Palache (1937) is 18.9 wt. per cent ZnO. This, approximately 22 mol per cent of the manganese, might be assumed as the maximum amount of zinc present in the structure at high temperature. If exsolution has indeed taken place, zinc must have been in 6-coordination. With separation of willemite on cooling, the zinc is in the more comfortable situation of 4-coordination. That only small amounts of zinc are accommodated in the crystal structure of tephroite is consistent with the general observations on the geochemistry of zinc. Newmann (1949) points out that in all the common zinc minerals with the exception of smithsonite, zinc is in 4-coordination. He further states that if it entered into common

structures in 6-coordination it would be camouflaged in the ferromagnesian minerals. Ridge (1952) in discussing the geochemistry of the ores of Franklin remarks, "If the zinc reported by the chemical analyses in tephroite is really in the crystal lattice and is not present as submicroscopic inclusions of zincite, it seems almost certain that the zinc is present as the unusual Zn^2 in 6-coordination."

Conclusions

The oriented intergrowth of willemite in tephroite speaks eloquently for its origin as a product of exsolution. With the slow cooling of natural tephroite the unmixing of Zn_2SiO_4 may have been nearly complete. Most certainly one can conclude that it contains much less zinc than has been reported in many chemical analyses. The variations that exist in the properties of tephroite result, therefore, from the substitution of Mg, Fe^{++}, and Ca for Mn^{++} rather than from the substitution of Zn.

REFERENCES

Bragg, W. L. and Zachariasen, W. H. (1930), The crystal structure of phenacite Be_2SiO_4 and willemite, Zn_2SiO_4: *Zeit. Krist.*, **72**: 518.

Brush, G. J. (1864), On tephroite: *Am. Jour. Sci. 2nd series*, **37**, 66–70.

Glasser, F. P. and Osborn, E. F. (1960), The ternary system MgO-MnO-SiO_2: *Jour. Am. Ceramic Soc.*, **43**, 132–140.

Gordon, S. G. (1922), Crystallographic notes on glaucochroite, willemite, celestite and calcite from Franklin, N. J.: *Acad. Nat. Sci. Phila. Proc.*, **74**, 105.

Larsen, E. S. and Berman, H. (1934), The microscopic determination of the nonopaque minerals: *U.S.G.S. Bull.*, **848**.

Metsger, R. W., Tennant, C. B. and Rodda, J. L. (1958), Geochemistry of the Sterling Hill zinc deposit, Sussex County, New Jersey: *Bull. G.S.A.*, **69**, 775–788.

Neumann, Henrich (1949) Notes on the mineralogy and geochemistry of zinc: *Min. Mag.*, **28**, 575–581.

O'Daniel, H. and Tscheischwili (1944), Structuruntersuchungen an tephroit Mn_2SiO_4, glaukochroit $(Mn,Ca)_2SiO_4$ und Willemit Zn_2SiO_4 von Franklin Furnace: *Zeit. Krist.*, **105**, 273.

Palache, C. (1928), Mineralogical notes on Franklin and Sterling Hill, New Jersey: *Am. Mineral.*, **13**, 297–329.

——— (1937), The minerals of Franklin and Sterling Hill, Sussex County, New Jersey: U.S.G.S. Prof. Paper 180.

Sahama, G. and Hytönen, K. (1958), Calcium-bearing magnesium-iron olivines: *Am. Mineral.*, **43**, 862.

Snow, R. B. (1943), Equilibrium relationships on the liquidus surface in part of the MnO-Al_2O_3-SiO_2 system: *Jour. Am. Ceram. Soc.*, **26**, 11–20.

Strunz, H., (1957), Mineralogische Tabellen. Akademische Verlagsgesellschaft, Geest und Portig K.-G., Leipzig.

von Breithaupt, A. (1823), Charakteristik des Mineral Systems: 3rd ed., pp. 211, 329.

Yoder, Jr. H. S., and Sahama, G. (1957), Olivine *x*-ray determinative curve: *Am. Mineral.*, **42**, 475–491.

Manuscript received July 1, 1960.

NOBLEITE, ANOTHER NEW HYDROUS CALCIUM BORATE FROM THE DEATH VALLEY REGION, CALIFORNIA*

RICHARD C. ERD, JAMES F. MCALLISTER, AND ANGELINA C. VLISIDIS,
U. S. Geological Survey, Menlo Park, Calif., and Washington, D. C.

ABSTRACT

Nobleite is a new hydrous calcium borate, $CaO \cdot 3B_2O_3 \cdot 4H_2O$, that has been found in the Furnace Creek borate deposits of the Death Valley region, California. Platy euhedral crystals of nobleite are produced by the weathering of colemanite and priceite veins in altered basaltic rocks of the Furnace Creek formation of late Tertiary age. The new mineral is associated with ulexite, gowerite, meyerhofferite, colemanite, several undescribed borates, ginorite, sassolite, a manganese oxide mineral, and gypsum.

Nobleite is biaxial (+), $\alpha = 1.500 \pm 0.003$, $\beta = 1.520 \pm 0.002$, $\gamma = 1.554 \pm 0.002$; $2V = 76°$ (calc.); $r > v$ weak; $X \wedge a = 29°$, $Y = b$, $Z \wedge c = -7°$. Hardness 3; measured specific gravity 2.09 ± 0.01.

Chemical analysis of the mineral gave: Li_2O 0.02, Na_2O 0.26, K_2O 0.06, CaO 16.96, SrO 0.11, Fe_2O_3 0.15, B_2O_3 60.80, H_2O 21.84; total 100.28 per cent.

Nobleite is monoclinic; the space group is $P2_1/a$; $a = 14.56 \pm 0.05$ Å, $b = 8.01_8 \pm 0.02$ Å, $c = 9.83_8 \pm 0.02$ Å, $\beta = 111° 45' \pm 10'$; $a:b:c = 1.816:1:1.227$; cell volume 1066 Å^3; cell contents $4[CaO \cdot 3B_2O_3 \cdot 4H_2O]$; calculated density 2.09_8.

The new mineral is named in honor of Dr. Levi F. Noble of the U. S. Geological Survey.

INTRODUCTION

The mineral described in this paper was first collected by McAllister in 1955 in the course of his study of the Furnace Creek borate district in the Death Valley area, California. His preliminary tests showed the material to be a borate having optical properties different from those of other naturally occurring borates. Further study by Erd and Vlisidis proved this material to be identical with the synthetic compound $CaO \cdot 3B_2O_3 \cdot 4H_2O$.

The naturally occurring hydrous calcium borate, $CaO \cdot 3B_2O_3 \cdot 4H_2O$ (or $CaB_6O_{10} \cdot 4H_2O$), is named nobleite in honor of Dr. Levi F. Noble, geologist in the U. S. Geological Survey since 1909, in further recognition of his fundamental contributions to geologic knowledge of the Death Valley region. Dr. Noble's broad interest in the region has included the geology of borates and the paragenetic sequence of colemanite after ulexite in some mines.

OCCURRENCE

Nobleite has been found at seven places that are widely spaced for twelve miles along virtually the length of the area containing borates between the floor of Death Valley and the Widow mines in the Greenwater Range south of Ryan. These localities are at least one mile and

* Publication authorized by the Director, U. S. Geological Survey.

not more than four miles apart on mining property of the United States Borax and Chemical Corporation. All but the southeasternmost one are within the boundary of Death Valley National Monument. The number of localities indicates little more than how far the search for the new mineral has been carried.

The mineralogical observations in this paper were made on material from a locality 0.6 mile NNW of the De Bely mine or 1.1 miles in a straight line S. 18° E. from the junction of the Corkscrew Canyon road and California highway 190.

The nobleite is associated with other borate minerals produced by the weathering of colemanite and priceite veins in altered olivine basalt and basaltic clastic rocks (McAllister, 1958; Erd and others, 1959, p. 912–913) in the Furnace Creek formation (Noble, 1941, p. 955–956) of late Tertiary age. The new mineral generally is in surficial, weathered material on and near the source veins. The weathered matrix now consists chiefly of montmorillonite, analcime, and some magnetite. It contains along with borate minerals some gypsum, thenardite, a manganese oxide mineral, and limonite. The newly formed borates in surficial material at nobleite localities include ulexite, gowerite, meyerhofferite, colemanite, an undescribed calcium borate, a magnesium borate, ginorite, and sassolite. An apparently exceptional occurrence of the most coarsely crystalline nobleite was found in the Corkscrew mine by Mr. Sutherland, who describes it below. Two other occurrences underground, about 10 feet vertically from the surface in the Hard Scramble claim and 300 feet below the surface at the Widow No. 3 mine, are more similar to the others, for they are in efflorescences on mine workings in priceite- or colemanite-bearing altered basalt.

At every locality where the original colemanite or priceite veins are exposed (six out of the seven places), some of the nobleite encrusts the veins, which generally show corrosion. Some aggregates of subhedral nobleite crystals retain the general form of diverging clusters of the original coarse colemanite. A crust of meyerhofferite in one specimen lies between the colemanite and some of the nobleite. Clusters of gowerite crystals are attached to nobleite aggregates from four of the localities and some of this gowerite in turn supports individual crystals of nobleite (Fig. 1). A still undescribed calcium borate at one place fills in between the microblades of gowerite on the nobleite. Much of the nobleite forms a coherent open meshwork of tabular crystals, commonly intergrown with fluffy ulexite, an undescribed manganese oxide, or doubly terminated microcrystals of colemanite. Like closely associated ginorite and sassolite, clots of euhedral nobleite are also irregularly spaced through a nearly incoherent matrix of weathered basaltic surficial debris.

Some of the ginorite is interspersed among the larger crystals of nobleite, coating them and filling in between as if at least this ginorite formed later than this nobleite.

According to field relationships, the origin of the nobleite in surficial material can be attributed with some confidence to weathering of borate minerals in the Tertiary rocks. How recently it has continued to crystallize since the present topography was formed remained unanswered until

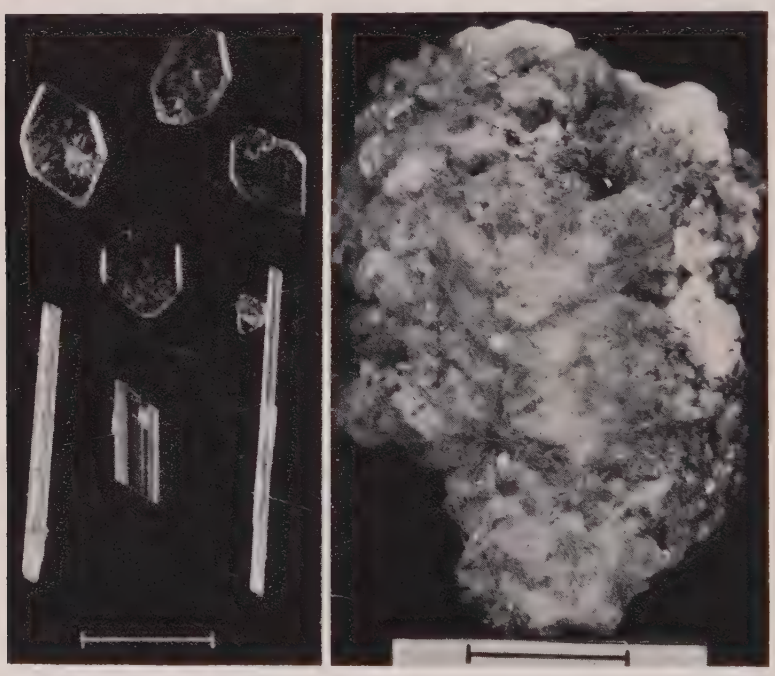

a *b*

FIG. 1. (*a*) Crystals of nobleite (at top) and gowerite from north of the De Bely mine, Death Valley. Crystals of nobleite may be seen adhering to the gowerite crystal on the right. Bar at bottom indicates one mm. (*b*) Nobleite crystals from the Corkscrew mine, Death Valley. Bar at bottom indicates one cm. Photographs by Elliot C. Morris.

nobleite was found in the efflorescence coating man-made surfaces less than forty years old.

The largest, best-formed crystals of nobleite (Fig. 1) were obtained from the Corkscrew mine in December 1957, by J. A. Sutherland,[1] who at the time was unaware that the new mineral from nearby localities was being described for publication. He had previously collected a small

[1] 1261½ Neola St., Los Angeles 41, California.

amount of the material in November 1956. Mr. Sutherland contributes the following description of the occurrence of the material he collected:

The nobleite in the Corkscrew mine was found on colemanite in several geodelike cavities which were joined by small fissures. This enabled the tracing of nobleite in this occurrence. The lower cavity was entirely coated with nobleite, while the upper cavities were only partially covered. The lower cavity showed the largest crystals and some of the most perfectly formed. The upper cavities showed smaller crystals of good form, though they are not as translucent as the crystals of the lower cavity. A few isolated crystals were noticed on colemanite in fissures below the lower cavity. The crystals range in size from less than 1 mm. to more than 3 mm. There were only two minerals in direct association with the nobleite, colemanite as mentioned and ulexite. Nobleite appears to be a solution deposition and of later origin than the colemanite and probably earlier than the ulexite. No ulexite was found directly on nobleite but several tufts of ulexite crystals were found in the upper cavities and showed no apparent damage or etching from a later solution.

The Corkscrew mine is 1.6 miles in a straight line S. 20° W. from the junction of the Corkscrew Canyon road and California highway 190, as shown on the topographic map of the Furnace Creek quadrangle.

Crystallography

X-ray data

The crystallography of nobleite, determined by single-crystal x-ray precession techniques, is given in Table 1, together with the calculated and observed densities. The diffractometer powder pattern (Table 2) was indexed from the single-crystal data in Table 1, and all calculated d-spacings are listed in Table 2 for $d \geq 2.500$ Å. Observed powder data are given both for the mineral and for synthetic material. Nobleite shows strong preferred orientation in its x-ray powder pattern due to the platy habit and perfect cleavage parallel to (100); this effect is much less pronounced in the pattern of the synthetic nobleite.

Morphology

Nobleite occurs as a coherent open mesh-work of platy euhedral crystals or as mammillary coatings formed by plates arranged subparallel to {100}. Fig. 2 illustrates a typical habit for nobleite crystals. The {100} plate form is commonly elongated [010] or [001]. Large crystals have a hexagonal aspect (Fig. 1*a*), but smaller crystals are commonly rhomb-shaped by truncating {011} forms. The acute angle of the rhombs, measured with the microscope, is 78° (78°25′, calc., from x-ray data). Common forms observed are: {100}, {001}, {110}, {011}, and {111}. These forms were identified by comparing interfacial angles measured under the microscope with angles calculated from the x-ray cell constants. Contact twinning, with (100) as twin plane and composi-

TABLE 1. CRYSTALLOGRAPHIC DATA FOR NOBLEITE, $CaO \cdot 3B_2O_3 \cdot 4H_2O$*

	Symmetry: monoclinic	
	(1)† $P2_1/a$	(2)† $P2_1/n$
a	14.56 ± 0.05 Å	14.23 ± 0.05 Å
b	$8.01_6 \pm 0.02$	$8.01_6 \pm 0.02$
c	$9.83_8 \pm 0.02$	$9.83_8 \pm 0.02$
β	$111°45' \pm 10'$	$108°11' \pm 10'$
$a:b:c$	1.816:1:1.227	1.775:1:1.227
Cell Volume	1066 Å^3	
Cell Contents	$4[CaO \cdot 3B_2O_3 . 4H_2O]$	
Density (calc.)	2.09_8 g.cm.$^{-3}$	
Specific Gravity (meas.)	$D_4^{20°}$ 0, 2.09 ± 0.01 (mineral)[a]	
	2.10^b 2.09^c (synthetic)	

* Single-crystal x-ray data obtained by Joan R. Clark, U. S. Geological Survey (written communication, 1959); a quartz-calibrated precession camera was used with Mo/Zr radiation, $\lambda MoK_\alpha = 0.7107$ Å, and film measurements were corrected for both horizontal and vertical film shrinkage.

† Transformation, $P2_1/a$ to alternative setting $P2_1/n$: $\bar{1}0\bar{1}/010/001$.

[a] Determined by Erd for clear inclusion-free crystals using the sink-float method with a mixture of bromoform and carbon tetrachloride.

[b] Determined by Vlisidis using a fused silica Adams-Johnston pycnometer with ethyl alcohol (95% by volume) as the liquid medium; synthetic nobleite prepared by W. T. Schaller, U. S. Geological Survey.

[c] Chelishcheva (1940, p. 511) on synthetic material.

tion surface is common. Such twins show symmetrical extinction in sections containing [010]. Typical dimensions of individual crystals from north of the De Bely mine are 0.6 by 0.3 by 0.1 mm. One specimen from the Corkscrew mine contains crystals up to 3 mm. in length, covered with a dust of later nobleite crystals having an average diameter of 0.01 mm.

PHYSICAL AND OPTICAL PROPERTIES

Nobleite exhibits perfect {100} and indistinct {001} cleavages; the fracture is uneven. The mineral is sectile, flexible in thin crystals or cleavage flakes, and inelastic. The hardness is about the same as that of calcite (3).

Individual crystals of nobleite are colorless and transparent, but fine-grained aggregates and the streak of the mineral are white. The luster is subvitreous, but is pearly on cleavage plates. Nobleite is neither fluorescent nor thermoluminescent.

TABLE 2. *X*-RAY DIFFRACTION DATA AND UNIT CELL OF NOBLEITE

Indexed on monoclinic unit cell: $P2_1/a$; $a=14.56\pm0.05$ Å, $b=8.01_6\pm0.02$ Å, $c=9.83_8\pm0.02$ Å, $\beta=111°45'\pm10'$.

	Nobleite North of De Bely mine, Death Valley[1]			$CaO\cdot3B_2O_3\cdot4H_2O$ Synthetic[2]	
hkl	*d* (calc.)[3] Å	*d* (meas.) Å	I	*d* (meas.) Å	I
001	9.138				
110	6.897				
$\bar{2}01$	6.766	6.79	100	6.78	100
200	6.764				
$\bar{1}11$	6.086	6.06	3	6.05	5
011	6.027				
$\bar{2}11$	5.171	5.18	9	5.18	20
210	5.170				
111	5.064				
$\bar{2}02$	4.674	4.68	5	4.67	9
201	4.671				
002	4.569	4.58	2	4.57	6
$\bar{1}12$	4.191				
$\bar{3}11$	4.126				
$\bar{2}12$	4.038	4.05	3	4.04	7
211	4.036				
020	4.009				
012	3.970				
310	3.930	3.94	5	3.93	8
120	3.844			3.83	3
$\bar{1}21$	3.684				
021	3.671	3.65	2	3.66	3
$\bar{4}01$	3.641				
$\bar{3}12$	3.611				
112	3.515	3.51	1	3.51	2
220	3.449	3.45	5	3.45	22
$\bar{2}21$	3.449				
121	3.417				
$\bar{4}02$	3.383	3.39	31	3.39	12
400	3.382				

(*continued on next page*)

[1] Radiation: Fe, unfiltered; only lines due to $\lambda FeK_\alpha=1.9373$ Å radiation are listed. Shows preferred orientation so that intensities shown are not directly comparable with those of the synthetic compound. Diffractometer chart X-493.

[2] Radiation: Cu/Ni, $\lambda CuK_\alpha=1.5418$ Å. Diffractometer chart X-1456. Synthetic material prepared by R. C. Erd.

[3] All calculated spacings listed for $d_{hkl}\geq2.500$ Å.

TABLE 2. (*continued*)

	Nobleite North of De Bely mine, Death Valley[1]			$CaO \cdot 3B_2O_3 \cdot 4H_2O$ Synthetic[2]	
hkl	*d* (calc.)[3] Å	*d* (meas.) Å	I	*d* (meas.) Å	I
$\bar{4}11$	3.315				
$\bar{2}03$	3.267	3.27	2	3.27	4
202	3.266				
311	3.249				
$\bar{4}12$	3.117				
410	3.116	3.12	7	3.11	12
$\bar{1}22$	3.107				
$\bar{3}21$	3.080	3.08	4	3.08	10
003	3.046				
$\bar{2}22$	3.043	3.05	3	3.05	10
221	3.042				
$\bar{2}13$	3.026				
212	3.025				
022	3.013				
$\bar{1}13$	3.004	3.006	5	2.998	14
320	2.996				
$\bar{3}13$	2.904			2.912	3
$\bar{4}03$	2.848				
401	2.847	2.849	5	2.849	15
$\bar{3}22$	2.847				
013	2.847				
122	2.800	2.805	2	2.801	7
$\bar{5}11$	2.730	2.734	1		
$\bar{4}21$	2.695				
$\bar{4}13$	2.684	2.685	1	2.691	2
411	2.683				
$\bar{5}12$	2.671				
321	2.660				
130	2.622	2.614	1	2.622	2
113	2.610				
312	2.594				
420	2.585				
$\bar{4}22$	2.585				
$\bar{1}31$	2.570				
031	2.565	2.566	9	2.567	13
510	2.563				
$\bar{2}23$	2.533				
222	2.532				
$\bar{1}23$	2.520				
		2.489	1	2.481	3
		2.464	1	2.462	3
		2.410	5	2.413	3

TABLE 2. (*continued*)

	Nobleite North of De Bely mine, Death Valley[1]			$CaO \cdot 3B_2O_3 \cdot 4H_2O$ Synthetic[2]	
hkl	*d* (calc.)[3] Å	*d* (meas.) Å	I	*d* (meas.) Å	I
		2.309	7	2.304	9
		2.256	4	2.246	5
		2.171	4	2.171	3
		2.119	2		
		2.098	5	2.096	23
		2.067	2	2.060	8
		2.022	2	2.019	6
		1.986	3	1.985	12
		1.963	5	1.965	6
		1.905	1	1.903	4
		1.881	1	1.881	2
				1.848	2
		1.831	0.5	1.831	4
		1.805	1	1.807	3
		1.788	0.5	1.787	2
		1.744	2	1.743	4
		1.721	1	1.724	3
		1.692	4	1.692	2
		1.636	0.5	1.637	1
		1.615	0.5	1.613	1
				1.585	1
				1.547	1
		1.521	0.5	1.519	1
	plus additional lines all with $I \leq 2$				

Nobleite is colorless in all orientations in transmitted light. It is biaxial (+) with the following optical properties:

	n	
α	1.500 ± 0.003	$2V = 76°$ (calc.)
β	1.520 ± 0.002	$r > v$, weak
γ	1.554 ± 0.002	$X \wedge a = 29°$, $Y > b$, $Z \wedge c = -7°$

Nikolaev and Chelishcheva (1940, p. 129) report $\alpha = 1.505$ and $\gamma = 1.552$ for the synthetic compound.

CHEMICAL PROPERTIES

Analysis

Large (1 mm. in diameter) and nearly inclusion-free crystals of nobleite were selected for analysis. The sample, weighing 0.500 g., was dissolved with 30 ml. of 1 N HCl. This solution was adjusted to a pH of 2.5 and

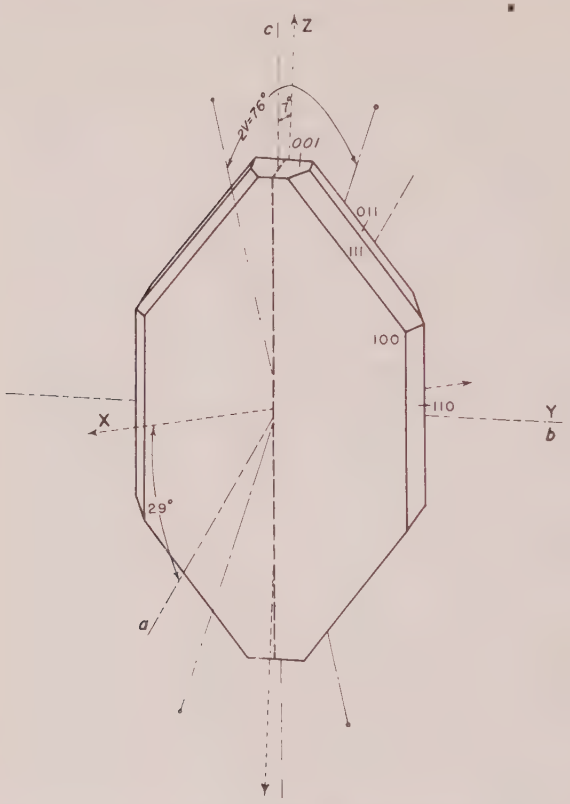

FIG. 2. Typical habit and optical orientation of nobleite. Interfacial angles are approximate.

then passed through an ion exchange column in order to separate B_2O_3 from the cations. Mannite was added to the effluent and B_2O_3 was titrated with NaOH in the usual way. The cations were recovered from the column and determined by the standard methods of quantitative analysis as outlined by Hillebrand and others (1953). Total water was measured by the Penfield method.

The results of the analysis are given in Table 3.

Synthesis

The compound $CaO \cdot 3B_2O_3 \cdot 4H_2O$ was first reported by Ditte (1873, p. 784) who prepared it by dissolving $CaCO_3$ in a boiling concentrated solution of boric acid. Its synthesis was subsequently reported by Meyerhoffer and Van't Hoff (1907), Van't Hoff (1907, p. 653), Sborgi (1913, p. 640-641), Nikolaev and Chelishcheva (1940), and Kurnakova (1953, p. 46). Dr. W. T. Schaller, who has been working for a long period

TABLE 3. CHEMICAL ANALYSIS OF NOBLEITE

	Weight per cent*		Molecular proportions		Ratios	Calculated composition for $CaO \cdot 3B_2O_3 \cdot 4H_2O$
CaO	16.96		.3024	.3035	1.01	16.64
SrO†	0.11		.0011			
B_2O_3	60.80		.8731		2.92	61.98
H_2O	20.82	21.84	1.2123		4.05	21.38
H_2O^-	1.02					
Fe_2O_3	0.15					
Na_2O†	0.26					
K_2O†	0.06					
Li_2O†	0.02					
Insoluble residue	0.08					
	100.28					100.00

* A. C. Vlisidis, analyst.

† Determinations made by Leonard Shapiro using a Beckman Model DU flame spectrophotometer.

of time on the synthesis of calcium borates (as a part of a larger study on borates), has prepared this compound in various ways (personal communication, 1958).

The fine-grained nobleite (to 4 μ in diameter) used in obtaining the x-ray powder data reported in Table 1 was synthesized by Erd as follows: 1.6 g. CaO and 10.0 g. H_3BO_3 were stirred in 25 ml. H_2O for 30 hours at 48° C.; the resulting product was held at 68° C. for 10 days; finally the precipitate was filtered, washed successively with distilled water, methyl alcohol, and acetone and air-dried at room temperature.

Solubility data

Nobleite is slightly soluble in cold water; moderately soluble in hot water. Nikolaev and Chelishcheva (1940, p. 128) in their study of the solubility isotherm of the system $CaO—B_2O_3—H_2O$ at 25° C. found that after 153 days the composition of the liquid phase in equilibrium with nobleite (as the only solid phase) was B_2O_3 1.34, CaO 0.044, (and H_2O 98.616) per cent. Calculation of the CaO as nobleite shows 2.71 g. of nobleite and 21.4 g. of boric acid per liter of H_2O to be in solution under equilibrium conditions. Although not directly comparable, this solubility of nobleite in a solution of boric acid may be contrasted with the solubility of gowerite in water = 6.03 g./liter (Gode, 1949).

The mineral dissolves readily in cold dilute acids and strong alkalies;

is slowly soluble in a 30 per cent solution of hydrogen peroxide, in xylol, and in glycerol; and is very slightly soluble in methyl alcohol. Nobleite reacts with dilute sulfuric acid to produce crystals of gypsum and boric acid.

Pyrognostics

Before the blowpipe, nobleite decrepitates and then fuses to an opaque enamel bead. In the closed tube test, nobleite decrepitates strongly, exfoliates slightly, and finally becomes a frothy glass. The water driven off during the heating has a pH of about 3 indicating a loss of B_2O_3.

Rapidly heated to 465° C. in an electric furnace, crystals of nobleite were found to have exfoliated perpendicular to {100} and to have turned silvery white. Outlines of the original crystals are still sharp at this temperature; however, most of the material has become a glass ($n = 1.558$) with many inclusions rendering it almost opaque. With continued heating the glass softens at about 580° C. and melts completely by 610° C.

Chemical nomenclature and relationships

The name "triborate" was first applied to the compound $CaO \cdot 3B_2O_3 \cdot 4H_2O$ by Meyerhoffer and Van't Hoff (1907, p. 104) and this term has been used by subsequent workers (for example, Kurnakova, 1953) to refer to this compound and, in a general sense, to the class of borates having a ratio of B_2O_3 MO = 3. The equally established term "hexaborate" (derived from the empirical formula $MB_6O_{10} \cdot xH_2O$) has been used (Gode, 1949; Gode and Kesans, 1953) to refer to the same class of borates and to $CaO \cdot 3B_2O_3 \cdot 5H_2O$. However, crystal chemistry provides a logical and systematic basis for classification of hydrated borates (Christ, 1960). The crystal structure of gowerite $CaO \cdot 3B_2O_3 \cdot 5H_2O$, is currently being studied (Christ and Clark, 1960) together with those of other members of the $CaO \cdot 3B_2O_3 \cdot xH_2O$ series (Christ and Clark, written communication, 1959). Further studies by one of us (R. C. Erd), using differential thermal analysis, dehydration data, and *x*-ray powder techniques, are in progress in order to elucidate the relationships of the members of this series to one another and to other hydrated borates. The results obtained to date indicate that there is no simple hydration-dehydration relationship between nobleite and gowerite.

ACKNOWLEDGMENTS

We greatly appreciate the cooperation of the United States Borax and Chemical Corporation and the National Park Service, and the help we have received from several of our colleagues of the United States

Geological Survey. Especially, we are indebted to Joan R. Clark for her *x*-ray study of the single crystals and for a most helpful critical review of this paper; to W. T. Schaller for many helpful discussions and for the loan of synthetic nobleite specimens, to C. L. Christ for much useful advice, and to Daniel E. Appleman who carried out the computation of the *d*-spacings on a digital computer.

REFERENCES

Chelishcheva, A. G. (1940), Heating curves and specific weights of synthetic borates: *Comptes rendus (Doklady) Acad. Sci. U.R.S.S.*, **28,** 508–511.

Christ, C. L. (1960), Crystal chemistry and systematic classification of hydrated borate minerals: *Am. Mineral.*, **45,** 334–340.

Christ, C. L. and Clark, J. R. (1960), *X*-ray crystallography and crystal chemistry of gowerite, $CaO \cdot 3B_2O_3 \cdot 5H_2O$: *Am. Mineralog.*, **45,** 230–234.

Ditte, Alfred (1873), Production par voie sèche de quelques borates cristallisés: *Acad. Sci. Paris Comptes rendus*, **77,** 783–785.

Erd, R. C., McAllister, J. F., and Almond, Hy (1959), Gowerite, a new hydrous calcium borate, from the Death Valley region, California: *Am. Mineral.*, **44,** 911–919

Gode, H. K. (1949), Calcium hexaborate: *Latvijas PSR Zinatnu Akad. Vestis 1949*, No. 10 (Whole No. 27), 101–116. Abstract in *Chem. Abstracts*, **48,** 69 *e*, 1954.

Gode, H. K. and Kesans, A. D. (1953), Sintezy boratov v vodnykh rastvorakh (Syntheses of borates in aqueous solutions), *in* Khimiîa boratov (Chemistry of the borates), 29–43, *Izdatelstvo Akad. Nauk. Latv. S.S.R.*, Riga, 9953.

Hillebrand, W. F., Lundell, G. E. F., Bright, H. A., and Hoffman, J. I. (1953), Applied inorganic analysis, 2d ed., 1034 p. John Wiley and Sons, Inc., New York.

Kurnakova, A. G. (1953), Troĭnye i chetnerye sistemy s bornoĭ kislotoĭ (Ternary and quaternary systems containing boric acid) *in* Khimiîa Boratov (Chemistry of the borates), 45–66, *Izdatelstvo Akad. Nauk. Latv. S.S.R.*, Riga, 1953.

McAllister, J. F. (1958), Borate minerals from weathering of late Tertiary borates in the Furnace Creek district, Death Valley, California (abs.): *Geol. Soc. America Bull.*, **69,** 1695.

Meyerhoffer, Wilhelm and Van't Hoff, J. H. (1907), Krystallisirte Calciumborate: *Liebig's Ann.*, **351,** 100–107.

Nikolaev, A. V. and Chelishcheva, A. G. (1940), The 25° isotherm of the systems: $CaO+B_2O_3+H_2O$ and $MgO+B_2O_3+H_2O$: *Comptes rendus (Doklady) Acad. Sci. U.R.S.S.*, **28,** 127–130.

Noble, L. F. (1941), Structural features of the Virgin Spring Area, Death Valley, California: Geol. Soc. America Bull., **52,** 941–1000.

Sborgi, Umberto (1913), Sistema CaO-B_2O_3-H_2O a 30°: *Atti. Accad. Lincei*, 5th ser., **22,** 636–642.

Van't Hoff, J. H. (1907), Untersuchungen über die Bildung der ozeanischen Salzablagerungen. LI. Borocalcit und die künstliche Darstellung von Ascharit: *Sitzungsber. Konigl. preuss. Akad. Wiss., 1907*, 652–654.

Manuscript received June 30, 1960.

PHASE EQUILIBRIA AT LIQUIDUS TEMPERATURES IN THE SYSTEM IRON OXIDE-TITANIUM OXIDE AT LOW OXYGEN PRESSURES*

J. B. MacChesney† and Arnulf Muan, *The Pennsylvania State University, University Park, Pa.*

Abstract

Phase relations in the system iron oxide-titanium oxide were determined by heating oxide mixtures at oxygen pressures defined by the iron-wüstite equilibrium. The mixtures were either heated in iron crucibles in a nitrogen atmosphere, or enclosed in sealed vitreous-silica tubes together with an iron-wüstite buffer. Compositions of mixtures prepared under these conditions were found to deviate somewhat from those of the join FeO-TiO_2. Mixtures of high iron content contained some Fe^{3+}, whereas mixtures of high titanium oxide content contained some titanium of valence states below +4.

Introduction

The experimental study at high temperatures of phase relations in iron oxide containing systems is difficult, and only after the major breakthrough in 1932 by Bowen and Schairer could systematic progress on such systems be achieved. By equilibrating oxide phases in iron crucibles in a purified nitrogen atmosphere, practically all iron of the oxide sample is present as Fe^{2+}. Later it has become practical also to study phase relations in iron oxide containing systems by other techniques which permit controlled variations of oxygen partial pressures over wide ranges (see for instance a review paper by Muan, 1958).

The work to be described in the following represents one unit of study of the complicated ternary system Fe—Ti—O. The authors have previously reported on their investigation of this system in air (MacChesney and Muan, 1959). The present paper deals with phase relations in an atmosphere of very low oxygen partial pressure, that at which iron and its lowest oxide, wüstite ($Fe_{1-x}O$), coexist in equilibrium. The experimental procedures adopted for realizing this situation are described in a later section.

Previous Work

Several studies of phase relations in systems containing the oxides of iron and titanium have been reported in the literature. Investigations of the bounding binary systems Fe—O and Ti—O in particular have been extensive.

Discussions of equilibria in the system Fe—O are found in papers by Greig, Posnjak, Merwin and Sosman (1934), by Darken and Gurry (1945, 1946), and recently by Phillips and Muan (1960).

* Contribution No. 59-113 from College of Mineral Industries, The Pennsylvania State University, University Park, Pennsylvania.

† Present address: Bell Telephone Laboratories, Murray Hill, New Jersey.

The Ti—O system has attracted considerable interest in recent years. Magneli *et al.* (1958), as well as Andersson *et al.* (1957), have made very comprehensive studies of the phases present in this system. The data obtained by those groups will serve to refine the approximate diagram for Ti—O which was inferred by DeVries and Roy (1954) on the basis of scattered data available in the literature.

Some of the general features of the ternary system $FeO—Fe_2O_3—TiO_2$ are fairly well established. Three solid solution series are known to exist in the system: cubic magnetite-ulvospinel ($FeO \cdot Fe_2O_3—2FeO \cdot TiO_2$),* hexagonal hematite-ilmenite ($Fe_2O_3—FeO \cdot TiO_2$), and orthorhombic pseudobrookites ($Fe_2O_3 \cdot TiO_2—FeO \cdot 2TiO_2$). In the first of these, magnetite-ulvospinel, a continuous solid solution exists at high temperatures, with exsolution taking place below 600° C. (Kawai, Kume and Sasajima, 1954; Vincent and Wright, 1957). Controversies exist in the literature with respect to the continuity of the hematite-ilmenite solid solution series. Ramdohr (1926, 1950, 1953) reported that hematite and ilmenite form a continuous solid solution series above 600° C., whereas Pouillard (1950) found that two solid solution phases exist together in equilibrium at 950° C., the miscibility gap extending approximately from 33 to 67 mole %. Basta (1953) showed that complete miscibility exists between the two end members at 1050° C., and Nicholls (1955) in a recent review refers to the work of Ramdohr (1926) and of Posnjak and Barth (1934) as indicating that complete solid solubility exists between ilmenite and hematite above 1050° C.

The only systematic work on phase equilibria in the system iron oxide-titanium oxide at liquidus temperatures under strongly reducing conditions seems to be that of Grieve and White (1939). They used differential thermal analysis techniques, measuring temperatures with tungsten-molybdenum thermocouples and containing the oxide mixtures in molybdenum crucibles in vacuo or in an inert atmosphere. Phase relations as determined in their study are illustrated in Fig. 1. The diagram shows only two compounds, $2FeO \cdot TiO_2$ (ulvospinel, which they incorrectly named pseudobrookite) and $FeO \cdot TiO_2$ (ilmenite), in addition to "FeO" (wüstite) and TiO_2 (rutile). It is difficult to understand their results in light of those obtained in the present investigation.

Experimental Method

General Procedure

Phase relations were determined by the quenching technique. Preheated mixtures of iron oxide and titanium oxide were held in iron crucibles in carefully controlled atmospheres and at accurately meas-

* This phase as well as others appearing in the system may have oxygen contents deviating somewhat from the stoichiometric values listed here for sake of simplicity.

ured temperatures until equilibrium was established. The samples were then quenched rapidly to room temperature and the phases present identified by microscopic and x-ray examination. Compositions of mixtures at equilibration temperatures were determined by chemical analysis of quenched samples.

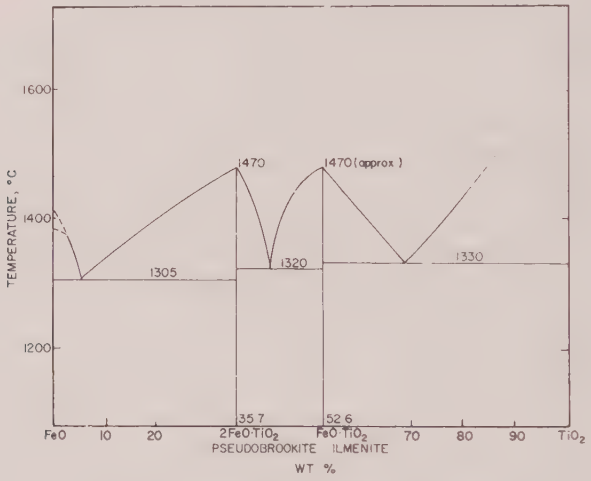

FIG. 1. Diagram illustrating phase relations at liquidus temperatures in the system $FeO—TiO_2$, after Grieve and White (1939).

Starting Materials

"Baker Analyzed" reagents, Fe_2O_3 and TiO_2, were used as starting materials in most of the experiments. The oxides were dried at approximately 400° C. for 12 hours, mixed in desired proportions, ground under alcohol and heated to melting or sintering in a gas-air combustion furnace. Prior to their use in the equilibration runs these mixtures (prepared during our previous investigation of the system iron oxide-titanium oxide in air) were brought close to equilibrium with the oxygen partial pressure prevailing when iron and wüstite coexist in equilibrium. This was accomplished by containing the samples in iron crucibles in a nitrogen atmosphere at approximately 1300° C.

As the work advanced, the above mixtures were supplemented with a new set of mixtures prepared from TiO_2 and iron oxide which was obtained by high-temperature ($\sim$1300° C.) oxidation of pure metallic iron in nitrogen gas containing a small amount of oxygen as an impurity.

Control of Atmosphere

A few introductory runs were carried out in iron crucibles in nitrogen atmosphere, following the procedure developed by Bowen and Schairer

(1932). However, FeO contamination of the sample by oxidation of the iron crucible, as well as loss of liquids by creep on crucible walls caused difficulties in the present investigation. More reliable results were obtained in experiments carried out by a technique illustrated in Fig. 2. An iron-wüstite buffer* is sealed together with the oxide sample into a vitreous silica tube to maintain a fixed oxygen partial pressure at any chosen temperature. Oxidation of the crucible and accompanying contamination of the sample could be minimized by placing the tube in the furnace in such a manner that the crucible and its contents were at the hot zone while the buffer was at a slightly (~20° C.) lower temperature.

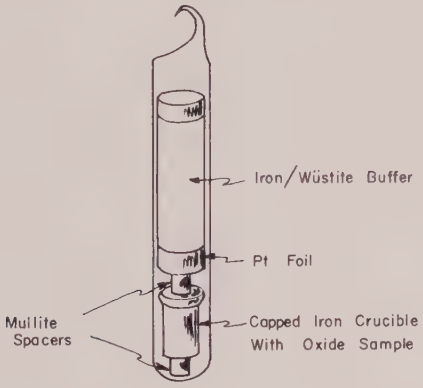

FIG. 2. Sealed vitreous silica tube assembly used for studying the system iron oxide-titanium oxide in the present investigation. The iron crucible and iron-wüstite buffer were held away from the silica wall by means of mullite spacers and platinum foil which was wrapped around the ends of the buffer. This precaution prevented attack on the tube by iron oxide liquid formed at temperatures in excess of 1369° C.

Furnaces, and Temperature Measurement

Equilibration runs were carried out in vertical tube furnaces with resistance windings of platinum or an 80% platinum 20% rhodium alloy. Temperatures were kept constant to approximately ±3° C. by means of a commercial Tagliabue Celectray Controller connected to a platinum-90% platinum 10% rhodium thermocouple inserted close to the hot spot of the furnace.

Temperatures were measured before and after each run with a platinum-90% platinum 10% rhodium thermocouple calibrated against

* This buffer consisted of an iron slug coated with a layer of wüstite formed by oxidation of the iron in air at approximately 1200 ° C. When sealed in a vitreous silica tube, the buffer maintained within the tube an oxygen partial pressure corresponding to the equilibrium coexistence of metallic iron and wüstite at any specific temperature.

standards with melting points defined as follows: Gold (Au), 1063° C.; diopside ($CaMgSi_2O_6$), 1391.5° C.; pseudowollastonite ($CaSiO_3$), 1544° C. Temperatures thus defined are according to the Geophysical Laboratory Scale, which is almost identical to the 1948 International Scale up to 1550° C. Temperatures above 1550° C. reported in the present paper are on the 1948 International Scale.

Examination of Quenched Samples

Phases present in quenched samples were determined by *x*-ray and microscopic examination. Examination of polished samples in reflected light was found more informative than observations under the petrographic microscope because of the opacity of the samples. The recognition of dendrites as opposed to primary crystals was at times very difficult. In some cases, dendritic growth was so rapid that the quench specimen was honeycombed with large euhedral crystals. Therefore, the use of crystal size and shape as criteria for identification of primary crystals was not entirely satisfactory. The accumulation of primary crystals at the bottom of the specimen, however, was quite useful in this regard. It was often possible to observe a distinct boundary between the liquid and the accumulated primary crystals. A second reliable guide was the presence of characteristic dendritic patterns or textures. For instance, liquids with pseudobrookite as primary crystalline phase were found to produce a characteristic quench pattern which resembled a coarsely woven cloth.

Total iron oxide content as well as Fe^{3+} Fe^{2+} ratios of mixtures before and after equilibration were determined by wet chemical analysis. The following analytical methods were used:

For determination of total iron oxide, samples containing less than 60 wt. % TiO_2 were dissolved by boiling them in a mixture of 20 ml. 1:3 H_2SO_4 and five ml. HF. The resulting solution was then diluted to 100 ml. with five % (by volume) H_2SO_4 and passed through a Jones Reductor. The emerging solution contained all iron as Fe^{2+} and all titanium as Ti^{3+}. Following the procedure of Grimaldi, Stevens and Carron (1943), three ml. of a 0.0001 molar cupric sulfate solution was added as catalyst and the solution aerated for 10 to 15 minutes to quantitatively oxidize titanium to the tetravalent state while leaving the iron in the divalent state.* The solution was then titrated with a 0.01 N potassium permanganate solution.

Samples containing more than 60 wt. % TiO_2 required fusion with potassium pyrosulfate ($K_2S_2O_7$) to put them into a soluble form. A weighed amount of the reagent (two to five grams) was added to the 50 mg. sample and heated to a temperature at which melting occurred without rapid dissociation to the pyrosulfate. The fusion generally required between 30 and 45 minutes to completely dissolve the sample. After cooling, the

* Grimaldi *et al.* (1943) reported that no oxidation of divalent iron occurred during 20-minute aeration by this method. A check run made in the present study on a sample of known composition confirmed this.

salt cake was dissolved by boiling in five % (by volume) H_2SO_4. The solution was then reduced, aerated and titrated as described above. It was found that the reagents used in this technique made a small but significant contribution to the total number of milliequivalents needed for titration of the ferrous iron concentration. This quantity was determined and the analysis corrected accordingly.

Samples for determination of divalent iron were placed in a covered platinum crucible and brought to boiling in 20 ml. of 1:3 H_2SO_4. When steam was evolved, five ml. of HF was added and the solution allowed to boil for five to 10 minutes. The crucible was then plunged into a 600 ml. beaker containing five % H_2SO_4 saturated with boric acid. Copper sulfate was added, the solution aerated for 10 to 15 minutes and titrated with 0.05 N potassium permanganate. This method of course was applicable only to samples which were soluble by acid treatment (<60 wt. % TiO_2).

Another analysis was carried out in order to determine the sum of Fe^{2+} and Ti^{3+}. Samples for this purpose were mixed with 10 ml. of a ferric sulfate solution (two mg. $Fe_2(SO_4)_3$ per ml.) prior to acid treatment, and the solution was titrated with 0.05 N permanganate without addition of copper sulfate and aeration of the solution beforehand. According to Hillebrand *et al.* (1953), this procedure prevents Ti^{3+} from decomposing water in the presence of platinum. From the quantity of permanganate required to titrate this solution, the total milliequivalents of reduced oxides could be calculated. Subtraction of the number of milliequivalents of potassium permanganage required to titrate the ferrous iron from the value for the total reduced oxides left a remainder which could be calculated as trivalent titanium. The assumption is made that all iron in these crystalline samples is in the divalent state when trivalent titanium is detected. This assumption seems justified in view of the far greater stability of Ti^{4+} than of Fe^{3+} in oxide structures, as discussed in a previous paper (MacChesney and Muan, 1959).

Results and Discussion

Results of equilibration runs are illustrated graphically in Fig. 3. A similar procedure has been used in the construction of this diagram as has been described in previous papers from our laboratories (see for instance Muan, 1958). Points representing compositions of condensed phases in the ternary system (Fe—Ti—O) have been projected onto the join FeO-TiO_2 to give a diagram with the appearance of a binary system.

The essential features of the diagram at oxygen pressures dealt with in the present study are as follows: Liquidus temperatures first decrease as TiO_2 is added to iron oxide, from 1369° C. for wüstite to approximately 1312° C. at the "eutectic" temperature where wüstite,* ulvospinel, liquid with approximately 10 wt.% TiO_2 and gas coexist in equilibrium. Further addition of TiO_2 results in a rise in liquidus temperature, with ulvospinel as primary phase. A maximum is reached at 1395° C. and approximately 33 wt.% TiO_2. Temperatures then decrease toward a second "eutectic" located at approximately 47 wt.% TiO_2 and 1363° C., where the phases present are ulvospinel, ilmenite, liquid and gas. Ilmenite is the next phase to appear in order of increasing TiO_2 con-

* This phase, as well as others appearing in the present system, are solid solutions in which the iron to titanium ratios vary.

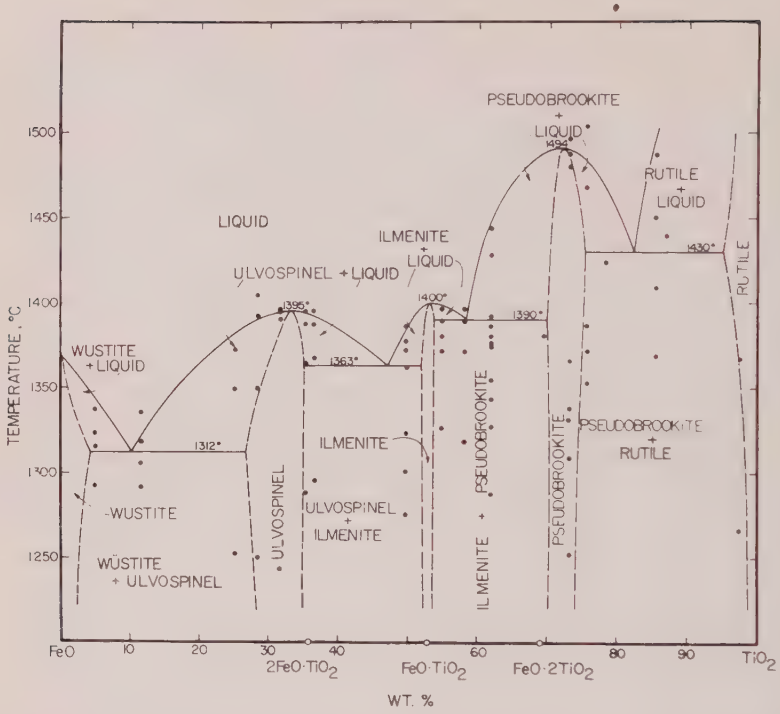

FIG. 3. Phase diagram for the system iron oxide-titanium oxide at oxygen pressures defined by the iron-wüstite equilibrium. For sake of simplicity the phase relations are shown in a projection onto the join FeO-TiO_2. Solid dots represent equilibration runs, and heavy lines are boundary curves separating the various phase areas, as labeled on the diagram. Dash curves represent boundary curves whose location is uncertain.

tent, and a maximum exists on the liquidus curve at approximately 1400° C. and 53 wt.% TiO_2. After a slight drop in liquidus temperatures to 1390° C., the third "eutectic" point at approximately 58 wt.% TiO_2 marks the coexistence of the phases ilmenite, pseudobrookite, liquid and gas. Further increase in TiO_2 content causes liquidus temperatures to increase to approximately 1494° C., the maximum melting temperature of the pseudobrookite phase. This point, located at approximately 69 wt.% TiO_2, is followed by a decline in liquidus temperature to the fourth "eutectic" at 1430° C. and approximately 80 wt.% TiO_2. Finally, liquidus temperatures increase toward the melting point of what is believed to be an oxygen-deficient rutile phase (probably ~1800° C.).

The partial pressure of oxygen in the gas phase, as calculated from the iron-wüstite equilibrium (Darken and Gurry, 1945), varies from approximately $10^{-10.7}$ atm. at 1312° C. to approximately $10^{-9.1}$ atm. at 1494° C.

The diagram in Fig. 4 is presented in order to show compositions of mixtures heated at temperatures ranging from 1250 to 1350° C. The composition area bounded by the points FeO, Fe_2O_3, and TiO_2 is shown as an equilateral triangle, and arrows indicate directions to the apices of the triangle Fe-Ti-O, of which the area in Fig. 4 is a part. Light dash-dot lines represent the solid solution joins magnetite-ulvospinel, hematite-ilmenite and pseudobrookites. The dash curve connects points (solid dots) representing analytically determined compositions of various mixtures. Projection of spinel composition points onto the joint FeO-TiO_2 results in points located on the FeO side of the stoichiometric composition (see Fig. 3), whereas the opposite situation prevails for the pseudobrookite phase.

In addition to the phases mentioned in the previous text and illustrated in the diagram of Fig. 3, globules of metallic iron were observed in all quenched samples obtained in this investigation. Evidence presented in the following suggests that iron is not an equilibrium phase under the experimental conditions used, but that its presence is caused instead by complicated kinetic characteristics of the reactions. Inasmuch as the sample is kept at a temperature slightly higher than that of the iron-wüstite buffer, the oxygen partial pressure of the gas phase is slightly lower than that corresponding to the wüstite-iron equilibrium at the temperature of the sample. Hence wüstite, if present as a pure phase in the sample, would tend to be reduced to metallic iron, causing a transport of oxygen from the sample to the buffer. However, when iron oxide is combined with TiO_2 to form the phases ulvospinel, ilmenite or pseudobrookite, the FeO activity of the sample is reduced enough to prevent deposi-

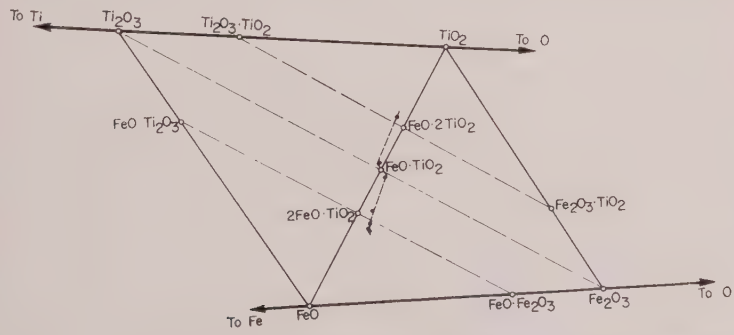

FIG. 4. Diagram of a part of the system Fe–Ti—O to show approximate compositions of oxide mixtures equilibrated at the oxygen partial pressures of the iron-wüstite equilibrium in the temperature interval 1250–1350° C. Solid dots represent compositions determined by chemical analysis, and the dash curve has been drawn to pass approximately through these points. Light dash-dot lines represent solid solution joins (magnetite-ulvospinel, hematite-ilmenite, and pseudobrookites).

tion of metallic iron under equilibrium conditions in spite of the temperature difference between sample and buffer. (See data on free energies of formation of these phases from the oxide components, as listed for instance by Michaud and Pidgeon (1954).)

The following mechanism is suggested for explaining the occurrence of globules of metallic iron in all quenched samples in the present investigation: The starting materials for the equilibration runs, prepared by pre-heating at lower temperatures, have higher Fe_2O_3 FeO ratios than those corresponding to the final equilibrium state. The samples, when put into the quench furnace at the equilibration temperature, try to establish the "correct" oxidation state by reducing the amount of Fe_2O_3 and increasing the amount of FeO present. There are two possible ways in which this can be accomplished. One is for the sample to give off oxygen to the gas phase according to the equation

$$2Fe_2O_3 = 4FeO + O_2$$

The other is a reaction of Fe_2O_3 of the oxide sample with metallic iron of the crucible according to the equation

$$Fe_2O_3 + Fe = 3FeO$$

The FeO formed by the latter process may be reduced partially to metallic iron by the prevailing atmosphere before FeO reacts with TiO_2 to form phases in which the divalent iron is stabilized. This inferred mechanism is supported by the following observations made on the quenched samples: Ridges and other relief features on the inside surface of the crucibles appeared to have been leveled by contact with the sample. Microscopic examination of the crucible surface showed embayment of areas where contact with the sample was maintained. Globules of metallic iron were localized near contact with the crucible. The latter observation is particularly significant, for if the initial sample was homogeneous and the oxygen pressure was constant throughout the volume of the sealed-silica tube, then the distribution of metallic iron should have been uniform within the volume of the sample upon reduction in situ. On the other hand, iron emplaced as a result of reaction with the crucible material would be concentrated near the contact with the container.

The data obtained in the present investigation show that the pseudobrookite structure is stable under the reducing conditions prevailing when FeO is in equilibrium with metallic iron. This observation confirms the findings of Akimoto and Nagata (1957) who reported that a complete solid solution series exists between $Fe_2O_3 \cdot TiO_2$ and $FeO \cdot 2TiO_2$ at 1200° C. In contrast to this, Grieve and White (1939) presented a phase diagram for the system "FeO TiO_2" which does not incorporate

pseudobrookite as a phase, and in addition shows other disagreements with results obtained in the present study. It is believed that their use of molybdenum crucibles in poorly defined atmospheres may be the reason for the deviating results.

Summary

Phase relations in the system iron oxide-titanium oxide have been determined at oxygen partial pressures defined by the equilibrium between wüstite and metallic iron. Equilibration runs were made by keeping oxide mixtures in iron crucibles in nitrogen atmosphere or by sealing the mixtures together with an iron-wüstite buffer into tubes of vitreous silica. Compositions of mixtures prepared under these conditions were found to deviate somewhat from those of the join FeO-TiO_2. Mixtures containing large percentages of iron oxide showed excess Fe^{3+} whereas Ti^{3+} was inferred (from chemical analysis) to be present in samples of high titanium oxide content.

Four "eutectic" points have been determined in the system "FeO-TiO_2." The phase assemblage, approximate liquid composition and temperature of each are as follows: At approximately 1312° C. wüstite, ulvospinel, liquid (approximately 90 wt.% FeO,* 10 wt.% TiO_2) and gas are in equilibrium. The phases ulvospinel, ilmenite, liquid of composition 53 wt.% FeO, 47 wt.% TiO_2 and gas coexist in equilibrium at 1363° C. The third point at 1390° C. marks the existence of ilmenite, pseudobrookite, liquid of composition 42 wt.% FeO, 58 wt.% TiO_2 and gas in equilibrium. At 1430° C. pseudobrookite, rutile, liquid of approximate composition 20 wt.% FeO, 80 wt.% TiO_2 are in equilibrium with a gas phase.

In addition to the phases mentioned above, globules of metallic iron were observed in quenched samples. Phase rule consideration shows that metallic iron cannot be an equilibrium phase. It is proposed that the metal is incorporated into the sample from the crucible. This reaction, being more rapid than the exchange of oxygen between sample and buffer, results in the precipitation of an amount of metallic iron equivalent to that incorporated from the crucible.

Acknowledgments

This work was carried out as part of a research project on oxide systems sponsored by the American Iron and Steel Institute. The authors are indebted to E. F. Obsorn for his critical reading of the manuscript.

* Total iron oxide content calculated as FeO.

References

Akimoto, S. and Nagata, T. (1957), The $TiFe_2O_5$ Ti_2FeO_5 Solid Solution Series: *Nature*, **179,** 37–38.

Andersson, S., Collen, B., Kuylenstierna, U. and Magneli, A. (1957), Phase Analysis Studies on the Titanium-Oxygen System: *Acta Chem. Scand.*, **11,** 1641–1652.

Basta, E. Z. (1953), Ph.D. Thesis, Bristol.

Bowen, N. L. and Schairer, J. F. (1932), The System FeO-SiO_2: *Am. J. Sci.*, **224,** 177–213.

Darken, L. S. and Gurry, R. W. (1945), The System Iron-Oxygen: I, The Wüstite Field and Related Equilibria: *J. Am. Chem. Soc.*, **67,** 1398–1412.

Darken, L. S. and Gurry, R. W. (1946), The System Iron-Oxygen: II, Equilibrium and Thermodynamics of Liquid Oxide and Other Phases: *J. Am. Chem. Soc.*, **68,** 798–816.

DeVries, R. C. and Roy, R. (1954), A Phase Diagram for the System Ti-TiO_2 Constructed from Data in the Literature: *Bull. Am. Ceram. Soc.*, **33,** 370–372.

Greig, J. W., Posnjak, E., Merwin, H. E. and Sosman, R. B. (1935), Equilibrium Relationships of Fe_3O_4, Fe_2O_3 and Oxygen: *Am. J. Sci.*, **30** (5th Series), 239–316.

Grieve, J. and White, J. (1939), The System FeO-TiO_2: *Journ. Roy. Techn. Coll.*, **4,** 441–448.

Grimaldi, F. S., Stevens, R. E. and Carron, M. K. (1943), Determination of Iron in the Presence of Chromium and Titanium with the Jones Reductor: *Ind. and Eng. Chem.*, **15,** 387–388.

Hillebrand, W. F., Lundell, G. E. F., Bright, H. A. and Hoffman, J. I. (1953), Applied Chemical Analysis: John Wiley and Sons, New York.

Kawai, N., Kume, S. and Sasjima, S. (1954), Magnetism of Rocks and Solid Phase Transformation in Ferromagnetic Minerals: *Proc. Japan. Acad.*, **30,** 588–593.

Magneli, A., Andersson, S., Westman, S., Asbrink, S. and Homberg, B. (1958), Studies on the Crystal Chemistry of Titanium, Vanadium and Zirconium Oxides at Elevated Temperatures: Final Tech. Rept. No. **1,** Dept. of Army Contracts No. Da-91-508-NUC-254.

Michaud, G. G. and Pidgeon, L. M. (1954), The Selective Reduction of Iron in Ilmenite and the Oxygen Pressure of TiO_2-y Rutile: *Can. Mining and Metal. Bull.*, **47,** 307–309.

Muan, A. (1958), Phase Equilibria at High Temperatures in Oxide Systems Involving Changes in Oxidation States: *Am. J. Sci.*, **256,** 171–207.

Nicholls, G. P. (1955), The Mineralogy of Rock Magnetism: *Advanc. Physics*, **4,** 113–190.

Phillips, B. and Muan, A. (1960), Stability Relations of Iron Oxides: Phase Equilibria in the System Fe_3O_4-Fe_2O_3 at Oxygen Pressures up to 45 Atmospheres: *J. Phys. Chem.*, **64,** 1451–1453.

Posnjak, E. and Barth, T. F. W. (1934), Notes on Some Structures of the Ilmenite Type: *Zeit. Krist.*, **88,** 271–280.

Pouillard, E. (1950), Sur le Comportement de l'Alumine et l'Oxyde de Titane vis-à-vis des Oxydes de Fer: *Ann. de Chim.*, **5,** 164–214.

Ramdohr, P. (1926), Beobachtungen an Magnetit, Ilmenit, Eisenglanz und Ueberlengugen über das System FeO, Fe_2O_3, TiO_2: *Neues Jahrb. Min., Abt. A, Beil.-Bd.*, **54,** 320–379.

Ramdohr, P. (1960), Die Erzmineralien und ihre Verwachsungen: Akadamie Verlag, Berlin.

Ramdohr, P. (1953), Ulvospinel and its Signficance in Titaniferous Iron Ores: *Econ. Geol.*, **48,** 677–687.

Sidgwick, N. V. (1950), The Chemical Elements and Their Compounds: Oxford University Press, London.

Vincent, E. A. and Wright, J. B. (1957), Heating Experiments on Some Natural Titaniferous Magnetites: *Min. Mag.*, **31,** 624–688.

Manuscript received June 14, 1960.

THE AMERICAN MINERALOGIST, VOL. 46, MAY–JUNE, 1961

DIFFRACTOMETER PATTERNS OF A.P.I. REFERENCE CLAY MINERALS

MARTIN W. MOLLOY AND PAUL F. KERR, *Columbia University, New York, N. Y.*

ABSTRACT

The widely used studies published by the American Petroleum Institute on reference clay minerals are supplemented by revised *x*-ray diffraction information based on the original specimens. Chemically analyzed samples of kaolinite, dickite, halloysite, nontronite, montmorillonite, illite, attapulgite and pyrophyllite are re-examined by recent *x*-ray diffractometer techniques. Spacing and intensity measurements and the corresponding diffractometer patterns are furnished for specimens oriented to enhance the basal reflections, subjected to glycolation and given 550° C. heat treatment. Constant instrument settings permit diffraction intensity comparison between different specimens, treatments, and species. The interpretation of the *x*-ray diffraction patterns in terms of the structural and thermal stability of the minerals is discussed.

INTRODUCTION

In 1950, cooperative studies of reference clay minerals, localities, and occurrence were published as reports on Research Project 49 of the American Petroleum Institute. Among the data presented were chemical analyses, electron micrographs, infra-red spectra, pH data, *x*-ray powder film measurements, semi-quantitative spectrographic analyses, base-exchange data, magnetic susceptibility, particle size determinations, optical measurements, and staining tests.

Since the publication of the A.P.I. studies there has been considerable development in the field of electronic devices for measuring the intensity and position of *x*-ray reflections. The convenience and accuracy of *x*-ray diffractometers in distinguishing and analyzing the clay minerals have led to the widespread use of diffractometer equipment in clay mineralogy. Visual recognition of the diffractometer pattern, together with profile characteristics such as peak amplitude, sharpness, and asymmetry are important improvements made possible by strip-chart recording. The facility with which structural changes such as lattice expansion and collapse may be observed, and even recorded continuously, has led to the replacement of film methods for many theoretical, and most routine, applications.

The data reported in A.P.I. Project 49 have frequently been quoted, and since the specimens were widely distributed numerous supplementary measurements have been published. In view of the scientific application the reference clay minerals have received, revised data on the original specimens should be of value. It is the purpose of this paper to give an improved sequence of *x*-ray diffractometer patterns and measurements on selected A.P.I. clay minerals uniformly applicable to the set as a

whole. In view of the widespread use of the technique of orienting clay mineral specimens to enhance basal *x*-ray reflections, it is of additional interest to furnish patterns and data of the reference clay standards oriented in this manner. Similarly, the employment of organic compounds to expand, and thereby distinguish the montmorillonite-type lattices, and the use of heat treatment to collapse the lattice of the kaolin group, are now common techniques for the analysis of clay minerals. Diffractometer patterns for the A.P.I. standards subjected to these treatments are also given, together with diffraction intensity and spacing measurements when these differ significantly from the untreated specimen.

The reference clay minerals studied include kaolinite, dickite, nonhydrated halloysite, nontronite, montmorillonite, illite, attapulgite and pyrophyllite. The particular minerals and specimens chosen were restricted to the chemically analyzed material. In most cases it was possible to study more than one specimen of a particular mineral, thus verifying the diffraction reflections which were obtained. In addition, the specimens of kaolinite yielded in their diffractometer patterns a representative range in crystallinity.

Clay minerals are rarely monomineralic or entirely free from impurities. While the American Petroleum Institute clay mineral set includes some of the most satisfactory reference clays which have been collected, it must be remembered that impurities were frequently noted in the original descriptions. It is possible by *x*-ray diffractometer techniques to identify impurities indicated by thermal, optical, or other techniques. Glycolation provides a method for recognition of small amounts of expanding-lattice, montmorillonoid minerals, and the interpretation of mixed-layer structures which were only theoretical possibilities at the time of the original A.P.I. study. Additional thermal, *x*-ray, and electron micrographic observations have increased knowledge of clay structures and the behavior of clay lattices during expansion and heat treatment. Similarly, the developments in mica polymorph studies during the past ten years have considerably clarified the illite problem.

In preparing the discussions and interpretations of the *x*-ray diffractometer patterns, the authors have drawn extensively from Brindley (1951), "The Identification and Structure of the Clay Minerals"; Grim (1953), "Clay Mineralogy"; and Mackenzie (1957), "The Differential Thermal Investigation of Clays." Many of the conclusions from the original American Petroleum Institute Research Project 49 report (Kerr *et al.*, 1951) have also been incorporated in the present paper.

This study has been carried on with the assistance of a graduate fellowship in geology awarded by the Union Carbide Ore Co., a division of the Union Carbide Corporation.

Instrumentation

A portion of the original A.P.I. specimen remaining after chemical analysis has been crushed, dispersed in distilled water, and sedimented onto glass slides. The entire specimen has been used, not merely the suspended fraction, so that the diffraction pattern represents the material used for chemical analysis.

An improved Norelco *x*-ray Diffractometer was used for the patterns after precise alignment and checking. The electronic circuit was equipped for pulse height analysis to reduce the background of hard radiation scatter. The patterns were completed within a short period to minimize the effect of equipment drift, and the instrument settings were maintained without change throughout this time.

The patterns were run with Ni filtered Cu radiation ($\lambda = 1.5418$ Å) at 40 kv, 17 ma potential, scanning speed of 1° 2θ per minute, with 1° and .003″ slits and a 17 cm. goniometer radius. Instrument settings of: scale factor 4, multiplier .6, time constant 4 sec., proportional counter voltage 1470 vdc, amplifier gain 50, base line 23 v, and channel width 11 v, were employed for all the patterns. The pulse height analyzer settings were chosen to discriminate in favor of Cu Kα radiation, sacrificing about 10 per cent of the initial intensity in the process, but supressing the background by a larger factor.

The scans were limited to the 4–60° 2θ range which corresponds to spacings from 22 to 1.55 angstroms. Three sedimented slides were prepared for each specimen by warm air drying. One was used as the untreated sample. A second was sprayed with a fine mist of diethylene glycol monobutyl ether until saturation, and then used as the glycolated specimen. The last slide was placed in an electric furnace at 550° C., $\pm 10°$ C., for two hours, and then slowly cooled.

The instrument settings were intentionally maintained constant throughout the examination of all specimens so that intensity measurements might be compared directly. The background reading was not subtracted from the measurements in order to eliminate this arbitrary factor. Two types of intensity measurements are presented, the relative (I_{REL}), and the absolute (I_{ABS}). The relative measurements given in per cent of the strongest reflection permit comparison with other published patterns, while the absolute intensities in units above the base allow comparison between different specimens, treatments, and species in this work. Thus the influence of admixed kaolinite upon the intensities in the diffractometer pattern of halloysite may be estimated, as well as the range in the degree of crystallinity among the kaolinites themselves.

The diffractometer patterns have been measured by direct overlay on a precise template reading in dÅ. The template aids the search for, and

determination of, minor or missing peaks, as well as the distinction of several overlapping patterns produced by the same specimen.

The chemical analyses of the A.P.I. specimens are given in Table I. Other data may be obtained by reference to the original descriptions (Kerr, *et al.*, 1951).

Kaolinite

X-ray diffractometer patterns of kaolinite (Fig. 1) are characterized by intense (001) and (002) reflections accompanied by a series of lesser peaks. Glycolation yields no noteworthy shift in the spacing or intensity of the peaks observed in the untreated pattern. Heating the specimens to 550° C. results in complete destruction of this pattern.

The number, intensity, and sharpness of the diffraction peaks recorded for a particular kaolinite sample depend primarily on the degree of crystallinity of the specimen. Brindley and Robinson (1946), and Murray and Lyons (1956) have presented studies showing the range in

TABLE I CHEMICAL ANALYSES FOR AMERICAN PETROLEUM INSTITUTE REFERENCE CLAY MINERALS[1]

A. P. I. Number	Weight Per Cent															Per Cent Clay Mineral	Per Cent Impurity	TOTAL
	SiO_2	Al_2O_3	Fe_2O_3	FeO	MgO	CaO	Na_2O	K_2O	H_2O^+	H_2O^-	TiO_2	MnO	C	Other				
Kaolinite $Al_4Si_4O_{10}(OH)_8$																		
1a	45.48	38.84	0.19	--	0.17	0.24	0.24	0.42	13.66	0.71	0.86	--				97.19	2.81	100.81
8	45.11	37.02	1.24	0.17	0.11	0.22	0.36	0.71	13.44	0.80	1.30	--				93.26	6.74	100.48
9a	46.07	38.07	0.33	--	0.01	0.38	0.27	0.43	13.47	0.43	0.50	--	--	SO_3 Trace		96.39	3.61	99.96
10[2]																		
17	45.72	39.82	0.01	--	Trace	Trace	0.16	0.36	13.67	0.55	0.42	Trace	--			97.44	2.56	100.80
Dickite $Al_4Si_4O_{10}(OH)_8$																		
15a	43.95	39.72	--	0.01	Trace	0.86	0.12	0.52	14.59	0.10	0.07					94.43	5.57	99.89
15c	44.48	40.05	--	0.01	Trace	0.51	0.16	0.15	14.42	0.06	0.02					96.20	3.80	100.22
Halloysite $Al_4Si_4O_{10}(OH)_8$																		
12a	42.72	38.59	0.17	0.13	Trace	Trace	0.18	0.44	14.14	4.38	Trace	0.01	--			91.06	8.94	100.76
13	43.98	38.46	--	0.03	Trace	0.32	0.14	0.48	14.59	2.58	0.01					93.4	7.1	100.59
Nontronite $Fe^{+3}_{2.00}(Al_{.33}Si_{3.67})O_{10}(OH)_2Na_{.33}$																		
33b	40.54	5.19	31.24	0.39	0.06	1.92	0.14	0.24	6.00	14.75	--	--	-	Li_2O				100.47
Montmorillonite $(Al_{1.67}Mg_{.33})Si_4O_{10}(OH)_2Na_{.33}$																		
19	50.95	16.54	1.36	0.26	4.65	2.26	0.17	0.47	8.28	15.01[3]	0.32	0.01	0.01					100.28
22	51.52	17.15	5.65	0.32	2.80	1.72	0.15	0.85	8.55	11.22	0.48	--						100.41
23	49.91	17.20	2.17	0.26	3.45	2.31	0.14	0.28	7.70	15.77	0.24	0.04	Trace	Li_2O				99.47
27	58.53	19.61	3.10	0.13	2.65	0.25	1.68	0.31	6.21	7.89	0.12							100.48
28	51.69	18.65	4.00	0.23	1.64	0.24	0.08	0.17	7.89	14.82	0.16	--	--	CO_2				99.62
Illite $(Al_{1.45}Fe_{.44}Mg_{.15})(Al_{1.27}Si_{3.73})O_{10}(OH)_2(K,Ca)$																		
35	56.91	18.50	4.99	0.26	2.07	1.59	0.43	5.10	5.98	2.86	0.81							99.50
36	57.41	17.96	4.99	0.26	2.25	0.64	0.15	5.75	6.70	2.97	0.82							99.90
		#																
Attapulgite $Mg_5Si_8O_{20}(OH)_2 \cdot 8H_2O$																		
14	51.90	8.56	3.10	0.19	10.07	2.01	0.03	0.39	11.51	9.79	0.24	--						99.85
Pyrophyllite $Al_{2.00}Si_4O_{10}(OH)_2$																		
47	77.43	16.51	0.47	--	0.05	0.41	0.22	1.26	22.87	0.11	0.18	--						99.51

[1] Kerr *et al.*, Research Project 49, American Petroleum Institute, No. 7, pp. 43-45, 48-50, 52-55, 57-58 (1951).
[2] Ledoux & Company, Teaneck, New Jersey Analysis #615328., A.P.I. No. 10 omitted in A.P.I. Research Project 49

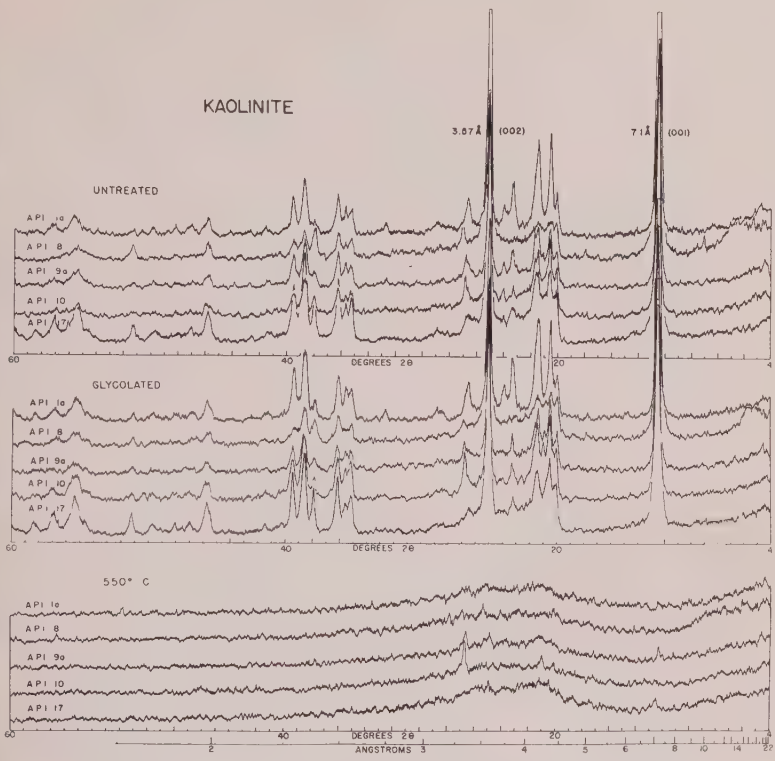

FIG. 1. X-ray diffractometer patterns of oriented A.P.I. Kaolinite.

crystallinity observed in kaolinites, and the gradual merging, broadening, and loss of diffraction lines with decrease in crystallinity. Similar effects may be noted by a comparison of measurements in Table II. In all cases, however, the (001) and (002) reflections at 7.1 and 3.58 Å, respectively, were recorded, together with groups of lines in the 4.5–3.6, 2.56–2.34, and 1.67–1.48 Å ranges.

The diffractometer pattern of the untreated sample is usually sufficient to distinguish kaolinite from other non-kaolin minerals. If the 14 Å (001) reflection of chlorite is not observed, the (003) reflection at 4.7 Å is usually present. Heating the sample to 550° C. will destroy the kaolinite pattern, leaving a chlorite pattern visible, together with other impurities which are thermally stable at that temperature. Montmorillonite is visible in the pattern of A.P.I. 8 (Fig. 1) with a small reflection at 14 Å which shifts to a larger spacing upon glycolation. Approximately 2 per cent quartz is responsible for the small, sharp peak recorded at 3.34Å in the heat treated pattern of A.P.I. 10.

TABLE II. X-RAY DIFFRACTOMETER SPACING AND INTENSITY MEASUREMENTS FOR ORIENTED A. P. I. KAOLINITE

KAOLINITE																							
Untreated																							
ASTM 5-0413[1]			A. P. I. 1a[2]			A. P. I. 8[3]			A. P. I. 9a[4]			A. P. I. 10[5]			A. P. I. 17[6]								
(hkl)	dA	I_{REL}	dA	I_{ABS}	I_{REL}	dA	I_{ABS}	I_{REL}	dA	I_{ABS}	I_{REL}	dA	I_{ABS}	I_{REL}	dA	I_{ABS}	I_{REL}						
						(13.5-14.7)	25	20															
						(10.1)	18	14															
(001)	7.15	100	7.12	78	100	7.16	~132	100	7.13	~102	100	7.14	~108	100	7.13	~135	100						
						(5.01)	11	8															
	4.45	50	4.44	23	29	4.44	21	16	4.45	20	20	4.44	24	22	4.44	26	19						
	4.35	60	4.35	44	56	4.36B	21	16	4.38	29	28	4.34	30	28	4.35	34	25						
	4.17	60	4.17B	42	54				4.17	30	29	4.16	35	32	4.17	32	24						
						4.13B	21	16															
	4.12	30							4.12	26	25	4.12	31	29	4.13	32	24						
	3.84	40	3.84	26	33				3.83B	20	20	3.83	17	16	3.83	19	14						
	3.73	20	3.73	17	22				3.73	16	16	3.72	16	15	3.73	16	22						
(002)	3.57	100	3.57	59	76	3.57	~114	87	3.57	71	68	3.57	79	73	3.57	~123	91						
	3.37	40	3.37	20	26				3.35	19	19	3.37	17	16	3.37B	16	12						
						3.30	21	16															
	3.14	20																					
	3.09	20	3.09	11	14	3.09	13	10							3.09	11	8						
	2.75	20	2.76	10	13				2.76	10	10												
	2.55	70	2.56	15	19	2.56	14	11	2.56	14	14	2.55B	15	14	2.55	22	16						
	2.52	40	2.52	16	21	2.52	13	10	2.53	15	15	2.51	13	12	2.52	20	15						
	2.486	80	2.48	20	26	2.49	17	13	2.49	19	19	2.48	16	15	2.49	29	22						
(003)	2.374	70	2.38	11	14	2.38	18	14	2.39	12	12	2.37	13	12	2.38	23	17						
	2.331	90	2.33	27	35	2.32	17	13	2.34	24	24	2.32B	20	18	2.33	39	29						
	2.284	80	2.28	20	26	2.29	14	11	2.29	18	18	2.28	14	13	2.29	27	20						
	2.243	5	2.24	8	10	2.23	9	7															
	2.182	30	2.17	9	12				2.18B	8	8				2.18B	9	7						
	2.127	20	2.11	8	10	2.10B	8	6	2.11	7	7				2.12	8	6						
						2.09	7	7															
	2.057	5	2.05	7	9																		
	1.985	70	1.99	12	15	2.00B	13	10	1.99B	10	10	1.98B	10	9	1.99	17	13						
	1.935	40	1.93	10	13				1.95	8	8				1.94	11	8						
	1.892	20	1.89	9	12																		
	1.865	5	1.87	7	9																		
	1.835	40	1.82B	8	10				1.83	8	8				1.84	9	7						
	1.805	5	1.80	7	9																		
(004)	1.778	60	1.78	7	9	1.79	11	8	1.79	9	9	1.78	6	6	1.79	11	8						
	1.704	5	1.70	7	9																		
	1.682	10	1.68	11	14	1.68B	11	8	1.68	12	12	1.68	10	9	1.68B	19	14						
	1.659	80	1.66B	12	15				1.67	11	11	1.66	7	6	1.67	13	10						
	1.616	70	1.62B	9	12				1.62	9	9	1.62	7	6	1.62	15	11						

[1] Unoriented specimen; Brindley and Robinson, Min. Mag., 27, 242-254 (1946).
[2] Unlayered; Murfreesboro, Arkansas. B = broad.
[3] Crude; Bath, South Carolina. Montmorillonite and halloysite reflections are enclosed in parentheses.
[4] White; Mesa Alta, New Mexico
[5] Birch Pit, Macon, Georgia.
[6] Lewiston, Montana.

The distinction of kaolinite from other kaolin minerals is not as simple. Hydrated halloysite may be distinguished in the untreated pattern of A..I. 8 (Fig. 1) by the (001) spacing of 10.1 Å. However, non-hydrated halloysite, dickite, and nacrite yield patterns that are not greatly different from kaolinite.

Comparison of Figs. 1, 2, and 3 shows the principal similarities and differences between the *x*-ray diffractometer curves of kaolinite, dickite, and non-hydrated halloysite. The halloysite curve is far more diffuse than the curves for dickite or kaolinite, and the lattice spacings (Table

TABLE III. X-RAY DIFFRACTOMETER SPACING AND INTENSITY MEASUREMENTS FOR ORIENTED A. P. I. DICKITE

DICKITE								
Untreated								
ASTM 2-0104[1]			A. P. I. 15a[2]			A. P. I. 15c[3]		
(hkl)	dA	I_{REL}	dA	I_{ABS}	I_{REL}	dA	I_{ABS}	I_{REL}
(001)	7.2	100	7.17	∿158	100	7.12	∿163	100
	4.4	80	4.43	36	23	4.41	34	21
			4.24	18	11	4.25	21	13
	4.14	80	4.12	48	30	4.11	47	29
			3.93	16	10	3.93	16	10
	3.78	60	3.78	18	11	3.78	31	19
(002)	3.58	90	3.57	∿145	92	3.58	∿155	96
			3.48	18	11	3.48	15	9
	3.43	40	3.42	22	14	3.42	26	16
	3.27	20	3.24B	8	5	3.24B	8	5
	3.10	40	3.09	10	6	3.08B	9	6
						3.07	11	7
			3.04	14	9			
	2.93	40	2.92	13	8	2.92	15	9
	2.80	40				2.79	11	7
	2.56	70	2.56	15	10	2.56	19	12
	2.51	80	2.50	23	15	2.50	28	17
			2.42	26	16	2.42	14	9
(003)	2.39	60	2.38B	24	15	2.39	30	18
	2.33	90	2.32	36	23	2.31	49	30
			2.23	7	4			
	2.20	30	2.19B	10	6	2.19	12	7
			2.17	10	6	2.18B	11	7
	2.10	30	2.09	8	5			
			2.07	8	5			
	1.98	70	1.98	14	9	1.98	20	12
			1.94	11	7	1.94B	8	5
			1.92	9	5	1.92	6	4
	1.90	30	1.90	10	6	1.90	9	6
						1.88	9	6
	1.86	70	1.86	7	4	1.85B	7	4
(004)	1.79	60	1.79	14	9	1.79	17	11
			1.69B	10	6	1.68B	9	5
	1.65	80	1.66	11	7	1.65	20	12
			1.61B	8	5			
			1.59	7	4	1.59	7	4
	1.56	60	1.56B	9	5	1.56	12	7

[1] Unoriented specimen; Red Mountain, Colorado. McVay, L., and Thompson, J. Am. Cer. Soc., 11, 382 (1928): Gruner, J. W., Z. Krist, 83, 394 (1932): Nagelschmidt, G., Z. Krist., 87, 120 (1934).

[2] San Juanito, Chihuahua, Mexico. B = broad.

[3] San Juanito, Chihuahua, Mexico; different portion of pit.

IV) are somewhat larger than the corresponding spacings for the two other minerals (Tables II and III). Dickite, however, is somewhat similar to kaolinite in the number, spacing, sharpness, and intensity of the reflections. The main differences are in the larger number and increased sharpness of the dickite reflections, and in small changes in diffraction spacings. The dickite pattern, unlike kaolinite, persists upon careful heating to 550° C., the distinction between the two minerals being particularly apparent after heat treatment.

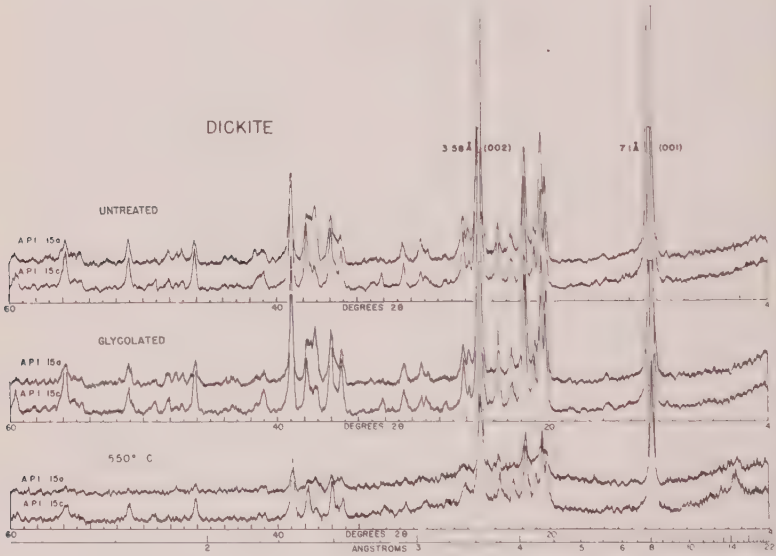

FIG. 2. *X*-ray diffractometer patterns of oriented A.P.I. dickite.

Differences in *x*-ray pattern and thermal behavior among the kaolin minerals are best revealed by reference to structural considerations. The basic structure common to the members of the group is that of kaolinite. This consists of a planar network of silica tetrahedra, joined at the base and with vertices pointing in the same direction. The vertices of the silica tetrahedra in turn are crosslinked in an octahedral pattern with aluminum and hydroxyl ions to form a stable, layer-like unit with a thickness of approximately 7 Å. Stacking these one-layer units above each other results in the kaolinite structure. The stacking pattern results in either a triclinic (kaolinite *T*) or pseudo-monoclinic (kaolinite p*M*) form. According to Gruner (1932), Ksanda and Barth (1935), and Hendricks (1938a), the dickite structure is formed by a stacking of two-layer units, and nacrite (Hendricks, 1938b) by a stacking of six-layer

kaolinite units. Thus, if the polymorph notation of Ramsdell (1947) is extended to kaolinite as proposed by Holdridge and Vaughn (Mackenzie, 1957, p. 98), then dickite would be kaolinite $2M$, and nacrite kaolinite $6M$.

Halloysite is apparently a kaolinite-like structure with considerable disorder in the arrangement, and perhaps also in the components, of the lattice. The mineral seems to be a species distinct from kaolinite as there is no intergradation known between the two. When fully hydrated, the halloysite lattice is thicker than kaolinite by approximately one layer of water. The resulting structure is asymmetric, curling to form long tubes. Upon dehydration the tubes often unroll and split, as seen in the excellent electron micrographs of Bates *et al.* (1950).

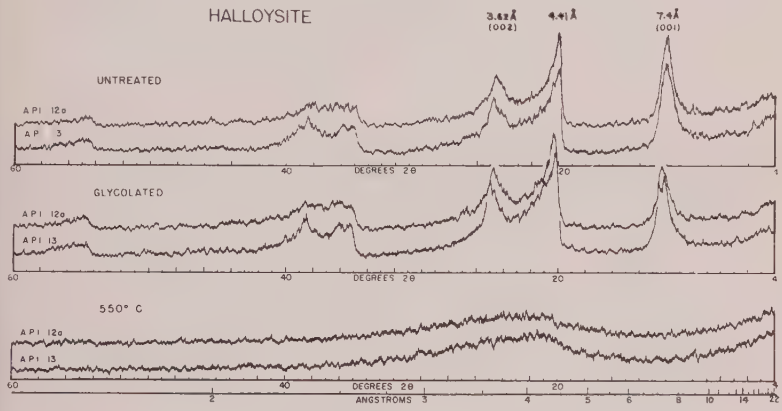

FIG. 3. *X*-ray diffractometer patterns for oriented, non-hydrated A.P.I. halloysite.

DICKITE

Dickite is a less common member of the kaolin group (Ross and Kerr, 1931), structurally similar to kaolinite, differing principally in the stacking of the layers.

The *x*-ray diffractometer patterns of dickite (Fig. 2) are distinguished by a series of sharp, intense reflections which are unaffected by glycolation, but reduced in intensity upon heating to 550° C. The two most intense peaks occur at 7.1 and 3.58 Å, representing, respectively, (001) and (002) reflections. Unlike kaolinite, where the diffraction pattern is destroyed at approximately 530° C., the pattern of dickite persists until above 600° C., at which point dehydration is complete. Differential thermal analysis records show dehydration as an endothermic reaction near 675° C., a considerably higher peak temperature than prevails

for other minerals of the kaolin group. This emphasizes the thermal stability of the dickite structure.

Electron micrographs show well-crystallized, euhedral plates with elongate hexagonal outlines, approximately 1-10 microns in diameter. Individual crystals of the mineral may be 1 mm. or more in diameter, sufficiently large to be easily visible to the unaided eye. Many smaller crystals are observable with an ordinary microscope, emphasizing excellent crystallinity, since the most ordered minerals usually give the largest crystals.

The two-layer unit cell of dickite is similar to the less common nacrite, a six-layer kaolinite structure, and the two are believed to be randomly and intimately intergrown in the San Juanito specimens (A.P.I. 15*a* and 15*c*). The diffraction patterns (Table II) indicate that the samples are otherwise pure, with quartz absent, and only a trace of chlorite in the 14 and 4.7 Å peaks of the heat treated A.P.I. 15*c* specimen.

Halloysite

The partly hydrated and fully hydrated forms of halloysite differ in the presence of a single molecular layer of water in the fully hydrated form. This results in an increase from the 7.4 Å (001) spacing of the non-hydrated form to 10.1 Å in hydrated halloysite.

The two specimens examined in this study were of the non-hydrated form, with an *x*-ray diffractometer pattern (Fig. 3) characterized by three weak, diffuse reflections at 7.4, 4.4 and 3.62 Å, and a series of smaller peaks in the 2.3–2.6 Å vicinity (Table IV). The diffuse diffraction pattern apparently results from considerable disorder in both the stacking and degree of hydration of the structural layers.

Although some workers have reported the formation of an organic-halloysite complex when the hydrated form is glycolated, there is no shift noted in the structural spacing of the non-hydrated specimens.

Heating halloysite to 550° C. results in a complete destruction of the *x*-ray diffractometer pattern (Fig. 3). This represents both the non-reversible loss of water from the hydrated form below 100° C., and the progressive loss of hydroxyl ions in octahedral coordination in the range from 400 to 500° C.

Nontronite

Nontronite is the iron-rich member of the montmorillonite group. Since the *x*-ray diffractometer patterns of nontronite summarize the behavior of the montmorillonite minerals, they are given first.

The few, diffuse reflections recorded for nontronite in Fig. 4 represent only (00*l*) and (*hk*0) spacings. The lack of crystallographic order in the

stacking of the layers causes the absence of true (*hkl*) reflections. The strongest peak, (001), ranges between 9.2 and 15.8 Å in the untreated specimen, depending upon the number of water layers, and the nature of the cations in the intersilicate position. Thus the lattice is of the "expandable" variety. The only other distinct reflection occurs at 4.5 Å and is about one half the intensity of the (001) peak (Table V). The intense background in the nontronite patterns is caused by fluorescence of iron under the copper radiation.

TABLE IV. X-RAY DIFFRACTOMETER SPACING AND INTENSITY MEASUREMENTS FOR ORIENTED, NON-HYDRATED A. P. I. HALLOYSITE

HALLOYSITE								
Untreated								
ASTM 2-0229[1]			A. P. I. 12a[2]			A. P. I. 13[3]		
(hkl)	dA	I_{REL}	dA	I_{ABS}	I_{REL}	dA	I_{ABS}	I_{REL}
(001)	7.48	60	7.4B	39	98	7.4B	39	100
	4.44	100	4.41B	40	100	4.42B	37	95
			4.34	28	70	4.34	32	82
(002)	3.62	40	3.62B	25	63	3.58B	26	67
	2.60	80	2.58B	12	30	2.57B	16	41
			2.52B	13	33	2.50-2.52	16	41
			2.49B	13	33			
(003)	2.33	80	2.32-2.39	14	35	2.33	19	49
						2.29B	16	41
			1.99	8	20			
	1.70	60	1.67-1.70	8	20	1.67-1.70	11	28
	1.64							

[1] Unoriented specimen; Toller Graben, Elbingerode, Harz, Germany. Nagelschmidt, G., Z. Krist., 87, 131 (1934).

[2] Blue; Bedford, Indiana. B = broad.

[3] Eureka, Utah.

Glycolation of the specimen results in the characteristic expansion of the lattice as the polar organic molecules orient themselves in the intersilicate position. The degree of expansion depends upon the particular organic molecule employed. Glycerol results in a (001) spacing of approximately 17.8 Å, while diethylene glycol monobutyl ether, employed in this study, caused an expansion to 15.4 Å. The 4.5 Å reflection is reduced slightly in intensity by the treatment, but does not shift in position.

Heat treatment of nontronite to 550° C. results in a decrease in the (001) spacing to approximately 9.6 Å; a decrease in the intensity of (001)

and 4.5 Å peaks; and the appearance of a strong, broad reflection at approximately 3.16 Å, probably corresponding to (003), a spacing which is not present in the untreated or glycolated structures. As this peak also appears in the heat treated patterns of montmorillonite, it is seemingly characteristic of the group. The 9.6 Å spacing represents the anhydrous nontronite structure after the loss of intersilicate water between 150–250° C., and partial loss of hydroxyl ions coordinated about Fe^{+3} ions in the octahedral position. The hydroxyl ions are not completely driven off until about 950° C., and the *x*-ray diffraction pattern persists until this point. The nature of the residual cations trapped in the intersilicate position after the loss of the H_2O with which they were

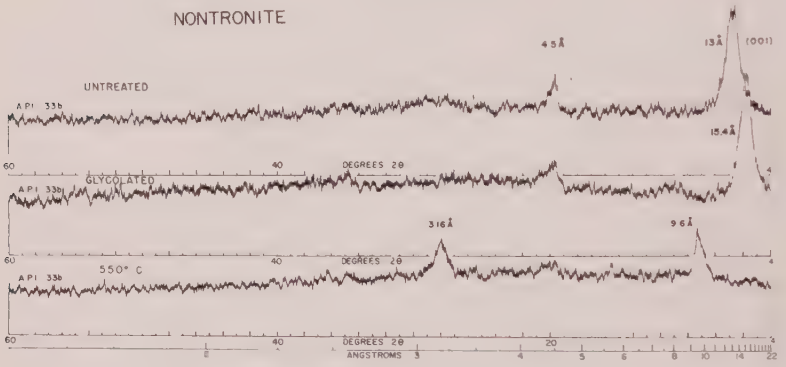

FIG. 4. *X*-ray diffractometer patterns for oriented A.P.I. nontronite.

coordinated will largely determine the position of (001) in the range 9.2–9.8 Å.

The problems introduced by mixed-layer structures in the diffractometer patterns of the group will be discussed under montmorillonite.

MONTMORILLONITE

The structural features of nontronite are characteristic for the entire montmorillonite group. *X*-ray diffractometer patterns of the untreated specimens (Fig. 5) show a few, diffuse reflections which are more intense than the corresponding peaks of nontronite. The most intense peak (Table VI) ranges in spacing from 12–15 Å, depending upon the number of water layers in the intersilicate position. The next more intense peak occurs at approximately 4.5 Å, and an asymmetric increase in background intensity is noted in the vicinity of 2.5 Å.

These three reflections persist in the glycolated patterns, with the characteristic expansion of (001) spacing. Diethylene glycol mono-

TABLE V. X-RAY DIFFRACTOMETER SPACING AND INTENSITY MEASUREMENTS FOR ORIENTED A. P. I. NONTRONITE

NONTRONITE									
Untreated						Glycolated		550° C.	
ASTM 2-0008[1]			A. P. I. 33b[2]						
(hkl)	dA	I_{REL}	dA	I_{ABS}	I_{REL}	dA	I_{ABS}	dA	I_{ABS}
(001)	15.4	100	13.1-13.5	63	100	15.4B	68	9.6	42
								5.70	28
	4.56	100	4.51	38	60	4.49-4.51	36	4.49B	29
			3.49	31	49			3.51	28
						3.29	33		
						3.18	31	3.16B	38
	3.11	20							
	3.03	20							
								2.84	27
	2.64	80							
	2.56	80				2.59B	33	2.57B	25
								2.47	25
	2.43	40							
	1.72	40	1.79	25	40			1.74	22
	1.67	40				1.69	27		

[1] Unoriented specimen; Nontron, Dordogne. Nagelschmidt, G., Min. Mag., 25, 140-155 (1938).

[2] Manito, Washington. B = broad.

butyl ether was employed in this study to expand the montmorillonite lattice. A number of organic molecules cause similar expansion, and MacEwan (1948) and others have described the organic complexes formed, and the expansion observed.

As in the case of nontronite (Fig. 4), upon heating to 550° C., montmorillonite collapses to an anhydrous spacing of about 9.6 Å for (001) and a pronounced reflection appears near 3.17 Å. The 4.5 Å spacing decreases slightly to about 4.42 Å, while the asymmetric peak near 2.5 Å remains unchanged.

The five montmorillonite patterns shown in Fig. 5 are somewhat complicated by the presence of several intense extraneous reflections. These are particularly noted in the patterns of A.P.I. 27 Five of the intense peaks in this pattern are caused by quartz ("Q"). The remaining reflections are best explained (Table VI) as caused by a mixed-layer structure of montmorillonite-chlorite ("M-C").

The montmorillonite species are particularly subject to the phenom-

enon of mixed-layer structure. The basic illite, chlorite, vermiculite, and montmorillonite structures are similar; the main distinction being in the composition of the intersilicate layer. Although the different compositions of this layer result in considerably different unit cell spacings in the *c* direction, the structures are often found interlayered in both random and regular patterns. The (001) series of reflections occur in an integral sequence in the regular mixed-layer clays, in distinction to the random mixed-layer structures. A new field has developed in the interpretation of mixed-layer clay structures (Earley *et al.*, 1956; Weaver, 1956, 1958).

Electron micrographs of montmorillonite samples show irregular flakes with only slightly more evidence of crystallinity than allophane. Hectorite, saponite, and nontronite may show lath-like forms, occasionally with striations parallel to their length, indicating cleavage resulting from

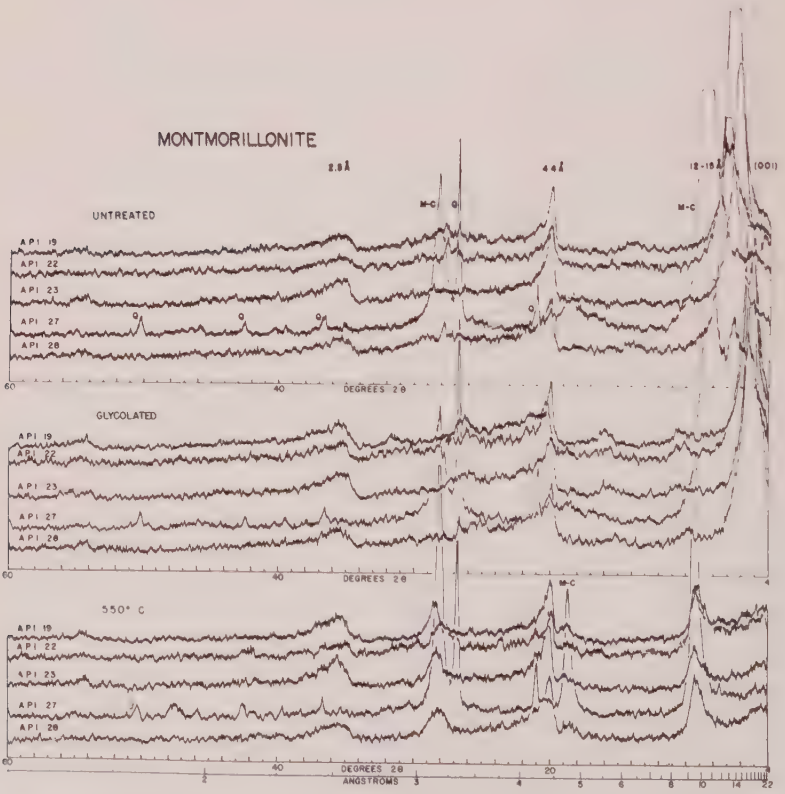

FIG. 5. *X*-ray diffractometer patterns of oriented A.P.I. montmorillonite. Impurity reflections are labeled: Q = quartz; M-C = montmorillonite-chlorite.

TABLE VI. X-RAY DIFFRACTOMETER SPACING AND INTENSITY MEASUREMENTS FOR ORIENTED A.P.I. MONTMORILLONITE

a. Untreated. b. Glycolated. c. 550° C.

a. Untreated

ASTM 3-0010[1]			A.P.I. 19[2]			A.P.I. 22[3]			A.P.I. 23[4]			A.P.I. 27[5]			A.P.I. 28[6]		
(hkl)	dA	IREL	dA	IABS	IREL	dA	IABS	IREL	dA	IABS	IREL	dA	IABS	IREL	dA	IABS	IREL
												22	48	23			
(001)	15.3	100	13.6	~200	100	12.5B	63	100	14.5	~115	100	13.6	~210	100	12.9B	~110	100
	5.1	40															
												4.8B	24	11			
	4.6	80	4.47B	34	17	4.46B	30	48	4.44	40	35	4.43	19	9	4.42B	33	30
	4.27	30										(4.26)	28	13	4.25	26	24
			3.34	20	10	3.33	24	38	3.38	18	16	(3.34)	82	39			
			3.23	20	10	3.24	25	40				3.21	45	21	3.19	24	22
												3.17	69	33			
	3.08	50				3.02	20	32	3.09	18	16						
			2.92	15	8				2.95	16	14						
	2.76	10															
	2.56	70	2.49-2.59	11	5	2.52-2.57	14	22	2.51-2.58	20	17	2.55	13	6	2.49-2.59	18	16
	2.50	40										2.47B	16	8			
												(2.28)	12	6			
	2.24	20							2.23	15	13	(2.23)	17	8			
									2.08	14	12	(2.12)	13	6			
												(1.81)	15	7			
	1.69	30							1.69	14	12	(1.68)	10	5			
									1.62	12	10						

b. Glycolated

A.P.I. 19[2]		A.P.I. 22[3]		A.P.I. 23[4]		A.P.I. 27[5]		A.P.I. 28[6]	
dA	IABS	dA	IABS	dA	IABS	dA	IABS	dA	IABS
16.6	~160	16.5	~150	16.7	98	16.3	80	17.4	~170
						13.5	87		
						10.8	~175		
		8.8	20					8.9-9.2	19
		8.35	19						
				7.03	13				
								6.48	15
5.49-5.62	14			5.57	15			5.86	16
4.45	32	4.42	34	4.41-4.49	32	4.45	20	4.48	35
				(4.26)	30				
		4.19	26						
		4.10	25	4.14	21				
						3.73	13		
								3.63	20
								3.56	21
		3.43	25	3.45B	19			3.45-3.50	20
3.33-3.41	20					(3.34)	84	3.35	22
		3.29	23						
		3.20B	22			3.21	35	3.21	16
						3.17	53		
		2.96	18					2.94	14
2.83	12								
2.50-2.58	17	2.52-2.59	20	2.52-2.60	17			2.49-2.59	17
2.48	15					2.46	14	2.44	15
						(2.28)	11	2.29	13
						(2.12)	11		
						(1.81)	13		
				1.70	10				
1.69	11	1.69B	13	1.68	11			1.69	12
				1.64	10				
						1.56	9		

c 550° C

A.P.I. 19[2]		A.P.I. 22[3]		A.P.I. 23[4]		A.P.I. 27[5]		A.P.I. 28[6]	
dA	IABS	dA	IABS	dA	IABS	dA	IABS	dA	IABS
						22*	21		
						12.0	21		
9.4-9.6	25	9.4-9.8	37	9.4-9.7	25	9.7	~145	9.4-9.7	34
						7.62	12		
						4.78*	55		
4.64	13								
4.42-4.45	18	4.40-4.50	27	4.42	34			4.44	34
				4.29	22				
						(4.26)	27		
		4.21	20	4.21	22				
								4.17	23
		3.77B	17						
		3.31	19			(3.34)	83		
		3.23	22						
3.11-3.16	20	3.17	23	3.10-3.20	23	3.19	~120	3.10-3.22	21
		3.00	16			2.97*	14		
2.41-2.59	15	2.42-2.60	15	2.51	20	2.47	15	2.45-2.68	15
				2.45-2.47	16				
						(2.28)	11		
		2.10-2.14	13			(2.11B)	12		
						1.99B	10		
						1.91-1.92	11		
						(1.81)	11		
1.68-1.69	8			1.69B	11				

1 Unoriented specimen; Algiers. Favejee, J.C.L., Z. Krist., 100, 433 (1939).
2 Polkville Mine; Polkville, Mississippi. B = broad.
3 Itawamba Mine; Amory, Mississippi.
4 Chambers, Arizona.
5 Belle Fourche, South Dakota. Quartz reflections are enclosed in parentheses
6 Little Rock, Arkansas.
*Spacings similar to montmorillonite-chlorite heated to 550°C., Earley et al., Am. Mineral., 41, 262.

strains induced in the structure by differences in the ionic radii of octahedrally coordinated cations. Variation in the spacing and intensity of x-ray reflections similarly indicate differences among the montmorillonite minerals.

Illite

The term illite is applied to the mica-like clay mineral with a 10 Å c-axis spacing and a non-expanding lattice. Yoder and Eugster (1955) suggest the use of illite as a field term describing polymorphic forms of

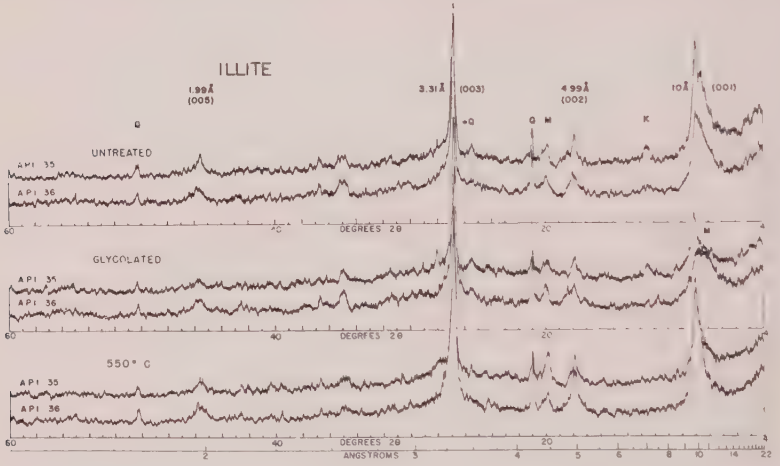

Fig. 6. X-ray diffractometer patterns for oriented A.P.I. illite. Impurity reflections are labeled: M = montmorillonite; Q = quartz; K = kaolinite.

mica, which may be interlayered with montmorillonite. The principal difference between illite and muscovite-sericite is in the degree of crystallinity which reflects the greater compositional range permitted in the illite lattice. X-ray diffractometer charts of illite show a few, broad, diffuse, weak reflections (Fig. 6), in contrast to the numerous sharp, strong peaks of muscovite and sericite (Table VII). Electron micrographs reveal the platy, irregular aggregates of illite, against the large, clean-cut plates of sericite and muscovite.

Except for a series of sharp quartz reflections, the x-ray diffractometer patterns of illite (Fig. 6) are characterized by several weak, broad peaks. These remain constant in spacing and intensity after glycolation. Heat treatment causes no shift in lattice spacing, but results in a slight increase in the peak intensities (Table VII).

The asymmetry of the 10.0 Å, (001) reflection probably indicates the presence of mixed-layer structures of montmorillonite-illite. Upon glycolation this reflection is reduced in intensity and in A.P.I. 36 shifts to slightly larger spacings. After heating to 550° C., the intensity is restored and the peak becomes symmetrical, indicating the collapse of the hydrated montmorillonite lattice to the anhydrous spacing, and a possible increased ordering of the illite lattice components.

Differential thermal analyses of these illite specimens (Kerr *et al.*, 1951) reveal a series of reactions upon heating, which may be attrib-

TABLE VII. X-RAY DIFFRACTOMETER SPACING AND INTENSITY MEASUREMENTS FOR ORIENTED A.P.I. ILLITE

	ILLITE																			
	Untreated										Glycolated						550° C.			
	MUSCOVITE ASTM 7-25[1]		ASTM 9-343[2]		A.P.I. 35[3]			A.P.I. 36[4]			A.P.I. 35[3]		A.P.I. 36[4]		A.P.I. 35[3]		A.P.I. 36[4]			
(hkl)	dA	I_{REL}	dA	I_{REL}	dA	I_{ABS}	I_{REL}	dA	I_{ABS}	I_{REL}	dA	I_{ABS}	dA	I_{ABS}	dA	I_{ABS}	dA	I_{ABS}		
					(10.4B)	47	78				(16.5)	21								
(001)	10.08	100	10.0	100	10.0	60	100	10.0	42	100	10.0	34	10.0	31	10.0	46	10.0	61		
					(7.15B)	19	32				(7.12)	15								
(002)	5.04	37	4.95	20	4.98	23	38	4.98B	20	48	4.99	18	4.98	18	4.99	21	4.99B	25		
	4.49	90	4.48	90	4.47	20	33	4.47B	18	43	4.41-4.51	16	4.48	18	4.48	22	4.48	17		
	4.35	27																		
					(4.26)	26	43	(4.26)	27	64	(4.26)	21	(4.26)	27	(4.26)	23	(4.26)	28		
	4.11	16																		
	3.66	60	3.69	20	3.66	17	28													
					3.51	20	33				3.52	17			3.51	18				
					(3.34)	73	120	(3.34)	79	188	(3.34)	51	(3.34)	80	(3.34)	74	(3.34)	87		
(003)	3.36	100	3.33	90	~3.30	28	47	~3.30	30	71	~3.30	23	~3.29	32	~3.29	26	~3.30	32		
			3.17	5	3.19	22	37	3.21	22	52	3.18	21			3.19	20				
	3.07	50									3.07	16								
								(2.96-2.98)	16	38			(2.97)	16			(2.98)	15		
			2.87	10				2.88	16	38			2.89	15	2.90	14				
					2.84	16	27				2.84	14	(2.84)	15						
	2.689	16	2.61	60																
	2.582	50																		
	2.565	90	2.51	10	2.54-2.59	16	27	2.54-2.60	17	40	2.55-2.57	13	2.57B	16	2.55-2.57	14	2.55-2.59	12		
(004)	2.550	22																		
	2.450	11	2.42	40	2.45	16	27	2.45B	16	38			2.44	14	2.45	13	2.45	11		
	2.380	12						(2.28)	12	29							(2.28)	10		
	2.156	20	2.16	20				2.18	12	29							(2.11)	11		
(005)	2.013	32	1.986	10	1.99	17	28	1.99B	15	36	1.99B	10	1.99B	12	1.99B	13	2.00B	14		
					(1.81B)	13	22	(1.81)	12	29	(1.81)	9	(1.81)	9	(1.80B)	10	(1.81)	11		
	1.668	18	1.667	30	1.68	11	18	1.68	13	31										
											1.65-1.68	9								
	1.653	12			1.65	11	18													
	1.635	12			1.63	11	18				1.61	8								

[1] Synthetic 1M type; Yoder and Eugster, Geochim. et Cosmochim. Acta., 8, 225 (1955). Reflections with relative intensity less than 10 are not listed
[2] Carden Wood, Aberdeenshire; Walker, G. F., Min. Mag., 29, 72-84 (1950)
[3] Fithian, Illinois. B = broad. Quartz, montmorillonite, and kaolinite reflections are enclosed in parentheses
[4] Morris, Illinois. Quartz reflections are enclosed in parentheses.

uted to montmorillonite and kaolinite, with which illite is frequently interlayered. The diffractometer pattern of A.P.I. 35 indicates the presence of both of these minerals, while kaolinite is absent in A.P.I. 36.

The coincidence of the (003) reflection of illite with the 3.34 Å, most intense quartz peak, has resulted in certain problems. Although other reflections are present, quartz is often overlooked because of the masking of the most intense peak. Similarly, the precise spacing of the illite (003) reflection is difficult to determine because of the overlap of the intense quartz peak. Because of intensity ratios of the (001) and (003) muscovite peaks, and the asymmetrical small angstrom side of this reflection on the illite patterns, it is believed that the (003) reflection of illite approximates 3.30 Å, and these peaks are separately listed in Table VII.

Attapulgite

The clay-like mineral attapulgite is considered to be a finely crystalline relative of the palygorskite group.

A single intense reflection of 10.5 Å and a series of weak, broad lines at lesser angstrom spacings constitute the *x*-ray diffractometer pattern of attapulgite (Fig. 7). The intensities are slightly decreased and some peaks broadened by glycolation. Heating to 550° C. for two hours causes almost complete destruction of the pattern; the peaks which remain are primarily caused by montmorillonite and quartz (Table VIII).

The collapse of the attapulgite structure upon heating is a result first of the loss of H_2O and then of octahedrally coordinated OH ions. Dehydroxylation of the structure is almost complete at 550° C.

Unlike the other minerals examined in this study, attapulgite is not a sheet silicate structure. Bradley (1940) has described the mineral as a framework formed by the cross-linking of double-ribbed sheets. The double-ribbed effect represents the alternate pointing of the silica tetrahedra vertices to opposite sides of the "tetrahedral" layer. The channelways thus formed contain the H_2O molecules.

Electron micrographs reveal long straight fibers approximately 0.1×3 microns in width and length. Cleavage parallel to the ribs is considered responsible for the fiber-like habit.

Pyrophyllite

Pyrophyllite, the dioctahedral analogue of talc, was included in the original set of A.P.I. reference clays.

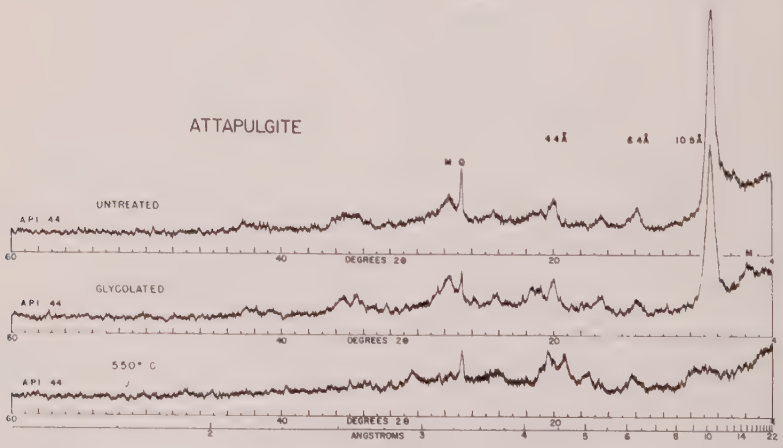

Fig. 7. *X*-ray diffractometer patterns of oriented A.P.I. attapulgite. Impurity reflections are labeled: Q = quartz; M = montmorillonite.

TABLE VIII. X-RAY DIFFRACTOMETER SPACING AND INTENSITY MEASUREMENTS FOR ORIENTED A. P. I. ATTAPULGITE

ATTAPULGITE										
Untreated						Glycolated		550° C.		
ASTM 5-0099[1]			A. P. I. 44[2]							
(hkl)	dA	I_{REL}	dA	I_{ABS}	I_{REL}	dA	I_{ABS}	dA	I_{ABS}
			(13.1)	33	36	(16B)	28		
(110)	10.50	100	10.5	91	100	10.5	72		
								(9.6B)	20
(200)	6.44	60	6.42B	18	20	6.43B	14		
								6.23	17
(130)	5.42	40	5.32-5.49	15	16	5.44	15		
						5.35	14	4.95-5.12	17
			4.65	14	15	4.65	14	(4.62B)	24
(040)	4.49	80	4.45B	20	22	4.48	22		
								4.34	25
			(4.26)	17	19	(4.26)	19	(4.26)	20
(310)	4.18	20	4.14	17	19	4.14B	19		
(240)	3.69	40	3.67	17	19	3.67-3.71	16		
(330)	3.50	20	3.48	15	16	3.49	15		
			(3.34)	32	35	(3.34)	24	(3.34)	25
(400)	3.23	100	3.22	23	25	3.21B	22		
						3.13	19		
(420)	3.03	10				3.04	14		
								(2.94)	18
			2.80	13	14	2.79	12		
			2.69	14	15				
(440)	2.61	80				2.61B	15		
			2.50-2.63	16	18			(2.57)	14
(510)	2.55	20				2.51-2.55	15		
			(2.46)	14	15				
			2.40	11	12				
			2.39	12	13	2.39B	9		
(530)	2.38	20	2.38	11	12				
(600)	2.15	40	2.14	12	13	2.15	11		
			(2.13)	11	12	(2.12B)	11		
			2.10B	12	13				
(390)	1.82	10	1.82	10	11	1.82	8		
(800)	1.62	10				1.62	9		

[1] Unoriented specimen; Attapulgus, Georgia. Bradley, W. F., Am. Mineral., 25, 405-410 (1940).

[2] Attapulgus, Georgia. Quartz and montmorillonite reflections are enclosed in parentheses. B = broad.

The sharp, intense reflections seen in the *x*-ray diffractometer patterns (Fig. 8) indicate excellent crystallinity, but only a few of the reflections are caused by pyrophyllite. The majority of the peaks represent well crystallized impurities including quartz, muscovite, and kaolinite or dickite (Table VIII), which comprise about 30 per cent of this specimen.

The diffraction pattern of pyrophyllite is unaffected by glycolation, and only slightly intensified by heating to 550° C. Dehydration is not noted, while dehydroxylation of the mineral has only begun at this

temperature and is not complete until above 780° C. Similarly, the low base exchange and isomorphous replacement reported for pyrophyllite explain the lack of response to glycolation.

Additional reflections have been noted in the pyrophyllite pattern by Gruner (Table IX) and others. Most are masked by the numerous impurity peaks, but the 4.15 Å spacing is absent. Otherwise, comparison of the A.P.I. with the A.S.T.M. pyrophyllite pattern is satisfactory.

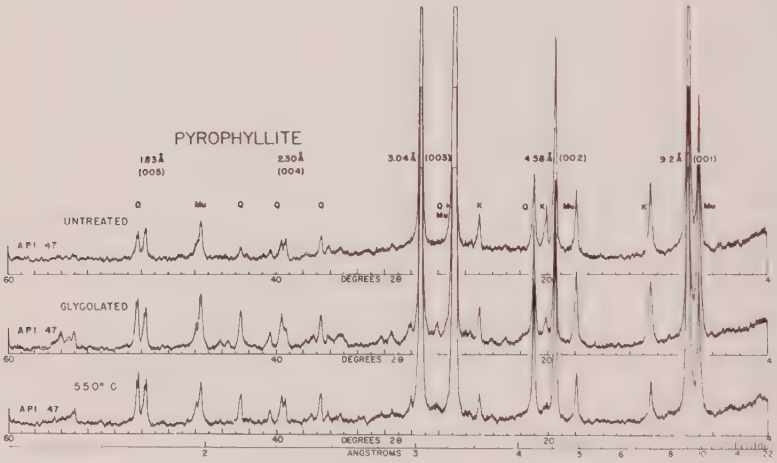

FIG. 8. *X*-ray diffractometer patterns of oriented A.P.I. pyrophyllite. Impurity reflections are labeled: Mu = muscovite; K = kaolinite or dickite; Q = quartz.

The isomorphism of talc and pyrophyllite structures, one dioctahedral, the other trioctahedral, presents difficulties in the distinction of these minerals. The main *x*-ray diffraction differences are the absence of the strong 3.13 and 2.62 Å talc spacings in the pyrophyllite pattern.

CONCLUSION

X-ray diffractometer techniques furnish an effective method for identifying and differentiating the clay minerals. Data for reference clay minerals from other forms of analysis are supplemented by diffractometer patterns and spacing-intensity measurements on the original chemically analyzed specimens of A.P.I. Research Project 49. Clay lattice spacing shifts and reactions observed in these *x*-ray charts are understandable in terms of changes within the clay mineral structure.

In conclusion, a schematic chart of diffractometer patterns (Fig. 9) is given for the clay minerals described. Extraneous lines have been re-

TABLE IX. X-RAY DIFFRACTOMETER SPACING AND INTENSITY MEASUREMENTS FOR ORIENTED A. P. I. PYROPHYLLITE

PYROPHYLLITE									
Untreated					Glycolated		550° C.		
ASTM 2-0613[1]			A.P.I. 47[2]						
(hkl)	dA	I_{REL}	dA	I_{ABS}	I_{REL}	dA	I_{ABS}	dA	I_{ABS}
			(10.0)	67	48	(10.0)	76	(10.0)	59
(001)	9.14	40	9.2	∿140	100	9.2	∿110	9.2	∿150
			(7.16)	37	26	(7.16)	28	(7.16)	20
			(5.01)	32	23	(5.00)	31	(4.98)	24
(002)	4.57	50	4.58	89	64	4.59	65	4.57	88
			(4.47)	26	19	(4.47)	14	(4.47)	12
			(4.26)	38	27	(4.26)	48	(4.26)	57
	4.15	20							
	3.87	5	3.87	11	8	3.87	7		
						(3.72)	7		
			(3.59)	23	16	(3.59)	18	(3.57)	15
						(3.49B)	13	(3.48B)	12
	3.34	20-40	(3.34)	∿150	100	(3.34)	∿140	(3.34)	55
						(3.19)	13		
(003)	3.04	100	3.04	∿140	100	3.04	∿125	3.04	∿150
						(2.98)	12		
			(2.87)	12	9	(2.87)	9	(2.86)	10
			(2.78B)	10	6	(2.79B)	7	(2.79)	9
			(2.56B)	11	8	(2.57B)	8		
	2.52	20	(2.50)	11	8	(2.51)	7	(2.51)	7
			(2.46)	15	11	(2.45)	15	(2.45)	15
	2.40	40	(2.39)	9	6			(2.40B)	8
(004)	2.29	20	2.30	14	10	2.30B	10	2.30	10
			(2.28)	13	9	(2.29)	16	(2.28)	15
			(2.23)	9	6	(2.24)	8	(2.23)	9
	2.14	10-20	(2.14)	8	5				
			(2.13)	10	7	(2.12)	16	(2.12B)	15
	2.07	10				(2.07)	6		
	2.04	10						(2.01)	20
			(2.00)	20	14	(2.00)	23	(2.00)	12
			(1.98)	12	9	(1.99)	12		
	1.88	5				(1.89)	4	1.86B	21
(005)	1.83	40	1.83	18	13	1.83	18		
			(1.81)	17	12	(1.82)	21	(1.82B)	24
			(1.68B)	8	5	(1.68)	9	(1.69B)	10
						(1.67)	9		
	1.64	20-40							

[1] Unoriented specimen; Tres Ceritos, Mariposa County, California. Gruner, J. W., Z. Krist., 88, 415 (1934).

[2] Processed; Robbins, North Carolina. Reflections primarily caused by quartz, muscovite, and kaolinite are enclosed in parentheses.

moved, the symmetry or asymmetry of each peak is imitated, and the intensities are absolute in terms of the equipment used. The corresponding chemical composition of the minerals is based on the analyses of A.P.I. Research Project 49. Dotted lines indicate the approximate level of background radiation in the charts.

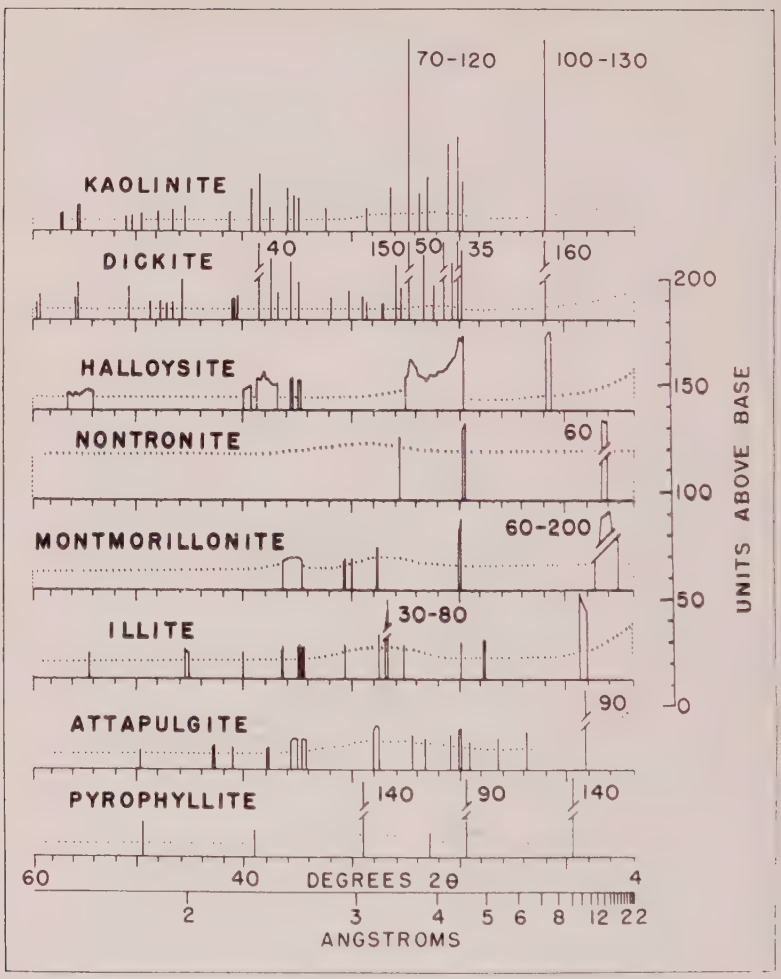

FIG. 9. Schematic diagram of A.P.I. diffractometer patterns. Intensity, spacing, width and symmetry of the principal reflections are imitated. Intensity is measured in units above base. The dotted line indicates the background level.

REFERENCES

BATES, T. F., HILDEBRAND, F. A., AND SWINEFORD, A., 1950, "Morphology and Structure of Endellite and Halloysite," *Amer. Mineral.*, **35**, 463–484.

BRADLEY, W. F., 1940, "The Structural Scheme of Attapulgite," *ibid.*, **25**, 405–410.

BRINDLEY, G. W., ed., 1951. *X-ray Identification and Structure of the Clay Minerals.* Mineralog. Soc. Gr. Brit., Monogr., 345 p.

———, AND ROBINSON, H., 1946, "Randomness in the Structures of Kaolinitic Clay Minerals," *Trans. Faraday Soc.*, **42B**, 198–205.

Earley, J. W., Brindley, G. W., McVeagh, W. J., and Vanden Heuvel, R. C., 1956, "A Regularly Interstratified Montmorillonite-chlorite," *Amer. Mineral.*, **41,** 258–267.

Grim, R. E., 1953, *Clay Mineralogy*, 384 p. McGraw-Hill Book Co., New York.

Gruner, J. W., 1932, "Crystal Structure of Dickite," *Z. Krist.*, **83,** 394–404.

Hendricks, S. B., 1938a, "On the Structure of the Clay Minerals: Dickite, Halloysite, and Hydrated Halloysite," *Amer. Mineral.*, **23,** 295–301.

———, 1938b, "Crystal Structure of Nacrite and the Polymorphism of the Kaolin Minerals," *Z. Krist.*, **100,** 509–518.

Kerr, P. F., *et al.*, 1951, "Preliminary Reports, Reference Clay Minerals," *Amer. Petrol. Inst.*, Research Project **49**.

Ksanda, C. J., and Barth, T. F. W., 1935, "Note on the Structure of Dickite and Other Clay Minerals," *Amer. Mineral.*, **20,** 631–637.

MacEwan, D. M. C., 1948, "Complexes of Clays with Organic Compounds, I," *Trans. Faraday Soc.*, **44,** 349–367.

MacKenzie, R. C., ed., 1957, *The Differential Thermal Analysis of Clays*. 456 p. Mineralog. Soc., Clay Minerals Group, London.

Murray, H. H., and Lyons, S. C., 1956, "Correlation of Paper-coating Quality with Degree of Crystal Perfection of Kaolinite," *Clays and Clay Minerals;* Proc. 4th Nat. Conf. on Clays and Clay Minerals; Publ. 456, Nat. Acad. of Sci., Nat. Research Council.

Ramsdell, L. S., 1947, "Studies on Silicon Carbide," *Amer. Mineral.*, **32,** 64–82.

Ross, C. S., and Kerr, P. F., 1931, "The Kaolin Minerals," *U. S. Geol. Survey Prof. Paper* 165E.

Weaver, C. E., 1956, "The Distribution and Identification of Mixed-layer Clays in Sedimentary Rocks," *Amer. Mineral.*, **41,** 202–221.

———, 1958, "Geologic Interpretation of Argillaceous Sediments," *Bull. Amer. Assoc. Petrol. Geol.*, **42,** No. 2, 254–309.

Yoder, H. S., and Eugster, H. P., 1955, "Synthetic and Natural Muscovites," *Geoch. Cosmoch. Acta*, **8,** 225–280.

Manuscript received July 15, 1960.

NEW RESULTS FROM LEAD-ALPHA AGE MEASUREMENTS*

T. W. Stern and H. J. Rose, Jr., *U. S. Geological Survey, Washington 25, D. C.*

Abstract

Improvement in the spectrochemical method for determining lead in zircon increases the usefulness of the lead alpha (Larsen) age method. Good agreement is found between the lead alpha ages and those obtained by isotope dilution analyses on twelve samples. These samples have calculated ages ranging from 400 to 1200 million years. New lead analyses and revised lead-alpha ages are presented for 19 samples previously analyzed.

Introduction

A number of zircons previously analyzed by isotope Pb-U methods have been dated by the lead-alpha (Larsen) method using an improved spectrochemical procedure for determining lead (Rose and Stern, 1960). The new analytical technique differs from the previous method (Waring and Worthing, 1953) in that the standards used are more nearly similar in chemical and physical properties to natural zircons. Comparative results for lead determined by both spectrochemical methods indicate that the new analyses yield significantly higher lead values and lead-alpha ages than produced by earlier determinations.

Analytical Data

The lead contents determined by spectrochemical and isotope dilution techniques and the measured and calculated alpha activities for 12 samples are given in Table 1. The table lists all Precambrian samples presently available and presents comparative results for splits of the same sample.

The average deviation between the spectrochemical lead values and the lead contents determined by isotope dilution analyses is about 2%, with the isotope dilution values on the average greater. The average deviation between measured and calculated alpha activity is about 6%, with the calculated activities generally higher.

A sample of monazite, SQ-81, from Mountain Pass, San Bernardino County, California, which had been previously dated by isotope dilution analysis and by the lead-alpha method was investigated in the present study. A lead content of 1760 ppm was obtained with the new spectrochemical method compared with an average value of 1130 ppm found previously (Jaffe, 1955, p. 1253). The present determination agrees with isotope dilution analyses by G. R. Tilton and L. R. Stieff who found 1770 and 1740 ppm of lead, respectively (Gottfried and others, 1959, p. 25).

* Publication authorized by the Director, U. S. Geological Survey.

TABLE 1.—COMPARISON OF LEAD CONTENTS AND ALPHA ACTIVITIES

Sample No.	Zircon sample, and supplier	Pb(ppm)		Alpha activity		Th:U
		Spectrochemical method[1]	Isotope dilution	Measured	Calculated from isotope dilution U and Th[2]	
1	Kensington granite gneiss, Washington, D. C., G. R. Tilton (Cooke, C. W., 1951).	97[3]	98	568	567	.20
2	Rare-earth vein, Laurel Gap, Tenn., G. R. Tilton	165	161	697	684	.31
3	Beech granite, Roan Mountain, Tenn., G. R. Tilton	54	58	235	242	.67
4	Granite gneiss, Crossnore, N. C., G. R. Tilton	33	32	100	99	.14
5	Gneiss, Shenandoah, Park, Va., G. R. Tilton	78	83	183	179	.32
6	Cranberry gneiss, Deyton Bend, N. C., G. R. Tilton	57	60	124	129	.43
7	Storm King granite, N. Y., G. R. Tilton (Berkey, C. P., 1907)	335	337	676	838	.16
8	McDonald mine Hybla, Ontario, G. R. Tilton	970[4]	1045	1488	1743	.59
9	Baltimore gneiss, Spring Mills, Pa., G. R. Tilton	187	168	372	390	.32
10	Pegmatite, San Gabriel Mts., Calif., L. T. Silver	37	41	78	81	.30
11	Old Whitestone Farm, Natural Bridge, N. Y., A. F. Buddington and H. D. Holland	110[5]	127	224[6]	283	—[7]
12	Wilson Creek gneiss, Mortimer, N. C., Tilton	168	160	433	484	.26

[1] Average of duplicate determinations of a 15 mg. sample.

[2] Sample from San Gabriel Mts., California isotopically analyzed by L. T. Silver, California Institute of Technology. All other samples isotopically analyzed by G. R. Tilton and G. L. Davis, Geophysical Laboratory, Carnegie Institute of Washington. Alpha activities were calculated from the analyses.

[3] Analyses by Nola B. Sheffey, U. S. Geological Survey, Washington, D. C.

[4] Sample diluted with 8 parts zircon base (68 per cent zirconia and 32 per cent silica) prior to lead analysis.

[5] Single determination on a 4 mg sample.

[6] Alpha activity measurement by H. W. Jaffe, U. S. Geological Survey, Washington, D. C

[7] All alpha activity due to uranium, thorium not detectable.

In addition to the 12 samples for which isotope dilution analyses were available, new lead determinations were made on some samples previously dated by the lead-alpha method for which sufficient material was available (Table 3).

DISCUSSION

The new lead-alpha ages (Table 2) are in good agreement with the ages obtained by isotopic methods. The results for the 19 samples in Table 3 indicate, however, that although some of the lead analyses previously

TABLE 2.—COMPARISON OF LEAD-ALPHA AGES OF ZIRCON WITH LEAD-URANIUM AND LEAD-THORIUM AGES IN MILLIONS OF YEARS

Sample No.	Sample	Pb-Alpha		$\frac{Pb^{206}}{U^{238}}$	$\frac{Pb^{207}}{U^{235}}$	$\frac{Pb^{207}}{Pb^{206}}$	$\frac{Pb^{208}}{Th^{232}}$	Reference
		Assumed Th:U ratio 1:1	Calculated Th:U ratio					
1	Kensington granite gneiss, Washington, D. C. (Cooke, 1951)	410	430	400	420	510	350	G. R. Tilton and others (1959)
2	Rare-earth vein, Laurel Gap, Tennessee	560	580	585	640	820	360	"
3	Beech granite, Roan Mountain, Tennessee	540	560	555	585	700	425	"
4	Granite gneiss, Crossnore, North Carolina	770	790	690	720	800	680	"
5	Gneiss, Shenandoah National Park, Virginia	980	1000	1070	1100	1150	1110	"
6	Cranberry gneiss, Deyton Bend, North Carolina	1040	1070	1080	1140	1270	950	"
7	Storm King granite, Bear Mt. Near York. (Berkey) 1907)	1120	1140	960	990	1060	850	G. R. Tilton and others (1958)
8	McDonald mine, Hybla Ontario	1420	1430	1350	1190	900	435	G. L. Davis and others (1957)
9	Baltimore gneiss, Spring Mills, Pennsylvania	1130	1160	1010	1045	1120	950	G. R. Tilton, written communication
10	Pegmatite, San Gabriel Mts., California	1070	1100	1200	1200	1200	1210	L. T. Silver and others (1960)
11	Old Whitestone Farm Natural Bridge, N. Y.	1100	1130	1025	1065	1140	—	G. R. Tilton and others (1957)
12	Wilson Creek gneiss, Mortimer, North Carolina	890	920	800	860	1020	670	G. R. Tilton and others (1959)

reported are in satisfactory agreement with the new determinations, most of the new determinations are significantly higher than the earlier lead analyses. Thus the new lead-alpha ages for these samples are significantly older. No systematic variation has been found between the old and new determinations and hence no single empirical factor can be applied to the earlier analyses.

The new lead-alpha ages are reported to the nearest 10 million years. The analytical error is assessed at approximately 10 per cent. This error is assigned to deviations in the spectrochemical and counting techniques and excludes errors due to variations in Th, U and geological factors that are more difficult to evaluate. The lead-bearing minerals other than zircon, present as a sample contaminant, are generally eliminated during careful microscopic examination prior to analysis. A more difficult problem is that of nonradiogenic lead contained within the zircon sample

TABLE 3.—REDETERMINATION OF SOME LEAD-ALPHA AGES

Rock types, locality and supplier	α/mg/hr.	Mean lead ppm (duplicate determinations)		Lead-alpha ages Million years		Remarks
		Previous method	Present method	Previous method	Present method	
Nordmarkite N-7, Oslo, Norway, Henry Faul	177[1] 173	19	18	*265*	260	C. L. Waring, oral communication (1960)
Reddish biotite granite SA-1, Jebal Rafa, Saudi Arabia, G. F. Brown	3,840	390	560[2]	247	350	Jaffe, and others (1959)
Coarse gray porphyritic granite, SA-2, Eastern side of eastern batholith, Saudi Arabia, G. F. Brown	460 360	66.5 48	117[2] 125[2]	*349* *323*	600 800	Jaffe, and others (1959)
Granite rock, SA-3, Jebal Zaba, Saudi Arabia, G. F. Brown	2,083 1,970	303 307	530[2] 570[2]	*351* *377*	600 680	Jaffe and others (1959)
Swarthmore granodiorite, A.W.P.-5, Intermediate replacement type East Lake Park, Philadelphia area, Pa. A. W. Postel	220	21.5	44[3]	*238*	480	Jaffe and others (1959)
Swarthmore granodiorite A.W.P.-6, Intermediate replacement type, Clifton Heights, Philadelphia area, Pa., A. W. Postel	250	23.5	48[3]	*230*	460	Jaffe, and others (1959)
Biotitic Wissahickon schist, A.W.P.-7, near Falls Bridge, Fairmont Park, Philadelphia area, Pa., A. W. Postel	135	23.5	52[3]	*418*	880	Jaffe, and others (1959)
Biotitic Wissahickon schist, A.W.P.-10, Gully Run, South of West Manayunk, Philadelphia area, Pa., A. W. Postel	125	22	45[2]	*422*	840	Jaffe, and others (1959)
Arenite, RN-2, Ocoee series, Great Smoky Mts., Gatlinburg quadrangle, Tennessee, R. B. Neuman	287	107	112[3]	*859*	890	Jaffe, and others (1959)
Arenite, RN-13, Ocoee series, Great Smoky Mts., Tunderhead quadrangle, Tennessee, North Carolina, R. B. Neuman, D. Carroll	136	37	48	*640*	820	Jaffe, and others (1959)
Quartz diorite, SV-1, Roadcut, north edge of town of San Vicente, Baja, California, D. Gottfried, L. R. Stieff, and T. W. Stern	123 152	5.05	6.1	*102*	100	Jaffe, and others (1959)
Baltimore gneiss, BL-1, Cross-cutting pegmatite along a deformed fault plane, River Road, Southeast of Spring Mill, Pa., Betsy Levin	160 141	44	52	*654*	850	D. Gottfried, personal communication

(*continued on next page*)

[1] Alpha activity measured by H. W. Jaffe.

[2] Spectrographic examination of 5 mg sample, single determination.

[3] Spectrographic examination on 15 mg sample, single determination.

TABLE 3 (*continued*)

Rock types, locality and supplier	α/mg/hr.	Mean lead ppm (duplicate determinations)		Lead-alpha ages Million years		Remarks
		Previous method	Present method	Previous method	Present method	
Baltimore gneiss, BL-2. Pegmatized band, River Road, Southeast of Spring Mill, Pa., Betsy Levin	144 130	41	61	670	1060	D. Gottfried, oral communication (1960)
Baltimore gneiss, BL-3, Concordant felsic band, River Road, southeast of Spring Mill, Pa., Betsy Levin.	191 173	51	81	630	1060	D. Gottfried, oral communication (1960)
Baltimore gneiss, BL-4, Light felsic band in gneiss, 1 mile southeast of Spring Mill, Pa., Betsy Levin.	237 228	62.5	105	620	1040	D. Gottfried, oral communication (1960)
Baltimore gneiss? BL-5, Concordant felsic garnetiferous band, north side of Glen Mills Quarry, Glen Mills, Pa., Betsy Levin.	663 608	104	215	380	820	D. Gottfried, oral communication (1960)
Baltimore gneiss? BL-6, Cross-cutting folded pegmatite in altered gabbro. Glen Mills quarry, Glen Mills, Pa., Betsy Levin.	234 211	41	44	405	500	D. Gottfried, oral communication (1960)
Cranberry gneiss, Deyton Bend, North Carolina, G. R. Tilton	124	39	57	734	1040	D. Gottfried, oral communication (1960), Tilton and others (1959)
Scarn at Old Whitestone Farm, Natural Bridge, New York, A. T. Buddington, H. D. Holland	224	66	110	771	1100	G. R. Tilton and others, (1957)

(Tilton and others, 1957). In addition, igneous rocks may contain mixed zircons, and the possible effects of the xenocrysts on the lead-alpha age are not easily evaluated. Any of these factors would tend to give older lead-alpha ages.

The calculated alpha activities in Table 1 were derived from the equation

$$\alpha = 0.366\,\mathrm{U} + 0.089\,\mathrm{Th}$$

where α is in units of alpha counts per milligram per hour, and the Th and U contents are in parts per million.

The age equations (Gottfried and others, 1959, p. 14–17) are

$$t = \left[\frac{2632 + 624\,\mathrm{Th{:}U}}{1 + 0.312\,\mathrm{Th{:}U}}\right]\frac{\mathrm{Pb}}{\alpha} = C\,\frac{\mathrm{Pb}}{\alpha}$$

and

$$t_0 = t - 1/2\, kt^2$$

The age equation, t, is used for samples which are younger than 200 million years and, t_0, for samples which are older than 200 million years. For most zircons, the Th:U ratios vary within an order of magnitude of a 1:1 ratio, and in the absence of thorium and uranium analyses, ages are calculated based on a 1:1 Th:U ratio. This assumption gives a value of 2485 for C and introduces an error in the calculation when the Th:U ratio deviates from 1:1. When the Th:U ratio is actually less than 1:1, the apparent age will be younger than the age derived from the actual ratio. This situation exists for the 12 samples given in Table 2. Both of the calculated lead-alpha ages are reported. The actual Th:U ratios are given in Table 1. The maximum error introduced by assuming a fixed 1:1 ratio is about 5 per cent for the samples reported. Recent work at the U. S. Geological Survey has shown that Th:U ratios may be measured by x-ray fluorescence to a lower limit of 50 ppm for each element. The Th:U ratios may then be used in the age calculation.

Based on the assumption that lead in zircon is primarily of radiogenic origin, the lead-alpha method has been considered to be most nearly comparable to the Pb^{206}/U^{238} isotopic age. As indicated in Table 2, when the Pb-U ages are concordant, the lead-alpha age may be expected to agree favorably. It is known, however, that the Pb/U ages obtained from zircon concentrates of Precambrian rocks commonly are discordant. Few data are at present available for discordant zircons and the correlation between lead-alpha and discordant Pb-U isotopic ages remains to be investigated.

The lead-alpha method is of great value as a reconnaissance tool. Its speed and simplicity are particularly advantageous. Only small amounts of zircon are required; 75 milligrams for the nondestructive alpha measurement, and 15 milligrams for each lead determination. With the refinement recently achieved in the determination of lead in zircon, the usefulness of the technique will be extended further. The method is of particular value for preliminary scanning of zircon samples prior to isotopic analysis and is a useful supplement to potassium-argon and rubidium-strontium age determinations.

Acknowledgments

The authors are indebted to G. R. Tilton of the Geophysical Laboratory, Carnegie Institute of Washington, D. C., and L. T. Silver, California Institute of Technology for samples of zircon which they had

dated by isotopic methods. These samples were used in the present study.

We are indebted to S. S. Goldich for numerous helpful suggestions during the preparation of this paper.

References

Berkey, C. P., 1907, Structural and stratigraphic features of the basal gneisses of the Highlands: *New York State Museum, Bull.* **107.**

Cooke, C. W., and Cloos, Ernst, 1951, Geologic map of Prince Georges County and the District of Columbia: *Maryland State Dept. Geology, Mines and Water Resources.*

Davis, G. L., Tilton, G. R., Aldrich, L. T., Wetherill, G. W., and Faul, Henry, 1957, The age of rocks and minerals: *Carnegie Institute of Washington Year Book* **56,** 164–171.

Gottfried, David, Jaffe, H. W., and Senftle, F. E., 1959, Evaluation of the lead-alpha (Larsen) method for determining ages of igneous rocks: *U. S. Geol. Survey Bull.* **1097A,** 1–63.

Jaffe, H. W., 1955, Precambrian monazite and zircon from the Mountain Pass rare earth district, San Bernardino County, California: *Geol. Soc. America Bull.* **66,** 1247–1256.

Jaffe, H. W., Gottfried, David, Waring, C. L., and Worthing, H. W., 1959, Lead-alpha age determinations of accessory minerals of igneous rocks (1953–1957): *U. S. Geol. Survey Bull.* **1097B,** 65–148.

Rose, Harry, Jr. and Stern, Thomas, 1960, Spectrochemical determination of lead in zircon for lead-alpha age measurements: *Am. Mineral.*, **45,** 1243–1256.

Silver, L. T., McKinney, C. R., Deutsch, Sarah, and Bolinger, Jane, 1960, Precambrian age determinations in some crystalline rocks of the San Gabriel Mountains of Southern California (abs.): *Jour. Geophysical Research*, **65,** p. 2522.

Tilton, G. R., Davis, G. L., Wetherell, G. W., and Aldrich, L. T., 1957, Isotopic ages of zircon from granites and pegmatites: *Am. Geophys. Union Trans.*, **38,** 360–371.

Tilton, G. R., Davis, G. L. Wetherill, G. W., Aldrich, L. T., and Jäger, Emilie, 1959, The ages of rocks and minerals: *Carnegie Institute of Washington Year Book* **58,** 170–178.

Tilton, G. R., Wetherill, G. W., Davis, G. L., and Hopson, C. A., 1958, Ages of minerals from the Baltimore gneiss near Baltimore, Maryland: *Geol. Soc. America Bull.* **69,** 1473.

Waring, C. L. and Worthing, Helen, 1953, A spectrographic method for the determination of trace amounts of lead in zircon and other minerals: *Am. Mineral.* **38,** 827–833.

Manuscript received July 20, 1960.

THE AMERICAN MINERALOGIST, VOL. 46, MAY–JUNE, 1961

ANALYTIC CLASSIFICATION AND QUADRIPLANAR CHARTING OF ANALYSES WITH NINE OR MORE COMPONENTS*

JOHN B. MERTIE, JR., *U. S. Geological Survey, Beltsville, Maryland*

ABSTRACT

Analytic methods are used for the classification of analyses having nine or more components, though under favorable conditions such analyses may also be charted. A square matrix of the third order is formulated with three columns that represent 3-dimensional Cartesian vectors extending outward from the origin. The end points of these vectors are triads of coordinates defined by the percentages of a given analysis. By means of a collineatory transformation, such a matrix is transformed to a new frame of reference wherein these vectors appear as intercepts on new axes of X, Y, and Z. Thus 9 numbers are reduced to 3 unique numerical indices.

The algebraic procedure required for a collineatory transformation consists in the solution of a cubic equation derived from the determinant of a characteristic matrix. The roots of this equation, known as characteristic roots, latent roots, or eigenvalues, are found to be the elements in the principal diagonal of a diagonalized matrix, whose other elements are zeros. The sum of these roots is called the trace or spectrum (T) of the transformed matrix. If the roots are real numbers, their three values together with (100-T) may be taken as quadriplanar coordinates for charting inside or outside a tetrahedron of reference. Thus each analysis may be represented by a single point, which may then be projected either apically or orthogonally onto one or more of the triangular faces of the tetrahedron, for a 2-dimensional representation. Complex roots cannot be charted, but the analyses of most igneous rocks yield real roots.

A refinement of this method by the use of symmetrical matrices eliminates complex roots, and thus renders charting universally feasible. Symmetry with respect to the principal diagonal is produced before diagonalization by post-multiplying an unsymmetrical matrix of the third order by its transpose. A generalization of this operation consists in post-multiplying a rectangular array of the order 3×4, 3×5, 3×6, or in general $3\times(3+k)$ by its transpose. This constitutes a third method which provides for the classification and charting of 12, 15, 18, or in general $9+3k$ variables; and if one or two zeros are introduced into the rectangular arrays, any number of variables in excess of 9 may be analyzed. The insertion of one to four zeros in a square matrix of the third order, before it is multiplied by its transpose, makes it possible to handle 8, 7, 6, or 5 variables. These three methods are not interchangeable; instead one is selected and used for the required purpose.

INTRODUCTION

The classification and charting of a number of variables, especially the components of analyses that sum to 100, is a matter of perennial interest to most scientific workers. In two earlier papers the writer (1948, p. 324–336 and 1949, p. 706–716) presented methods for charting 5, 6, and 7 variables on the triangular and tetrahedral boundaries of hypertetrahedra of 4, 5, and 6 dimensions; but suitable coordinate nets could not be devised for more than 7 variables. These, however, were essentially multiple charts, in that the variables were charted as triads with reference

* Publication authorized by the Director, U. S. Geological Survey.

to bounding triangles, or at most as tetrads with reference to bounding tetrahedra. Such graphs had the advantage that the variations of 3 or 4 components between consecutive analyses were shown; but the variations of all the components of the analyses could not simultaneously be charted. This is the dilemma in dealing with many variables.

An alternative solution of this problem is a group classification and charting of analyses, whereby the initial variables are so combined as to formulate a smaller number of composite variables. This condensation, however, must be accomplished by algebraic processes such that the new variables are unique, that is, they cannot assume identical values from the components of different analyses. An example of the improper combination of variables would be to add or multiply three components of an analysis. This sum or product would not constitute a unique composite variable, as the same numerical value could be obtained from different analyses. An analogy of the contemplated process, if one were dealing with an equation of 9 variables, would result if this equation was partially differentiated for 3 variables, say

$$\frac{\partial f}{\partial x}, \quad \frac{\partial f}{\partial y} \text{ and } \frac{\partial f}{\partial z};$$

and if the new equation was charted with regard to these three partial derivatives after numerical values had been assigned to the other variables. But we are dealing with percentages, or numbers, not with functions, and a process must be devised to combine these into a small number of unique numbers that can be interpreted either as numerical indices of the analyses or as numerical data for empirical charting. It has seemed best to accomplish this objective by the formulation of 3 new variables, each of which is a function of all the components of an analysis. This, however, is group classification and group charting, which will show distinct differences between total analyses, but will not ordinarily show quantitatively the mode of variation of the individual components of analyses. The thinking and perception of the operator must become adjusted to this different objective.

Matrices will be utilized to develop the proposed method. Most geologists are familiar with the elementary properties and uses of determinants, as that topic is treated in courses of college algebra. Matrices, however, are less well understood, for which reason a brief description of the nature of a matrix seems desirable. Perhaps the best way to describe a matrix is to show the differences between it and a determinant. A determinant, as is well known, is a square array of numbers, symbols, or functions in rows and columns, say 3 rows and 3 columns, or in general n

rows and n columns, enclosed by 2 vertical bars. As the array is square its order may be stated merely by the use of a single digit, calling it a determinant of the nth order. A matrix is a similar array enclosed by double instead of single vertical bars, but it may be either square or rectangular. If rectangular, its order is stated by 2 digits specifying respectively the number of rows and columns, say the order of 3×4, 8×5, or in general $m\times n$.

A more fundamental difference between a matrix and a determinant is that the matrix is merely an array of elements with assigned meanings, according to the problem under investigation, but with no composite value. A determinant, on the other hand, is a square array of elements, which represents a complex function, that has a determinable numerical or algebraic value. In fact, a determinant may be regarded as a function of some square matrix, such that it may be written as $|A|=f(\|A\|)$. Both matrices and determinants may be subjected, not merely to the elementary operations of addition, subtraction, multiplication, division, involution, and evolution, but also to more highly involved algebraic processes, though the manipulative rules are different. A special kind of algebra, called matrix algebra, has been developed for the treatment of matrices.

The operations of ordinary arithmetic and algebra are controlled by five laws, which are as follows:

1. Commutative principle in addition (and subtraction)
2. Commutative principle in multiplication (and division)
3. Associative principle in addition (and subtraction)
4. Associative principle in multiplication (and division)
5. Distributive principle in combined addition and multiplication.

If one or more of these laws is voided, a new type of algebra results, that operates only by the non-voided principles. Thus the commutative principle is voided in the multiplication and division of matrices, wherefore the so-called matrix algebra has been evolved. If both the second and fourth laws are voided, the Cayley algebra results; and other algebras may similarly be developed. In this paper, square and rectangular matrices are multiplied, for which reason the operation of matrix multiplication should be understood; but no further applications of matrix algebra are required.

Matrices originated as tabulations of coefficients in systems of linear equations, providing a shorthand device for the solution of such equations. They are now utilized, however, for many other purposes, according to prior agreement as to the meaning of their elements. They are extensively used in the study of vectors, tensors, and related entities; in variate statistical analysis; in multiple factorial analysis; and in numer-

ous other applications. In this paper, the utilization of matrices is rather empirical, but is related to vectorial and factorial analysis.

Formulation of Matrix

Consider a system of three-dimensional Cartesian coordinates, with a vector that starts at the origin and extends outward into the first octant to a point defined by 3 coordinates. The values of these coordinates will be taken as the percentages of SiO_2, Al_2O_3 and Fe_2O_3 in a rock analysis recomputed to total 100%. A second vector, likewise starting at the origin, will be connected to a point determined by the percentages of FeO, MgO, and CaO; and a third vector will similarly be constructed, using the percentages of Na_2O, K_2O, and R, where R means the sum of the remaining components of the analysis. These triads are tabulated as three columns to form a square matrix of the third order, though rows instead of columns could equally well be utilized. This matrix may now be operated upon algebraically in such a way that its three component vectors will be transformed to a new system of Cartesian coordinates wherein each vector will become an intercept on one of the new coordinate axes. The terminal of a 3-dimensional intercept has three coordinates, of which two are zeros; and hence for a specified axis it may be identified by a single number. Therefore each of the three original vectors will similarly be represented by a single number, thus reducing nine percentages to three numerical indices.

A change in origin is accomplished in ordinary analytical geometry by stating the coordinates and rotation of the new frame of reference in terms of the old one, and in making the transformation by means of enabling equations. In the present transformation, however, no such data are given but two limiting geometric conditions serve to localize the new frame of reference. One of these is that the coordinates of the three intercepts shall lie on the extension of the three original vectors; the other is that a triangle formed by connecting the ends of the three intercepts shall be parallel to and therefore similar to the triangle formed by joining the terminals of the three original vectors. Owing to these limitations, such a change in the frame of reference is called a collineatory or similarity transformation.

Derivation and Solution of Cubic Equation

A square matrix of the third order, formulated in the manner outlined above, is used to obtain a cubic equation, from which the required numerical indices are derived. Such a matrix, called A, is shown below in generalized form, using the double subscript type of notation for its nine elements. The required transformation is obtained by subtracting from

A the quantity λI, where I is the unit or identity matrix, and λ is a general variable.

$$\|A - \lambda I\| = \begin{Vmatrix} a_{11} & a_{12} & a_{13} \\ a_{21} & a_{22} & a_{23} \\ a_{31} & a_{32} & a_{33} \end{Vmatrix} - \lambda \begin{Vmatrix} 1 & 0 & 0 \\ 0 & 1 & 0 \\ 0 & 0 & 1 \end{Vmatrix} = \begin{Vmatrix} a_{11} - \lambda & a_{12} & a_{13} \\ a_{21} & a_{22} - \lambda & a_{23} \\ a_{31} & a_{32} & a_{33} - \lambda \end{Vmatrix}.$$

As every square matrix defines a determinant, the matrix $\|A-\lambda I\|$ may now be interpreted as the determinant $|A-\lambda I|$, which is expanded to obtain its algebraic value. This is accomplished, not by the ordinary method of clearing a determinant of the third order, but by means of one of Laplace's expansions, which permits the writing of the coefficients of λ as minor determinants, thus:

$$|A - \lambda I| = -\lambda^3 + (a_{11} + a_{22} + a_{33})\lambda^2 - \left[\begin{vmatrix} a_{11} & a_{12} \\ a_{21} & a_{22} \end{vmatrix} + \begin{vmatrix} a_{22} & a_{23} \\ a_{32} & a_{33} \end{vmatrix} + \begin{vmatrix} a_{11} & a_{13} \\ a_{31} & a_{33} \end{vmatrix} \right] \lambda + \begin{vmatrix} a_{11} & a_{12} & a_{13} \\ a_{21} & a_{22} & a_{23} \\ a_{31} & a_{32} & a_{33} \end{vmatrix}$$

This reduces to

$$\begin{aligned} f(\lambda) = & -\lambda^3 + (a_{11} + a_{22} + a_{33})\lambda^2 \\ & - [(a_{11}a_{22} + a_{22}a_{33} + a_{11}a_{33}) - (a_{12}a_{21} + a_{23}a_{32} + a_{13}a_{31})]\lambda \\ & + [(a_{11}a_{22}a_{33} + a_{12}a_{23}a_{31} + a_{13}a_{21}a_{32}) - (a_{13}a_{22}a_{31} + a_{23}a_{32}a_{11} + a_{33}a_{12}a_{21})] \end{aligned}$$

Written in generalized form and equated to zero, this equation becomes

$$\lambda^3 + b\lambda^2 + c\lambda + d = 0$$

where b and d are negative coefficients, though their numerical values may prove to be either positive or negative. A critical examination of the make-up of coefficients b, c, and d will convince the most skeptical person that the cubic equation in lambda obtained from the percentages of one analysis cannot be duplicated by similar data from any other analysis. The matrix $\|A-\lambda I\|$ is known as the characteristic matrix of A; the cubic equation in lambda is called the characteristic equation of A; and the roots of this equation are designated as characteristic roots, latent roots, or eigenvalues.

The nature of the roots of a general cubic equation may be predicted from its discriminant, that is,

$$\Delta = 18bcd - 4b^3d + b^2c^2 - 4c^3 - 27d^2$$

If the sign of this discriminant is positive, there are three real roots; if the sign is negative, there are one real and two conjugate complex roots. A third alternative, where $\Delta = 0$, will not materialize in dealing with decimal fractions. A trigonometric solution is used if the roots are real; otherwise Cardan's solution is employed. These standard methods of

solving cubic equations will be found in any textbook on the theory of equations, such as that written by Dickson (1939, p. 42–51).

Special mention should be made of a small book by Salzer, Richards, and Arsham (1958), entitled a "Table for the solution of cubic equations." Only 6 of the 161 pages of this book refer to real roots so that these, with the permission of the authors, could be photographed and made available to anyone interested in these methods. For the general cubic, the argument of these tables is a quantity

$$\theta = \frac{q^2}{p^3}, \quad \text{where} \quad p = c - \frac{b^2}{3}, \quad \text{and} \quad q = d - \frac{bc}{3} + \frac{2b}{27};$$

but for the cubics solved in this paper, it must be remembered that the coefficients b and d are negative. The tables yield the values of $f_1(\theta)$, $f_2(\theta)$, and $f_3(\theta)$; and the three roots are

$$\lambda_n = -\frac{q}{p} f_n(\theta) - \frac{b}{3}.$$

It should be noted that the value of λ_1, as used in this manuscript, is derived from $f_3(\theta)$, λ_2 from $f_2(\theta)$, and λ_3 from $f_1(\theta)$. On the other hand, the real root of a Cardan solution, which is derived from $f_1(\theta)$ of the tables, is designated by the writer as λ_1. Even with the preliminary computations required, these tables obviate a large part of the labor of solving cubic equations by standard methods.

Application of Eigenvalues

An important theorem of matrix algebra states that any nonsingular ($|A| \neq 0$) matrix with distinct latent roots may be reduced by a collineatory transformation to a diagonal matrix, wherein the elements of the principal diagonal are the latent roots or eigenvalues of the given matrix. All other elements of the diagonal matrix are zeros. This process, called the diagonalization of a matrix, is shown below, first in generalized form where λ_1, λ_2, and λ_3 are the latent roots of the characteristic cubic; and second in specific numerical form, where the 9 elements of the original matrix are the percentages in a mean analysis of 90 biotite granites, and the 3 elements in the diagonal matrix are the derived eigenvalues.

$$\begin{Vmatrix} a_{11} & a_{12} & a_{13} \\ a_{21} & a_{22} & a_{23} \\ a_{31} & a_{32} & a_{33} \end{Vmatrix} \rightarrow \begin{Vmatrix} \lambda_1 & 0 & 0 \\ 0 & \lambda_2 & 0 \\ 0 & 0 & \lambda_3 \end{Vmatrix}$$

$$\begin{Vmatrix} 71.66 & 1.10 & 3.06 \\ 14.49 & 0.87 & 4.13 \\ 1.46 & 1.97 & 1.26 \end{Vmatrix} \rightarrow \begin{Vmatrix} 71.967 & 0 & 0 \\ 0 & -1.709 & 0 \\ 0 & 0 & 3.532 \end{Vmatrix}$$

This diagonal matrix is unique except for the order in which the latent roots are enumerated, as the transformation does not assign the intercepts represented by these numbers to particular axes of the new frame of reference. Obviously, therefore, the elements of the principal diagonal, which constitute the numerical indices of this method, could be written in the order $a_{11}a_{22}a_{33}$, $a_{11}a_{33}a_{22}$, $a_{22}a_{11}a_{33}$, $a_{22}a_{33}a_{11}$, $a_{33}a_{11}a_{22}$, or $a_{33}a_{22}a_{11}$. In reality a geometric study will show that at least 6 frames of reference will satisfy this transformation. This indeterminacy has been overcome in the following way. A cubic equation with real roots is solved by means of several algebraic substitutions, of which the last makes use of the trigonometric function cos X. After the first root is obtained from cos X, the other roots are obtained respectively from cos $(120°+X)$ and cos $(240°+X)$. The roots λ_1, λ_2, and λ_3 in the principal diagonal are enumerated in this order.

Twenty groups of analyses of igneous rocks and 4 of mafic minerals taken from granitic rocks were selected to show the application of this method. These are presented in Table 1.

The eigenvalues derived from these 24 groups of analyses are shown in the first three columns of Table 2. It will be noted that 22 of the derived cubics yield real roots, and that the exceptions are the rock ijolite and the mineral biotite. In general it appears that most igneous rocks can be represented by 3 real numerical indices, though exceptions other than the two cited have also been found.

Certain relationships appear in these eigenvalues. The values of λ_1 are near yet invariably greater than the percentages of SiO_2 in the original analyses, but no linear relationship exists, as most of the differences range from 0.2 unit to 2.8 units, though larger differences result from the two Cardan solutions. Negative values of λ_2 are characteristic of the granites, adamellite, tonalite, syenite, monzonite, nepheline syenite, shonkinite, and muscovite. The lamprophyres and monzonite have larger values of λ_3 than the more felsic granitic rocks; hornblende and augite show still larger values; and pyroxenite and peridotite are characterized by the highest values of λ_3. Somewhat different relationships exist for eigenvalues derived from symmetrical matrices.

The sum of each set of three real eigenvalues, which in Table 2 ranges from 50 to 82, is known as the trace or spectrum of the diagonal matrix and is designated as T. The eigenvalues corresponding to each trace could empirically be charted as trilinear coordinates referred to an equilateral triangle having one side equal to the specified trace, and T unit divisions along each side of the triangle. This plotting, however, would not be convenient, as many triangles of different sizes would have to be shown.

TABLE 1. ANALYSES OF IGNEOUS ROCKS AND GRANITIC MAFIC MINERALS

Analyses		Petrographic character	SiO_2	Al_2O_3	Fe_2O_3	FeO	MgO	CaO	Na_2O	K_2O	R
Group	No.										
1	7	High-silica granite (Johannsen)	74.88	11.66	1.66	1.40	0.05	0.65	3.99	4.87	0.84
2	2	Two-mica granite (Johannsen)	75.52	14.82	1.27	0.73	0.20	1.72	3.47	4.58	0.69
3	90	Biotite granite (Tschirwinsky)	71.66	14.49	1.46	1.10	0.87	1.97	3.06	4.13	1.26
4	34	Adamellite (Johannsen)	67.76	14.97	1.60	2.11	1.45	2.76	3.67	4.09	1.59
5	19	Tonalite (Johannsen)	66.29	15.68	1.22	3.11	2.15	4.57	4.24	1.42	1.32
6	184	Gabbro (Johannsen)	49.14	17.45	3.75	5.95	6.60	10.59	2.58	1.00	2.94
7	161	Basalt (Daly)	48.78	15.85	5.37	6.34	6.03	8.91	3.18	1.63	3.91
8	9	Pyroxenite (Johannsen)	51.10	2.45	1.92	6.61	27.22	6.90	0.26	0.06	3.48
9	10	Peridotite (Johannsen)	41.95	5.74	4.65	6.82	26.97	6.04	1.11	0.63	6.09
10	32	Minette (Johannsen)	51.13	14.24	3.76	4.39	6.09	6.37	2.40	4.95	6.67
11	54	Kersantite (Johannsen)	52.96	15.66	4.25	4.41	5.79	6.01	3.28	3.10	4.54
12	15	Vogesite (Johannsen)	50.31	15.38	3.71	5.29	6.33	7.58	3.03	2.74	5.63
13	14	Spessartite (Johannsen)	53.07	15.81	3.05	4.83	6.27	7.61	3.60	2.40	3.36
14	10	Syenite (Rosenbusch)	60.06	16.16	2.63	3.37	3.29	4.26	3.08	5.21	1.94
15	6	Monzonite (Rosenbusch)	53.66	15.88	3.73	4.52	4.54	7.77	3.65	4.11	2.44
16	7	Normal diorite (Rosenbusch)	54.88	17.34	2.97	6.23	4.64	7.46	3.48	1.52	1.48
17	43	Nepheline syenite (Daly)	54.63	19.89	3.37	2.20	0.87	2.51	8.26	5.46	2.81
18	20	Essexite (Rosenbusch)	48.60	17.51	4.42	5.72	4.00	8.88	4.30	2.28	4.29
19	16	Shonkinite (Rosenbusch)	46.71	14.82	5.45	4.41	5.66	8.36	4.87	4.90	4.82
20	6	Ijolite (Rosenbusch)	44.32	18.41	3.78	4.71	4.34	9.86	9.35	1.98	3.25
21	4	Muscovite, granitic (Johannsen)	45.66	31.45	4.21	0.94	0.90	0.63	0.82	10.50	4.89
22	34	Biotite, granitic (Tschirwinsky)	36.52	17.00	7.61	14.67	9.32	0.88	1.13	8.19	4.68
23	4	Hornblende, granitic (Johannsen)	48.05	5.30	2.43	9.95	13.97	15.94	1.44	0.90	2.02
24	4	Augite, granitic (Tschirwinsky)	50.80	4.17	5.44	6.62	12.36	18.61	1.28	0.29	0.43

Such unequal triangles, however, will fit at different altitudes within a tetrahedron with a base of 100 unit divisions of the same magnitude; and it is clear that such parallel triangles will lie at distances of $(100-T)$ above the basal triangle of the tetrahedron. Therefore the 3 eigenvalues, $\lambda_1=\alpha$, $\lambda_2=\beta$, and $\lambda_3=\gamma$, and the corresponding altitude $(100-T)=\delta$, as shown in the first four columns of Table 2, will constitute 4 quadriplanar coordinates suitable for charting each analysis as a single point within, or for one or more negative eigenvalues, outside a tetrahedron of reference.

TABLE 2

No.	Quadriplanar coordinates				Trilinear coordinates (Apical projection)			Trilinear coordinates (Orthogonal projection)		
	λ_1	λ_2	λ_3	100-T	α	β	γ	α	β	γ
1	75.194	−1.393	1.970	24.23	99.24	−1.84	2.60	83.27	6.68	10.05
2	72.748	−2.251	2.913	26.59	99.10	−3.07	3.97	81.61	6.61	11.78
3	71.967	−1.709	3.532	26.21	97.53	−2.32	4.79	80.70	7.03	12.27
4	68.361	−1.752	4.191	29.20	96.55	−2.47	5.92	78.10	7.98	13.92
5	67.192	−0.047	2.616	30.24	96.32	−0.07	3.75	77.27	10.03	12.70
6	51.870	2.545	4.265	41.32	88.39	4.34	7.27	65.64	16.32	18.04
7	51.595	1.572	5.554	41.28	87.86	2.68	9.46	65.36	15.33	19.31
8	51.771	3.453	26.576	18.20	63.29	4.22	32.49	57.84	9.52	32.64
9	44.428	5.830	24.751	24.99	59.23	7.77	33.00	52.76	14.16	33.08
10	52.827	0.525	10.538	36.11	82.69	0.82	16.49	64.86	12.56	22.58
11	54.809	0.911	7.570	36.71	86.60	1.44	11.96	67.04	13.15	19.81
12	52.520	1.433	8.317	37.73	84.34	2.30	13.36	65.10	14.01	20.89
13	55.048	0.770	6.882	37.30	87.80	1.23	10.98	67.48	13.20	19.32
14	61.219	−2.160	6.230	34.71	93.77	−3.31	9.54	72.79	9.41	17.80
15	55.538	−2.093	7.195	39.36	91.59	−3.45	11.86	68.66	11.03	20.31
16	57.289	0.122	3.589	39.00	93.92	0.20	5.88	70.29	13.12	16.59
17	56.105	−1.492	3.697	41.69	96.22	−2.56	6.34	70.00	12.41	17.59
18	51.463	0.266	5.161	43.11	90.46	0.47	9.07	65.83	14.64	19.53
19	49.234	−0.881	8.837	42.81	86.09	−1.54	15.45	63.50	13.39	23.11
20	48.018	1.946 ±	4.270i	48.09						
21	46.426	−0.716	5.741	48.55	90.23	−1.39	11.16	62.61	15.47	21.92
22	44.525	2.998 ±	3.712i	49.48						
23	49.697	0.986	13.356	35.96	77.60	1.54	20.86	61.69	12.97	25.34
24	51.694	0.0125	11.883	36.41	81.29	0.02	18.69	63.83	12.15	24.02

rence. The charting of negative trilinear and quadriplanar coordinates has been described in an earlier paper by the writer (Mertie, 1949, p. 707–710).

Perspective drawings would be required to show the positions of many points located by quadriplanar coordinates. Obviously one could not take the time and trouble to do this, and it therefore seems best to project these points onto one or more of the triangular faces of the tetrahedron of reference. A perspective drawing of the inside of a lined tetrahedron is shown in Fig. 1 to illustrate two ways of making the required

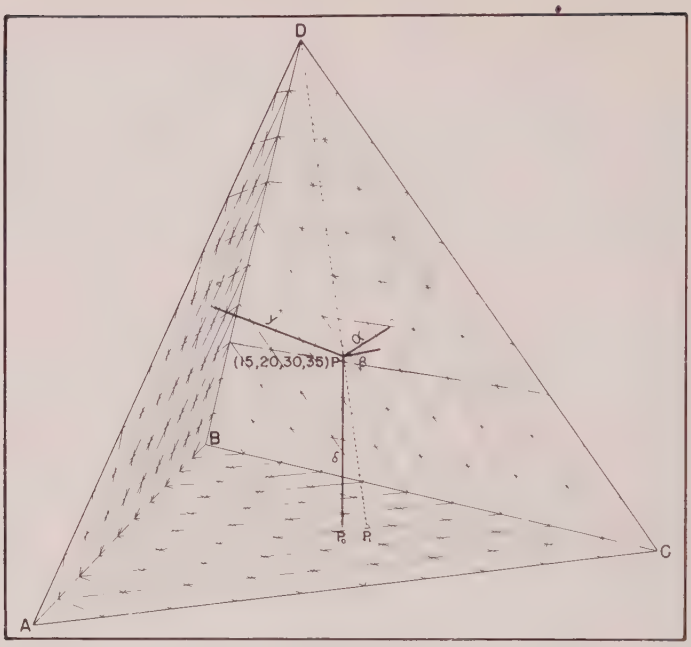

FIG. 1. Perspective drawing of inside of lined tetrahedron, showing apical and orthogonal projections of quadriplanar coordinates.

projection. The point P may be projected apically by the line DP to P_1, in which case the trilinear coordinates of P on the triangle ABC will be the quadriplanar coordinates α, β, and γ, recomputed to 100%. A second method is to project P orthogonally onto ABC, in which case the trilinear coordinates of P_0 will be

$$\left(\alpha+\frac{\delta}{3}\right), \quad \left(\beta+\frac{\delta}{3}\right), \quad \text{and} \quad \left(\gamma+\frac{\delta}{3}\right).$$

This formula may be generalized for the boundaries of hypertetrahedra. By either method, however, a single projection is inadequate, as two points with different quadriplanar coordinates could by either of the two cited methods occupy identical positions in the projection. Moreover, one point that was projected apically might coincide with another point projected orthogonally; but if the projections were reversed, these two points would no longer be superposed. Therefore a projection into one plane of all points by both methods of projection will assure that at least two of the four projected positions of two original points will be unique.

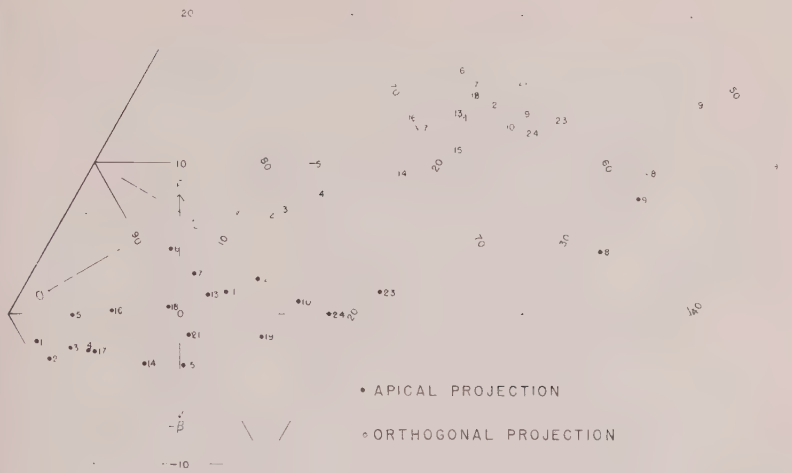

FIG. 2. Projection of quadriplanar coordinates on base of tetrahedron.

The relative positions of the quadriplanar coordinates derived from 19 igneous rocks and 3 granitic minerals are shown in Fig. 2, projected both apically and orthogonally, in order to avoid projections on two triangular faces. The numerical data for these two projections are given respectively in columns 5–7 and 8–10 of table. 2. It happens that these values cause no identical superpositions produced from any of the suggested causes, though points 4 and 17, when apically projected, are close together. By orthogonal projection, however, they are far apart. For this particular assemblage of analyses, a somewhat greater dispersion of points is attained by orthogonal projection. In both projections, the granitic rocks lie at one end of the sequence, the ultrabasic rocks at the other end, and the other 15 rocks and minerals at various intermediate positions.

Variations in the charted positions of analyses resulting from differences in the percentages of specified components are not ordinarily apparent. However, some idea of the magnitude and direction of displacement of a particular point could be obtained in the following way. Suppose that an analysis showing 5% K_2O is so changed that it becomes 2%. This decrement might be added to the percentage of Na_2O, or proportionately to Na_2O and CaO, or it might be distributed throughout the analysis. After the disposition is made, however, a new cubic equation and a new set of eigenvalues may be computed; and for some specific distribution of the 3% K_2O, the displacement of the projected point will be apparent.

Symmetric Matrices

The method of classification and charting so far outlined has the defect that complex numbers may emerge as the latent roots of matrices derived from some analyses; and in applying this method to many kinds of analyses, complex roots might become very prevalent. A refinement of the first method permits the elimination of all complex roots, though the process adds two arithmetical steps. A matrix of real elements that is symmetrical to its principal diagonal is known to have a characteristic equation that yields only real roots. The matrices heretofore used can be rendered symmetrical in the following way. If the rows and columns of a matrix are interchanged, a second matrix is produced that is called the transpose of the first. Either addition or multiplication of a matrix A and its transpose A′ will yield a new matrix that is symmetrical with regard to its principal diagonal. Addition, however, does not insure uniqueness, so that multiplication, which is a combination of multiplication and addition, is used. But owing to this process, the elements of AA′ become large and unwieldy; and they are therefore reduced to total 100 by dividing each element by S/100, were S is their sum. This method of producing a symmetrical matrix, and of obtaining its eigenvalues, is illustrated below for the rock ijolite.

Ijolite, 9 components, from 3×3 matrix

$$AA' = \begin{Vmatrix} 44.32 & 4.71 & 9.35 \\ 18.41 & 4.34 & 1.98 \\ 3.78 & 9.86 & 3.25 \end{Vmatrix} \times \begin{Vmatrix} 44.32 & 18.41 & 3.78 \\ 4.71 & 4.43 & 9.86 \\ 9.35 & 1.98 & 3.25 \end{Vmatrix}$$

$$= \begin{Vmatrix} 2073.87 & 854.89 & 244.36 \\ 854.89 & 361.68 & 118.82 \\ 255.36 & 118.82 & 240.89 \end{Vmatrix}$$

Divided by 51.1256, we get

$$\begin{Vmatrix} 40.56 & 16.72 & 4.78 \\ 16.72 & 7.07 & 2.33 \\ 4.78 & 2.33 & 4.71 \end{Vmatrix} \rightarrow \begin{Vmatrix} 48.13 & 0 & 0 \\ 0 & 0.13 & 0 \\ 0 & 0 & 4.09 \end{Vmatrix}$$

This process leads to an important generalization. Given an analysis of 12 components which are written as a 3×4 matrix, whose transpose is therefore a 4×3 matrix. These two matrices are conformable for multiplication, as expressed in the language of matrix algebra, and their product AA′ becomes a symmetrical matrix of the third order, which is diagonalized as in the original method. An example is given below where ijolite is taken with 12 instead of 9 components, by the separate enumeration of MnO, H_2O, TiO_2, and P_2O_5. The matrix AA′ is nonsingular, and the latent roots are shown to be real numbers.

Ijolite, 12 components, from 3×4 matrix

$$AA' = \begin{Vmatrix} 44.32 & 4.71 & 9.86 & 0.68 \\ 18.41 & 0.13 & 9.35 & 1.36 \\ 3.78 & 4.34 & 1.98 & 1.08 \end{Vmatrix} \times \begin{Vmatrix} 44.32 & 18.41 & 3.78 \\ 4.71 & 0.13 & 4.34 \\ 9.86 & 9.35 & 1.98 \\ 0.68 & 1.36 & 1.08 \end{Vmatrix}$$

$$= \begin{Vmatrix} 2084.13 & 909.66 & 208.23 \\ 909.66 & 428.22 & 90.14 \\ 208.23 & 90.14 & 38.21 \end{Vmatrix}$$

Divided by 49.6660, we get

$$\begin{Vmatrix} 41.96 & 18.32 & 4.19 \\ 18.32 & 8.62 & 1.81 \\ 4.19 & 1.81 & 0.77 \end{Vmatrix} \rightarrow \begin{Vmatrix} 50.48 & 0 & 0 \\ 0 & 0.34 & 0 \\ 0 & 0 & 0.53 \end{Vmatrix}$$

This method may be extended to 3×5, 3×6, and in general 3×(3+k) rectangular arrays, where k is positive. This generalization and its extension thus constitute a third method for the classification and charting of analyses having 12, 15, 18, or in general 9+3k components that total 100. But the number of variables need not necessarily be divisible by 3, as one or two zeros may be substituted for absent components in any rectangular array, before post-multiplication by its transpose.

The classification and charting of fewer than 9 variables constitutes another topic. It might be thought that a 3×2 matrix, involving 6 variables, could be multiplied by its transpose, thus producing a symmetrical matrix of the third order analogous to those obtained from 3×5, 3×6, and 3×(3+k) matrices. But the symmetrical matrix thus obtained will be found to be singular, and therefore unusable.[1] A 2×3 matrix also involves 6 variables, but when multiplied by its transpose yields a square matrix of the second order which will have a quadratic characteristic equation. The eigenvalues derived from such an equation are not unique.

Fewer than 9 variables, however, can be handled by another method. Given a nonsingular square matrix of the third order, such as heretofore shown in generalized form. For the production of 8, 7, 6, or 5 variables, zeros may be substituted as follows:

For 8 variables, let $a_{12}=0$; for 7 variables, let $a_{12}=a_{21}=0$; for 6 variables, let $a_{12}=a_{21}=a_{23}=0$; and for 5 variables, let $a_{12}=a_{21}=a_{23}=a_{32}=0$.

Any of these four alternatives will yield a usable cubic characteristic equation. An example is given below of a weighted mean analysis of all

[1] Theorem. If any real matrix of the order $m\times(m+k)$ and rank $r=m$ be post multiplied by its transpose, two alternatives exist: if k is nonnegative, the resulting symmetrical matrix AA′ of the mth order is nonsingular; but if k is negative, the matrix AA′ is singular.

the platinum metals produced by the Goodnews Bay Mining Co., of Alaska, from 1934 to 1959, inclusive. The mean analysis and its matrix are given below:

Platinum	84.38 per cent	84.38	0	1.35
Iridium	11.49			
Osmium	2.21	0	2.21	0
Ruthenium	0.18			
Rhodium	1.35	11.49	0.18	0.39
Palladium	0.39			

The characteristic equation of this matrix is

$$\lambda^3 - 86.98\lambda^2 + 204.7384\lambda - 38.4467 = 0,$$

whose discriminant is positive, so that the latent roots are real. It therefore is unnecessary to render the matrix symmetrical before diagonalization. The derived eigenvalues are 84.564, 0.206, and 2.210; and $100-T = 13.02$. This may readily be charted either by the apical or orthogonal projection.

Square matrices of the fourth order contain 16 elements; and therefore 4×4, 4×5, 4×6, and in general $4\times(4+k)$ matrices could be used for 16, 20, 24, or in general $16+4k$ variables, where k is nonnegative. The derived characteristic equations, however, are quartics, which are more laborious to solve than cubics; and the five resulting coordinates must be charted on the boundaries of hypertetrahedra of four dimensions. For these reasons, and because matrices of the third order suffice for 9 or any larger number of variables, the utilization of matrices of the fourth order is not recommended.

Summary Statement

Three general methods have been presented for the classification and charting of analyses that are recomputed to total 100 per cent. The first method employs unsymmetrical matrices of the third order, from each of which three eigenvalues and a trace are derived. These are utilized in quadriplanar charting unless the eigenvalues include complex numbers. A second method uses the same original matrices, but they are rendered symmetrical before diagonalization, thus eliminating complex eigenvalues. A third method uses rectangular arrays of the order $3\times(3+k)$ that are transformed into symmetrical matrices of the third order, after which they are treated as in the first and second methods. This permits the classification and charting of 12, 15, 18, or in general $9+3k$ variables. By substituting one or two zeros in the rectangular matrices, the third method allows all analyses with more than 9 components to be utilized.

And by substituting from one to four zeros in square matrices of the third order, before multiplication by their transposes, either the first or the second method permits the use of analyses with 8, 7, 6, or 5 components.

It must be understood that numerical indices and graphs which result from these three methods are not comparable. Even analyses of 12 components, classified and charted by the third method, cannot be tabulated or graphed with similar data obtained by the same method from 15 or more components. A choice of methods that suits the problem in hand is first made; thereafter only one method is used for each group of related analyses.

Bibliography

Mathematics is like geology and mineralogy in that no single exposition includes a complete discussion of all phases of a subject; and therefore for particular topics numerous books are needed. The appended bibliography of books on matrices and related topics is not intended to be an enumeration of all the principal treatises on these subjects. The dozen cited books on matrices include only treatises of comparatively recent origin that have been consulted by the writer in the preparation of this paper. They range from elementary treatments to others that are too advanced to be readily assimilated by a non-mathematician, such as the writer; but even the more abstruse of these discussions contain items that may not elsewhere be available. An example is the volume by Frazer, Duncan, and Collar (1957), which is an advanced treatise; yet it includes four introductory chapters on matrix algebra that are readily understandable and contain many numerical examples of great value.

References

Aitken, A. C., 1942, Determinants and matrices, second edition: Oliver and Boyd, Edinburgh, 135 p.

Bellman, Richard, 1960, Introduction to matrix analysis: McGraw-Hill Book Co., Inc., New York, 328 p.

Browne, E. T., 1958, Introduction to the theory of determinants and matrices: Univ. of North Carolina Press, Chapel Hill, 270 p.

Dickson, L. E., 1939, New first course in the theory of equations: John Wiley and Sons, Inc., New York, 185 p.

Ferrar, W. L., 1941, Algebra, a text-book of determinants, matrices, and algebraic forms: Oxford Univ. Press, London, 202 p.

Frazer, R. A., Duncan, W. J., and Collar, A. R., 1957, Elementary matrices and some applications to dynamics and differential equations, second edition: Cambridge Univ. Press, London, 416 p.

Gantmacher, F. R., 1954, A theory of matrices; part 2, entitled "Applications of the theory of matrices": Translated from Russian and revised in 1959 by J. L. Brenner, D. W. Bushaw, and S. Evanusa: Interscience Publishers, Inc., New York, 317 p.

Hohn, F. E., 1958, Elementary matrix algebra: The Macmillan Co., New York, 305 p.

MacDuffee, C. C., 1953, Vectors and matrices: Mathematical Association of America, Buffalo, 203 p.

Mertie, J. B., Jr., 1948, Charting five, six, and seven variables on hypertetrahedral faces: *Am. Mineral.*, **33,** 324–336.

———, 1949, Charting five and six variables on the bounding tetrahedra of hypertetrahedra: *Am. Mineral.* **34,** 706–716.

Perlis, Sam, 1952, Theory of matrices: Addison-Wesley Press, Inc., Cambridge, 237 p.

Salzer, H. E., Richards, C. H., and Arsham, Isabelle, 1958, Table for the solution of cubic equations: McGraw-Hill Book Co., Inc., New York, 161 p.

Thomson, Godfrey, 1951, The factorial analysis of human ability, fifth edition: Univ. of London Press, Ltd., 383 p.

Thurstone, L. L., 1947, Multiple-factor analysis; a development and expansion of "The vectors of mind": Univ. of Chicago Press, Chicago, 535 p.

Turnbull, H. W., and Aitken, A. C., 1952, An introduction to the theory of canonical matrices: Blackie and Son, Ltd., London, 200 p.

Wade, T. L., 1951, The algebra of vectors and matrices: Addison-Wesley Press, Inc., Cambridge, 189 p.

Manuscript received June 25, 1960.

DILLNITE AND ITS RELATION TO ZUNYITE

J. Konta and L. Mráz, *Institute of Petrography, Caroline University, Prague, Czechoslovakia.*

Abstract

New data on dillnite from Banská Belá, Czechoslovakia, are given. Dillnite is cubic, and occurs in minute tetrahedrons, with $n=1.563$ and $G=2.87$. The formula is $Al_{16}Si_6O_{25}(OH, F)_{18}Cl$. A new analysis has been made, with special attention to the determination of OH, F and Cl.

Dillnite and zunyite form a series in which OH and F can substitute for each other within broad limits, but the content of Cl is nearly constant. Zunyite has a low F content and higher refractive index, and the name dillnite is used for material with high F content and lower index.

Introduction

Dillnite from Banská Belá (formerly Dilln) near the old mining region of Banská Štiavnica in Czechoslovakia, was described in 1849 by A. Hutzelmann. A historical survey of dillnite has been given (Konta, 1955). According to six published analyses, dillnite contains 22.33–24.97 SiO_2, 53.00–56.40 Al_2O_3, and the loss on ignition is 18.4–21.75%.

Until recently, dillnite was not considered to be a specific mineral, but rather a mixture of kaolinite and diaspore. During a systematic study of the clay minerals of Czechoslovakia, dillnite was reexamined in our laboratory by *x*-ray, D.T.A., gravimetric thermal analyses and determination of the refractive index. It was found that it is not a mixture, but a specific mineral (Konta, 1955). As the material studied was named dillnite in 1849, one of the authors (J.K.) did not think it necessary to now change the name.

Dr. W. T. Schaller, of the U. S. Geological Survey, noticed that the *x*-ray pattern of dillnite as reported (Konta, 1955) was practically identical with those of zunyite, and suggested to us that further investigation was needed. It was then that the F and Cl content of dillnite was discovered.

Optical Data

The dillinite from Banská Belá occurs in minute tetrahedrons, mostly below 2 microns in size. It is isotropic, and the refractive index of 1.563 is essentially lower than those of known zunyites (Table 1). This value (originally given as 1.559) was confirmed by Drs. J. Kouřimský and V. Šípek, from the National Museum in Prague.

It was thought possible that the lower index of dillnite might be caused by a thin film of some amorphous material such as opal or allophane. However, after successive boiling for 30 minutes in HCl,

HNO_3 and finally HF, with washing with hot water after each acid treatment, the refractive index remained unchanged.

Determination of Volatile Constituents

Since the determination of F, Cl and OH in this insoluble silicate presents a difficult analytical problem, we describe briefly the methods used. The data were obtained on finely pulverized dillnite, sieved through a 200-mesh screen (aperture 0.074 mm.), and dried at 110° until the weight was constant.

Table 1. Refractive Indices of Dillnite and Zunyite (Na Light)

This paper	J. Kouřimský	V. Šípek
	Dillnite	
1.563	1.563±0.003	1.563±0.001 (single crystal) 1.564 (aggregates)
	Zunyite	
Zuñi Mine, Colorado (Quoted by Nell, 1930 1.595 Gossner and Mussgnug 1.6022 M. Albis	Lake Balkhash 1.590–1.594 Astashenko and Moleva, 1939 Postmasburg, S. Africa 1.600±0.001 Vermaas, 1952	
1.589±0.003 E. S. Larsen	Palembang, Sumatra 1.595 Druif, 1948	

Total loss on ignition

Three 1 gm. samples were heated repeatedly to 1000° C. until the weight was constant, and the loss in weight was determined to be 20.75, 20.72 and 20.70% respectively. A 2 gm. and a 1 gm. sample were heated at 1100° C. until the weight was constant, and showed losses of 20.97 and 21.04% respectively.* The value of 21.04% was considered to be the most reliable.

The dehydration data and the D.T.A. curves are given in the paper of Konta (1955). The newly obtained curves are the same.

Volatile components remaining in the ignited sample

The samples which had the loss of 20.97 and 21.04% were used to determine the residual amounts of F and Cl. For the first, this proved to be Cl 0.23–0.20%; F 0.15%. For the second sample, Cl 0.12%; F 0.07–0.05%. Fluorine remains in smaller quantity than chlorine, although its

* After the emptying of the powder, some still adhered to the walls and bottom of the crucible in the 2 gm. sample. The 1 gm. sample came out in a smooth-surfaced single piece.

original content is nearly six times as great. The chlorine can be released only with great difficulty, from which it seems apparent that it is more firmly bound in the structure of dillnite than is fluorine.

Determination of hydroxyl

During ignition all three volatile components escape simultaneously. Hence the determination of OH was done by a modified method of Penfield (1894). Three different ½ gm. samples of powdered dillinite were each mixed with 0.5 gm. of PbO (dried at 600° C.) and placed in small glass bulbs made of high temperature glass. The mixture was covered with 0.5 gm. of PbO. These determinations gave the values 6.35, 6.65 and 6.41%, with an average of 6.47% of H_2O. The water gave negative tests for F and Cl.

TABLE 2. CONTENT OF FLUORINE IN DILLNITE FROM BANSKÁ BELÁ, CZECHOSLOVAKIA

							Average value
	a	*b*	*c*	*d*	*e*		
Fluorine determined by pyrohydrolysis in platinum apparatus	12.34	12.31	12.37	12.38	12.39	12.46	12.38% F
	g	*h*	*i*				
Fluorine determined in glass apparatus:	12.52	12.48	12.61				12.54% F
Final average value							12.46% F

Determination of fluorine

Results of the determination of F in dillnite by two different methods are given in Table 2. First, F was determined on 6 different 0.1 gm. samples (*a*-*f*) by pyrohydrolysis in a platinum apparatus according to Fresenius *et al.* (1949) and Warf *et al.* (1954). The catalyst was U_3O_8. Final volumetric determination of HF was done by 0.05 M thorium nitrate after previous neutralizing and by addition of buffer (pH = 3.8) in the presence of alizarine sodium monosulfonate as indicator.

Other determinations were made in a glass distilling apparatus after the method of Willard and Winter (1933), modified by Richter (1942) and by the volumetric method of Hoskin and Ferris (1936). Three 0.2 gm. samples of dillnite (*g*-*i*) were analyzed. Final determination was

made by titration with 0.05 M. thorium nitrate as stated above. The experiences of Romo and Roy (1957) and of Turková (1957) were taken into consideration in this determination.

We consider the determination of fluorine in the glass-apparatus to be more reliable, because the analyzed specimens were fused in a mixture with 1 to 2 grams of sodium and potassium carbonate and thus completely decomposed. The liberation of fluorine during the dissolving of the carbonate fusion was complete.

A final determination of the hydrofluoric acid after pyrohydrolytic treatment was also made by titration with sodium hydroxide solution. Phenolphtalein was used as indicator. The results differed considerably (14.76%, 16.32% and 15.46%), and are too high, as follows from the comparison of the sum of the determined amounts of fluorine, chlorine, and hydroxyl water with the total loss of ignition. Therefore we consider the determination of fluorine by sodium hydroxide solution to be less accurate, even after the correction for chlorine.

Determination of chlorine

This was determined by two methods after water extraction of finely pulverized dillnite fused with sodium and potassium carbonate. In the first three samples the chlorine was determined by potentiometric titration of the extraction of the carbonate fusion, neutralized with nitric acid, after removing the silicic acid and the sesquioxides. The titration was done with $AgNO_3$, as described in detail by E. Müller (1942). The values obtained were 2.26, 2.17, 2.30; average 2.25% Cl. In the remaining three samples the Cl was determined gravimetrically as AgCl, after removing the silica and sesquioxides (according to Hillebrand *et al.* 1953), with values of 2.19, 2.16, 2.16; average 2.17% Cl, giving a final average of 2.21% Cl.

Determination of SiO_2, Al_2O_3 and other oxides

Owing to the high fluorine content it was necessary to use a different method than usual for the silicate analysis. All of the existing analyses of dillnite (collected in the paper by J. Konta, 1955) are in error because of the presence of fluorine. If it is not first removed, it has an adverse influence during the whole analysis. Part of the Si volatilizes as SiF_4, after the dissolution of the carbonate fusion during the coagulation of the silicic acid from the chloride solution, and also during the dehydration of the silica by ignition. Thus the real content of SiO_2 may be reduced several per cent. The presence of fluorine also affects the determination of CaO, for part of the F forms CaF_2, which is weighed with the SiO_2

TABLE 3. NEW CHEMICAL ANALYSIS OF DILLNITE FROM BANSKÁ BELÁ, CZECHOSLOVAKIA

	No. 1	No. 2	No. 3	Average	Mol Quotients	Atomic ratios
SiO_2	26.55	26.61	26.30	26.48	0.4409	Si 0.4409
TiO_2	0.76	0.79	0.80	0.78	0.0098	Ti 0.0098
Al_2O_3	56.21	56.00	56.30	56.17	0.5510	Al 1.1020
Fe_2O_3	0.05	0.07	0.05	0.06	0.0004	Fe 0.0007
CaO	0.82	0.79	0.88	0.83	0.0142	Ca 0.0142
MgO	0.19	0.19	0.18	0.19	0.0047	Mg 0.0047
MnO	0.01	0.01	0.01	0.01	0.0001	Mn 0.0001
H_2O^+	6.47	6.47	6.47	6.47	0.3591	OH 0.7182
F	12.50	12.50	12.50	12.50	0.6579	F 0.6157
				(−0.8)	(−0.0422)	
Cl	2.20	2.20	2.20	2.20	0.0620	Cl 0.0620
Less O for F, Cl	5.66	5.66	5.66	5.66		O 1.8637
	100.10	99.97	100.03	100.03		Al:Si:O=15:6:25 OH:F:Cl∼10:8:1

and partially with the Al_2O_3, whose apparent content is thus increased, with the CaO being correspondingly decreased.

The influence of boron was eliminated by the evaporating of the borax fusion with methyl alcohol saturated with dry HCl. After complete removal of boron, the SiO_2 was determined as usual. The other oxides were determined as follows: Al_2O_3 was determined gravimetrically by orthohydroxyquinoline, by drying at 140° C.; TiO_2, Fe_2O_3 and MnO were determined colorimetrically; CaO and MgO were determined complexiметrically, CaO with calcion as indicator (Körbl and Vydra, 1957), and MgO with eriochrome black (Přibil, 1953).

Table 3 gives the results of the quantitative chemical analysis of dillnite from Banská Belá from three 0.5 gm. samples. After the subtraction of 0.8% F, which is probably present as fluorite (Konta, 1955), the approximate formula of dillnite is

$$Al_{15}Si_6O_{25}(OH, F)_{18}Cl$$

Comparison of these results with earlier analyses shows that errors were mainly in the determination of SiO_2 and CaO, as well as in hydroxyl water, F and Cl.

Density of dillnite

The density determined pycnometrically at 20° C. is 2.87. In the original work there is a misprint: namely 2.67_5.

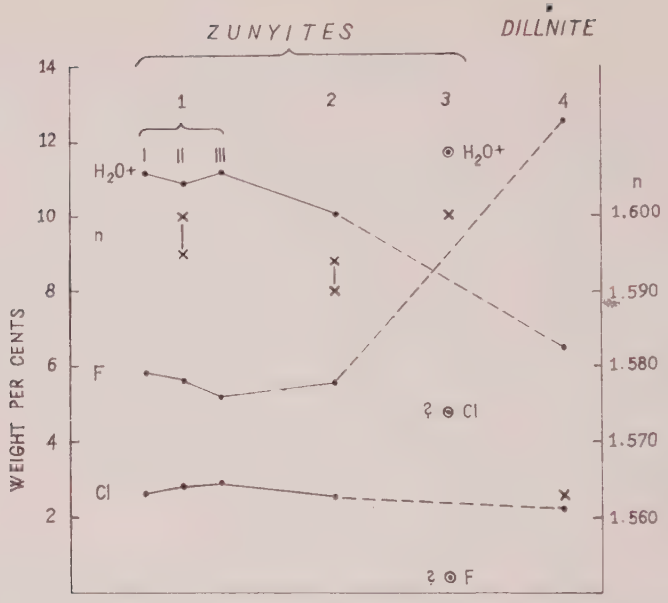

FIG. 1. The chief differences in chemical composition and refractive indices (indicated by x) of zunyites and dillnite.

(1) Zunyite from Zunyi mine, Colorado. (Nel, 1930, writes "Zuni" mine). Gossner and Mussgnug (1929): I H_2O^+ 11.12%, F 5.81, Cl 2.62; II H_2O^+ 10.89, F. 5.61, Cl 2.91; III H_2O^+ 11.12, F 5.19, Cl 2.90, $n=1.595$ (detd. by the authors), $n=1.6022$ (detd. by M. Albis, 1921) and quoted by Nel, (1930).

(2) Zunyite from Karabas, near Lake Balkhash in Kazakhstan. Astashenko and Moleva (1939) H_2O^+ 10.03, F 5.52, Cl 2.56, $n=1.590$–1.594.

(3) Zunyite from Postmasburg, South Africa. Vermaas (1952) H_2O^+ 11.65, F 0.40, Cl 4.80, $n=1.600\pm0.001$.

(4) Dillnite from Banská Belá, Czechoslovakia. H_2O^+ 6.47, F 12.46, Cl 2.2, $n=1.563$.

The Relation of Dillnite to Zunyite

From the determined data, it is evident that dillnite and zunyite form an isomorphous series in which within fairly broad limits the fluorine and hydroxyl can replace each other. The content of chlorine is relatively constant in all of the samples studied (Fig. 1).

The formula of zunyite given by Pauling (1933) as $Al_{13}Si_5O_{20}(OH,F)_{18}Cl$ seems to correspond better with the results on dillnite than the formulas $Al_8Si_3O_{12}(OH,F,Cl)_{12}$ (Palache, 1932) and $Al_{13}Si_5O_{20}(OH,F,Cl)_{19}$ (Vermaas, 1952).

Material with lower fluorine and higher refractive index is named zunyite, and that with higher content of fluorine and lower index is named dillnite.

Acknowledgments

The authors wish to express their gratitude to Dr. W. T. Schaller of the U. S. Geological Survey in Washington for calling our attention to the close relation of dillnite to zunyite and for his interest in the progress of this work, and to Dr. J. Kouřimský and Dr. V. Šípek from the National Museum in Prague for the determination of the refractive index of dillnite.

References

Astashenko, K. I. (1939), Zunyite, the zunyite rocks and associated ores: *Izvest. Akad. Nauk SSSR, ser. geol.*, No. **5,** 158–167.

Astashenko, K. I. and Moleva, V. A. (1939), Zunyite and zunyite rocks of Karabas: *Doklady Akad. Nauk SSSR*, **22,** 327–330.

Druif, J. H. (1948), On the occurrence of diaspore and zunyite in detrital sediments of Palembang: *Mededeelingen van het Algem. Proefstation voor de Landbouw* (*Communic. General Agricult. Experim. Station*), *Buitenzorg, Java*, No. **67,** 5.

Fresenius, R., Kurtenacker, A., Eichler, A. and Santer, O. (1949), Bericht über die Fortschritte der analytischen Chemie: *Zeits. anal. Chemie*, **129,** 410–423.

Gossner, B. and Mussgnug, F. (1926), Die chemische Zusammensetzung von Zunyit: *Centralbl. f. Mineralogie etc., Abt. A*, 149–155.

Hillebrand, W. F. (1884), Proc. Col. Soc., **1,** p. 124. Quoted in Dana's System of mineralogy. 6th edition, (436).

Hillebrand, W. F., Lundell, G. E. F., Bright, H. A. and Hoffman, J. I. (1953), Applied inorganic analysis with special reference to the analysis of metals, minerals and rocks. 2nd ed., New York.

Hoskins, W. N. and Ferris, C. A. (1936), A method of analysis for fluoride: *Ind. Eng. Chem. Anal.* ed., **8,** 6–9.

Hutzelmann, A. (1849), Ueber den Dillnit und Agalmatolith, die Begleiter des Diaspors von Schemnitz: *Poggend. Annalen Phys. und Chemie, 3. Reihe*, **18,** 575–578.

Konta, J. (1955), Dillnit—ein spezifisches Tonmineral: *Chemie der Erde*, **17,** 223–232.

Körbl, J. and Vydra, F. (1957), Metallochromic indicators, IV. Note on the preparation and properties of "calcein": *Chemické listy*, **51,** 1457–1461, Prague.

Müller, E. (1942), Die Elektrometrische Massanalyse. 6th edition, Dresden-Leipzig, (117–125).

Nel, L. T. (1930), A new occurrence of zunyite near Postmasburg, South Africa: *Miner. Mag.*, **22,** 207–221.

Palache, Ch. (1932), Zunyite from Guatemala: *Am. Mineral.*, **17,** 304–307.

Pauling, L. (1933), The crystal structure of zunyite, $Al_{13}Si_5O_{20}(OH, F)_{18}Cl$: *Zeits. Krist.*, **84,** 442–452.

Penfield, S. L. (1894), Ueber einige Methoden zur Bestimmung des Wassergehaltes: *Zeits. f. anorg. Chemie*, **7,** 22–32.

Přibil, R. (1953), Komplexony v chemické analyse. (The complexions in chemical analysis.) Naklad. Českosl. akademie věd, Prague, pp. 162 (on p. 59, 70–71).

Richter, F. (1942), Die colorimetrische Bestimmung von Fluor in einfachen und komplexen Fluoriden mittels Zirkon-Alizarin-Farblackes: *Zeits. anal. Chemie*, **124,** 161–215.

Romo, L. A. and Roy, R. (1957), Studies of the substitution of OH^- by F^- in various hydroxylic minerals: *Am. Mineral.*, **42,** 165–177.

Turková, J. (1957), Volumetric estimation of microgram quantities of fluorine in a car-

bonate and phosphate by a modified method of Willard and Winter: *Universitas Carolina, series Geologica,* **3,** 227–245.

Vermaas, F. H. S. (1952), Zunyite from Postmasburg, South Africa: *Am. Mineral.*, **37,** 960–965.

Warf, J. C., Cline, W. D. and Tevebaugh, R. D. (1954), Pyrohydrolysis in the determination of fluoride and other halides: *Anal. Chem.*, **26,** 342–346.

Willard, H. H. and Winter, O. B. (1933), Volumetric method for determination of fluorine: *Ind. Eng. Chem., Anal. ed.*, **5,** 7–10.

THE AMERICAN MINERALOGIST, VOL. 46, MAY-JUNE, 1961

FIRST U. S. OCCURRENCE OF MANGANOAN CUMMINGTONITE, TIRODITE

CURT G. SEGELER, *Brooklyn, New York.*

ABSTRACT

Tirodite, a Mn amphibole, was discovered in an Indian manganese deposit in 1938. It has now been found in the form of transparent pink crystals at Talcville, New York. The properties are compared with those of cummingtonite. Since the Talcville material is very low in Fe, the specific gravity and refractive indices are lower than those reported for the Indian material. $\alpha=1.620$, $\beta=1.630$ and $\gamma=1.635$. New chemical analyses are given of the tirodite and two tremolites from Talcville.

INTRODUCTION

During a recent visit to the International Talc Co. mines at Talcville, N. Y., in search for more specimens of groutite (Segeler, 1960), some light pink fibrous masses were found, in which were embedded distinct bladed pink crystals an inch in width and up to three inches long. (Fig. 1). The pink crystals were well known to the mine operators, and had been analyzed by Mr. Orton Smalley, the mine chemist. The high Mn and low Ca contents suggested that this material is not tremolite. Dr. Brian Mason of the New York Museum of Natural History kindly made an *x*-ray powder photograph, which was found to resemble that of cummingtonite. Three lines not found in cummingtonite are present, and the intensities of some lines vary.

The name cummingtonite refers to the monoclinic Fe-Mg amphibole. The new mineral is clearly a Mn-Mg amphibole, and is sufficiently different to be identified by a varietal name. In 1851, Erdmann found an Fe-Mn amphibole which he called dannemorite, after its Swedish locality (Dana, 1884). This is now regarded as a varietal name of cummingtonite. However, the new Talcville mineral does not resemble dannemorite.

Before proposing a new name for this variety, a search was made in the Indian Geologic Survey Records. Dunn and Roy (1938) described a Mn-amphibole which they had found at a manganese mine at Tirodi, India, and named it tirodite. Bilgrami (1955) reported the same mineral from the Sitasgoni Mine, Chikla, India. He also repeated the analysis of a specimen from Tirodi. His data do not closely match those of the Talcville material, but this is probably due to the difference in Fe content. The same mineral has also been reported from Nagpur, India, by Zwaan and van der Plas (1958). Their *x*-ray data are in general agreement with the data given in this paper.

A specimen of tirodite from Tirodi, India, has been compared with the

FIG. 1. Typical specimen of tirodite from Talcville, N. Y.

Talcville material. *X*-ray powder photographs taken by Dr. Brian Mason of these two tirodites match very closely (Fig. 2) and the optical data, other than the refractive indices, check very well.

PROPERTIES OF TIRODITE

Tirodite occurs at Talcville in transparent pink blades embedded in a matrix of fibrous pink anthophyllite. Both the association and occurrence are quite different from the Indian material.

Monoclinic: cleavage (110) perfect. (100) imperfect. Striated parallel to *c*, and shows

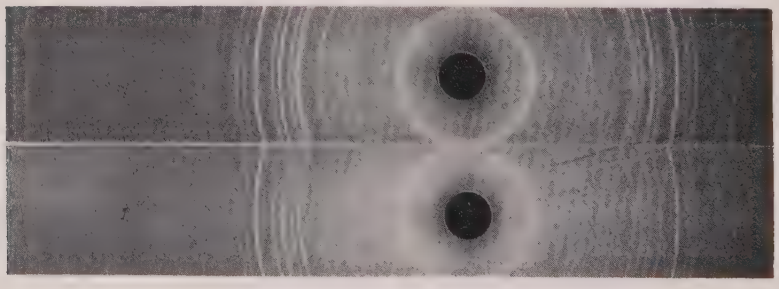

FIG. 2. *X* ray powder photographs of tirodite. Above Talcville, N. Y.; below Tirodi, India. FeK_α radiation.

TABLE 1. CHEMICAL ANALYSES OF TIRODITE AND TREMOLITE

	Tirodite						Tremolite	
	Talcville (1)						Talcville (1)	
	Pink	Rose	Chikla (2)	Tirodi (3)	Tirodi (2)	Chavel-tice (4)	Dark purple Hexago-nite	White
SiO_2	58.80	58.78	53.26	53.26	53.25	53.69	58.96	59.16
TiO_2			0.78		0.79			
Al_2O_3	1.20	0.58	2.26	1.25	2.31	1.65	1.48	0.88
Fe_2O_3		0.72	2.60	2.63	1.81	0.32		
FeO			1.12	1.06	1.62	5.94		
MgO	24.80	25.86	29.16	31.21	28.42	20.50	24.32	24.18
CaO	2.72	2.38	1.10	1.11	3.42	1.20	12.12	12.44
MnO	10.08	8.70	6.24	8.25	4.66	16.10	1.55	0.30
Na_2O			1.39	1.56	1.25			
K_2O			0.09	0.07	0.06			
H_2O	2.54	1.26	1.87	0.05	2.04	0.70	2.47	2.79
Total	100.14	99.28	99.87	100.50	99.63	100.19	100.25	100.90

Analyses as follows:

1. Orton Smalley, International Talc Co.
2. Bilgrami (1955).
3. Dunn and Roy (1938).
4. Rabbitt, No. 90 (1948).

many parting lines parallel to (001). $=73°$. Brittle. Hardness 6.5; G = 3.07. Optical properties: biaxial; $\alpha=1.620$, $\beta=1.630$, $\gamma=1.635$; $2V=74°$ on universal stage; $X=a$, $Y=b$, $Z:c=16°$. Pleochroism: X colorless, Y yellowish, Z colorless.

In Table 1, the chemical analyses of tirodites and two tremolites from Talcville are given, and compared with tirodite from other localities. Table 2 compares the *x*-ray powder photograph data of tirodite and cummingtonite.

Rabbitt (1948) discussed the role of MnO in anthophyllite and cummingtonite. He listed two specimens (41 and 43) from Edwards, N. Y. as the purest anthophyllites known. On earlier maps Talcville was not usually shown, but Edwards is an old community, and is nearest to present day Talcville. It is therefore quite probable that these two specimens are also from Talcville. They seem to be quite similar to the matrix in which the tirodite crystals are embedded. They contained 2.53

TABLE 2. COMPARISON OF X-RAY DATA FOR TIRODITE AND CUMMINGTONITE
CAMERA DIAMETER 114.6 MM.; FeK_α, Mn FILTER

Tirodite (Talcville)		Cummingtonite (New Zealand)		Tirodite		Cummingtonite	
d	I	*d*	I	*d*	I	*d*	I
9.03	7	9.41	4	2.19	4	2.21	5
8.35	9	8.51	10	2.09	2	2.11	2
5.16	2	5.28	1	2.04	1	2.05	2
4.85	4	4.87	1	1.973	1	1.961	2
4.53	5	4.60	1	1.870	2	—	
4.17	2	4.17	2	1.811	1	1.801	1
3.88	6	3.90	3	1.707	3	—	
3.44	3	3.51	3	1.661	5	1.667	3
3.36	3	3.38	2	1.629	2	1.639	1
3.25	5	3.28	3	1.598	3	1.605	2
3.09	8	3.10	9	—	—	1.561	1
2.98	6	3.01	2	1.517	4	1.526	3
2.74	10	2.77	10	1.492	1	—	—
2.61	4	2.64	6	1.415	4	1.410	5
2.52	6	2.53	7	1.380	2	1.389	1
2.32	3	2.31	2	1.298	4	1.336	1
2.26	1	2.24	1	1.187	3	1.305	4

and 2.77% Mn, respectively. It appears likely that geologic conditions favored Mn enrichment to the point where tirodite was formed. Such Mn concentration has previously been mentioned as a possible explanation for the formation of groutite at this locality.

Rabbitt stated that *x*-ray data for the specimen from Chaveltice, Czechoslovakia (No. 90) showed it to be monoclinic, and that in light of its composition, it was dannemorite. In order to evaluate this conclusion, and also to furnish a more complete picture of the MnO:FeO:MgO ratios in some of these amphiboles, the diagram of Fig. 3 was prepared. The following analyses were used: tirodites from Table 1; cummingtonites from Rabbitt's Table 7, and from Mason (1953); and dannemorite from Dana and No. 84 of Rabbitt.

It seems that the groupings of the points is significant. The tirodites, low in FeO, approach the ideal Mg-Mn amphibole. Cummingtonites show up as Fe-Mg amphibole, with little MnO. Dannemorite is recognizable as a Mn-Fe-Mg variety. No. 90 of Rabbitt, which he called dannemorite, appears to be more appropriately grouped with the tirodites.

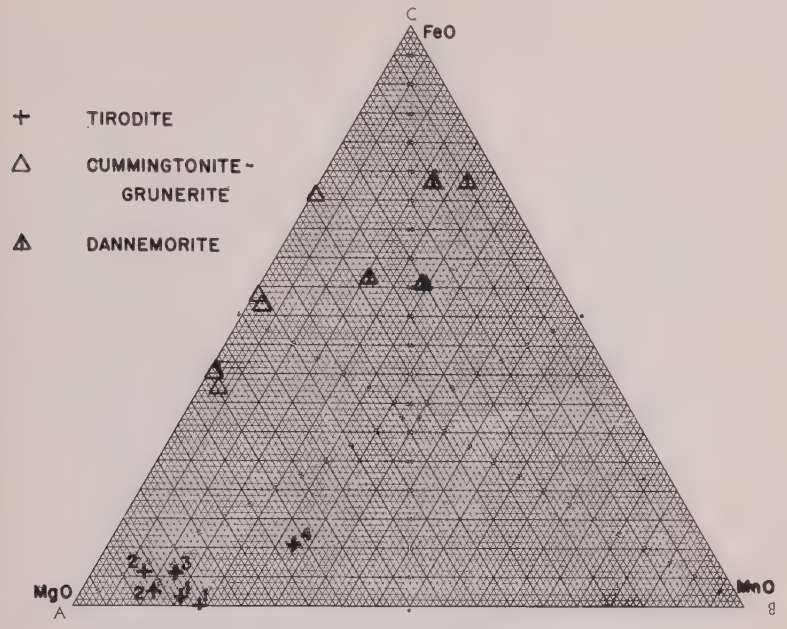

FIG. 3. Diagram showing relative amounts of MgO, FeO and MnO in tirodites (+), cummingtonite-grunerite (Δ), and dannemorite (Δ). The numbers for tirodite correspond to Table 1; cummingtonite-grunerite are from Rabbitt's Table 7; dannemorite from Dana and No. 84 of Rabbitt.

REFERENCES

BILGRAMI, S. A. (1955), Mn amphiboles from Chikla, Bhandara District, India: *Mineral. Mag.* (*London*), **30,** 633.

DUNN, J. A. AND ROY, O. C. (1938), Tirodite, a new Mn mineral: *Misc. Notes, Geol. Sur. India Records*, **73,** 295.

JAFFE, H. W., GROENEVALD MEIJER, W. O. J., AND SELCHOW, D. H. (1961); *Am. Mineral.*, **61,** this issue.

MASON, BRIAN (1953), Cummingtonite from the Mikonui River, Westland, New Zealand: *Am. Mineral.*, **38,** 862–865.

RABBITT, JOHN C. (1948), A new study of the anthophyllite series: *Am. Mineral.*, **33,** 263–323.

ZWAAN, P. C. AND VAN DER PLAS, L. (1958), Optical and x-ray investigation of some pyroxenes and amphiboles from Nagpur, Central Provinces, India: *Kon. Nederlandse Akad. Wetenschappen, Ser. B*, **61,** 265–277.

Manuscript received April 18, 1960.

MANGANOAN CUMMINGTONITE FROM NSUTA, GHANA

HOWARD W. JAFFE, W. O. J. GROENEVELD MEIJER AND D. H. SELCHOW,
Union Carbide Ore Company, Research Center, Tuxedo, N. Y.

ABSTRACT

Manganoan cummingtonite (Mg:Mn:Ca:Fe=60:35:3:2) from a manganese carbonate rock, Nsuta, Ghana, contains more manganese and less iron than any cummingtonite previously described. The unit cell dimensions are: $a_0=9.531$ Å, $b_0=18.10$ Å, $c_0=5.326$ Å, $\beta=102°\ 15'$. Crystals are pale greenish white, acicular-prismatic, non pleochroic and colorless in transmitted light; $\alpha=1.628$, $\beta=1.642$, $\gamma=1.650$, $2V=74°$, biaxial negative, $Z\wedge c=22°$. G.=3.12 (obs.), 3.19 (cacl. from x-ray data), 3.12 (calc. from $(n-1)/d=K$). A revision in nomenclature of the series is suggested whereby cummingtonite, grunerite, and $Mn_7(Si_4O_{11})_{12}(OH)_2$ represent the Mg, Fe^{+2}, and Mn^{+2} end members of an essentially three-component system.

INTRODUCTION

Manganese-bearing amphiboles of the cummingtonite group, described by Sundius (1931) and Bauer and Berman (1930), are all rich in iron. Manganoan cummingtonite from Nsuta, Ghana, is unique in that it contains more manganese (19.2% MnO) and far less iron (1.2% FeO) than any amphibole of this group previously described. It occurs as slender acicular prisms (0.5×0.1 mm.) in a metamorphosed manganese carbonate rock (Fig. 1). The mineral is often intimately associated with a calcian, magnesian rhodochrosite ($n_\omega=1.786$), pure spessartite ($n=1.800$), rhodonite, talc, and minor quartz. At Nsuta, spessartite is a frequent product of low-grade metamorphism of sedimentary manganese carbonate and argillaceous and tuffaceous sediments, whereas rhodonite and cummingtonite are relatively uncommon. The latter minerals appear to have formed in localized shears in carbonate rock.

The cummingtonite group of amphiboles has the formula $X_7(Si_4O_{11})_2(OH)_2$, where X is predominantly Mg, Fe^{+2}, and Mn^{+2}. Manganoan cummingtonite from Nsuta has an X cation ratio of Mg:Mn equal to approximately 60:40. It has lower indices of refraction and specific gravity than its ferroan analogue, Mg:Fe=60:40, and is optically negative, whereas the latter is optically positive. Both manganoan and ferroan cummingtonites have virtually identical *x*-ray powder diffraction patterns which can be readily distinguished from those of the calcium- and sodium-rich amphiboles: tremolite, richterite, edenite, hornblende and others. This distinction results from the presence or absence of the relatively large Ca and Na ions which require eight-fold coordination. These may also occupy some of the normally vacant twelve-fold lattice positions. Warren (1930) has shown that Fe^{+2} and

Mg have six nearest oxygen neighbors closely approaching octahedral coordination in cummingtonite, whereas Ca is eight-fold coordinated in tremolite.

Mineralogy

Separation and purification

The sample was ground in stages to minus 60 mesh and sieved on 100, 200, and 325 mesh screens. Microscopic examination indicated that the optimum mesh of liberation of cummingtonite occurred in the 200–325

Fig. 1. Metamorphosed manganese carbonate rock from Nsuta, Ghana, showing acicular-prismatic manganoan cummingtonite in a matrix of granular calcian, magnesian rhodochrosite, quartz, and spessartite. Crossed nicols ×30.

mesh fraction. This fraction was separated in fresh methylene iodide (density = 3.3) to remove the spessartite garnet, rhodonite, and rhodochrosite. The float fraction, containing the cummingtonite was then separated in bromoform (density = 2.86) to remove quartz. The bromoform sink, composed essentially of cummingtonite (density = 3.12), was then leached in a dilute hydrochloric acid to remove adhering particles of carbonate. The concentrate was then shake-sifted in stages on glossy paper to remove any remaining granular minerals. Microscopic examination and a grain count of the concentrate indicated a purity of >99% cummingtonite prisms containing an estimated 5% of inclusions of spessartite garnet (Fig. 2). This was verified by analysis which yielded 1.1% Al_2O_3 equivalent to a maximum of 5.4% spessartite.

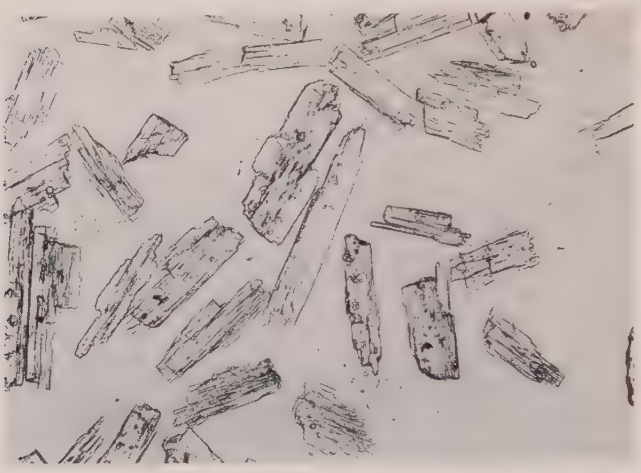

FIG. 2. Manganoan cummingtonite concentrate from carbonate rock. Many of the prisms contain small inclusions of spessartite. Plane polarized light ×45.

Unit Cell

Two small prismatic grains were studied with a single crystal *x*-ray goniometer by R. P. Dodge who obtained the value $b_0 = 18.10$ Å. Three spacings on the *x*-ray powder diffraction pattern at 3.06 Å, 2.61 Å, and 2.51 Å could be identified as the (310), (061), and ($\bar{2}02$) reflections, respectively, by analogy with other monoclinic amphiboles. From these data it was possible to calculate $a_0 \sin\beta$, $c_0 \sin\beta$, $\cos\beta$, β, $\sin\beta$, a_0 and c_0. Warren (1930), who analyzed the structures of the monoclinic amphiboles, noted that tremolite and the cummingtonites have the same space group, ($C_{2/m}$), and similar unit cell dimensions. The unit cell dimensions of manganoan cummingtonite from Nsuta, Ghana, are given in Table 1.

TABLE 1. MONOCLINIC UNIT CELL DATA FOR MANGANOAN CUMMINGTONITE FROM NSUTA, GHANA

$a_0 = 9.531$ Å	Cell volume = 897.9 Å^3
$b_0 = 18.10$ Å	Cell weight = 1725.4
$c_0 = 5.326$ Å	Cell formula = $(Mg, Mn, Ca, Fe)_{14}Si_{16}O_{44}(OH)_4$
$\beta = 102°15'$	Mg:Mn:Ca:Fe = 60:35:3:2
Density = 3.19 (calculated from *x*-ray data)	
3.12 (observed)	
3.12 (calculated from the law of Gladstone and Dale, $(n-1)/d = K$[1]	

[1] $(\alpha+\beta+\gamma)/3 = 1.640$. $K = 0.205148$.

X-ray powder diffraction data

An x-ray powder diffraction pattern of manganoan cummingtonite was obtained with a 57.3 mm. camera using FeK_α radiation ($\lambda = 1.93597$ Å) and a Mn filter. All of the lines measured, down to 1.163 Å, were indexed on the basis of the unit cell data given in Table 1. The x-ray powder diffraction data for manganoan cummingtonite from Ghana and ferroan cummingtonite from Sweden (Johansson, 1930) are compared in Table 2. Cummingtonites may be distinguished from all other monoclinic amphiboles by measurement of the (310) and the ($\bar{6}61$) and ($\bar{6}42$) spacings. These d values and a_0 increase directly with the Ca+Na content going from cummingtonite to edenite (Table 3). Figure 3 compares x-ray powder diffraction patterns of manganoan cummingtonite from Nsuta, Ghana with those of pure white tremolite from Fowler, New York, and dark greenish-black hornblende from a mafic shonkinite from Mountain Pass, California. Both the tremolite and hornblende, which contain essential amounts of the large cations Ca and Ca+Na, respectively, give very similar patterns. The cummingtonite, however, which does not contain significant amounts of either Ca or Na, yields an x-ray pattern that can be readily distinguished from that of either hornblende or tremolite. Noteworthy is the position of a strong line at 1.405 Å on this and other cummingtonite patterns compared with 1.43–1.44 Å in tremolites and hornblendes. This line indexes closer to ($\bar{6}42$) than to ($\bar{6}61$) for manganoan cummingtonite (this paper) and for ferroan cummingtonite of Johansson (1930). In the patterns of natural tremolite, hornblende and synthetic fluor-tremolite, fluor-richterite, and fluor-edenite, the corresponding line indexes much closer to ($\bar{6}61$) than ($\bar{6}42$). Whether a transposition or a true line shift, the position of this strong line serves to distinguish members of the cummingtonite group from all other calcium- and sodium-rich monoclinic amphiboles.

Optical properties

Manganoan cummingtonite from Nsuta, Ghana, occurs as pale greenish white, long prismatic to acicular crystals. It is colorless and non-pleochroic in transmitted light. Multiple twinning on (100) was observed on several crystals. In thin-section, the mineral cannot readily be distinguished from tremolite although the latter has a smaller extinction angle. The indices of refraction of Nsuta cummingtonite are, however, significantly higher than those of tremolite so that the two can be distinguished in immersion media. A manganoan cummingtonite with a lower Mn content than the Nsuta mineral could not be distinguished from tremolite by optical properties alone. Ferroan cummingtonite with

TABLE 2. *X*-RAY POWDER DIFFRACTION DATA FOR CUMMINGTONITES FROM NSUTA, GHANA AND UTTERSVIK, SWEDEN (FeK_α RADIATION, $\lambda = 1.9359$ Å, Mn FILTER)

Nsuta, Ghana			*hkl*	Uttersvik, Sweden	
I (obs.)	*d*(obs.)	*d*(calc.)		*d*(obs.)*	I
20	9.0	9.05	020	—	
80	8.25	8.28	110	8.32	50
20	4.83	4.84	$\bar{1}11$	—	
40	4.52	4.52	040	4.55	10
20	4.14	4.14	220	4.16	10
40	3.86	3.86	$\bar{1}31$	3.87	20
	—	3.59	$\bar{2}21$	3.60	10
30	3.42	3.44	131	3.46	40
		3.41	041		
40	3.24	3.24	240	3.26	50
100	3.06	3.06	310	3.07	40
30	2.96	2.98	221	2.99	10
		2.94	$\bar{1}51$	—	
10	2.75	2.76	330	2.76	100
90	2.73	2.74	151		
40	2.61	2.61	061	2.63	60
80	2.51	2.51	$\bar{2}02$	2.51	60
5	2.37	2.38	$\bar{2}61$	—	
		2.36	350	—	
20	2.29	2.29	$\bar{3}51$	2.30	50
10	2.24	2.24	421	—	
		2.22	$\bar{3}12$	2.23	10
60	2.17	2.18	261	2.19	70
20	2.08	2.09	202	2.10	20
		2.07	440	—	
		2.07	081	—	
10	2.03	2.03	351	2.04	20
10	1.954	1.954	$\bar{4}02$	1.957	20
10B	1.860	1.867	$\bar{1}91$	1.871	10
		1.853	510	—	
10	1.799	1.799	$\bar{5}31$	—	
40B	1.693	1.693	390	—	
	—	1.687	$\bar{5}12$	1.693	10
40	1.651	1.652	461	1.663	60
10	1.620	1.621	480	1.633	40
		1.620	1·11·0		
		1.620	043		
	—	1.594	$\bar{1}53$	1.600	20
40	1.588	1.588	531	—	
	—	1.553	600	1.561	10
	—	1.515	263	1.521	60
50	1.508	1.508	0·12·0		
5	1.486	1.486	0·10·2	—	

TABLE 2. (*continued*)

Nsuta, Ghana			*hkl*	Uttersvik, Sweden	
I (obs.)	*d*(obs.)	*d*(calc.)		*d*(obs.)*	I
5	1.455	1.454	3·11·0	1.465	10
80	1.405	1.405	$\bar{6}42$	1.409	90
	—	1.402	$\bar{6}61$		
5	1.376	1.378	512	1.386	20
		1.377	1·13·0	—	
	—	1.327	710	1.335	40
	—	1.301	004	1.305	10
60B	1.292	1.292	2·12·2	1.291	70
			751	1.280	40
			$\bar{4}04$	1.257	
			602	1.231	
			5·11·2	1.187	
60	1.182	1.183	770	—	
		1.181	642	—	
5	1.163	1.164	800	1.171	
40B	1.113			—	
40	1.056			—	
60	1.037			1.041	
30	1.030			—	
40	1.020			—	
40	1.011			—	
30	1.003			—	
40	0.991			—	
30	0.983			—	
20	0.976			—	
20	0.974			—	

* The ASTM card No. 2-0865 for this mineral contains several errors.

The *d* values cited here were recalculated from the original $\sin^2\theta$ values published by Johansson (1930).

B = broad.

Mg:Fe = 60:40 is optically positive (Sundius, 1931), whereas manganoan cummingtonite from Nsuta, with Mg:Mn = 60:40 is optically negative. The indices of refraction of the manganoan cummingtonite are significantly lower than the ferroan analogue as could have been predicted. The optical properties of manganoan cummingtonite from Nsuta and those of its ferroan analogue from Persberg are compared in Table 4.

CHEMISTRY

Analysis and composition

When it became apparent that the pure material that could be obtained was insufficient for a conventional wet chemical analysis, a

TABLE 3. VARIATION OF a_0, d_{310}, AND $d_{\bar{6}42-\bar{6}61}$ WITH THE Ca+Na CONTENT OF SEVERAL MONOCLINIC AMPHIBOLES

	1 Manganoan cummingtonite	2 "Cummingtonite"*	3 Fluor-tremolite	4 Fluor-richterite	5 Fluor-edenite
a_0	9.53 Å	9.58 Å	9.78 Å	9.82 Å	9.85 Å
d_{310}	3.06 Å	3.07 Å	3.11 Å	3.12 Å	3.12 Å
$d_{\bar{6}42}$ / $\bar{6}61$	1.405 Å	1.409 Å	1.430 Å	1.432 Å	1.435 Å
Ca+Na†	0.45	0.80	3.88	5.86	5.98

* According to the nomenclature proposed in this paper, this mineral is a magnesian grunerite as Fe>Mg or Mn (See Figure 4).

† Cations per 48 oxygens.

1. Nsuta, Ghana, new data.
2. Uttersvik, Sweden, Johansson (1930).
3. Synthetic, Comeforo and Kohn (1954).
4. and 5. Synthetic, Kohn and Comeforo (1955).

quantitative emission spectrographic method was developed by Mr A. L. Hallowell. SiO_2, Al_2O_3, MgO, MnO, FeO, and CaO were determined by internal standardization with cobalt using the following line pairs: Si 2438.8 Co 2989, Al 3082 Co 2989, Mn 2705.7 Co 2989, Mg 2790.8 Co 2989, Fe 2947.8 Co 2989, and Ca 3179 Co 2989. Siliceous manganese ores previously analyzed at the Research Center were used

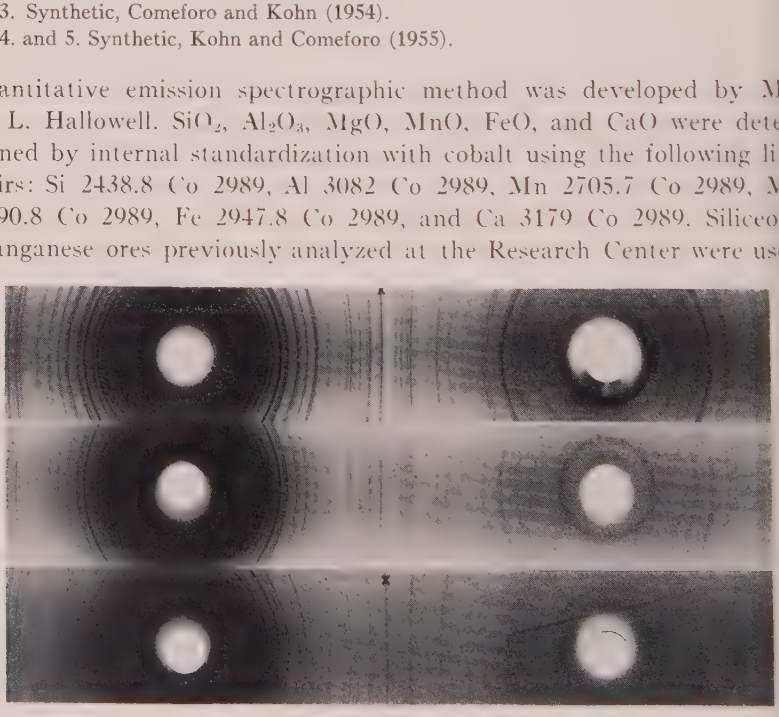

FIG. 3. X-ray powder diffraction patterns. (top) Hornblende, Mountain Pass, Cali X indicates the $\bar{6}61$ line. (middle) Tremolite, Fowler, N. Y. (bottom) Manganoa cummingtonite, Nsuta, Ghana. X indicates $\bar{6}42$ and $\bar{6}61$ lines. (Fe K_α radiation $\lambda = 1.93597$ Å, Mn filter).

s standards for obtaining the necessary working curves. Water was not etermined and is given by difference. Fluorine was determined to be bsent. In order to further check some of the spectrographic determinaions, MnO and MgO+CaO were determined by wet chemical methods n very small amounts of material. The agreement is satisfactory as ndicated in the tabulation of the analytical data (Table 5).

The formula for amphiboles of the cummingtonite-grunerite group nay be written as $X_7(Si_4O_{11})_2(OH)_2$ where X is occupied predominantly y divalent Mg, Fe, and Mn in six-fold coordination (Warren, 1930). Divalent Zn may occupy X positions as in the Franklin Furnace, New ersey, occurrence (Bauer and Berman, 1930), but this is uncommon.

Table 4. Optical Properties of Manganoan and Ferroan Cummingtonite

	1 Manganoan cummingtonite Mg:Mn=60:40	2 Ferroan cummingtonite Mg:Fe=60:40
α	1.628±0.002	1.640
β	1.642±0.002	1.647
γ	1.650±0.002	1.665
$\gamma-\alpha$	0.022	0.025
$Z\wedge c$	22°	20°
2V	74° (calc.)	65°
Optic sign	negative	positive

1. Nsuta, Ghana, new data.
2. Persberg, Sweden, Sundius (1930).

One of the characteristics of the cummingtonite-grunerite group is the bsence of essential amounts of the larger cations Ca and Na in X posiions and the similar absence of Al in tetrahedral positions occupied by Si. Both Ca and Na are coordinated by eight or more oxygens in tremolite and the alkalic amphiboles, depending on the degree of occupancy f the vacant 12-fold sites known to exist in tremolite (Warren, 1930 and Kohn and Comeforo, 1955).

The formula calculated from the analysis of manganoan cummingonite from Nsuta is as follows:

$$\underbrace{(Mg_{4.0}Mn_{2.3}Fe_{0.1}Ca_{0.2})}_{6.6}Si_{8.0}O_{21.8}(OH)_{1.8}$$

his represents one-half of the unit cell formula of cummingtonite. In able 5, the ratios obtained on a basis of anions and cations per unit cell Hey, 1939) are compared with those obtained on a basis of cations per

48 oxygens. Either calculation shows reasonably good agreement with the accepted unit cell formula of cummingtonite:

$$X_{14}(Si_4O_{11})_4(OH)_4$$

Relation between density, index of refraction and chemical composition.

The density of manganoan cummingtonite from Nsuta was measured by suspension of grains in acetone-diluted methylene iodide. The meas-

TABLE 5. SPECTROCHEMICAL ANALYSIS OF MANGANOAN CUMMINGTONITE FROM NSUTA, GHANA

(A. L. Hallowell, analyst)

Oxide	Determined[2]	Recalculated[3]	Anions per Unit Cell		Cations per Unit Cell		Cations on a basis of 48 oxygens
SiO_2	56.0	57.1	32.08	Si	16.04	16.04	16.32
Al_2O_3	1.1						
MnO	20.5*	19.2	4.57	Mn^{+2}	4.57		
MgO	18.1*	19.1	7.99	Mg	7.99	13.29	13.52
FeO	1.1	1.2	0.28	Fe^{+2}	0.28		
CaO	1.4*	1.5	0.45	Ca	0.45		
H_2O[1]	1.8	1.9	1.78	H	3.56	3.56	3.62
	100	100	47.15		32.89		

[1] H_2O by difference.

[2] SiO_2, Al_2O_3, MnO, MgO, FeO, and CaO were determined by internal standardization with cobalt using the following line pairs: Si 2438.8/Co 2989, Al 3082/Co 2989, Mn 2705.7/Co 2989, Mg 2790.8/Co 2989, Fe 2947.8 Co 2989, and Ca 3179 Co 2989.

[3] After deduction of 1.1% Al_2O_3, 2.0% SiO_2, and 2.3% MnO equivalent to 5.4% of spessartite garnet included in cummingtonite.

* Wet chemical determinations made on small samples as a check on the spectrographic results gave: MnO = 19.4 and MgO + CaO = 20.2.

Unit Cell Formula: (from analysis) $(Mg, Mn, Ca, Fe)_{13.3}Si_{15.9}O_{43.6}(OH)_{3.6}$

Mg:Mn:Ca:Fe = 60:35:3:2

ured value, 3.18, was then corrected for the presence of 5.4% spessartite occurring as inclusions in cummingtonite. A density of 4.185 (Yoder 1959, Fleischer, 1937, Skinner, 1956) was assumed for spessartite as it has a measured index of refraction of 1.800 and no calcium, indicating it to be an end member. The corrected value for the density of the manganoan cummingtonite is 3.12. The density calculated from the *x*-ray data (Table 1) and the chemical composition is 3.19 for Mg:Mn:Ca:Fe = 60:35:3:2.

The density was also calculated from the law of Gladstone and Dale

$(n-1)/d = K$ using the optical data (Table 4), the chemical composition (Table 5), and the specific refractive energy values (k) of Larsen and Berman (1934). These are $k_{MgO} = 0.200$, $k_{MnO} = 0.191$, $k_{CaO} = 0.225$, $k_{FeO} = 0.187$, $k_{SiO_2} = 0.207$, and $k_{H_2O} = 0.34$. The calculated density is 3.12, the same as that measured. Agreement between the measured density and that calculated from the law of Gladstone and Dale consistently is excellent for all amphiboles of very diverse composition (Jaffe, 1956).

Nomenclature

The present nomenclature of the cummingtonite-grunerite series is confused and inadequate. Sundius (1931) suggested that the name cummingtonite be reserved for the mineral containing 50–70 mol per cent of the magnesium component and that varieties richer in iron be named grunerite. Mason (1953) has noted that "this proposal would have the curious effect of requiring the original cummingtonite from Cummington, Massachusetts, to be called grunerite." The work of Sundius (1931) and others indicates that this group of minerals may be considered a three component system, with the end members represented by $Mg_7(Si_4O_{11})_2(OH)_2$, "kupfferite," $Fe_7(S_4O_{11})_2(OH)_2$, grunerite, and $Mn_7(Si_4O_{11})_2(OH)_2$, unnamed. Of these only the Fe end member, grunerite, is known to occur naturally. The fluorine analogue of the Mg end member, has however been synthesized by Bowen and Schairer (1935). Inasmuch as the name cummingtonite has priority over all others, the writers suggest that it be assigned to the Mg-dominant member of the series in place of "kupfferite," and that grunerite be retained for the Fe^{+2}-dominant member. The Mn^{+2}-dominant member has not been found or synthesized and a new name is deemed inappropriate. This classification would be more in keeping with the nomenclature of other isomorphous series. The proposed revision in nomenclature is as follows:

cummingtonite—$Mg_7(Si_4O_{11})_2(OH)_2$ with Mg > Fe or Mn
grunerite— $Fe_7(Si_4O_{11})_2(OH)_2$ with Fe > Mg or Mn
$Mn_7(Si_4O_{11})_2(OH)_2$ with Mn > Mg or Fe

The names, cummingtonite and grunerite, could be further qualified by prefixing the terms manganoan, ferroan or magnesian. This classification is illustrated in Fig. 4 on a ternary diagram showing the compositions of the natural cummingtonites and gruneries previously described by Sundius (1931), Winchell (1938), Bowen and Schairer (1935), and Mason (1953). Manganoan cummingtonite from Nsuta (Fig. 4) contains far less iron and more manganese than any of the other cummingtonites described in the literature. Inasmuch as this mineral al-

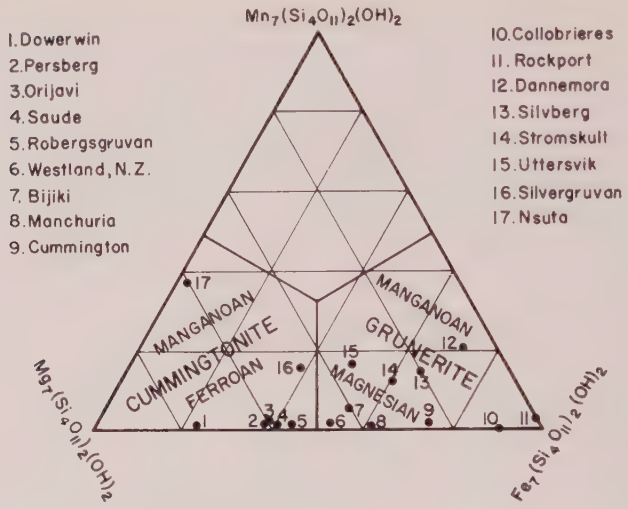

FIG. 4. Composition of cummingtonites and gruneries, and suggested nomenclature.

ready contains almost 40 mol per cent of the Mn component, and the ionic radius of Mn^{+2} is only 7 per cent larger than that of Fe^{+2}, the mineral should be capable of accepting a much larger amount of manganese. No attempt has been made by the authors to synthesize the end member.

ACKNOWLEDGMENTS

The authors are indebted to Mr. H. R. Spedden, Director of Research, Union Carbide Ore Company for collecting the samples described herein, for encouraging the study, and for technical suggestions. Thanks are also due to Mr. A. L. Hallowell, Union Carbide Nuclear Company, for the spectrographic analysis, and Dr. R. P. Dodge, Union Carbide Research Institute, for a single crystal measurement.

REFERENCES

ASANO, GORO (1949), Amphiboles of the grunerite cummingtonite series in banded iron ore from Manchuria: Jour. Jap. Assoc. Mineral., *Petrol., Econ. Geol.*, **32,** 92–98.

BAUER, L. H. AND BERMAN, H. (1930), Notes on some Franklin minerals: *Am. Mineral.* **15,** 340–348.

BOWEN, N. L. AND SCHAIRER, J. F. (1935), Grunerite from Rockport, Massachusetts, and a series of synthetic fluor-amphiboles: *Am. Mineral.*, **20,** 543–551.

COMEFORO, J. E. AND KOHN, J. A. (1954), Synthetic asbestos investigations, I: A study of synthetic flour-tremolite: *Am. Mineral.*, **39,** 537–548.

FLEISCHER, M. (1937), The relation between chemical composition and physical properties in the garnet group: *Am. Mineral.*, **22,** 751–759.

HEY, M. H. (1939), On the presentation of chemical analyses of minerals: *Min. Mag.*, **25** 402–412.

AFFE, H. W. (1956), Application of the rule of Gladstone and Dale to minerals: *Am. Mineral.*, **41,** 757–777.

OHANSSON, K. (1930), Vergleichende Untersuchungen an Anthophyllit, Grammatit und Cummingtonit: *Z. Krist.* **73,** 31–51.

OHN, J. A. AND COMEFORO, J. E. (1955), Synthetic asbestos investigations, II: *X*-ray and other data on synthetic fluor-richterite, -edenite, and -boron edenite: *Am. Mineral.*, **40,** 410–421.

ARSEN, E. S., JR. AND BERMAN, H. (1934), The microscopic determination of the non-opaque minerals: *U. S. Geol. Survey, Bull.* **848,** 2nd Ed., 30–32.

IASON, BRIAN (1953), Cummingtonite from the Mikonui River, Westland, New Zealand: *Am. Mineral.*, **38,** 862–865.

KINNER, B. J. (1956), Physical properties of end-members of the garnet group: *Am. Mineral.*, **41,** 428–436.

UNDIUS, N. (1931), Optical properties of grunerites and cummingtonites: *Am. Jour. Sci.*, **221,** 330–344.

WARREN, B. E. (1930), The crystal structure and chemical composition of the monoclinic amphiboles: *Z. Krist.*, **72,** 493–517.

WINCHELL, A. N. (1938), The anthophyllite and cummingtonite-grunerite series: *Am. Mineral.* **23,** 329.

ODER, H. S. (1951), Complete substitution of aluminum for silicon: the system $3MnO \cdot Al_2O_3 \cdot 3SiO_2$—$3Y_2O_3 \cdot 5Al_2O_3$: *Am. Mineral.*, **36,** 519–533.

Manuscript received June 14, 1960.

THE USE OF ZONE THEORY IN PROBLEMS OF SULFIDE MINERALOGY, PART III; POLYMORPHISM OF Ag_2Te AND Ag_2S

ALFRED J. FRUEH, JR., *Department of Geological Sciences, McGill University, Montreal, P.Q., Canada*

ABSTRACT

Three polymorphs of Ag_2Te exist between room temperature and the melting point. They are, in the order of increasing temperature: monoclinic, face-centered cubic, and body-centered cubic. The transformation temperature between the face-centered cubic and the body-centered cubic forms increases with a slight stoichiometric excess of Ag. The three polymorphs of Ag_2S are, in order of increasing temperature, monoclinic, body-centered cubic, and face-centered cubic. The transformation temperature between the body-centered cubic and the face-centered cubic forms decreases with a slight stoichiometric excess of Ag. An explanation, based on the relative shapes of the n (e) vs. E curves of the two cubic forms, is suggested to explain the increase of the stability range of the face-centered cubic structure with stoichiometric excess of Ag in both these compounds.

INTRODUCTION

The sulfides, selenides and tellurides of silver and copper have for many years been the subject of countless investigations by mineralogists and solid state workers. Some of the interest stems from the unusual property of combined electronic and ionic conductivity exhibited by these compounds. Of equal and related interest is the fact that each possesses a high-temperature or α-phase which is characterized by either a face-centered or body-centered array of anions, with a random or statistical distribution of the cations in the interstitial sites.

A now-classical structural investigation was conducted by Rahlfs (1935). He showed that the diffraction record of the high-temperature α modifications of Ag_2S and Ag_2Se could be explained by placing the sulfur or selenium atoms at the nodes of a body-centered cubic lattice and distributing 1.5 of the 4 silver atoms per cell in the 12(d) positions listed below and the remaining 2.5 silver atoms in the 24(h)+(6b) positions.

	(000; $\frac{1}{2}\frac{1}{2}\frac{1}{2}$+			
6(b)	$\frac{1}{2}00$	$0\frac{1}{2}0$	$00\frac{1}{2}$	
12(d)	$\frac{1}{2}0\frac{1}{2}$	$\frac{1}{4}\frac{1}{2}0$	$0\frac{1}{4}\frac{1}{2}$	
	$\frac{1}{2}0\frac{3}{4}$	$\frac{3}{4}\frac{1}{2}0$	$0\frac{3}{4}\frac{1}{2}$	
24(h)	uu0	$u\bar{u}0$	$\bar{u}u0$	$\bar{u}\bar{u}0$
	u0u	$u0\bar{u}$	$\bar{u}0u$	$\bar{u}0\bar{u}$
	0uu	$0u\bar{u}$	$0\bar{u}u$	$0\bar{u}\bar{u}$

where $u = \frac{5}{8}$.

Rahlfs further described the high-temperature or α modifications of Ag_2Te, $Cu_{1.8}S$ and Cu_2Se as structures in which the tellurium, selenium

r sulfur atoms occupied the corners and face-centers of a cubic cell, and he silver or copper atoms were distributed amongst the octahedral oles, the tetrahedral holes, and the 16-fold positions ($\frac{1}{3}$, $\frac{1}{3}$, $\frac{1}{3}$).

More thorough studies on the phase relations in the systems silver-ulfur and silver-tellurium by F. C. Kracek (1946), and by Kracek and Ksanda,* have revealed additional high-temperature phases. For the urposes of the present paper, the terms α and β will be dropped, and the omenclature utilized by Kracek will be followed. The crystalline hase that can exist in equilibrium with the liquid will be assigned the oman numeral I. Those phases stable at successively lower tempera-ures will be assigned numerals of increasing value.

Polymorphism of Ag_2S

The phase diagram in Fig. 1 shows the temperature range within which each of the three phases of Ag_2S is stable. The effect of stoichiom-try on the temperature of phase change should be noted. A stoichio-metric deficiency of Ag results in an increase in the temperature of the hase change from Ag_2S-II to Ag_2S-I from $586 \pm 3°$ C. to $622 \pm 3°$ C. A maller but similar change is shown between Ag_2S-III and Ag_2S-II.

The structure of Ag_2S-III was shown by Frueh (1958) to be mono-linic, based upon a slightly distorted body-centered cubic array of sul-ur atoms, with the silver atoms on two different but definite positions. One silver position lies between two sulfurs at 2.49 Å and 2.52 Å; the ther between three sulfurs at 2.50 Å, 2.61Å and 2.69 Å.

Ag_2S-II is the same phase referred to previously as α-Ag_2S, and hence as the body-centered cubic structure as determined by Rahlfs and de-cribed above.

A face-centered cubic structure for Ag-S-I has been suggested by Djurle (1958). Due to a very high background blackening, only one line f a Debye-Scherrer powder pattern could be seen by that author. However, all the I-modifications (Cu_2S-I, Ag_3CuS_2-I, $Ag_6Cu_4S_5$-I, AgCuS-I) along the "quasi-binary" line Cu_2S- Ag_2S produce a diffrac-ion record which can be indexed on the basis of a face-centered cubic ell with (220) as the most intense reflection. Djurle, assuming isomorph-sm in all the I-modifications, therefore suggested this same index (220) or the single discernible line of Ag_2S-I. This yields a cubic cell size at 00° C. of $6.269 \pm .02$ Å.

In the present investigation, three lines of d spacings, 3.17 Å, 2.24 Å nd 1.819 Å, were obtained on a powder diffraction of Ag_2S-I from Kongs-erg, Norway, by means of a Unicam high-temperature powder camera,

* F. C. Kracek and C. J. Ksanda, A paper on the Ag-Te system in preparation, private ommunication.

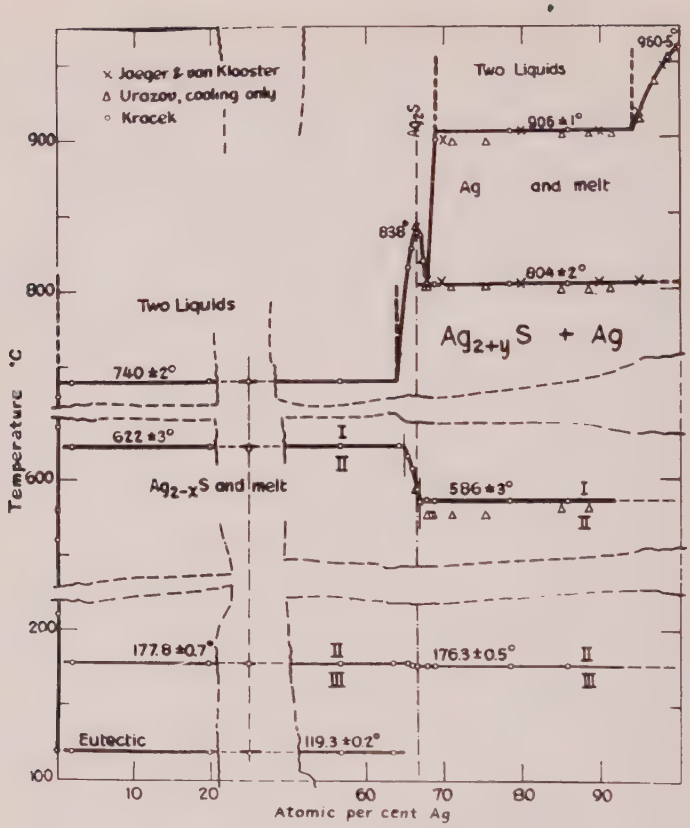

FIG. 1. Phase diagram of the system Ag-S from Kracek (1946).

at 650° C. These can be indexed either as the (100), (110) and (111) planes of a simple cubic cell of $a = 3.17$ Å, or as the (200), (220) and (222) planes of a face-centered cubic cell of $a = 6.34$ Å. Allowing but one formula weight of Ag_2S per unit cell, the calculated density of 12.84 makes the simple cubic cell of edge 3.17 Å an unlikely choice. On the other hand, the face-centered cubic cell of 6.34 Å edge could contain 4 formula weights and have a density of 6.42, which is a little less than the measured density of the room-temperature form (7.2).

POLYMORPHISM OF Ag_2Te

The phase diagram in Fig. 2 shows the temperature range of the stability of the three phases of Ag_2Te. Again, the effect of stoichiometry on the temperature of the phase change should be noted. In the case of the telluride, a stoichiometric deficiency of Ag results in a decrease in

The temperature of the phase change Ag_2Te-II to Ag_2Te-I from 802.3° C. to less than 700° C. A similar change is shown between Ag_2Te-III and Ag_2Te-II, where the transition temperature is lowered from 145° on the silver-excess side to 105° on the silver-deficient side.

The monoclinic structure of Ag_2Te-III was determined by Frueh (1959). Some shifting of tellurium as well as of silver atoms is necessary to transform this structure to the face-centered cubic structure of Ag_2Te-II, or α-phase, that was suggested by Rahlfs and described above.

The structure of Ag_2Te-I has not previously been determined. The powder diffraction record from a Unicam high-temperature camera at

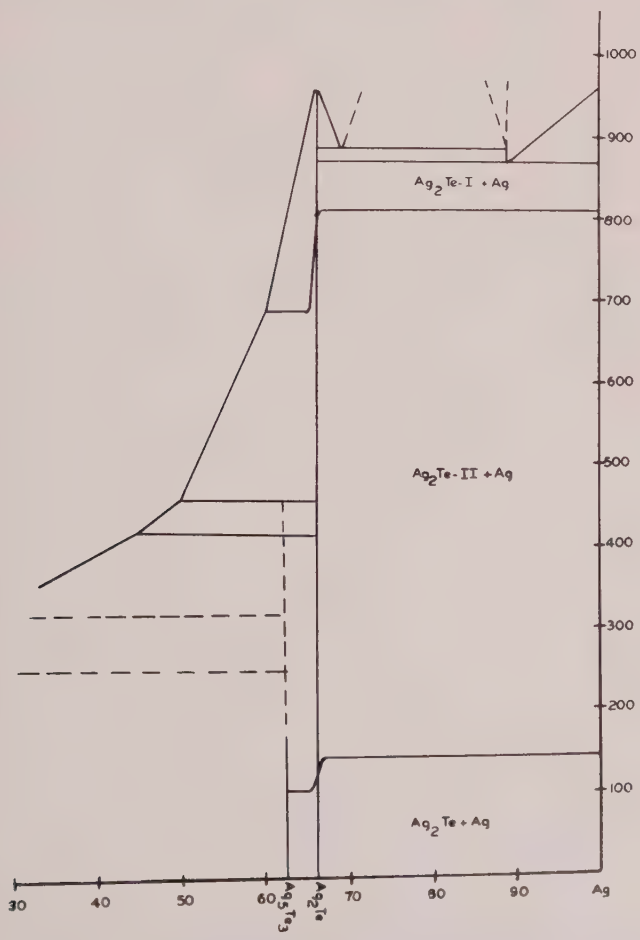

FIG. 2. Tentative phase diagram of the system Ag-Te after Kracek and Ksanda (private communication).

825° C. of a sample of hessite (Ag_2Te) from Bótes, Transylvania, revealed three diffraction lines of about equal intensity above an intense background. These lines had d spacings of 3.74 Å, 2.65 Å and 2.16 Å respectively, and could be indexed as the (110), (200) and (211) planes of a body-centered cubic cell of $a=5.29$ Å.

It would be unreasonable to suppose that a higher-temperature, and hence higher-entropy, form of Ag_2Te would have greater order with respect to the silver positions. Therefore, it is suggested that the structure of Ag_2Te-I is a body-centered arrangement of Te atoms (000, $\frac{1}{2}\frac{1}{2}\frac{1}{2}$), with the silver atoms randomly distributed about the interstitial positions. The randomness of the silver positions, rather than a statistical distribution amongst certain select positions, is borne out by the uniformity of the intensity, albeit weak, of the first three powder lines.

It was noted above that a deficiency of silver in Ag_2S increased the stability range of Ag_2S-II at the expense of Ag_2S-I, while a silver deficiency of Ag_2Te increased the range of Ag_2Te-I at the expense of Ag_2Te-II. However, in both cases the deficiency of silver increases the range of the body-centered phase, while a silver excess favors the face-centered phase.

In seeking a structural explanation for this phenomenon, one would expect that, as the cations are distributed in the interstices of the anion structure, the structure with the greater pore space would be favored when an excess of cations is present. This, however, does not seem to be the case, for the face-centered cell is more efficiently packed, having a pore space of only 26%, while the body-centered cell has a pore space of 32%. Nor is it likely that a treatment based upon packing of spheres and filling of holes would be valid for crystals as far from ideally ionic as Ag_2S and Ag_2Te.

A possible explanation of the phenomenon lies in a semi-quantitative interpretation of the possible band structure of the different phases. Of most interest is the Brillouin zone whose boundaries lie in the vicinity of the Fermi level and delimit the valence band. This particular zone has been referred to recently by Junod (1959) as the Jones zone. If we assume that all the outer-shell electrons contribute to the valence band, then the electron-to-atom ratio of the stoichiometric compounds of Ag_2S and Ag_2Te will be 8/3 or 2.67. The most intense line on the diffraction record of the face-centered phases is always the (220) reflection. The volume of the zone in k space bounded by the dodecahedron comprising this form in terms of electron-to-atom ratio is exactly 8/3.

The band structure of the body-centered phase of Ag_2S has been investigated by Junod (1959) who found that the cube bounded by the (200) form would have a volume of 8/3 electrons to atoms. If this form alone determined the Jones zone, Ag_2S-II would be a semiconductor. As

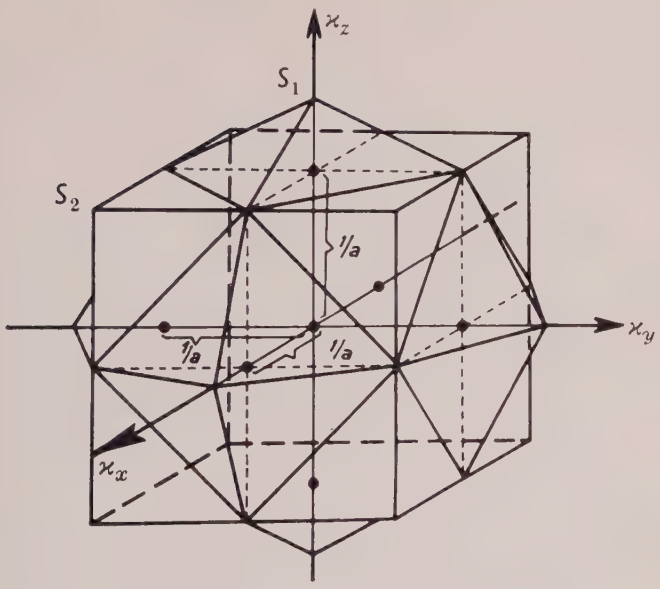

FIG. 3. "Jones" zone of Ag_2S-II, from Junod (1959).

his is in contradiction to observed electrical properties, Junod suggests hat there is some overlap, and that the true Jones zone must be constructed with the help of the (200) and (211) forms (Fig. 3).

Because a dodecahedron more closely approaches the shape of a phere than does a cube, the Fermi body will more quickly assume a pherical shape as it recedes from the zone boundary, and the slope of he N(e) vs. E curve in the vicinity of the zone boundary will be much teeper for the face-centered cubic cell than for the body-centered structure. The effect of the overlap in the body-centered phase will further xtend the curve to include more high-energy states. The approximation f these curves is illustrated in Fig 4.

A deficiency of silver in either Ag_2S or Ag_2Te will result in a deficiency f electrons in the valence band. The presence of the excess anions will erve to extend the framework of the solid, while the holes, in the form f Schottky defects, will be distributed throughout the structure. These lefects or holes can be considered as atoms that contribute *no* valence lectrons. Hence, the electron-to-atom ratio of the solid will diminish. With a reasoning similar to that used by Jones (1937) to explain the hase boundaries in the Hume-Rothery or electron phases of intermetallic compounds, we can see that the removal of a given number of lectrons from under the curve of gentler slope will result in a greater owering of the enegy of the electrons at the top of the band than if an qual number were removed from under the curve of steeper slope.

FIG. 4. Approximate n(e) vs E cirve for face-centered and body-centered cubic structures.

Thus, because more electrons are contained at a lower energy level in the body-centered phase when there is a silver deficiency, the stable range of this phase is increased at the expense of the face-centered phase.

ACKNOWLEDGMENTS

The author is indebted to Profesor Tom F. W. Barth and members of the staff of The Mineralogisk-Geologisk Museum, Oslo, Norway, where this work was initiated. He is also indebted to Dr. N. Norman and others of the Sentralinstitutt for Industriell Forskning, Oslo, for their generous cooperation in allowing me to use their research facilities. The continuation of this work has been made possible by a grant from the National Research Council of Canada.

REFERENCES

DJURLE, S. (1958), An *X*-ray study on the system Ag-Cu-S: *Acta Chem. Scand.*, **12,** 1427–1436.

FRUEH, A. J., JR. (1958), The crystallography of silver sulfide, Ag_2S: *Zeit. Krist.*, **110,** 136–144.

FRUEH, A. J., JR. (1959), The structure of hessite, Ag_2Te-III: *Zeit. Krist.*, **112,** 44–52.

JONES, H. (1937), The phase boundaries in binary alloys. Part 2. The theory of the α-β phase boundaries: *Proc. Phy. Soc.*, **49,** 250–257.

JUNOD, P. (1959), Zones de Brillouin, liaisons chimiques et node de conduction de Ag_2S et Ag_2Se: *Helv. Phys. Acta*, **32,** 581–614.

KRACEK, F. C. (1946), Phase relations in the system sulfur-silver and the transitions in silver sulfide: *Trans. Am. Geophys. Union*, **27,** 364–374.

RAHLFS, P. (1935), Über die kubischen Hochtemperaturmodifikationen der Sufide, Selenide und Telluride des Silbers und die einwertigen Kupfers: *Zeit. Physik. Chem.*, **B31,** 157–194.

Manuscript received July 24, 1960.

OPTICAL AND CHEMICAL STUDIES OF PYROXENES IN A DIFFERENTIATED TASMANIAN DOLERITE

IAN MCDOUGALL, *Australian National University, Canberra, A.C.T., Australia.*

ABSTRACT

At Red Hill in southern Tasmania a large near vertical dike-like intrusion of tholeiitic dolerite, one mile in width and about five miles in length crops out. In this body marked differentiation has given rise to a series of rocks varying continuously from undifferentiated dolerite to granophyre; the latter occurring in the highest parts of the intrusion. Five pyroxenes, separated from rocks representative of the differentiation series, have been chemically analyzed and the optical properties determined. These pyroxenes are a coexisting pigeonite and augite, two ferroaugites and a ferrohedenbergite. To outline the complete fractionation series a number of other pyroxenes have been determined optically. Orthopyroxene occurs as a primary phase in a zone approximately fifty feet wide in dolerites adjacent to, and including, the chilled contacts of the intrusion, but elsewhere pigeonite is the only Ca-poor pyroxene present. Pigeonite also has crystallized in the dolerites adjacent to the contacts, where it has, in some cases, partially inverted to orthopyroxene. A member of the augite series crystallizes in cotectic equilibrium with the pigeonite and during fractionation both pyroxenes become progressively enriched in Fe, primarily at the expense of Mg. At the limit of the two-pyroxene field pigeonite ceases to form but the Ca-rich pyroxene continues to crystallize, steadily increasing in Fe content with fractionation, ultimately to attain the composition of ferrohedenbergite in the more acid granophyres. The trend of crystallization with fractionation closely parallels that from the Skaergaard intrusion. Exsolution phenomenon occur in both series of pyroxenes throughout much of the sequence, but is virtually absent in the ferrohedenbergite, probably owing to the relatively low temperature of crystallization.

INTRODUCTION

During the last two decades considerable attention has been paid to the composition and course of crystallization of pyroxenes from basaltic magmas. The general trend of crystallization of pyroxenes during fractionation was outlined independently by Hess (1941) and Edwards (1942), who showed that normally two series of pyroxenes crystallize through the greater part of the cooling history of basic magma. They also recognized the relation between orthopyroxene and pigeonite and explained the significance of some of the exsolution textures. Hess (1941) noted that in the late fractionation stages only a single pyroxene phase crystallizes and suggested that this behavior might be accounted for by a solid solution with a minimum forming in the pyroxene system at the limit of the two-pyroxene field.

Poldervaart and Hess (1951) clearly summarized the relations between the different pyroxenes found in basaltic magmas and treated the exsolution textures in detail. To explain the cessation of crystallization of pigeonite at the limit of the two-pyroxene field, in addition to the hypothesis already suggested by Hess (1941), they proposed the alter-

native that Ca-poor pyroxene may react with the liquid to form fayalite olivine. The problem was again considered by Muir (1954) who outlined a further explanation of this behavior. Edwards (1942, p. 602) suggested that rapid crystallization at high temperature could result in complete miscibility in the pyroxene system, and Kuno (1955) has since shown that under certain conditions, probably rapid cooling, the immiscibility gap between the Ca-rich and Ca-poor series of pyroxenes does not in fact exist.

The Skaergaard intrusion of East Greenland is the only example in the literature from which adequate data is available on the behavior of pyroxenes with strong fractionation of basaltic magma. Following on the original investigation by Wager and Deer (1939), Muir (1951) and Brown (1957) have carried out detailed studies of the pyroxene phases, establishing the trend of crystallization. Brown also gives a comprehensive account of the exsolution and inversion phenomena.

Edwards (1942) in a broad study of the differentiation of the Tasmanian dolerites has considered the relations between the different pyroxenes in some detail, and explained the occurrence of the two separate series of pyroxenes on the basis of their atomic structure. The present paper records the results of a detailed chemical and optical investigation of the pyroxene phases occurring in the large Red Hill intrusion of Tasmania, in which an acid granophyre occurs; the differentiation thus being more marked than in any intrusion studied by Edwards. In the early and middle stages of fractionation of the magma of the Red Hill intrusion, and of the Tasmanian dolerites as a whole, representatives of the two main series have crystallized in cotectic equilibrium. In the late stages of fractionation, as exemplified in the Red Hill intrusion, a single pyroxene phase of the Ca-rich series has crystallized. The range in composition of the pyroxenes and their trend of crystallization with fractionation is closely comparable to that found in the Skaergaard Intrusion.

The Tasmanian Dolerites

The Tasmanian dolerites were intruded into an essentially flat-lying sequence of Permian and Triassic sediments as sheets, commonly exceeding 1,000 feet in thickness, and as irregular transgressive bodies, and large dike-like intrusions up to one mile in width. The dolerite, generally considered to be of Jurassic age (Banks, 1958, p. 234), crops out over an area exceeding 6,000 square miles, and originally probably extended over more than twice this area. Edwards (1942) has shown that the undifferentiated magma is of remarkably uniform composition throughout Tasmania, and recent work by the writer completely confirms this

finding. The dolerite magma belongs to the tholeiitic basalt association and it is closely allied in composition to the dolerites of the Karroo, the Palisadan province, the British Guiana and Brazilian dolerites and especially to those of Antarctica.

Edwards (1942) in his excellent chemical study of the Tasmanian dolerites outlined the differentiation trend and found that in the lower parts of the sheet-like intrusions rocks markedly enriched in magnesia occur, followed upwards by dolerites progressively enriched in iron relative to magnesia, with moderate absolute iron enrichment, and en-

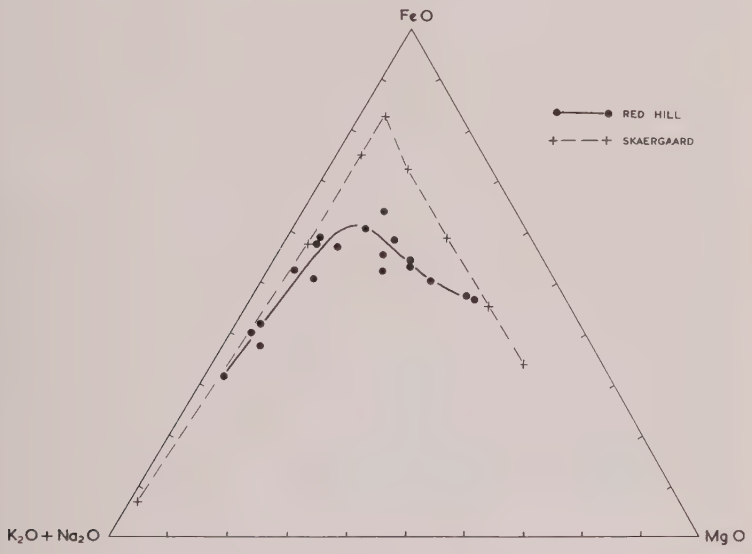

FIG. 1. Triangular diagram showing the differentiation trend in the Red Hill intrusion. The Skaergaard trend is included for comparison.

richment in alkalies and silica. In the Red Hill intrusion the differentiation has been more extreme and the latest products are granophyres, markedly enriched in iron, silica and alkalies and impoverished in magnesia and lime. The differentiation trend is illustrated in Fig. 1, where it is compared with that of Skaergaard. A detailed account of the field occurrence and petrology of the Red Hill intrusion will be presented elsewhere, and only a short summary of these is given here.

FIELD RELATIONS

The Red Hill intrusion is situated some 20 miles to the southwest of Hobart in southern Tasmania, and approximately 10 miles south of the Mount Wellington sheet, which Edwards (1942) has studied. The in-

trusion crops out as a large vertical dike-like body one mile in width, and can be traced in a north-south direction for over five miles. The structural interpretation indicates that this dike-like intrusion extends upwards for over 1,000 feet from the roof of an underlying dolerite sheet of approximately 1,300 feet in thickness (Fig. 2). The field evidence conclusively shows that this dike-like intrusion made room for itself by lifting the sediments in a similar manner to that in which the sheets were emplaced. The dike therefore possessed a roof of sediments, which have subsequently been removed by erosion.

Owing to the hilly topography in the Red Hill area a section of the intrusion 1,000 feet in height is available for study as well as an excellent

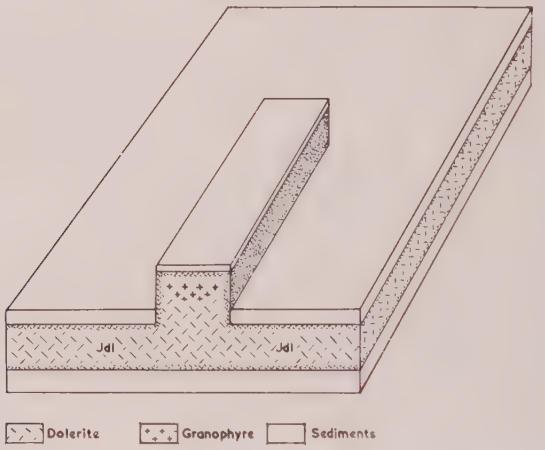

FIG. 2. Diagrammatic block diagram of the Red Hill intrusion.

river section at right angles to the trend of the dike. Because only the upper part of the dike-like intrusion is exposed, all the rocks revealed are more acid than the undifferentiated magma, as represented by the chilled contacts. However above the floor of the underlying dolerite sheet, out of which the Red Hill dike arose, more basic accumulative rocks must occur, comparable in composition to those of the magnesia-rich zone in the lower parts of the sheets, described by Edwards.

In the lowest exposed parts of the Red Hill intrusion the chilled dolerites adjacent to the intruded sediments pass gradationally into coarser varieties which become progressively more acid as the center of the dike is approached in a horizontal traverse. Here the rock is a medium grained dolerite which passes vertically upwards, by complete gradation, into increasingly more acid rocks and finally into granophyre towards the summit of Red Hill. This change in composition takes place

over a vertical height of the order of 600 to 800 feet and is brought about essentially by a steady increase in the quartz and potash feldspar at the expense of pyroxene and plagioclase; these latter two minerals changing progressively in composition throughout the sequence.

The petrological, mineralogical and field data conclusively show that the dolerite-granophyre association in the Red Hill intrusion has been produced by a process of differentiation of the dolerite magma by means of fractional crystallization and the gravitational movement of phases.

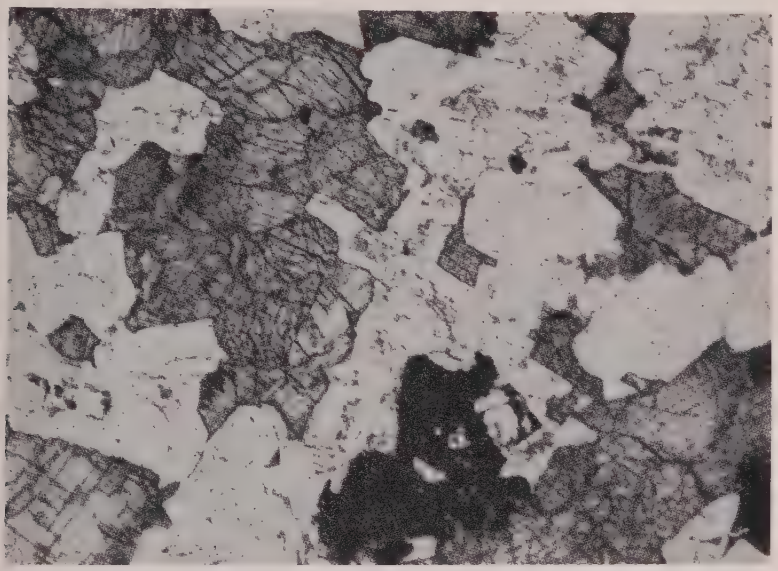

FIG. 3. Typical normal quartz dolerite (specimen M210) consisting of pigeonite and augite (dark, high relief) molded on plagioclase laths (colorless), with a large opaque crystal of iron ore. Scale mark is 1 mm. in length.

SUMMARY OF THE PETROGRAPHY

Invariably at the contacts with the sediments the dolerite is chilled to a glassy or very fine grained rock containing a few per cent of microphenocrysts. These are predominantly of euhedral orthopyroxene, although in some cases small augite and plagioclase microphenocrysts also occur. When crystalline the groundmass consists of minute granules of pyroxene and small laths of plagioclase (An_{65}). The groundmass pyroxene in such cases appears to consist of augite and orthopyroxene.

Away from the contacts the dolerite increases rapidly in grain size. The bulk of the dolerite is medium grained and consists essentially of pyroxene, plagioclase (An_{60}–An_{70}), an intersertal mesostasis composed of

quartz and potash feldspar, usually in micrographic intergrowth, with iron ore as an important accessory. The pyroxene is strongly molded on plagioclase laths to give a subophitic texture (Fig. 3).

In a zone extending up to 200 feet from the chilled vertical contacts of the Red Hill intrusion three varieties of pyroxene occur in the dolerite: orthopyroxene, pigeonite and augite. The primary orthopyroxene increases in grain size to about 1 mm. as compared with about 0.3 mm. in the chilled contacts. It generally builds prismatic crystals, which, however, are rarely euhedral owing to interference by plagioclase laths. The primary orthopyroxene persists for about 50 feet from the chilled contacts and is not found elsewhere in the exposed part of the intrusion. It is commonly mantled by pigeonite.

Within a few feet of the chilled margins of the Red Hill intrusion the groundmass pyroxene can definitely be identified as pigeonite and augite in approximately equal proportions. Both increase rapidly in grain size and within 100 feet of the contact attain an average size of about 1 mm. The two pyroxenes are indistinguishable in thin section except by the optic angle. Both are usually anhedral, rarely subhedral, but commonly somewhat elongate, and include plagioclase laths subophitically. Some of the pigeonite grains in a zone up to 200 feet from the contacts have partially or completely inverted to orthopyroxene, which contains exsolution lamellae, probably of augitic composition (Poldervaart and Hess, 1951).

Apart from the zone immediately adjacent to the contacts, the pyroxene of the quartz dolerites consists of pigeonite and augite only. Generally they are present in about equal proportions, except in the more acid dolerites, transitional to granophyre, when the pigeonite decreases in amount. The proportion of pyroxene in the quartz dolerites ranges from about 35% to less than 15% by volume; the highest concentration occurring in the dolerites adjacent to the chilled contacts, and the lowest proportion in the more acid dolerites in the central and higher parts of the intrusion, below the granophyre. The two clinopyroxenes, anhedral to subhedral in form and molded strongly on plagioclase laths, average between 1 and 2 mm. in size, and usually occur as individual crystals surrounded by areas of rather finer grained plagioclase and mesostasis. However in some cases several grains of pyroxene have crystallized in close proximity to one another to form large irregular plates up to 5 mm. across. Not uncommonly the pigeonite and augite are intergrown with one another, each having the same crystallographic orientation.

The quartz dolerite in the central parts of the dike passes upwards gradationally into fayalite granophyre essentially by a progressive increase in the proportion of quartz and potash feldspar at the expense of

pyroxene and plagioclase. A fayalitic olivine (Fa_{90}) makes its appearance at this level and coincides with a marked decrease and final disappearance of pigeonite. The pyroxene of the augite series, a ferroaugite, continues to crystallize. The fayalite granophyres have a texture very similar to that of the quartz dolerites, except that the pyroxene is much smaller in amount, usually less than 10% by volume. The pyroxene is strongly molded on plagioclase laths (Fig. 4). The plagioclase constitutes some 40% to 50% by volume of the fayalite granophyre and has a

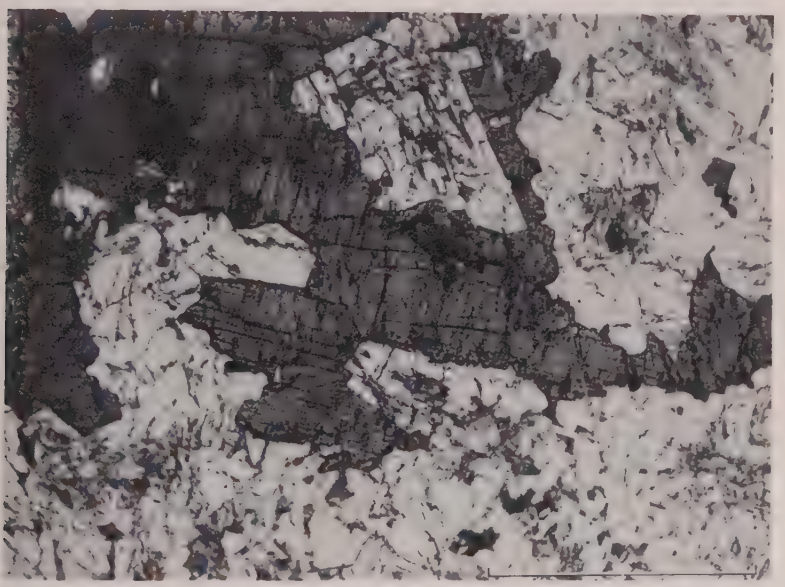

FIG. 4. Ferroaugite of fayalite granophyre strongly molded on colorless plagioclase laths. Scale mark is 1 mm. in length.

composition about An_{60}. The quartz and potash feldspar, forming 30% to 50% of the rock, occurs in well developed granophyric intergrowths or in some cases as anhedral grains. Iron ore is present as a major accessory and usually to the extent of about 2% by volume.

The granophyre, into which the fayalite granophyre passes upwards gradationally by a further increase in the proportion of quartz and alkali feldspar, contains only a single ferromagnesian phase, a ferrohedenbergite, the fayalitic olivine having ceased to crystallize. The granophyre consists essentially of ferrohedenbergite (5% to 9% by volume), plagioclase (An_{50} An_{15}) present to the extent of 15% to 30%, very abundant quartz and potash feldspar (50% to 70%), which is usually intergrown to give the rock the typical granophyric texture, and a variable amount of

iron ore. The pyroxene has a distinctly different habit from that in the quartz dolerites and fayalite granophyres, since it occurs as independent elongate crystals, which, however, rarely exhibit crystal faces, owing to strong interference by other minerals (Fig. 5). In some thin sections seemingly unconnected fragments of pyroxene, all of the same orientation, may extend over a distance in excess of 10 mm.

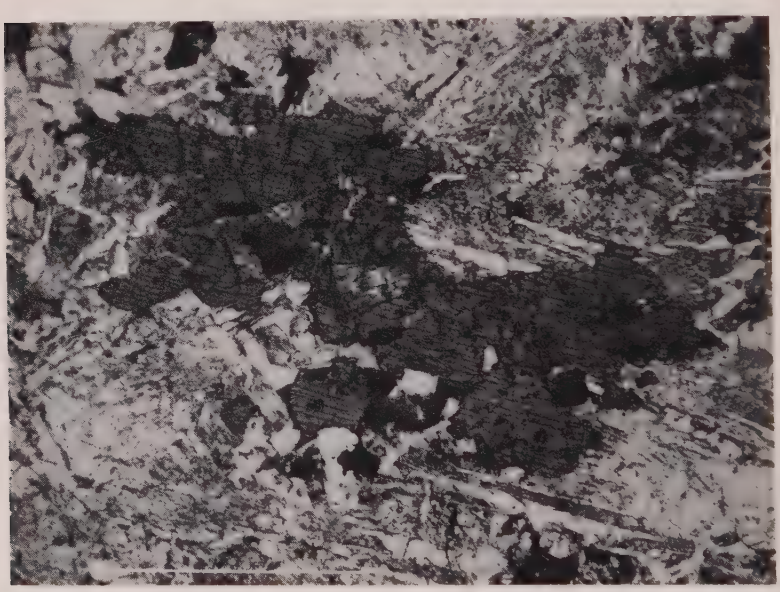

FIG. 5. Elongate but irregularly shaped ferrohedenbergite in granophyre from Red Hill. Iron ore granules are associated with the pyroxene. The light areas consist of quartz and alkali feldspar in granophyric intergrowth and also plagioclase laths. Scale mark is 1 mm. in length.

METHODS OF DETERMINATION OF OPTICAL PROPERTIES

The methods employed in the determination of the optical properties of the pyroxenes were essentially those of Hess (1949). Refractive indices were determined by the usual immersion methods on the crushed pyroxene fraction. The index being measured was bracketed between liquids 0.005 apart, and the final determination, carried out under sodium light, was by mixing the liquids until the index was exactly matched. The index of the liquid was then measured with an Abbe refractometer. The β index of clinopyroxenes with optic plane $\|(010)$ was measured on (100) parting tablets (Hess, 1949, p. 627), and α and γ were determined by the minimum and maximum index found in the crushed sample. This method

for α and γ is not as accurate as determination of them by calculation, from the birefringence, since the pyroxene is generally slightly zoned. Hence the birefringence, derived from the refractive indices, tends to be a little high. The determination of the indices of pigeonites was carried out on grains whose orientation was checked, in each case, by observing the interference figure (Hess, 1949, p. 628). When it was not possible to separate the clinopyroxene from the rock, crystals with an optic axis vertical were dug out of a slide and the β index measured. The composition of the pyroxene was then determined from the β index and the 2V, by referring to the graph of Hess (1949, p. 634). The orthopyroxenes from the chilled marginal zones of the intrusion, were determined from measurements of α and γ on a separated sample of the pyroxene, and referring to the graph of Poldervaart (1950, p. 1076). Measurements of the optic angle were also used as an independent check. The accuracy of the refractive index determinations is considered to be better than ± 0.001.

The optic angle of each of the pyroxenes was determined on a universal stage, using the conoscopic method of orientation, by direct rotation from optic axis to optic axis in sodium light. After applying the appropriate index corrections the accuracy of the determinations is better than $\pm 1°$.

Chemical Analyses of the Pyroxenes

Five chemical analyses have been made of pyroxenes from four of the main rock types of the Red Hill intrusion (Table 1). The analyses were carried out, in most cases, on pure material, separated by using the isodynamic magnetic separator in conjunction with heavy liquids. It was found impossible to completely eliminate the augite from the pigeonite of the quartz dolerite (M210); a correction was made to the analysis for 10% augite impurity, and then recalculated to 100%. The alkalies were determined by flame photometer and the total iron colorimetrically, but the remainder of the analysis was carried out by classical methods.

The generalized formulae for clinopyroxene, after Berman (1937), Hess (1949) and Kuno (1955) is:

$$W_{1-p}(X, Y)_{1+p}Z_2O_6$$

where

$W = Ca^2, Na^1, K^1$
$X = Mg^2, Fe^2, Mn^2, Ni^2$
$Y = Al^3, Fe^3, Cr^3, Ti^4$
$Z = Si^4, Al^3, Ti^4, Fe^3$

The analyses (Table 1) have been recalculated on the basis of six oxygen atoms (Table 2), using the method outlined by Hess (1949, p. 625), in

TABLE 1. CHEMICAL ANALYSES OF PYROXENES FROM FOUR MAIN ROCK TYPES OF THE RED HILL INTRUSION

	3	3A	4	5	6	
SiO_2	51.32	48.31	49.63	48.00	46.59	
Al_2O_3	1.55	0.53	1.34	1.17	0.95	
Fe_2O_3	0.87	1.35	1.53	1.20	1.82	
FeO	14.71	31.33	20.94	26.65	28.93	
MnO	0.30	0.62	0.47	0.53	0.53	
MgO	13.64	10.13	9.98	4.71	1.04	
CaO	15.96	6.08	14.47	16.50	18.08	
Na_2O	0.25	0.16	0.20	0.18	0.25	
K_2O	0.13	0.11	0.11	0.12	0.17	
TiO_2	0.42	0.58	0.67	0.75	1.50	
H_2O	0.44	0.80	0.28	0.30	0.31	
	99.59	100.00	99.62	100.11	100.17	
					Purple	Green
NX	1.692	1.707	1.710	1.721	1.736	1.735
NY	1.697	1.708	1.717	1.727_5	1.744	1.742_5
NZ	1.720	1.740	1.738	1.751	1.765_5	1.764_5
$2V_z$	Av. 47° 45, 46, 46½, 47½, 48½ 48½	0, 0, 0, 10, 13, 17, 21; opt. plane ⊥ (010) } r 11½, 13, 19, 25, opt. plane ∥(010). } i, m	Av. 41½° 40, 41, 41½, 41¼, 42½, 43	Av. 50° 46 53½, 48½, 49.1/4, 49½, 49½, 49½, 50½, 51½, 51.1/4. Rims about 7° higher than cores.	Av. 54° 51.3 4, 52½, 53.¾, 54½, 58.1/4	Av. 57½° 56½, 56½, 57, 61,
					Pleichroism	
					X = Y-pale-purple Z = sl. darker purple	X = Y pale yellow green Z = green
Exsolution lamellae	(001)	(001)	(001)	(001)	None	
Atom % Ca	33.8	10.8	31.4	36.6	41.4	
Mg	40.1	43.4	30.0	14.5	3.3	
Fe*	26.1	45.8	38.6	48.9	55.3	

* $Fe = Fe^{2+} + Fe^{3+} + Mn$.

Samples:

3. Augite from quartz dolerite M210; centre of Red Hill Dike, Snug River.
3A. Pigeonite from quartz dolerite M210. Analysis corrected for 10% augite impurity (3) and recalculated to 100%.
4. Ferroaugite from quartz dolerite M395; centre of Red Hill Dike on the northern flank of O'Brien's Hill, 465 feet above Snug River.
5. Ferroaugite from fayalite granophyre M12; northern flank of Red Hill at road level (altitude 715 feet) and about 550 yards from western contact of the Red Hill Dike.
6. Ferrohedenbergite from granophyre M162; 200 feet above M12 on northern side of Red Hill.

Analyses by Ian McDougall.

TABLE 2. ANALYSES OF TABLE 1, RECALCULATED ON THE BASIS OF SIX O ATOMS

		3	3A	4	5	6
Z	Si	1.957	1.953	1.947	1.939	1.926
	Al	0.048	0.024	0.063	0.058	0.047
	Ti	—	0.019	0.002	0.004	0.036
WXY	Al	0.021	—	—	—	—
	Fe^{3+}	0.028	0.041	0.047	0.039	0.055
	Fe^{2+}	0.468	1.058	0.686	0.900	1.002
	Mn	0.009	0.019	0.017	0.017	0.017
	Mg	0.775	0.609	0.581	0.284	0.065
	Ca	0.653	0.264	0.610	0.716	0.803
	Na	0.018	0.012	0.014	0.015	0.020
	K	0.005	0.005	0.005	0.005	0.010
	Ti	0.012	—	0.019	0.020	0.011
Z		2.005	1.996	2.012	2.001	2.009
WXY		1.989	2.008	1.979	1.996	1.983
% Al in Z		2.4	1.2	3.1	2.9	2.3
% Ti in Z		—	0.8	0.1	0.2	1.8

which the electrical charges are always balanced between the several groups. According to Hess in a completely satisfactory analysis the number of cations to six oxygen atoms in the WXY and Z groups is 2.00 ± 0.02; all the analyses carried out on the Red Hill pyroxenes meet this requirement.

In the recalculation of four of the five analyses it has been necessary to include all the Al^3 in the Z group, and even then there is still a deficiency in charge, which must be made up by assuming that some Ti^4 and/or Fe^3 is also present in the tetrahedral position. It has usually been tacitly assumed that Ti^4 will enter the tetrahedral position preferentially (Hess, 1949; Muir, 1951), but, as pointed out by Kuno (1955) and Brown (1957), it is possible that Fe^3 may also occur in this position in the pyroxenes. The ionic radii for sixfold coordination are (Ahrens, 1952);

Si^4	Al^3	Ti^4	Fe^3
0.42 Å	0.51 Å	0.68 Å	0.64 Å

The Fe^3 ion is slightly smaller than Ti^4 and therefore may replace Si^4 more readily, but since Ti^4 is quadrivalent this ion may be preferentially included in this position. That Fe^3 can enter the tetrahedral position in silicates, and particularly in alkali feldspars, has been well demonstrated by Faust (1936), Rosenqvist (1951), and Coombs (1954). Kuno (1955)

shows that Fe^3 may also be present in the Z group in clinopyroxenes. Thus although the recalculation of the analyses of the Red Hill pyroxenes is made by assuming the Ti^4 preferentially enters into the tetrahedral position, this does not exclude the possibility that some Fe^3 occurs in this position.

The Variation in Composition of the Pyroxenes with Fractionation

Enrichment in Fe at the expense of Mg is the major variation in the composition of the pyroxenes during fractionation of the Red Hill magma, and this is accompanied by smaller variations in Ca (Fig. 6).

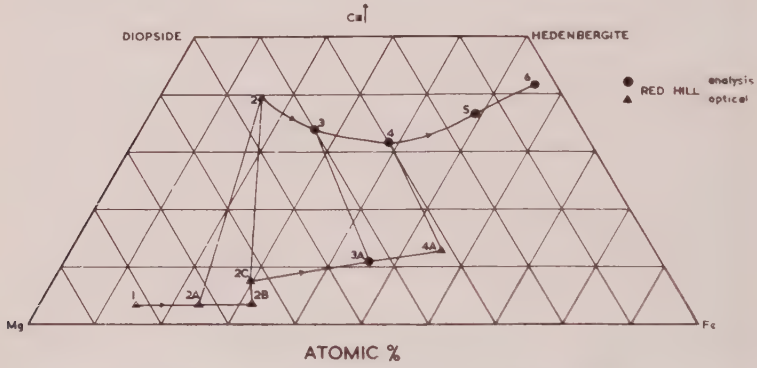

Fig. 6. Crystallization trend of the pyroxenes from the Red Hill intrusion. Tie lines join coexisting pyroxene phases. 1, 2A, 2B, orthopyroxene; 2C, 3A, 4A, pigeonite; 2, 3, augite; 4, 5, ferroaugite; 6, ferrohedenbergite.

These trends will be discussed below but reference will first be made to those cations which enter into the pyroxene lattice in small amount.

The Al content of the Red Hill pyroxenes is lower than in many analyzed clinopyroxenes (Hess, 1949; Muir, 1951; Kuno, 1955; Brown, 1957). As Brown (1957) found in the Skaergaard clinopyroxenes it decreases steadily with fractionation, and the amount of Al entering into the augite is somewhat higher than in the coexisting pigeonite.

With fractionation the Ti content of the clinopyroxene increases progressively, by contrast to Skaergaard, where there is but little change in Ti (Muir, 1951; Brown, 1957). Also Ti is present in greater amount in the pigeonite than in the associated augite; the reverse of the behavior in Skaergaard (Brown, 1957).

The Mn content of the pyroxenes from the Red Hill intrusion increases with the Fe^2 content; this being a consequence of the similarity in charge, electronegativity and ionic radius of the two ions (Wager and

TABLE 3. OPTICAL PROPERTIES OF PYROXENES

	1	1A	2	2A
α	1.675	1.675		
β	—		1.788	
γ	1.687			
2V	Av. 84°(−) 82½, 83, 84, 86, 86½ rim av. 62½(−)	Av. 84°(−) 80½, 82, 82, 84, 84, 85, 85½, 86 rim av. 62°	Av. 47°(+) 46½, 47, 47, 47, 47½, 48 core av. 7° higher than rim	Av. 69°(−) 62, 64, 66, 68, 68, 68, 74, 81.
Composition	Of_{15}	Of_{15}	$Ca_{39.5}Mg_{45}Fe_{15.5}$	Of_{24}

	2B	2C	4A
β		1.685	1.719
2V	58°(−)	Av. 18°(+) 17, 19. Opt. plane ⊥ (010)	Av. 12½° (+)12, 12, 14. Opt. plane ‖(010)
Composition	Of_{33}	$Ca_{7.5}Mg_{63}Fe_{29.5}$	$Ca_{13}Mg_{31.5}Fe_{55.5}$

1. Microphenocrysts of orthopyroxene in chilled dolerite M172; eastern contact of Red Hill dike
1A. Microphenocrysts of orthopyroxene in chilled dolerite M200; upper contact of northern sill, northeast of Longley.
2. Augite of M212; medium grained quartz dolerite about 40 feet from western contact of the Red Hill dike in Snug River.
2A. Primary orthopyroxene from quartz dolerite M212.
2B. Most iron-rich primary orthopyroxene from M212.
2C. Pigeonite from quartz dolerite M212.
4A. Pigeonite from M395.

Mitchell, 1951; Ringwood, 1955). Again, as expected, the Mn content of the pigeonite is considerably greater than that of the coexisting augite, because of the relatively higher Fe content of the pigeonite.

The amount of Fe^3 increases slightly with fractionation, and the pigeonite is relatively enriched in this constituent as compared with augite, the opposite to Brown's (1957, p. 518) findings in the pyroxenes of the Skaergaard intrusion.

The alkali content of the Red Hill pyroxenes remains uniformly low; there is no significant variation with fractionation.

In Fig. 6, together with the analyzed pyroxenes from Red Hill, are

plotted a number of pyroxenes whose compositions were estimated from optical data (Table 3).

At the chilled margins of the Red Hill dike, and indeed in the contacts of all the Tasmanian dolerites, small euhedral microphenocrysts of Mg-rich orthopyroxene (Of_{15}) occur embedded in either a glassy base or more commonly in a very fine-grained holocrystalline groundmass. It is apparent that this pyroxene began to crystallize some little time before emplacement of the dolerite magma. When crystallization began the magma was below the clinopyroxene-orthopyroxene inversion curve (Fig. 7), in the orthopyroxene stability field. The orthopyroxene is usu-

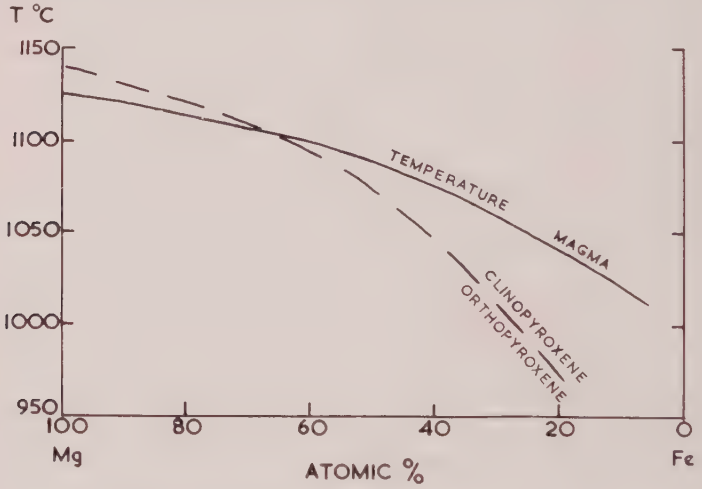

FIG. 7. Suggested temperature of crystallization of basaltic magma, and its relation to the orthopyroxene-clinopyroxene inversion curve (after Hess, 1941).

ally uniform in composition but commonly has a very thin rim which may be as iron-rich as Of_{29}.

Pyroxene in the groundmass of the contact rocks occurs as minute granules and appears to consist of both augite and orthopyroxene. However within a few feet of the contact pigeonite takes the place of orthopyroxene, so that the magma has crossed the inversion curve into the clinopyroxene stability field.

Primary orthopyroxene, mainly as phenocrysts, persists for about 50 feet from the chilled contacts of the Red Hill dike, after which pigeonite is the only Ca-poor primary pyroxene crystallizing. Dolerites from this marginal zone usually contain four different pyroxenes; primary orthopyroxene, orthopyroxene resulting from the inversion of pigeonite, pigeonite and augite. Therefore, because of the difficulty of separation,

it was necessary to determine these pyroxenes optically (Table 3). The primary orthopyroxene ranges in composition from Of_{16} to Of_{33} although zoning is not strongly developed. Pyroxene (2A) (Fig. 6) is the average of eight determinations and pyroxene (2B) is the most Fe-rich primary orthopyroxene determined. The assumption is made in plotting that the primary orthopyroxene contains the normal 3.5% Ca (Poldervaart and Hess, 1951). The orthopyroxene occurs as anhedral to prismatic crystals which may reach 2 mm. in size, and is commonly mantled by pigeonite which has, in some cases, subsequently inverted to orthopyroxene. Specimen (M212) contains about 40% pyroxene, but less than 1% of this is primary orthopyroxene.

Pyroxenes (2) and (2C) in Fig. 6 are the augite and pigeonite respectively, which together make up the bulk of the pyroxene in specimen (M212). The clinopyroxenes are anhedral to subhedral in form, and are molded strongly on plagioclase laths. They exhibit simple twinning (twin plane $\|(100)$), and usually have extremely fine exsolution lamellae $\|(001)$. When both twinning and the exsolution lamellae occur in the one crystal the well known herringbone structure results. Observations on the universal stage indicate that the pigeonite and augite are present in approximately equal proportions. The pigeonite is usually uniform in composition but the augite commonly has a core of variable size, which has a 2V averaging about 7° greater than the surrounding augite.

Pyroxenes (3) and (3A) represent the coexisting augite and pigeonite respectively from the normal, medium grained, quartz dolerite from the center of the Red Hill intrusion in Snug River (specimen M210). Except for an increase in grain size, and a decrease in proportion to approximately one fifth of the rock by volume, the pyroxenes are very similar in appearance and form to those in specimen (M212), just described. The pyroxenes have a distinct brown color and are not pleochroic. In some cases pigeonite and augite are intergrown with one another; where one pyroxene completely encloses the other, pigeonite is invariably in the core. Fine exsolution lamellae are usually present in both clinopyroxenes. The pigeonite from this rock is generally unzoned, except for the presence, in some cases, of a relatively thin outer rim. The optic angle shows considerable variation (Table 1) but the augite has a remarkably constant 2V, with zoning essentially absent.

Pyroxene (4) is the augite and (4A) the pigeonite from the dolerite immediately below the fayalite granophyre. This rock (M395) is about the most acid dolerite in which a member of both the augite and pigeonite series coexist. Because pigeonite is present in small amounts it was not possible to separate enough for analysis, so it was necessary to determine it optically (Table 3). Specimen (M395) is similar to the dolerite from

the summit of Mt. Wellington (Edwards, 1942), and Muir (1955, p. 562) has plotted analyses of the coexisting augite and pigeonite phases from this rock; the compositions of which lie very close to those from specimen (M395) (see Fig. 8).

The pyroxenes from specimen (M395) closely resemble those of specimen (M210) but they are generally of slightly coarser grain size. They are a purplish brown color, but in some cases they have a thin mantle of pale green pyroxene. The augite is mostly unzoned, but may have a thin rim which has a 2V up to 10° greater than the core. The associated pigeonite is also fairly uniform, and has a 2V of about 12° in the plane ||(010). As in the previously described clinopyroxenes simple twinning on (100) and fine exsolution lamellae ||(001) are present.

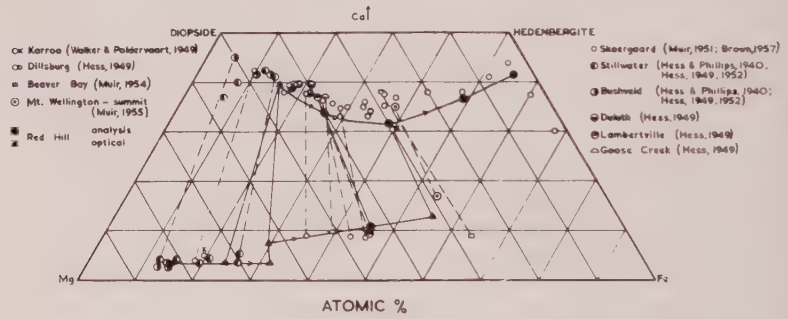

FIG. 8. Comparison of the Red Hill pyroxene trend with the compositions of pyroxenes from other slowly cooled tholeiitic intrusions.

With further fractionation the magma passed from the two-pyroxene field into that in which only one pyroxene forms, by the pigeonite ceasing to crystallize. The pyroxene of the augite series continues to crystallize throughout the fayalite granophyre and granophyre, and becomes progressively enriched in Fe and slightly enriched in Ca with fractionation.

The ferroaugite (5) was separated from the fayalite granophyre (M12) from Red Hill, and is the only pyroxene phase present in the rock. The ferroaugite occurs as anhedral to prismatic crystals which are usually molded strongly on plagioclase laths. Although normally occurring as independent crystals, in some cases several grains have formed adjacent to one another to produce large glomeroporphyritic plates. The pyroxene is purplish brown in color, and is commonly partially rimmed by a pale green variety whose 2V is 5° to 8° higher than the fairly uniform cores. Twinning is not developed, but thin continuous exsolution lamellae ||(001) are usually present.

The change from the ferroaugite (5) of the fayalite granophyre to the ferrohedenbergite (6), which is typical of the granophyre, takes place over a vertical distance of some 200 feet in the Red Hill dike. The pyroxene in the granophyre, as noted above, assumes an elongate, feathery, appearance. Commonly the crystals consist of an irregular intergrowth of two distinct varieties of pyroxene; one is pale purple, the other pale green, and both are faintly pleochroic. When intergrown the two varieties have the same optical and crystallographic orientation. However the refractive indices of the green variety are about 0.001 lower than those of the purple. Minute iron ore inclusions occur in some crystals, particularly in the green variety. The fine exsolution lamellae ||(001), so common in the less Fe-rich pyroxenes of the intrusion, are rarely present in the ferrohedenbergite, and simple twinning is never developed. The ferrohedenbergites occurring in other granophyres are very similar to the analyzed pyroxene, but in some rocks the green variety tends to predominate.

Wager and Deer (1939) and Muir (1951) record the presence of two pyroxenes, one brown and the other green, in some of the latest differentiates of the Skaergaard intrusion. Muir shows that both pyroxenes are ferrohedenbergites containing very little Mg and that their compositions differ by only a few mol per cent. Wager and Deer suggested from the textural relations that the green variety has arisen by inversion of iron-wollastonite and Muir follows this interpretation. The brown pyroxene is considered to be a primary phase and, in some cases, crystallizes in optical continuity with the green variety. Poldervaart (1944) also observed two distinct varieties of pyroxene in granophyre from the New Amalfi Sheet.

In the Red Hill granophyres there is no reason to suggest that either the green or purple pyroxenes are other than primary phases; apart from the color and slight differences in optical properties the two pyroxenes are very similar. No obvious explanation is forthcoming to account for the occurrence of the two pyroxenes which have apparently crystallized in equilibrium with one another; conceivably the observed relations may be the result of a small immiscibility gap appearing in this part of the pyroxene system.

Thus during fractionation of the Red Hill magma both series of pyroxenes show a progressive change in composition towards more Fe-rich varieties. In the Ca-rich pyroxene series Fe^2 continually replaces Mg throughout the whole sequence, and during the early and middle stages of fractionation Fe^2 is also replacing Ca to some extent, since the Ca content of these pyroxenes decreases in amount from about 40% of the total Ca+Mg+Fe to about 31%, at the limit of the two-pyroxene field.

However in the late stages of fractionation the Ca content steadily increases in amount to over 41% in the ferrohedenbergite of the granophyre, so that in addition to replacement of Mg by Fe^2, replacement of Mg by Ca also takes place.

The composition of the Ca-poor pyroxene during fractionation changes progressively by replacement of Mg by Fe^2, until the cessation of crystallization of the pigeonite at the limit of the two-pyroxene field. There is apparently little variation in the Ca content of these pyroxenes except that the orthopyroxene probably contains about $3\frac{1}{2}$% Ca of the total Ca+Mg+Fe (Poldervaart and Hess, 1951, p. 481), whereas the pigeonite contains about 10% Ca. Further analyses of pyroxenes of the Ca-poor series from the Red Hill intrusion would be extremely valuable in tracing in more detail, the variation in composition within this group during fractionation.

Comparison of the Red Hill Trends with the Trends in other Intrusions

A considerable literature now exists on the pyroxenes from moderately slowly cooled saturated basic intrusions, but the Skaergaard body is the only one in which the variation in composition of the pyroxenes has been traced throughout the fractionation of the magma (Muir, 1951; Brown, 1957). The analyzed pyroxenes from several of these intrusions, including Skaergaard, are plotted in Fig. 8, together with the Red Hill pyroxenes; the similarity in trend is most striking, particularly between Skaergaard and Red Hill. The Red Hill pyroxenes of the augite series have a slightly lower Ca content than the Skaergaard pyroxenes, but, as in Skaergaard (Brown, 1957), there is a minimum in the Ca content at the limit of the two-pyroxene field. At this stage there is a change from a gradual decrease in Ca to one of gradual Ca enrichment. An important point, which holds for Skaergaard also, is that there is no evidence for any marked compositional break, in the augite series, at the limit of the two-pyroxene field.

The trend with fractionation in the Ca-poor pyroxene series is also very similar to that of Skaergaard. The crystallization begins with an Mg-rich orthopyroxene, which gradually becomes more Fe-rich, and then at an Mg:Fe ratio of approximately 70:30 gives way to pigeonite, which itself becomes progressively enriched in Fe during fractionation, until the limit of the two-pyroxene field is attained, when it ceases to crystallize.

The variation in composition of the Red Hill pyroxenes during fractionation also agrees in general with the trends proposed by Poldervaart and Hess (1951), who collected data from a number of different intru-

sions, at several fractionation stages, to give the course of crystallization of pyroxenes within a single, strongly fractionated, basaltic body.

The Limit of the Two-Pyroxene Field

It has been long established that a single pyroxene phase of the augite series crystallizes during the late stages of fractionation of tholeiitic basaltic magma, instead of both a Ca-rich and a Ca-poor phase, which crystallize together in cotectic equilibrium in the early and middle stages. In the Red Hill intrusion the limit of the two-pyroxene field occurs at an Mg:Fe ratio of about 40:60 in the pyroxenes; in Skaergaard the corresponding ratio is about 50:50, and Poldervaart and Hess (1951) give the value of 45:55 for tholeiites in general.

Several explanations have been advanced to account for the cessation of crystallization of the Ca-poor pyroxene phase. Poldervaart and Hess (1951, p. 479) suggested that there may be reaction of the pigeonite with the liquid to form a fayalitic olivine. At essentially the same stage as the pigeonite disappears in the Red Hill intrusion a fayalitic olivine makes its appearance as a primary phase. There is no petrographic evidence of a reaction relation between the two minerals; the olivine has usually crystallized as discrete, large grains, not associated with pyroxene. It appears that the fayalite, rather than causing the cessation of crystallization of the pigeonite, has begun to form at this stage because of the disappearance of the pigeonite, owing to the marked absolute enrichment in Fe as well as the very strong enrichment in Fe relative to Mg in the liquid. Muir (1954, p. 384) concludes from his studies of Skaergaard, Beaver Bay and New Amalfi pyroxenes that the disappearance of Ca-poor pyroxene could not be due to a reaction relation with fayalitic olivine, and Brown (1957, p. 525) also arrives at the same conclusion as regards the Skaergaard intrusion.

The laboratory investigations of Bowen and Schairer (1935) show that hedenbergite and ferrosilite form a solid solution series with a mimimum. Hess (1941) developed the idea proposed by Tsuboi (1932) that at the limit of the two-pyroxene field a solid solution with a minimum forms, so that only a single pyroxene phase crystallizes with continued fractionation. If this were the correct explanation it would be expected that the compositions of the augite and pigeonite phases would converge as the limit of the two-pyroxene field was approached. However the data from Skaergaard (Muir, 1951; Brown, 1957), and now from the Red Hill intrusion, shows that no such convergence of the compositions takes place; in fact the trend in the augite series is away from the pigeonite at the limit of the two-pyroxene field. Therefore this explanation does not appear to satisfy the observed facts.

A third alternative was proposed by Muir (1954, p. 384), who sug gested that, instead of the solidus surface dipping below the liquidus a the limit of the two-pyroxene field to produce a solid solution with a minimum, the liquidus minimum, which intersects the solvus, migrate toward the Ca-rich side of the solvus and passes beyond it, so that only a single Ca-rich pyroxene would then form. Such a mechanism ca account for the disappearance of the pigeonite, and the continuity in th crystallization of the pyroxenes of the augite series, without any majo change in trend, when the limit of the two-pyroxene field is reached.

Exsolution and Inversion Phenomena in the Pyroxenes

When pyroxenes, which have crystallized from tholeiitic basalti magma, are cooled moderately slowly, exsolution or unmixing of on pyroxene phase from another may take place, leading towards the at tainment of a more ordered state, and is the result of the decrease i stability of one component in the other with decreasing temperatur (Hess, 1941; Edwards, 1942; Poldervaart and Hess, 1951; Brown, 1957

Edwards (1942, p. 584, p. 587) noted the presence of a pronounce parting $\parallel(001)$ in both the pigeonite and augite of the Tasmanian dole ites. Under high magnification it is found that this parting is produce by very fine exsolution lamellae; Muir (1955, p. 562) recognized suc lamellae in the ferroaugite from the summit of Mt. Wellington. In bot the augite and pigeonite these lamellae are very similar; they range i thickness from 0.0005 to 0.002 mm., with exceptional lamellae up t 0.003 mm.; they are spaced from 0.003 to 0.01 mm. apart, and constitut about 15 to 20% of each crystal. The lamellae have an orientation ver similar to that of the host clinopyroxene, making them difficult to di tinguish. They can be detected in practically all grains which are sui ably oriented in the thin section, and usually occur throughout a crysta

The work of Hess (1941) and of Poldervaart and Hess (1951) indicat that the lamellae in augite are pigeonitic in composition, whereas thos occurring in pigeonite are composed of augite, and this has been co firmed by an *x*-ray study of an augite from Mt. Wellington by Bown an Gay (1959), who have shown that the lamellae are in fact composed pigeonite. There is no evidence to suggest that the exsolved pigeonite i the augite crystals has inverted to orthopyroxene, so that the exsolutio probably took place at a temperature above the pigeonite-orthop roxene inversion curve (Fig. 7).

In the Red Hill intrusion exsolution lamellae occur in the pigeoni right up to the stage when it ceases to crystallize, at the limit of the tw pyroxene field. In the augite series lamellae are present in all the pyro enes up to and including the ferroaugite of the fayalite granophyre, b

re generally absent from the ferrohedenbergite of the granophyre; the emperature at which these more Fe-rich pyroxenes crystallized must ave been too low for any exsolution to take place, because of the relaively slow rate of diffusion at these temperatures. In addition it is probble that no pyroxene of the pigeonite series is stable in this composition eld.

In the Red Hill intrusion the pigeonite contained in dolerites occurring n a zone up to 200 feet from the contacts, has, in some cases, partly or holly inverted to orthopyroxene on cooling, because the temperature ad fallen to below the pigeonite-orthopyroxene inversion curve (Fig. 7), nto the stability field of orthopyroxene. Hess (1941) first recognized his phenomenon and independantly Edwards (1942) noted it in the ower parts of the Tasmanian dolerite sills.

In many cases the pigeonite has only partially inverted, so that commonly the parent pigeonite and the secondary orthopyroxene occur ogether in the one crystal. The boundary between the two phases is vays sharp, if irregular, and in some cases the orthopyroxene ends bruptly along an augite exsolution lamellar in the pigeonite. The secndary orthopyroxene usually has uneven extinction, and contains the xsolved augite as fine lamellae, which are the continuation, and of the me thickness, as those occurring in the adjacent uninverted pigeonite Figs. 9, 10). The lamellae in the orthopyroxene are much more obvious han those in the pigeonite, because in the former their orientation is uite different from the orthopyroxene, whereas in the pigeonite the mellae of augite have a very similar orientation to that of the host.

According to Poldervaart and Hess (1951, p. 482) pigeonite crystalzes with some 9.5% Ca^2 ions of the total ($Mg^2+Fe^2+Ca^2$), although he analyzed pigeonite (3A) from specimen (M210) appears to contain bout 10.8% of the Ca^2 ion. Orthopyroxene, on the other hand, can acept only about $3\frac{1}{2}$% Ca^2 ion into its structure, so that when pigeonite nverts to orthopyroxene the excess Ca^2 is exsolved in the form of augite mellae or blebs. However the pigeonites in the Tasmanian dolerites ave exsolved much of the Ca in the form of augite lamellae before the nversion to orthopyroxene, so that generally the exsolution lamellae in he secondary orthopyroxene are related to the parent pigeonite rather han to the orthopyroxene.

Further confirmation that orthopyroxene with well developed augite mellae resulted from the inversion of pigeonite is provided by the reservation of the herringbone twin structure of the pigeonite (Figs. 9, 0).

Poldervaart and Hess (1951, p. 482) contend that "in the majority of ases of inversion of pigeonite to orthopyroxene, the orthopyroxene will

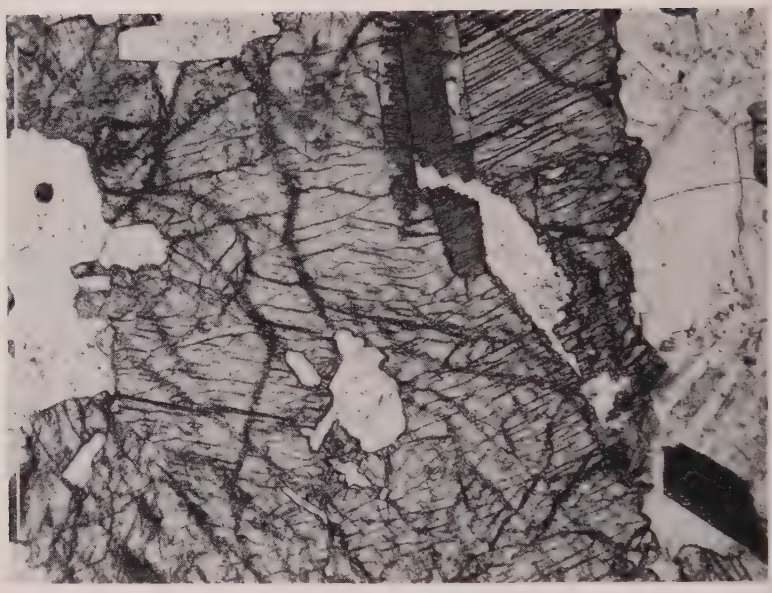

FIG. 9. Photomicrograph of pigeonite which has partially inverted to orthopyroxene. Some uninverted pigeonite showing a herringbone twin is present in the upper part of the field. The twin plane is (100) and the exsolution lamellae are parallel to (001), along which alteration has taken place. The remainder of the crystal is orthopyroxene. From quartz dolerite (specimen M212), about 40 feet from the western contact of the Red Hill Dike, Snug River. Plane light, scale mark is 1 mm. in length.

develop in such an orientation that it retains the *b* and *c* crystallographic axes of the parent pigeonite," but in the Red Hill intrusion this rarely occurs; an observation also made by Brown (1957) in his study of the Skaergaard pyroxenes. In the contact zones of the Red Hill dike, pigeonite commonly mantles primary orthopyroxene and assumes an orientation such that the *b* and *c* axes of the orthopyroxene are retained. If the pigeonite has subsequently inverted to orthopyroxene on cooling, the orientation of this secondary orthopyroxene, in some cases, is the same as the primary orthopyroxene, in agreement with Poldervaart and Hess's observations, but usually the orientation assumed is quite different. Also it is not uncommon to observe that a single pigeonite crystal, on inversion, has given rise to two or more areas of orthopyroxene which have different orientations; therefore even if one such area retained the *b* and *c* axes of the parent pigeonite the other(s) could not.

To further test the statement of Poldervaart and Hess a number of crystals of pigeonite, which had partially inverted to orthopyroxene, were plotted stereographically. In some cases the orientation of the orthopyroxene in relation to the parent pigeonite was quite random; in

FIG. 10. Same field as Fig. 9, but with crossed nicols. Note well developed exsolution lamellae in orthopyroxene, which are parallel to (001) of the original pigeonite. Relict twin plane of pigeonite preserved in secondary orthopyroxene. The orthopyroxene free of exsolution lamellae in the lower part of the field is probably primary.

other cases a relationship existed and the following orientations have been found:

$$\left\{\begin{array}{l} c \text{ orthopyroxene} = c \text{ pigeonite} \\ \text{plane } ab \text{ orthopyroxene contains } b \text{ pigeonite} \end{array}\right.$$

$$\left\{\begin{array}{l} b \text{ orthopyroxene lies in plane } ac \text{ pigeonite} \\ \text{plane } ac \text{ orthopyroxene contains } b \text{ pigeonite} \end{array}\right.$$

$$\left\{\begin{array}{l} a \text{ orthopyroxene lies in plane } ac \text{ pigeonite} \\ \text{plane } bc \text{ orthopyroxene contains } b \text{ pigeonite} \end{array}\right.$$

Thus the Red Hill orthopyroxenes, which have resulted from the inversion of pigeonite, exhibit a variety of orientations relative to the parent pigeonite. In a few cases the orthopyroxene retains the b and c axes of the parent pigeonite; generally, however, the orientation is random, although it is not uncommon to find that one crystallographic axis of the secondary orthopyroxene lies in a plane defined by two of the crystallographic axes of the parent pigeonite, and a plane of the orthopyroxene contains a crystallographic axis of the pigeonite.

The pigeonite only inverts to orthopyroxene in the marginal zones of the intrusion. These pigeonites, which are Mg-rich, have crystallized at

a temperature just above the pigeonite—orthopyroxene inversion curve (Fig. 7), and with cooling have been able to invert to orthopyroxene, because of the relatively fast rate of the inversion reaction at this temperature. Nevertheless, even in these rocks, less than half of the pigeonite has inverted, suggesting that the rate of cooling was such that the inversion could only be partially completed before the temperature decreased to a value at which it became too sluggish a reaction to take place. With increasing fractionation, away from the contacts of the intrusion, the pigeonite became progressively enriched in Fe and probably crystallized at an increasingly greater temperature above the inversion curve. By the time this pigeonite had cooled sufficiently to cross the inversion boundary, into the orthopyroxene stability field, the rate of the inversion reaction had become too slow, relative to the rate of cooling of the rock, because of the lower temperature of the phase boundary, for inversion to take place at all. Even in the central parts of the intrusion where the rate of cooling would have been the slowest, the inversion reaction has been too sluggish to occur.

Both the primary orthopyroxene and that which has resulted from the inversion of pigeonite, in some cases, contain exsolution lamellae of augite which are related to the orthopyroxene structure. These lamellae are very fine and of a similar thickness to those in the pigeonite, and are developed ||(100) of the host orthopyroxene. The lamellae are sporadically developed, even in the one crystal, and are not nearly as regular as those which occur in the clinopyroxenes. These augite lamellae have been exsolved from the primary or secondary orthopyroxenes as they cooled.

Summary and Conclusions

At the time of emplacement of the dolerite magma in the Red Hill intrusion an Mg-rich orthopyroxene (Of_{15}) was crystallizing, and after emplacement crystallization of this mineral continued for a short time until its composition reached Of_{30}, when pigeonite with approximately the same Mg:Fe ratio began to separate instead of the orthopyroxene. The pigeonite continued to crystallize with fractionation, and became progressively enriched in Fe^2 relative to Mg, with the Ca content remaining essentially constant. At an Mg:Fe ratio of about 40:60 the pigeonite ceased to crystallize at the limit of the two-pyroxene field, perhaps as the result of the liquidus minimum of the pyroxene system migrating to the Ca-rich side of the solvus. More analyses of the Ca-poor pyroxenes are obviously desirable but it is believed that the main trend has been demonstrated.

A member of the Ca-rich pyroxene series crystallized during the whole

If the cooling history of the Red Hill magma, except for the very early stages, just prior to intrusion, when only orthopyroxene was separating. The Ca-rich pyroxene crystallized in cotectic equilibrium first with orthopyroxene, adjacent to the chilled contacts, and then with pigeonite, until the latter ceased to form, when the Ca-rich pyroxene continued to crystallize independently in the more acid rocks. During fractionation the composition of the Ca-rich pyroxene changed progressively by successive replacement of Mg by Fe^2 with some variation in the Ca content. In the early and middle stages of fractionation the Ca content decreased steadily from about 40 to 31% of the total Ca+Mg+Fe, followed by a steady increase in the amount of Ca in the late stages to over 41% in the ferrohedenbergite of the granophyre.

The trend of crystallization in both pyroxene series is strikingly similar to that of the Skaergaard intrusion, but the pyroxenes of the augite series of Red Hill are always slightly lower in Ca than the corresponding pyroxenes from Skaergaard.

In both the Ca-poor and Ca-rich clinopyroxenes very thin exsolution lamellae parallel to (001) occur, and are the result of unmixing of one pyroxene phase from another owing to the decrease in stability with lowering of temperature. The lamellae in pigeonite are believed to be augitic in composition and those in the augite of pigeonitic composition. Exsolution lamellae are present in the pigeonite series right up to the stage when it ceases to crystallize, and in the augite series lamellae occur in all the pyroxenes up to and including the ferroaugite of the fayalite granophyre, but are generally absent from the ferrohedenbergite of the granophyre. The lack of exsolution lamellae in this Fe-rich pyroxene is probably the result of the relatively low temperature of crystallization and also that possibly no pyroxene of the pigeonite series is stable in this composition field.

In a zone up to about 200 feet from the chilled contacts of the Red Hill intrusion some of the pyroxene has partially or completely inverted to orthopyroxene. Elsewhere in the intrusion inversion has not taken place. This is probably related to the fact that the pigeonite in the marginal zones has crystallized close to the inversion curve and that the inversion rate is quite rapid at this relatively high temperature. In the more strongly fractionated rocks the pigeonite is more Fe-rich and has probably crystallized at a temperature somewhat above the inversion curve and on cooling, when passing into the orthopyroxene stability field the inversion reaction has been too slow as compared with the rate of cooling for it to take place.

The orthopyroxene resulting from the inversion of pigeonite rarely retains the *b* and *c* axes of the clinopyroxene but generally the orientation

is random, or else one crystallographic axis of the secondary ortho pyroxene lies in a plane defined by two of the crystallographic axes o the parent pigeonite and a plane of the orthopyroxene contains a crysta lographic axis of the pigeonite.

The recalculation of the chemical analyses of the pyroxenes indicate that in four out of the five cases some Ti^4 and or Fe^3, in addition to Al must replace Si in the tetrahedral position. With fractionation the minc constituents Ti, Mn and Fe^3 increase in amount whereas Al decrease and in the analyzed coexisting augite and pigeonite Ti, Mn and F are enriched in the pigeonite relative to the augite and Al is enriched i the augite.

Aknowledgments

This work was carried out while the writer was the holder of a Gener Motors-Holden's Limited Post-Graduate Research Fellowship and wish to express my thanks for their generous support. I desire to than Dr. G. Joplin and Dr. J. F. G. Wilkinson for the benefit of discussio with them during the course of this study.

References

Ahrens, L. H. (1952), The use of ionization potentials, I. Ionic radii of the element *Geoch. Cosm. Acta*, **2**, 155–169.

Banks, M. R. (1958), A comparison of Jurassic and Tertiary trends in Tasmania: *Dolerit A Symposium, Geol. Dept., Univ. of Tas.*, 231–264.

Berman, H. (1937), Constitution and classification of natural silicates: *Am. Mineral.*, **2** 333–415.

Bowen, N. L., and Schairer, J. F. (1935), The System MgO-FeO-SiO_2. *Am. Jour. Sc* **29**, 151–217.

Bown, M. G. and Gay, P. (1959), The identification of oriented inclusions in pyroxe crystals: *Am. Mineral.*, **44**, 592–602.

Brown, G. M. (1957), Pyroxenes from the early and middle stages of fractionation of t Skaergaard intrusion, East Greenland: *Mineral. Mag.*, **31**, 511–543.

Coombs, D. S. (1954), Ferriferous orthoclase from Madagascar: *Mineral. Mag.*, **30**, 40 427.

Edwards, A. B. (1942), Differentiation of the dolerites of Tasmania: *J. Geol.*, **50**, 451–48 579–610.

Faust, G. T. (1936), The fusion relations of iron-orthoclase: *Am. Mineral.*, **21**, 735–76

Hess, H. H. (1941), Pyroxenes of common magic magmas: *Am. Mineral.*, **26**, 515–53 573–594.

Hess, H. H. (1949), Chemical composition and optical properties of common clin pyroxenes. Part I: *Am. Mineral*, **34**, 621–666.

Kuno, H. (1955), Ion substitution in the diopside–ferropigeonite series of clinopyroxene *Am. Mineral.*, **40**, 70–93.

Muir, I. D. (1951), The clinopyroxenes of the Skaergaard intrusion, eastern Greenlan *Mineral. Mag.*, **29**, 690–714.

——— (1954), Crystallization of pyroxenes in an iron-rich diabase from Minnesot *Mineral. Mag.*, **30**, 376–388.

—— (1955), Transitional optics of some andesines and labradorites: *Mineral. Mag.*, **30,** 545–568.

OLDERVAART, A. (1944), The petrology of the Elephant's Head dike and the New Amalfi Sheet (Matatiele): *Trans. Roy. Soc. South Africa*, **30,** 85–119.

—— (1950), Correlation of physical properties and chemical composition in the plagioclase, olivine and orthopyroxene series: *Am. Mineral.*, **35,** 1067–1079.

OLDERVAART, A., AND HESS, H. H. (1951), Pyroxenes in the crystallization of basaltic magmas. *J. Geol.*, **59,** 472–489.

INGWOOD, A. E. (1955), The principles governing trace element distribution during magmatic crystallization. Part I: The influence of electronegativity: *Geoch. Cosm. Acta*, **7,** 189–202.

OSENQVIST, I. T. (1951), Investigations in the crystal chemistry of Silicates III. The relation haematite-microcline: *Norsk. Geol. Tids.* **29,** 65–76.

SUBOI, S. (1932), On the course of crystallization of basaltic magma: *Jap. J. Geol. Geogr.*, **10,** 67–82.

AGER, L. R., AND DEER, W. A. (1939), The petrology of the Skaergaard intrusion, Kangerdlugssuaq, East Greenland: *Medd. Om Grønland*, **105,** No. 4, 1–352.

AGER, L. R., AND MITCHELL, R. L. (1951), The distribution of trace elements during strong fractionation of basic magma: *Geoch. Cosm. Acta*, **1,** 129–208.

Manuscript received July 25, 1960.

THE DECOMPOSITION OF MICROCLINE, ALBITE AND NEPHELINE IN HOT WATER*

GEORGE W. MOREY AND ROBERT O. FOURNIER, *U. S. Geological Survey, Washington 25, D. C.*

ABSTRACT

The decomposition of microcline, albite, and potassium-bearing nepheline was investigated by slowly pumping distilled water at 295° C and 2500 psi over each sample for 13 days. The liquids collected from the bombs were analyzed for Na_2O, K_2O, Al_2O_3, and SiO_2. Microcline was partially decomposed to muscovite. The total amount of material in solution averaged 167 ppm and the pH averaged 7.9. Albite partially altered to boehmite, paragonite, and an amorphous material. The total amount of material in solution averaged 243 ppm and the pH averaged 7.9. An alteration profile was found in the nepheline sample container. Mainly muscovite plus minor analcite were found at the exit end of the container while mainly boehmite was found at the entrance end. The total amount of material in solution averaged 440 ppm and the pH averaged 9.7 with a high of 10.2. The ratio of sodium to potassium in the solutions leached from each of the minerals was greater than the ratio of sodium to potassium in the starting material.

INTRODUCTION

Three long-term experiments have been carried out to investigate the behavior of microcline, albite, and nepheline when water at 295° C and 2500 psi is pumped over each sample. Similar experiments using the same microcline and albite, but at different temperatures and pressures have been reported by Morey and Chen (1955). Khitarov (1958) also has conducted solution experiments on oligoclase using a continuous leaching technique. Hemley (1959) has measured the equilibrium quotients for the hydrolysis reactions of K-feldspar to mica+silica and of mica to kaolinite in the temperature range 200° to 500° C. at various high pressures. However, solubilities of all the components in the system were not measured by Hemley.

It is emphasized that all the solution results given in this paper represent rates of reaction under the conditions of the experiments, and not the equilibrium solution or equilibrium hydrolysis of the minerals under consideration.

APPARATUS

The apparatus is shown schematically in Fig. 1. The sample is contained within an 8-inch long, $\frac{1}{4}$ inch i.d. stainless steel tube fitted at one end with a porous stainless steel filter having a mean pore opening of 2 microns. The sample holder fits snugly into the middle of a two foot long steel bomb and is held in place by a stainless steel support tube. The encasing bomb has pressure fittings at each end. Water under pres

* Publication authorized by the Director, U. S. Geological Survey.

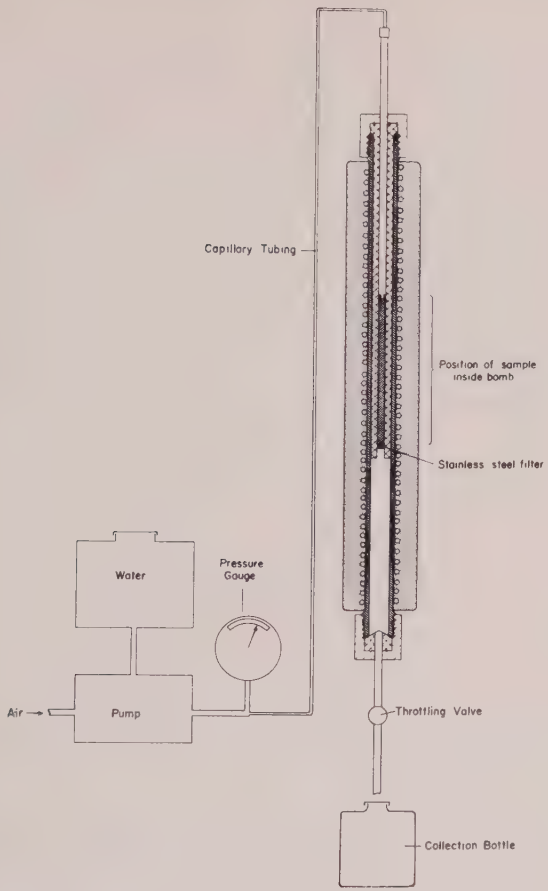

FIG. 1. Schematic diagram of pressure apparatus.

sure is introduced into the top of the bomb by means of an air-actuated diaphragm pump. The water passes down through the powdered samples and out of the bottom of the bomb where it is collected. The rate of flow of the fluid out of the bomb is controlled by a throttling valve. As liquid drips out of the bomb the resulting pressure drop in the high pressure system is sensed across the diaphragm in the pump. This actuates the pump automatically to send more water into the bomb to maintain the predetermined pressure. Friction in the pumping system may cause temporary pressure drops of 100 to 200 psi.

An electrical resistance furnace is wound directly around the outside of the bomb, sheet mica being used as an insulating material next to the bomb. Temperature control was by manual settings of a variac voltage regulator.

Temperature was measured by a platinum-10% rhodium thermocouple wrapped against the outside of the bomb adjacent to the middle of the sample container. Temperatures were continuously recorded on a multiple-record strip chart recorder. During the period when samples were collected the temperature did not vary more than ±5° C. from 295° C. There was no provision for measuring the temperature gradient along the length of the sample holder while liquid was being collected from the bomb. However, the temperature gradient was probably small as the furnace windings project six inches beyond each end of the sample holder. Also, in a similarly conducted experiment using a 10-inch long bomb and a furnace of different design, the authors found that an initial ten degree temperature gradient from the top to the bottom of the bomb was reduced to no temperature gradient within one minute after starting to drip liquid from the bomb.

TABLE 1.—CHEMICAL ANALYSES OF STARTING MATERIALS

[Analyst, Paula M. Montalto]

	Microcline	Albite	Nepheline
	(weight per cent)	(weight per cent)	(weight per cent)
SiO_2	65.06	68.06	42.34
Al_2O_3	18.90	20.00	34.22
Fe_2O_3	.06	.04	.06
CaO	.04	.15	.45
Na_2O	2.90	11.49	15.73
K_2O	13.30	.15	6.45
H_2O^+	.03	.01	.28
H_2O^-	.03	.01	.06
	100.32	99.91	99.59

STARTING MATERIALS

The minerals used as starting materials for the experiments reported here were 1) large crystals of perthitic microcline from the Derry mine in Quebec, 2) crystals of albite from Amelia County, Virginia, and 3) massive nepheline from Bancroft, Ontario. Chemical analyses of these minerals are tabulated in Table 1.

EXPERIMENTAL PROCEDURE

Each silicate was crushed to pass a 20-mesh screen and collected on an 80-mesh screen and the fines were removed by washing. Eight to nine grams of the dried sample were weighed into the sample holder. Each bomb was assembled and placed upright in a supporting rack. As

soon as the desired temperature was attained and stabilized, water was pumped into the bomb. Approximately 34 to 38 ml. of water at 295° C. and 2500 psi were maintained in the bombs at all times.* Each week day during an eight-hour period liquid was dripped at as uniform a rate as possible from the bombs into polyethylene bottles. The throttling valves were closed at night. During the first five days of liquid collection 50 to 100 ml. per day were obtained from each bomb. The average drip rate was 0.1 to 0.2 ml. per minute. Thereafter, generally 200 to 250 ml. per bomb per day were collected and the average drip rate was 0.8 to 1.0 ml. per minute. Most of the liquid was collected at the fairly slow uniform rates indicated by the average values. However, there were considerable variations in the rate of drip. There were extended periods when no liquid dripped from the bombs and other periods when the drip rate increased to as much as 4 ml. per minute.

The solutions were analyzed by colorimetric methods (Shapiro and Brannock, 1956) for K_2O, Na_2O, Al_2O_3, and SiO_2. We are grateful to Leonard Shapiro for his assistance in carrying out these analyses.

For the first five days of liquid collecting each of the liquid samples was individually analyzed. Then for four weeks each two day's collections were combined for analyses and for the last 14 weeks each week's collections were combined for one analysis.

No apparent precipitation of oxides from solutions occurred when the solutions were obtained from the bombs or upon standing at room temperature and pressure. At the end of 135 days no precipitate was found in the exit tubing of the bombs and no visible precipitate formed in the collection bottles. Samples of solutions from the two feldspars were analyzed for aluminum immediately after collection and again after 12 days. No change in the aluminum contents of the solutions were found. Both solutions had pH values of 7.9 and the concentrations of Al_2O_3 were 38 ppm for the albite solution and 27 ppm for the microcline solution. Similarly a nepheline solution of pH 9.5 gave identical results of 159 ppm Al_2O_3 in solution before and after eight months of storage.

At the termination of the experiments the alteration products left in the sample containers were examined optically and by *x*-ray.

Results

Microcline

The data obtained from the microcline experiment are summarized in Table 2. The initial weight of the microcline sample was 8.810 g.

* An exception was at the end of 33 days when the bombs were cooled and taken apart to investigate the progress of the alteration of the samples. The bombs were re-assembled and the experiments continued using the same then partially altered material.

After 135 days 2.075 g. or 23.6% of the sample had been dissolved in 12,460 g. of solution. This is 167 ppm of solids put into solution.

The molecular ratio of $(K_2O+Na_2O):Al_2O_3:SiO_2$ should be 1:1:6 if the microcline dissolved stoichiometrically. The measured ratio in solution was 1.60:1:9.85. If all the K_2O in solution is calculated to orthoclase, the orthoclase amounts to 1.063 g., or 51%; if the remaining Al_2O_3 in solution is calculated to albite, the albite amounts to 0.329 g. or 16%.

TABLE 2. MICROCLINE EXPERIMENTAL DATA

	SiO_2	Al_2O_3	K_2O	Na_2O	Total
Average solubility in ppm for first 33 days and 22 collections	147	25	15	12	199
Average solubility in ppm for the last 102 days and 39 collections	108	19	14	10	151
Average solubility in ppm for the total of all runs*	121	21	14	11	167
Grams dissolved in the first 33 days	.578	.098	.058	.049	.783
Grams dissolved in the last 102 days	.924	.161	.122	.085	1.292
Total grams dissolved	1.502	.259	.180	.134	2.075
Mole ratios for the first 33 days	10.00:1:	.640:	.823		
Mole ratios for the last 102 days	9:74:1:	.822:	.867		
Mole ratios for the total	9.85:1:	.752:	.850		

Temperature: 295° ±5° C.
Pressure: 2500±200 psi
Duration of experiment: 135 days

Initial weight of sample: 8.810 g.
Weight of liquid pumped over sample:
First 33 days— 3,941.5 g.
Last 102 days — 8,515.5 g.
Total —12,460.0 g.

* Calculated by dividing the total grams dissolved by the total amount of liquid pumped over the sample.

The remainder, 0.683 g. or 33%, is Na_2O and SiO_2 in the molecular ratio of 1:6.4. There has evidently been much decomposition, with extraction of Na_2O and SiO_2.

The dissolving liquid was distilled water having an initial pH of 5.8 caused by a small amount of dissolved atmospheric CO_2. The pH of the solution collected from the bomb varied from 7.7 to 8.2 and averaged 7.9.

The solution of oxides, particularly SiO_2, was greater during the first days of pumping water over the microcline than during the last. For the first five collections of liquid from the bomb, SiO_2 was found to be about 200 ppm and the total solids 270 ppm. The high values for silica

then tapered off and the values for the dissolved material were fairly constant for the remainder of the runs. Albite behaved in a similar manner.

This initial high solubility was probably due to strained surface conditions imparted to the feldspar grains as the original large single crystals were crushed. As soon as the molecular-sized "ragged areas" on the grain surfaces were dissolved away or hydrolyzed to mica, the

Table 3. Albite Experimental Data

	SiO_2	Al_2O_3	K_2O	Na_2O	Total
Average solubility in ppm for first 33 days and 22 collections	178	38	0.7	32	249
Average solubility in ppm for the last 102 days and 39 collections	171	38	0.6	31	241
Average solubility in ppm for the total of all runs*	172	38	0.7	32	243
Grams dissolved in the first 33 days	.637	.137	.003	.114	.891
Grams dissolved in the last 102 days	1.620	.363	.006	.298	2.287
Total grams dissolved	2.257	.500	.009	.412	3.178
Mole ratios for the first 33 days	7.91:1:	.02:	1.37		
Mole ratios for the last 102 days	7.58:1:	.02:	1.35		
Mole ratios for the total	7.65:1:	.02:	1.36		
Temperature: 295° ± 5° C.	Initial weight of sample: 9.257 g.				
Pressure: 2500 ± 200 psi	Weight of liquid pumped over sample:				
Duration of experiment: 135 days	First 33 days — 3,570 g.				
	Last 102 days — 9,497 g.				
	Total — 13,067 g.				

* Calculated by dividing the total grams dissolved by the total amount of liquid pumped over the sample.

amount of dissolved silica in the solutions decreased. The comparatively large initial solution values may in part be due to slower rates of pumping liquid over the samples. However, similar slow rates of liquid collec- were made at a later time without any increase in the amount of SiO_2 in solution.

No alteration products were apparent when the microcline was examined 33 days after the start of the experiment. After 135 days a large amount of unaltered feldspar still was present. Muscovite, partially coating most of the feldspar grains throughout the sample container, was the only alteration product found. If microcline is decomposed and leaves

only a residue of muscovite, the solution obtained from the bomb should contain excess $(K_2O+Na_2O):SiO_2$ in the molecular ratio 1:6. As already pointed out, the ratio found was 1:6.4.

Delicate, skeleton like portions of the perthite were found where water first came in contact with the microcline. The sodium-rich layers had been dissolved out, leaving behind portions of the potassium-rich layers.

Morey and Chen (1955) found that microcline from the Derry mine altered to both boehmite and muscovite at 350° C. and 5000 psi.

Albite

The data obtained from the albite experiment are summarized in Table 3. The intial weight of the albite sample was 9.257 g. After 135 days 3.178 g. or 34% of the sample had been dissolved in 13,067 g. of solution. This is 243 ppm. The pH of the distilled water pumped into the bomb was 5.8 and the pH of the solution collected from the bomb varied from 7.7 to 8.0 and averaged 7.9.

The experimentally measured molecular ratio of $(Na_2O+K_2O):Al_2O_3:SiO_2$ was 1.38:1:7.65. Excesses of 0.115 g. Na_2O and 0.486 g. SiO_2 exist in solution over the amounts which could combine with all the Al_2O_3 in solution for form albite. The amount of albite which could precipitate is 2.025 g. corresponding to 81% of the dissolved material.

After 135 days boehmite and paragonite were found partially coating albite grains throughout the sample container. No other alteration product was found by *x*-ray diffraction. However, a microscopic examination of the alteration products revealed that low birefringent blades of paragonite and granular boehmite are set in a gelatinous matrix. If paragonite and boehmite were the only alteration products the molecular ratio of the excess $Na_2O:SiO_2$ in solution should have been 1:6. The molecular ratio was measured to be 1:4.3. Such a ratio would be expected if an allophane-like material were forming.

In similarly conducted experiments Morey and Chen (1955) found that the Amelia albite altered to boehmite, analcite, and dioctahedral micas at 350° C. and 5000 psi. The mole ratio of excess $Na_2O:SiO_2$ in solution was 1:13.6. At 200° C. and 2000 psi they found that albite altered to boehmite and kaolinite and the mole ratio of excess $Na_2O:SiO_2$ in solution was 1:3.8.

Nepheline

The data obtained from the nepheline experiment are summarized in Table 4. The initial weight of the nepheline sample was 8.453 g. After 135 days 12,796 g. of liquid had passed over the nepheline, dissolving

5.630 g. of material or 67% of the sample. This amounts to 440 ppm. It should be noted, however, that the average parts per million was 491 for the first 33 days and only 416 for the last 102 days.

The pH of the CO_2-bearing distilled water pumped into the bomb was 5.8 and the pH of the solution collected from the bomb varied from 9.2 to 10.2. During the first 48 days of pumping liquid over the nepheline the pH varied from 9.9 to 10.2 and averaged 10.0. Later, as the nepheline

Table 4. Nepheline Experimental Data

	SiO_2	Al_2O_3	K_2O	Na_2O	Total
Average solubility in ppm for first 33 days and 22 collections	200	148	30	113	491
Average solubility in ppm for the last 102 days and 39 collections	188	118	24	86	416
Average solubility in ppm for the total of all runs*	192	127	26	95	440
Grams dissolved in the first 33 days	.793	0.587	0.121	0.450	1.951
Grams dissolved in the last 102 days	1.662	1.040	0.215	0.762	3.679
Total grams dissolved	2.455	1.627	0.336	1.212	5.630
Mole ratios for the first 33 days	2.29:1:.22:1.26				
Mole ratios for the last 102 days	2.66:1:.22:1.21				
Mole ratios for the total	2.57:1:.22:1.25				
Temperature: 295°±5° C.	Initial weight of sample: 8.453 g.				
Pressure: 2500±200 psi	Weight of liquid pumped over sample:				
Duration of experiment: 135 days	First 33 days— 3,969 g.				
	Last 102 days — 8,829 g.				
	Total —12,798 g.				

* Calculated by dividing the total grams dissolved by the total amount of liquid pumped over the sample.

grains became coated with alteration products the pH gradually decreased, reaching the lowest pH values toward the termination of the runs.

For the first 33 days the dissolved material had an average measured molecular ratio of $(Na_2O+K_2O):Al_2O_3:SiO_2$ of 1.48:1:2.29. From this solution 84% of the dissolved material or 1.637 g. could precipitate as nepheline. The remainder, after the subtraction of Na_2O, Al_2O_3, and SiO_2 for nepheline, is an excess of 0.138 g. Na_2O, 0.215 g. K_2O, and 0.412 g. SiO_2. The molecular ratio of excess $(Na_2O+K_2O):SiO_2$ is 1:0.61.

For the last 102 days the dissolved material had an average molecular

ratio of $(Na_2O+K_2O):Al_2O_3:SiO_2$ of 1.43:1:2.66. From this solution 79% of the dissolved material or 2.920 g. could precipitate as nepheline. This compares very closely with the 84% for the first 33 days. However, the molecular ratio of excess $(Na_2O+K_2O):SiO_2$ in solution is almost reversed. Instead of 1:0.61, it is 1:1.53. After substracting for nepheline there are excesses in solution of 0.132 g. Na_2O, 0.215 g. K_2O, and 0.412 g. SiO_2.

After 33 days a mixture of boehmite and muscovite was found replacing all the nepheline at the very top of the sample container, where fresh water first came in contact with the sample. At the exit end (bottom) of the sample holder the nepheline was unaltered. No trace of paragonite or analcite was found at this time.

When the experiment was terminated, after 135 days, mainly muscovite and small amounts of analcite were at the exit end of the container along with a few small residual grains of nepheline ensheathed by mica. In the middle and upper part of the container dioctahedral mica and boehmite mixtures were present. At the top of the container, where fresh water came in contact with the sample, only boehmite and minor amounts of paragonite were found. It is possible that paragonite may have been present elsewhere in the sample container, its presence masked by muscovite.

Discussion of Results

The dissolution and alteration of the minerals dealt with in this experimentation were carried out mainly in a dynamic open system. During the hours when samples were collected, the main movement of dissolved material was by a flushing action of liquid flowing in one direction into the top and out the bottom of the bomb. In such a system large concentration gradients of metal cations and of hydrogen ions (pH) result owing to the continued reaction of an increment of solution with solids as the solution moves through the bomb. Thus, the concentration and pH of the relatively dilute solution at the top of the sample holder may be appropriate for the formation there of one alteration product while at another point in the sample holder a different concentration and pH may be appropriate for the formation of a different alteration product.

In contrast, during the periods when no fluid was removed from the system, movement of material in solution was mainly by ionic diffusion and by convection of the liquid caused by temperature gradients. Both effects would tend toward equalizing the chemical potential of each ionic species throughout the sample holder. Thus, some alteration products which formed during the dynamic periods when liquid was ex-

tracted might become unstable in the presence of and react with quiescent liquids which remain in the bomb for relatively long periods. On the other hand, some alteration products would be expected to become stable over a much greater portion of the sample holder when there is opportunity for chemical potential gradients to be decreased.

Most of the alteration products probably formed during and shortly after the periods when water was dripped from the bombs. Only relatively small amounts of alteration products would be expected to form during "quiescent" periods for the following reasons. The starting materials are stable in the temperature-pressure environment of the experiments. Therefore, the starting materials will dissolve and alteration products will crystallize out of solution only until the chemical potential of each component is the same both in the solution and in each solid in which the component occurs. As soon as equilibrium is attained no further increase in the amounts of alteration products will take place as long as the temperature, pressure, and concentrations of ions in solution remain constant. During the periods when solution was dripped from the bombs the concentrations of ions in contact with solids at a given point within a bomb is constantly subject to change owing to liquid flow. In this case alteration products may continuously form in an attempt to reach equilibrium with each new portion of liquid passing by.

The alteration within the nepheline sample holder may be visualized as proceeding in the following manner: Decomposition of the nepheline was very rapid at the top of the container where fresh distilled water first came in contact with it. Muscovite was probably the first alteration product to form according to the hydrolysis reaction

$$3(Na, K)AlSiO_4 + H_2O \rightarrow (K, Na)Al_2(AlSi_3O_{10})(OH)_2 + Na_2O(soln).$$

This would account for the very high sodium content in the analyzed solutions during the first few days of the experiment. The first solution collected from the bomb contained 328 ppm Na_2O. Alteration proceeded from the top of the container downward. At a time when fresh nepheline still existed at the bottom, muscovite which had replaced nepheline in the top portion of the sample column began to decompose, leaving boehmite behind according to the reaction,

$$2(K, Na)Al_2(AlSi_3O_{10})(OH)_2 + 7H_2O \rightarrow 3Al_2(OH)_6 + (K, Na)_2O(soln) + 6SiO_2(soln).$$

This reaction led to an increase in solution of SiO_2 in respect to Na_2O and accounts for the reversal in the mole ratios of excess Na_2O:SiO_2 after the initial days of sample collection. Boehmite probably accompanied muscovite from a very early stage in the experiment.

Analcite probably began to form at a stage when the decomposition of muscovite in the upper part of the bomb allowed relatively high

concentrations of dissolved SiO_2 to pass over yet unaltered nepheline below.

It is difficult to account for the position of paragonite in the upper part of the sample holder accompanying boehmite. One possibility is that muscovite and paragonite formed concurrently. This would imply that paragonite is more resistant to breakdown by leaching than is muscovite. The paragonite certainly did not form as a decomposition product of muscovite as the ratio Na/K would not be high enough in

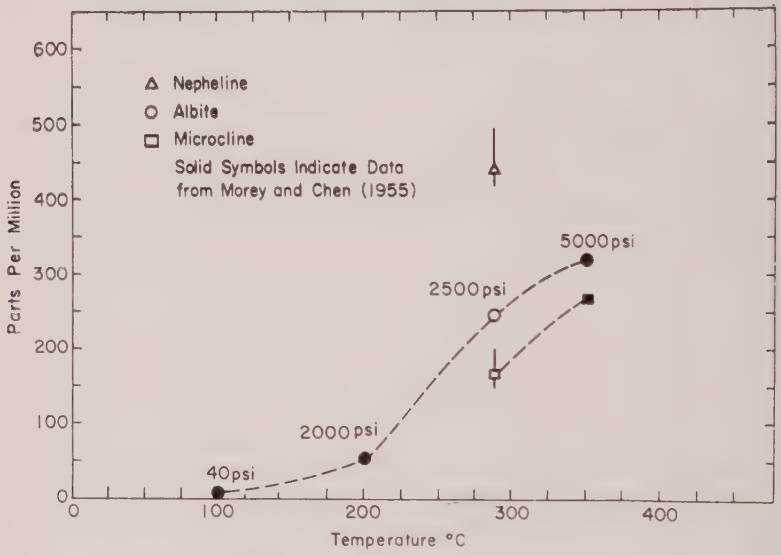

FIG. 2. Average total amounts of oxides in solution extracted from microcline from the Derry mine, albite from Amelia County, Va., and nepheline from Bancroft, Ontario. These are not equilibrium values, but rather chemical solution values obtained by decomposition of the samples under the conditions of the experiment.

solution. The paragonite might possibly form as a result of the decomposition of analcite. Another possibility is that the paragonite formed during quiescent periods when diffusion of sodium and silica back into the upper region of the sample holder may have allowed these components to react with boehmite. Potassium ions may not have migrated to the top of the container as rapidly as the sodium ions owing to their larger size and to rapid reactions forming muscovite lower in the container.

A comparison of the average total amounts of material in solution extracted from microcline from the Derry mine, albite from Amelia County, Va., and nepheline from Bancroft, Ontario, is shown in Figure 2.

The behavior of nepheline under the conditions of these experiments was markedly different from that of the two feldspars. Nepheline in the top of the container quickly reacted with fresh water coming in contact with it. Water at the top of the sample holder soon approached saturation with dissolved material and the rate of attack upon nepheline further down in the tube was slow. An alteration profile was thus set up with each successive increment of fresh solution attacking the nepheline a little further down in the sample holder. As the nepheline was used up and alteration products became more abundant, the chemical picture for the sample container as a whole gradually changed. This was reflected in a gradual change in quantities and proportions of dissolved materials in the solutions obtained from the bomb. A new chemical system gradually worked its way down in the sample holder as nepheline was successively used up at lower and lower levels.

The feldspars, on the other hand, were not rapidly decomposed when distilled water first came in contact with them at the top of the container. Concentration and pH gradients were never as large in the feldspar containers as in the nepheline container. Therefore, an alteration profile similar to that found in the nepheline container did not develop. An alteration profile formed only to the extent that there were more of the same kind or kinds of alteration products in the top of the sample container than in the bottom.

In all the experiments potassium tended to remain behind as muscovite and the solutions were enriched in sodium.

References

Hemley, J. J. (1959), Some mineralogical equilibria in the system K_2O-Al_2O_3-SiO_2-H_2O: *Am. Jour. Sci.*, **257**, 241–270.

Khitarov, N. I. (1958), On the reaction of oligoclase with water under conditions of high temperature and pressure: *Trudy Pyatogo Soveschchaniya Eksper. i Tekhn. Mineralog. i. Petrog.*, 208–213.

Morey, G. W., and Chen, W. T. (1955), The action of hot water on some feldspars: *Am. Mineral.*, **40**, 996–1000.

Shapiro, L., and Brannock, W. W. (1956), Rapid analysis of silicate rocks: *U. S. Geol. Survey Bull.*, **1036-C**.

Manuscript received July 27, 1960.

THE AMERICAN MINERALOGIST, VOL. 46, MAY-JUNE, 1961

X-RAY CRYSTALLOGRAPHY OF DAVIDITE

A. PABST, *University of California, Berkeley*

ABSTRACT

Partly or wholly metamict davidite from Pima County, Arizona and from Iveland, Norway, has been reconstituted to single crystals or twins by heating in air. The cell dimensions are a_0 10.37 ± 0.02, c_0 20.87 ± 0.02 Å. The space group is $R\bar{3}$ or $R3$. The suggested ideal content for the rhombohedral cell is $Y_6Z_{15}O_{36}$ or $3(Y_2Z_5O_{12})$, Y representing the larger cations, mostly Fe″ with some Ce, U, etc. and Z the smaller cations, mostly Ti with some Fe‴, V, Cr, etc. Davidites from seven localities yield the same powder diffraction pattern which can be fully indexed on this cell. Small amounts of contaminants, mostly rutile, can be identified in some reconstituted davidites. The reported morphology of davidite from Mozambique can be reconciled with the structure cell. Rough crystals of davidite from Billeroo, South Australia, also appear rhombohedral.

INTRODUCTION

The name davidite was applied by Mawson (1906) to a "bright black mineral" from Radium Hill, South Australia, shown "to contain over 50 per cent titania, a large quantity of iron, and a notable amount of rare earths, uranium, vanadium and chromium." An analysis was not published until ten years later (Cooke, 1916). The mineral at the type locality occurs in an intimate intergrowth with ilmenite and rutile from which it is difficult to separate a pure concentrate. Probably because of this the status of the species had been questioned even before the publication of Cooke's analysis (Crook and Blake, 1910) and long remained in doubt (Palache, Berman and Frondel, 1944, p. 542) though Mawson (1916) had reasserted its validity when the analysis was published. This may have been the reason for the caution exercised by Bannister and Horne (1950) when they referred to material they described as "A radioactive mineral from Mozambique related to davidite."

Studies by Kerr and Holland (1951) showed that davidite yields a characteristic DTA curve as well as *x*-ray powder diffraction pattern though analyses indicate wide variation in composition and in recent years davidite has been reported from many other localities in Australia (Whittle, 1954 and 1955, Lawrence, *et al.* 1957, Ramdohr and Lawrence, 1958). In spite of this its status continues to be questioned and Whittle (1959, p. 80) has recently stated "that davidite is perhaps not a finite mineral species, but that it could consist of a mechanical mixture of two or even more minerals, which are intimately associated at submicroscopic sizes."

The finding of davidite in Arizona which could be made to yield single crystal diffraction patterns (Pabst and Thomssen, 1959) has led to a unit cell and probable space group for davidite on the basis of which

powder patterns of davidite from many localities can be indexed. These results have been further supported by single crystal *x*-ray examination of davidite from Norway and by the reconciliation of the reported morphology of davidite from Mozambique and meager observations on the morphology of davidite from Billeroo, South Australia, with the lattice found by *x*-ray diffraction.

Material

Davidite specimens available for study included material from:

1. Pandora prospect, Quijotoa Mountains, Pima County, Arizona. (Several pieces collected by R. W. Thomssen, showing the association described by Thomssen (1961).)
2. Radium Hill, South Australia, the type locality. (Mawson 1906, 1944)
   a. (3×4″ specimen, mostly davidite intimately intergrown with ilmenite and rutile and much black mica, with which are mixed minor amounts of chalcopyrite and carbonates.)
   b. (A smaller specimen, similar to 2*a*, some parts nearly pure davidite.)
   Presumably equivalent to type material.
3. Crocker's Well, South Australia. Locality described by Whittle (1954).
   a. (Black, pitchy mass, 1½×1½″, with albite, mostly pale brownish in color, presumably due to many minute, high index, colored inclusions.)
   b. (A specimen similar to 3*a*, kindly lent for study by Mr. Joseph Urban.)
4. Billeroo, South Australia. Mentioned by Whittle (1959).
   a. (A small cluster of crystals, ca. 1×1″.)
   b. (3 larger, rough, single crystals, 22½, 17 and 8½ grams.)
5. Thackeringa, New South Wales, Australia.
   (1½″×2″. Small amount of davidite with a bit of anatase coating and large rutile crystals, some coarse gray quartz in fine granular yellowish matrix of quartz with a bit of mica.)
6. Portuguese East Africa (Mozambique). Geological setting described by Davidson and Bennett (1950), and by Roso de Luna and Freitas (1952), referred to as mavudzite by Pinto Coelho (1954). ("Rich mass," a 1×2″ rough fragment of pure davidite.)
7. Iveland, Setesdal, Norway.
   (1½×1½″ crystal fragment with a bit of adhering quartz and mica.)
   Specimens 2*a*, 4*a*, 5, 6, and 7 were purchased from the Scott Williams Mineral Co., specimens 2*b*, 3*a* and 4*b* from Specimen Minerals (Australia) Ltd.
   (See supplementary note (2) on page 718 of this paper)
   Other specimens examined (no davidite found):
8. Heavy mineral concentrates from east side of the Sierra Nevada, California. Said to contain "uranium-bearing ilmenite" (Shawe, 1953). Kindly supplied by Professor C. O. Hutton.
9. Coarse, heavy mineral concentrates. Red River placer gravels. Idaho County, Idaho. Reported to contain davidite (Armstrong and Weis, 1957, table 1, p. 28). Kindly supplied by L. L. Brown, U. S. Bureau of Mines, Albany, Oregon.

X-Ray Procedure

X-ray examination of davidites was carried out mostly on fragments. Untreated fragments were first mounted in Norelco powder cameras at

the tips of glass fibers and the x-ray diffraction recorded. Thereupon the fragments were dismounted, heat treated, remounted and again examined by x-ray diffraction. In some cases fragments were repeatedly treated and remounted for further examination to follow the course of changes. If single crystal diffraction was detected in either untreated or treated material the fragments were remounted on x-ray goniometer heads and fully examined by the Weissenberg or Buerger precession methods. X-ray photographs were also made from powdered material for the sake of obtaining more favorable conditions for recording powder patterns but only after the same material had been checked by the examination of fragments.

General Survey of Results

Davidites from all seven localities are initially metamict or show only faint x-ray indications of a remnant of structure. Upon heating all yielded the same x-ray powder diffraction pattern which can be indexed on the basis of a rhombohedral cell. The temperature at which reconstitution is effected varies in different davidites but once the reconstitution is complete no further changes are produced in the powder patterns by heating fragments to temperatures as high as 1375° C. Lima de Faria (1956, p. 8) noted that "it makes no difference whether davidite samples are heated at 1000° C. for 1 hour or for 24 hours."

Twelve fragments from Arizona and 9 from Norway were heated and examined by x-rays. All were reconstituted to single crystals, twins or coarse aggregates. No fragments from the other five localities were reconstituted in this way by heating, though 27 such fragments were examined, at least 4 from each locality. In most cases smooth arcs were observed in the powder patterns but the best patterns of reconstituted davidite from Radium Hill, the type locality, show some degree of orientation, suggesting that there might be a possibility of finding fragments of this material that could be reconstituted to single crystals.

Space Group and Cell Dimensions

Indexing of all patterns indicates a rhombohedral lattice and the Laue group is $\bar{3}$ so that the possible space groups are $R\bar{3}$ or $R3$, the latter if the c axis is polar as concluded from the morphology by Horne (Bannister & Horne, 1950, p. 102). The cell dimensions as determined from shrinkage-corrected Weissenberg or precession patterns of davidite from Arizona and Norway are a_0 10.37 ± 0.02 Å, c_0 20.87 ± 0.02 Å, averages of 11 and 6 determinations respectively, corresponding to a_r 9.178 Å, α 68° 48′, for the rhombohedral cell. The large indicated ranges of uncertainty span all values obtained. A greater precision was not

attained because of the diffuseness of high angle spots on most films and the high background on films with Cu or Co radiation due to high Ti content of the mineral. Powder patterns show no measurable back reflection lines but multiple correlation using 14 and 16 selected lines free of coincidence in the interval 3.0 to 1.4 Å on Co powder patterns of Arizona and Norway davidite respectively, made from powder rods 0.1 mm. thick and perfectly centered, yielded good checks of the values obtained from single crystals. Powder patterns of davidite from the five other localities gave no indication of differences in cell dimensions that would exceed the stated limits.

Indexed Powder Pattern

In Table 1 is given an indexed powder pattern of davidite from Arizona heated for one hour at 970° C. in air. The indexing has been completely checked by comparison with single crystal patterns giving proper consideration to intensities. All expected lines are observed and there are no surplus lines. Most of the indices listed in the table represent superposition of 2 and some of 4 sets of reflections. For instance, $41\bar{5}6$ represents $\{41\bar{5}6\}$, $\{41\bar{5}\bar{6}\}$, $\{51\bar{4}6\}$ and $\{51\bar{4}\bar{6}\}$. The relative intensities of spots representing these four sets, as observed on a single precession pattern, are 6, 5, 3 and 1. This statement can be taken to define the orientation adopted for indexing davidite single crystal patterns. In Table 1 the indices listed do not in all cases correspond to the set of reflections with highest intensity as in the example just given.

The indexed powder pattern agrees fairly well with patterns of davidite from Mozambique, specimen 1, published by Kerr and Holland (1951, table 2) and of "the Tete mineral after heating in air at 1000° C." published by Bannister and Horne (1950, Fig. 6, pattern A) as well as with patterns of davidite from Australian localities published by Lawrence *et al.* (1957) and by Whittle (1959), but includes a number of weaker lines not recorded by those observers. Similar patterns were obtained from all the davidites examined though some also showed extraneous lines to be discussed later. No change was observed in patterns obtained from fragments heated for longer periods or to higher temperatures. The highest temperatures employed were: specimen 1, 2 hours at 1375° C.; specimen 3*b*, $1\frac{1}{2}$ hours at 1150° C; specimen 4*a*, $1\frac{1}{4}$ hours at 1180° C. and specimen 6, 1 hour at 1220° C.

Density, Composition and Cell Content

In Table 2 are shown the chemical analyses of three of the davidites examined, two quoted from earlier publications. A somewhat different analysis of davidite with density 4.60 from the Tete district, Mozam-

TABLE 1. *X*-RAY POWDER DIFFRACTION PATTERN OF DAVIDITE FROM ARIZONA, RECONSTITUTED BY HEATING FOR ONE HOUR AT 970° C.

hkil	I	$d_{obs.}$	$d_{calc.}$	*hkil*	I	$d_{obs.}$	$d_{calc.}$	*hkil*	I	$d_{obs.}$	$d_{calc.}$
$10\bar{1}1$			8.25 Å	$30\bar{3}6$			2.267	$50\bar{5}2$			1.770
0003	18	6.86	6.96	$20\bar{2}8$			2.256	$20\bar{2}\cdot11$			1.748
$01\bar{1}2$			6.81	$13\bar{4}4$	50	2.248	2.248	$000\cdot12$	<5	1.741	1.739
$11\bar{2}0$	15	5.21	5.18	$21\bar{3}7$			2.240	$22\bar{4}9$			1.728
$10\bar{1}4$			4.51	$40\bar{4}1$			2.232	$33\bar{6}0$			1.728
$02\bar{2}1$			4.39	$04\bar{4}2$	‡		2.195	$41\bar{5}6$	22	1.708	1.707
$11\bar{2}3$	24	4.18	4.16	$31\bar{4}5$	40	2.139	2.139	$04\bar{4}8$			1.702
$20\bar{2}2$			4.12	$11\bar{2}9$			2.117	$05\bar{5}4$			1.698
$01\bar{1}5$	7	3.81	3.79	$22\bar{4}6$			2.079	$32\bar{5}7$			1.695
0006			3.48	$12\bar{3}8$	5	2.072	2.068	$24\bar{6}1$	‡		1.692
$02\bar{2}4$	72	3.42	3.40	$40\bar{4}4$			2.062	$33\bar{6}3$			1.677
$21\bar{3}1$	8	3.36	3.35	$32\bar{5}1$			2.048	$42\bar{6}2$			1.675
$12\bar{3}2$	20*	3.21	3.228	$10\bar{1}\cdot10$	5	2.029	2.033	$12\bar{3}\cdot11$			1.656
$20\bar{2}5$	50	3.065	3.057	$23\bar{5}2$			2.021	$50\bar{5}5$			1.650
$30\bar{3}0$	40	3.000	2.994	$04\bar{4}5$	12	1.982	1.977	$11\bar{2}\cdot12$	12	1.652	1.649
$11\bar{2}6$	100	2.895	2.889	$41\bar{5}0$			1.960	$13\bar{4}\cdot10$	40	1.601	1.600
$21\bar{3}4$	60	2.850	2.845	$32\bar{5}4$	25	1.919	1.916	$42\bar{6}5$	<5	1.572	1.572
$10\bar{1}7$			2.829	$13\bar{4}7$			1.911	$33\bar{6}6$	10	1.548	1.548
$30\bar{3}3$	22	2.755	2.748	$02\bar{2}\cdot10$	5	1.897	1.893	$31\bar{4}\cdot11$	15	1.509	1.509
$12\bar{3}5$	33	2.640	2.633	$41\bar{5}3$			1.886	$32\bar{5}\cdot10$	5	1.467	1.466
$22\bar{4}0$	18	2.595	2.593	$01\bar{1}\cdot11$			1.856	$52\bar{7}0$	40	1.439	1.438
$01\bar{1}8$			2.505	$23\bar{5}5$	10	1.849	1.847		8	1.419	
									10	1.376	
$02\bar{2}7$			2.484	$30\bar{3}9$			1.833		5	1.360	
									8	1.346	
$13\bar{4}1$	38†	2.480	2.473	$31\bar{4}8$	38	1.803	1.801		6	1.302	
									<5	1.275	
$22\bar{4}3$	25	2.429	2.429	$40\bar{4}7$			1.793		5	1.246	
$31\bar{4}2$			2.423	$05\bar{5}1$			1.789	plus ca. a dozen more weak, diffuse, lines.			
0009			2.319	$21\bar{3}\cdot10$	12	1.780	1.778				

Co radiation, Fe filter, Norelco 114.59 camera. Intensities estimated by comparison with standard intensity cale.

* Intensity reported for $12\bar{3}2$ is on hydrothermally reconstituted davidite. Ordinarily traces of the strongest rutile line at 3.245 obscure this.

† May be enhanced and slightly displaced towards lower angles by rutile line at 2.489 or by "subsidiary reflections" discussed in text.

‡ Lines in these positions reported in most published davidite patterns are probably attributable to (111) and (211) of rutile, spacings 2.188 and 1.687, intensities 22 and 50, NBS Circ. 539, vol. I, p. 45.

bique, has been published by Colin (1950). So far as known neither the davidites of Billeroo, Thackeringa and Crocker's Well, Australia, nor that from Iveland, Norway,* have been analyzed. Published analyses of davidites not examined during this study include one of material from Houghton, South Australia (Whittle, 1954) and three from the Mt. Isa-Cloncurry district, Queensland (Lawrence *et al.* 1957). Among the latter is an analysis of "davidite type 3" having a much higher density, 4.89,

* See supplementary note (2), page 718, this issue.

TABLE 2. CHEMICAL ANALYSES OF DAVIDITE

	1	2	3	4
Al_2O_3	—	—	0.37	0.39
SiO_2	—	0.06	1.69	0.34
TiO_2	54.3	54.5	54.37	55.20
V_2O_5	*	1.4	0.31	0.33
Cr_2O_3	*	0.17	0.87	0.91
Fe_2O_3	13.0	10.2	18.84	19.80
MgO	0.6	nil	0.73	0.77
CaO	1.5	0.3	1.28	
MnO	—	—	0.21	0.22
FeO	16.0	16.5	7.14	7.50
SrO	—	—	0.26	0.27
PbO	1.5	0.72	—	
ZrO_2	—	0.4	0.52	0.55
R.E.	8.3	5.6	8.96§	9.42
ThO_2	1.1	0.07	0.43	0.45
UO_2	4.6*	9.8†	3.56	3.74
Na_2O	—	0.15‡	0.03	0.03
K_2O	—	—	0.08	0.08
H_2O^+	—	0.05	0.17	
H_2O^-	—	—	0.00	
Total	100.9	99.92	99.82	100.00
Sp. Gr.	—	4.46	4.42	

* Represents U_3O_8, Cr_2O_3 and V_2O_5.

† Uranium reported as UO_3

‡ Alkali metals as Na_2O.

§ Includes Ce_2O_3 (1.5–2%), Sc_2O_3, Y_2O_3, etc.

1. Radium Hill, South Australia. W. T. Cooke (1916).
2. Tete district, Mozambique. Bannister and Horne (1950, Analysis 1, Table I).
3. Pandora prospect, Quijotoa Mountains, Pima County, Arizona. C. A. Ingamells, analyst.
4. Analysis of column 3 adjusted to a total of 100% after deducting sphene equivalent to 1.28% CaO and omitting water.

and higher uranium content, 20.16% U_3O_8, than any other recorded davidite.

Additional information on the composition of the Arizona davidite was obtained from an *x*-ray fluorescence spectrogram and counts on selected peaks kindly run by Mr. Kenneth Johnson of the Kearney Foundation of Soil Science. The spectrogram showed lines for Y, Ce, La and Gd and no others among the elements included under rare earths in the analysis.

Spectrographic examinations of the Arizona and Norwegian davidites by Mr. George Gordon of the Division of Mineral Technology showed them to have similar compositions but with these differences: less Mg, Si, Ca, Th and U but more V, Mn and Sc in the Norwegian than in the Arizona material.

The specific gravity recorded in Table 2 for the Arizona davidite was determined by pycnometer on the concentrate used for analysis. Similar values were obtained on individual fragments by Berman balance. No reliable specific gravity has been reported for the Radium Hill davidite and the available samples of this provide no material suitable for a determination. A selection of new specific gravity determinations of davidite follows:

Specimen	Locality	Method	Sp. Gr.
3*a*	Crocker's Well	Jolly balance	4.49
4	Billeroo	Jolly balance	4.38
7	Norway	Berman balance	4.37

The weight loss after heating was determined for fragments of the Arizona, Crocker's Well and Norwegian material to be about 0.3%. The Arizona davidite increased in sp. gr. to about 4.55 on heating, whereas changes in the others were within the limits of uncertainty.

In Table 3 are shown the results of cell content calculations for the three davidites for which analyses are given in Table 2. For the Arizona davidite the figures of the adjusted analysis, column 4, Table 2, were used. The same cell volume, 1,943.6 Å^3, was assumed for all. Since it seems probable that davidite in its reconstituted state contains no hydroxyl, water was excluded from consideration. In the absence of a specific gravity determination for the Radium Hill davidite the calculation for this shown in column 1 was adjusted to an oxygen content of 35 atoms for the rhombohedral cell, close to the average for the other two davidites as given in columns 2 and 3. Following Bannister and Horne (1950, p. 107), "V_2O_5 and U_3O_8, reported together in the analysis, have been arbitrarily assigned the values 1.4 and 3.2% respectively" for the Radium Hill davidite.

Bannister and Horne (1950) derived the provisional formula $AB_3(O, OH)_7$, where A represents smaller and B larger cations, for davidite. Five such formula units in the rhombohedral cell are indicated. The ratios of A + B/O for the Mozambique and Arizona davidites agree with this fairly well. If Fe''' is counted with the B cations, as was done by Bannister and Horne, their number is too large, 16.71 instead of 15.00, in the Arizona davidite. This is connected with the fact that Fe^3 exceeds Fe^2 in this davidite. An adjustment to the formula can be obtained by counting a part of the ferric iron with the B cations.

TABLE 3. CELL CONTENTS OF DAVIDITE

	1	2	3	4	5	6
Al	—	—	0.13	—	—	0.13
Si	—	0.02	0.09	—	0.02	0.09
Ti	11.87	11.87	11.95	12.21	12.28	12.14
V	0.38	0.27	0.06	0.39	0.28	0.06
Cr	—	0.04	0.21	—	0.04	0.21
Fe'''	2.85	2.21	4.27	2.93	2.29	4.34
Σ′	15.10	14.41	16.71	15.53	14.91	16.97
Mg	0.26	—	0.33	0.27	—	0.34
Ca	0.46	0.09	—	0.47	0.09	—
Mn	—	—	0.05	—	—	0.05
Fe''	3.87	3.99	1.80	3.98	4.13	1.83
Sr	—	—	0.05	—	—	0.05
Pb	0.09	0.06	—	0.09	0.06	—
Zr	—	0.06	0.08	—	0.06	0.08
Ce*	0.89	0.59	0.99	0.92	0.61	1.01
Th	—	0.01	0.03	—	0.01	0.03
U	0.20	0.61	0.24	0.21	0.63	0.24
Na	—	0.08	0.01	—	0.08	0.01
K	—	—	0.03	—	—	0.03
Σ''	5.77	5.49	3.61	5.94	5.67	3.67
Σ(Σ′+Σ'')	20.87	19.90	20.32	21.47	20.58	20.64
O	35.00	34.70	35.44	36.00	36.00	36.00
Sp. Gr.	4.45 (calc.)	4.46 (meas.)	4.42 (meas.)	4.58 (calc.)	4.61 (calc.)	4.49 (calc.)

Columns 1 and 4, Radium Hill, South Australia.
Columns 2 and 5, Tete district, Mozambique.
Columns 3 and 6, Pima County, Arizona.
* R. E. treated as Ce_2O_3. See text for other details.

The specific gravities used in the cell content calculations were determined on metamict material. It seems probable that somewhat higher values, as indicated by the increase in specific gravity on heating the Arizona davidite, would be appropriate for the crystalline material. This could lead to a cell content of 36 oxygens (see columns 4 to 6, Table 3) and possibly to a formula $Y_6Z_{15}O_{36}$, or $3(Y_2Z_5O_{12})$, for the rhombohedral cell, perhaps corresponding to no atoms on the 3-fold axes, a not unlikely situation. Probably only a determination of the structure, not contemplated at present, could firmly establish the ideal cell content and formula.

Relation to Ilmenite

It has been suggested by Shawe (1953, p. 38) that davidite is but a "uranium-bearing ilmenite." The cell dimensions of ilmenite, a_0 5.082, c_0 14.027 Å (Crystal Data, p. 453), if multiplied by 4/2 and 3/2 respectively, give a multiple cell with a_0 10.164 and c_0 21.041, very close to the dimensions, 10.37 and 20.37, for davidite. The content of the rhombohedral cell corresponding to this multiple of the ilmenite cell would be $Fe_{12}Ti_{12}O_{36}$. The cells can be compared on the basis of the volumes per oxygen atom. This is 17.34 Å^3 for ilmenite and either 18.51 or 18.00 for davidite, depending on whether there are 35 or 36 oxygens

Fig. 1. Davidite, Norway, heated to 960° C. 30° *hki*0 precession photograph of twin on (52$\bar{7}$0). Mo-Zr, 28 hours.

per rhombohedral cell. The volume per oxygen in close packing is 13.01 or 15.09 corresponding to the radii 1.32 or 1.40 Å. One may speculate that the structure of a davidite cell is related to the structure of a multiple of the ilmenite cell by the omission of one eighth of the cations and the partial subsitution of others by cations of higher charge. Such a possibility is not excluded by the marked difference in the diffraction patterns whose aspect is largely determined by the heavier atoms.

Twinning as Revealed by *X*-Rays

The third crystal of Arizona davidite examined by *x*-rays showed a repetition of spots in *hki*0 to *hki*3 precession patterns indicating twinning on a plane parallel to *c*. No indications of such twinning were found in other crystals of Arizona davidite but the same kind of twinning was observed in all of the reconstituted fragments of Norwegian davidite of which single crystal patterns were taken.

Manifestation of the twinning in an *x*-ray diffraction pattern is shown in Fig. 1. The interpretation is shown in the reciprocal lattice diagram in Fig. 2 which is reproduced to the same scale. Within the range of a 30°

Mo *hki*0 precession pattern only the reciprocal lattice points $52\bar{7}0$, $39.1\bar{2}.0$ and $10.4\cdot\bar{1}\bar{4}.0$ and their symmetrical equivalents are in common for the two lattices. The *hki*0 section of the combined lattices shows the symmetry $6mm$, intensity differences of equivalent spots arising from the two parts of the twin being disregarded. Upper level sections parallel to *hki*0 show only the symmetry $3m$. In *hki*1 and *hki*2, only the points plotted in Fig. 3 are in common for the two lattices. $(52\bar{7}0)$ or equivalents, which are symmetry planes for the rhombohedrons $\{13\bar{4}1\}$ and $\{4\bar{1}\bar{3}2\}$, may be taken as the twin planes.

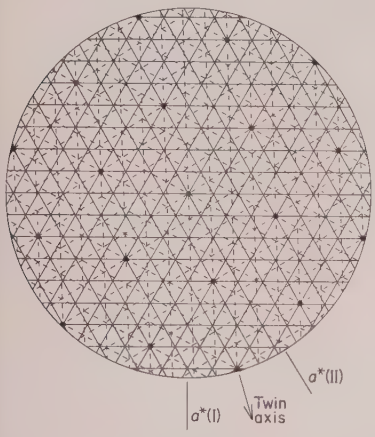

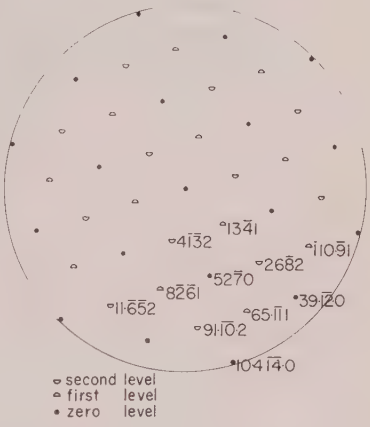

Fig. 2 (left). The *hki*0 plane of the reciprocal lattice of davidite, twinned on $(52\bar{7}0)$. Same scale as Fig. 1. Small black circles are lattice points common to both parts of twin. Intersections of lattice lines correspond to points for which $h-k-l=3n$ only. Same scale as Fig. 1.

Fig. 3 (right). Common reciprocal lattice points on the zero, first and second levels of a davidite twin on $(52\bar{7}0)$. Same scale as Fig. 2.

The common sets of reciprocal lattice points, $\{52\bar{7}0\}$, $\{13\bar{4}1\}$ and $\{4\bar{1}\bar{3}2\}$, correspond to the strongest reflections of their levels. The simplest indices that can be assigned to these sets of points are $\{11\bar{2}0\}$, $\{10\bar{1}1\}$ and $\{01\bar{1}2\}$, corresponding to an hexagonal cell with $a_0=2.878$ and $c_0=20.87$ Å.

Subsidiary *X*-Ray Reflections

On Fig. 1 there may be noted weak arcs or short tangential streaks, regularly distributed in a trigonal or hexagonal pattern. The most prominent of these are close to the position of $13\bar{4}0$, a "forbidden" reflection for a rhombohedral lattice. On the zero layer of a *c*-axis rotation pattern these streaks are reduced to spots which are slightly diffuse. Three such spots, the innermost one corresponding to the streaks near

1340, the others on either side of 52$\bar{7}$0, are indicated by arrows on the zero line of the *c*-axis rotation pattern of which one quadrant is shown in Fig. 4. On this pattern another arrow indicates a line of slightly diffuse spots between the 4th and 5th layer lines. Weissenberg resolution of this level shows only streaks similar to the subsidiary streaks on the zero level, whereas resolution of the 4th and 5th levels shows only sharp reflections. In accordance with expectation both sharp spots and diffuse streaks are present on the 9th level. No streaks were seen on other levels nor were any observed on *h*0$\bar{h}l$ or *hh*$\bar{2}\bar{h}l$ patterns.

The diffuse subsidiary streaks are present in the indicated regions on all well exposed patterns of twins as well as single crystals. A single crystal of the Arizona davidite and a twin of the Norwegian davidite, first reconstituted at 980 and 960° C. respectively and used for a survey of the subsidiary streaks, were further heated to 1170° C. Reexamination by c-axis rotation and *hki*0 Weissenberg patterns showed no change in the subsidiary streaks. In powder patterns corresponding lines are not recorded with the possible exception of the strong streaks near 13$\bar{4}$0 which may account for the diffuse shoulder usually seen on the low angle side of the 13$\bar{4}$1 line.

The subsidiary layer level, close to a "4½ level", corresponds to a *c* axis spacing of 4.64. This is very close to the spacing of the third level of ilmenite, 4.68. Likewise the spacing of 13$\bar{4}$0, 2.488, is close to that of 11$\bar{2}$0, 2.541, of ilmenite.

Differences in Localities

Extraneous phases in untreated material

X-ray examination of untreated fragments revealed no impurities in the davidites from Arizona, Norway or Mozambique and only a trace of anatase in one fragment from Thackeringa. Some fragments from the Crocker's Well specimens are completely *x*-ray amorphous but one fragment of specimen 3*a* showed streaky spots near 3.3, 2.7 and 1.7 Å and two fragments of specimen 3*b* showed weak diffuse lines near 3.5. Faint rutile lines are detectable in the patterns of some untreated fragments from both of the Billeroo specimens even though detached from what seem to be single crystals.

The Radium Hill davidite is intimately intergrown with rutile, partly in coarse crystals, ilmenite and possibly other black, opaque minerals as has been noted by others. The complexity of the intergrowth is indicated by the autoradiograph of specimen 2*a* shown in Fig. 5. Many untreated fragments were examined by *x*-rays. Those which could be converted to davidite or to mixtures including davidite all showed faint rutile lines and some also diffuse ilmenite spots in the untreated state. It seems not improbable that the cryptocrystalline rutile in untreated

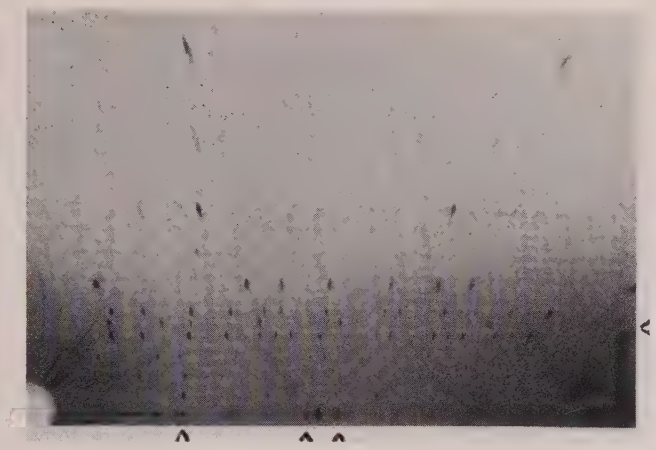

FIG. 4. One quadrant of c-axis rotation pattern of davidite, Arizona. Co-Fe, 16 hours. Arrows indicate features discussed in text.

Radium Hill davidite and in some fragments of the Billeroo davidite corresponds to the extremely fine-grained rutile isolated from davidite by Whittle (1959).

X-ray evidence of other phases in reconstituted davidite

Traces of cryptocrystalline rutile can be found by x-rays in most davidites reconstituted by simple heating in air. The four strongest rutile lines, with d and I 3.245–100; 2.489–41; 2.188–22 and 1.687–50, are close to possible davidite lines. The presence of rutile is suggested by the variation in intensity of this set of lines relative to the intensities of all other lines which remain nearly constant in the patterns. Examples of this variability can be found in several sets of published patterns, for

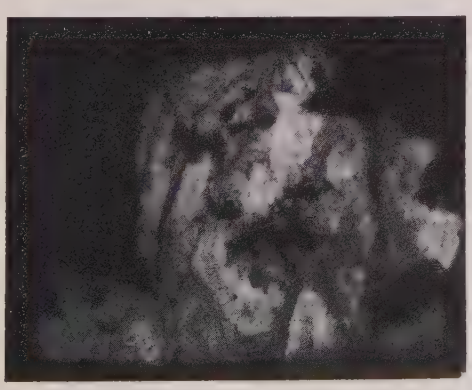

FIG. 5. Autoradiograph of polished surface of specimen 2a, Radium Hill, South Australia. Natural size. Compare Plate XXI, Mawson (1944).

instance those of Lawrence *et al.* (1957, table III), who report *d* and *I* 1.71-4, 1.69–4 for their specimen 1 and 1.70–10, 1.69–1 for their specimen 2, the second line of this pair being due to rutile which is present in much smaller amount in specimen 2. Reconstitution of davidite under hydrothermal conditions, to be reported in detail at some future date, yields material giving no trace of rutile lines.

Pseudobrookite lines were found in several patterns obtained from heated fragments of Radium Hill davidite. In two cases these fragments

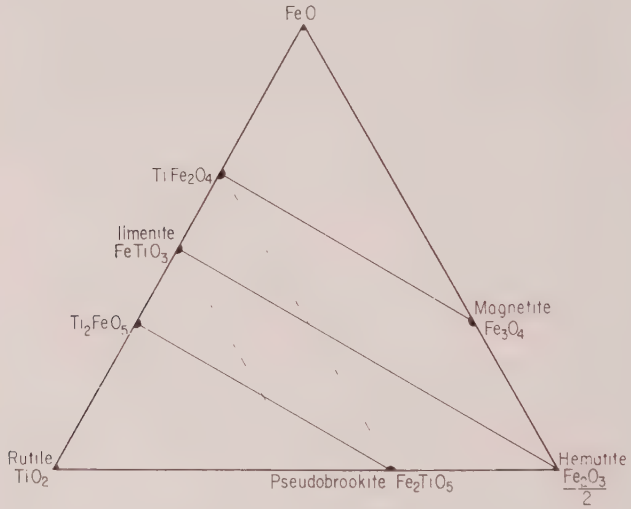

FIG. 6. Concentration triangle for the system FeO-Fe_2O_3-TiO_2. Following Gorter (1957 components are formulated so that each has the same number of metal atoms in order tha the several mix-crystal series may be represented by parallel lines. Dashed lines show th trends of composition changes with oxidation or reduction.

showed diffuse ilmenite spots before treatment but not after heating The Radium Hill fragment yielding the best pseudobrookite patter showed only rutile spots before heating and some of these remained though weakened, in the pattern of the heated fragment. Banniste (Bannister and Horne, 1950, footnote p. 110) reported that heate ilmenite yields a pseudobrookite pattern and wrote the equatio $2FeTiO_3 + O \rightarrow Fe_2TiO_5 + TiO_2$ to represent the change though no TiO lines were observed. It is now known that a complete series of pseudo brookite structure exists with the composition range Fe_2TiO_5 to $FeTi_2O$ as shown on Fig. 6. Such phases may arise by oxidation of phases in th Ti-rich portion of the series $FeTiO_3$-Fe_2O_3 or by reaction between phase or combinations of phases in any part of this series and TiO_2. No pseudo

brookite lines were observed in patterns from untreated Radium Hill fragments. Oxidation would be most effective if powder is heated in air. It may be presumed to be less effective when fragments are heated.

Weak, diffuse, unidentified lines appeared in *x*-ray diffraction patterns of several heated fragments of davidite from Mozambique near 5.9 or 3.7, from Crocker's Well near 4.7, or near 4.7 and 2.70 or near 6.0 and 3.18, and in one pattern of powdered Arizona davidite near 6.1 and 4.7. These cannot be matched with lines of any expected phases. Though some of these lines appeared in several patterns their occurrence seems to be accidental. At least a few of them, *e.g.* the 4.7 line from a Crocker's Well davidite fragment, persist after heating at higher temperature, $1\frac{1}{4}$ hours at 1150° C. It may be that these lines arise from unknown phases formed during the reconstitution of the davidite, possibly in part by reaction with original impurities. No systematic study of these extraneous lines, present on only a few photographs, was carried out.

Differential thermal analysis

Kerr and Holland (1951) published differential thermal analysis curves of davidite from Mozambique and reported that "samples after heating to 710° C. give no distinct lines even after extended exposure, but patterns of samples heated to 830° C. and 1020° C. give groups of lines that are identical." Mr. Larry Godwin kindly ran differential thermal curves to 920°C. on powdered davidite from Crocker's Well (specimen 3a) and from Arizona, using a constant heating rate of 12 degrees per minute. The curve obtained from the Crocker's Well davidite is somewhat similar to those for the Mozambique davidite published by Kerr and Holland, with a principal exothermic peak at 660° C. and a lower, broader, exothermic peak at 820° C. The differential thermal curve for Arizona davidite, on the other hand, shows no peaks. Powder diffraction photographs of the two samples after the DTA runs are nearly identical, showing the full davidite pattern plus a weak line near 2.70 from the Crocker's Well material only.

Degree of metamictness

The degree of metamictness differs markedly in the several davidites. All but the Arizona davidite are *x*-ray amorphous in the untreated state. Untreated fragments of this yielded *x*-ray photographs showing a few faint, diffuse, single-crystal spots. These are so weak that any *x*-ray pattern prepared from powdered material might be interpreted as indicating an *x*-ray amorphous substance.

Sharp single crystal patterns were obtained from a fragment of Arizona davidite heated to 775° C. for 2 hours. Fragments heated to 915° C.

or higher yielded the same patterns. The powder pattern of material used for a DTA run to 920° at 12° per minute, which had been above the presumed temperature of reconstitution only about 25 minutes, showed sharp lines that could be fully indexed on the lattice derived from the single crystal patterns.

No lower limit can be set for the temperature at which reconstitution occurs. After the lattice had been established it was possible to orient untreated fragments showing a few faint spots and to interpret the rather weak precession and Weissenberg pattern obtained from them on the basis of this lattice. On these patterns, obtained from 3 untreated fragments, spots corresponding to spacings greater than 3.5 Å are absent and spots corresponding to spacings less than about 1.5 are most diffuse and usually not observable. The absence of the low angle spots is attributable to absorption and that of the high angle spots to the smallness of the volumes within which a degree of order sufficient for *x*-ray diffraction persists. However, the remnants of order in this davidite are enough to determine the reconstitution of the fragments to single crystals upon heating. It may be recalled that Mügge's (1922) studies on the optical properties of partly metamict crystals indicated that intermediate stages may consist of a web- or sponge-like crystal whose meshes are filled with amorphous substance.

Fragments of the davidite from Norway are *x*-ray amorphous. A fragment heated for 44 hours at 510° C. acquired about the same degree of crystallinity found in untreated fragments of Arizona davidite. Fragments heated to various temperatures in the range 680 to 960° C. all yielded sharp patterns of similar character. Though no remnant of crystallinity can be detected by *x*-rays in untreated Norway davidite, the fact that reconstitution invariably leads to single crystals or twins suggests that metamictization of this davidite was not complete. According to Pellas (1954, p. 454) radiation damaged material will appear *x*-ray amorphous when 20 per cent of its atoms have been displaced.

Several fragments of Crocker's Well davidite, which may show faint lines even before heating, were heated at relatively low temperatures for long periods. Several weak diffuse lines that might be correlated with the principal groups of davidite lines appeared in a fragment heated for 44 hours at 510° C. Continued heating of this and other fragments below 600° C. for up to five days failed to produce sharp patterns, but all such fragments yielded sharp patterns on further heating at higher temperatures. Similar observations were made on davidite from Mozambique but in this case a fragment heated to 510° for 44 hours yielded no lines and only three weak lines were produced by the same fragment after further heating at the same temperature for a total of 106 hours.

TABLE 4. COORDINATE ANGLES FOR DAVIDITE FROM MOZAMBIQUE

As recorded by Horne (Bannister and Horne, 1950, p. 102)				Calculated for axial ratio 2.013		
Lower	Upper	ϕ	ρ	*hkil*	ϕ	ρ
$\bar{c}$	$\bar{c}(0001)$	—	0°	(0001)	—	0°
	$h(21\bar{3}0)$	11°	90	$(21\bar{3}0)$	10°54′	90
	$-h(12\bar{3}0)$	−11	90	$(12\bar{3}0)$	−10 54	90
	$-l(25\bar{7}0)$	−14	90	$(25\bar{7}0)$	−13 54	90
$-\bar{n}$	$(03\bar{3}4)$	−30	50	$(01\bar{1}2)$	−30	49 16
	$o(11\bar{2}1)$	0	70	$(22\bar{4}3)$	0	69 34
$\bar{p}$	$(22\bar{4}1)$	0	80	$(44\bar{8}3)$	0	79 27
	$s(52\bar{7}8)$	14	51	$(527\cdot12)$	13 54	50 25
	$t(41\bar{5}6)$	19	50	$(41\bar{5}9)$	19 06	49 48
	$-u(34\bar{7}3)$	− 5	73	$(68\bar{1}4\cdot9)$	− 4 43	72 20
$-\bar{v}$	$(34\bar{7}2)$	− 5	78	$(34\bar{7}3$	− 4 43	78 18
$-\bar{w}$	$(12\bar{3}3)$	−11	54	$(24\bar{6}9)$	−10 54	53 48
$-\bar{x}$	$(26\bar{8}9)$	−16	52	$(4\cdot12\cdot\bar{1}6\cdot27)$*	−16 06	51 19
$-\bar{y}$	$(13\bar{4}4)$	−16	55	$(13\bar{4}6)$	−16 06	54 24
$-\bar{z}$	$(16\bar{7}8)$	−22	52	$(16\bar{7}\cdot12)$	−22 24	51 47

* See text for comment and alternative interpretation.

No observations were made on Billeroo, Thackeringa or Radium Hill davidite heated at temperatures below 950° C. At this temperature all of the davidites are fully reconstituted in less than an hour, possibly within minutes.

Among the davidite specimens examined the least metamict are those from Arizona, followed by the specimen from Norway. It may not be a coincidence that the Arizona davidite is youngest, probably being late Cretaceous-early tertiary (Thomssen, 1961), and that the Norwegian davidite has a lower uranium content than analyzed davidites.

MORPHOLOGY

The morphology of davidite from Mozambique was described by Horne (Bannister and Horne, 1950) on the basis of contact goniometer measurements on large rough crystals. He stated that "the mineral appears to belong to the ditrigonal pyramidal class" and, adopting the axial ratio 1.37, recorded coordinate angles to one degree for 15 forms. His angle table is reproduced in the first four columns of table 4, form names being omitted. The axial ratio of the structure cell, $c_0/a_0 = 2.013$, being close to three halves the axial ratio adopted by Horne, the indices given in column 5 have been obtained from Horne's indices by the transformation $100/010/00\frac{3}{2}$. The calculated coordinate angles all agree with

Horne's reported measurements within the limits to be expected from rough goniometer measurements but this must not be taken as confirming the indices either as originally given or as transformed. $-\bar{x}$ may be considered to be (268·13), with $\rho = 52°\ 12'$, and simpler indices might also be found for some of the other forms.

Unfortunately no traces of morphology can be found on the Arizona or Norway davidites which have been reconstituted to single crystals but some crude observations on forms are possible on the crystals from Billeroo, South Australia. On the smallest of these a pinacoid (or pair of pedions), a rhombohedron with ρ close to 63° and some smaller steeper faces can be recognized. The larger crystals show fewer faces and are rougher but on the largest a 63° angle can also be found. For $c\ a = 2.013$, $\rho_{11\bar{2}2}$ is 63° 35′ and $\rho_{44\bar{8}9}$ is 60° 48′. The commonest rhombohedral form on ilmenite is $\{22\bar{4}3\}$ referred to the axial ratio 1.3846. Transformed as indicated above this would be $\{44\bar{8}9\}$.

Though it has not been possible to connect the morphology with the structure lattice by single crystal *x*-ray diffraction from faceted crystals the observations suggest that the structure lattice found in the reconstituted davidites does correspond to the lattice of original single crystals from Mozambique and Billeroo and that this is indeed the original lattice of davidites generally.

Acknowledgments

Thanks are due to Mr. R. W. Thomssen for bringing the Arizona davidite to my attention, for supplying ample material and for permitting publication of the chemical analysis of this davidite, the cost of which was defrayed by The Anaconda Company. Thanks are also due to Mr. Joseph Urban for lending specimen *3b*; to Professor C. O. Hutton and Mr. L. L. Brown for providing material for study; to Dr. F. A. Mumpton for suggesting the hydrothermal treatment; to Mr. Daniel Weill for carrying out this treatment and for diffractometer curves of untreated and reconstituted davidite; to Mr. Kenneth Johnson for an *x*-ray spectrograph examination, and to Mr. Larry Godwin for differential thermal analyses. Funds for the purchase of specimens were provided by the Committee on Research of the University of California.

References

Armstrong, F. C., and Weis, P. L. (1957), Uranium-bearing minerals in placer deposits of the Red River Valley, Idaho County, Idaho: *U. S. Geol. Survey Bull.*, **1046-C**, 25–36.

Bannister, F. A., and Horne, J. E. T. (1950), A radioactive mineral from Mozambique related to davidite: *Min. Mag.*, **29**, 101–112.

Colin, L. L. (1950), Uses of tannin in chemical analysis; *Journ. of the Chemical, Metallurgical and Mining Society of South Africa*, **50**, 314–319.

Cooke, W. T. (1916), Chemical notes on davidite: *Trans. Proc. Roy. Soc. S. Aust.*, **40,** 267.
Crook, T., and Blake, G. S. (1910), On carnotite and an associated mineral complex from South Australia; *Min. Mag.*, **15,** 271–284.
Davidson, C. F., and Bennett, J. A. E. (1950) The Uranium deposits of the Tete district, Mozambique; *Min. Mag.*, **29,** 291–303.
Gorter, E. W. (1957), Chemistry and magnetic properties of some ferrimagnetic oxides like those occurring in nature; *Advances in Physics*, **6,** 336–361.
Kerr, Paul F., and Holland, H. D. (1951), Differential thermal analyses of davidite: *Am. Mineral.*, **36,** 563–572.
Lawrence, L. J., See, G. T., McBride, Fiona, and Hofer, Hans (1957), Davidites from the Mt. Isa-Cloncurry district, Queensland: *Ec. Geol.*, **52,** 140–147.
Lima de Faria, J. (1956), The standard thermal treatment in the identification of metamict minerals by X-ray powder patterns: *Boletim do Museu e Laboratorio da Faculdade de Ciencias da Universidade de Lisboa, No.* **24,** 7a Serie, 9 pages.
Mawson, D. (1906), On certain new mineral species associated with carnotite in the radio-active ore body near Olary: *Trans. Proc. Roy Soc. S. Aust.*, **30,** 188–193.
——— (1916), Mineral notes: *Trans. Proc. Roy. Soc. S. Aust.*, **40,** 262–266.
——— (1944) The nature and occurrence of uraniferous mineral deposits in South Australia: *Trans. Roy. Soc. S. Aust.*, **68,** 334–357.
Mügge, O. (1922), Über isotrop gewordene Kristalle: *Cbl. Min.*, 721–739, 753–765.
Palache, Charles, Berman, Harry, and Frondel, Clifford (1944), Dana's system of mineralogy, 1, 7th ed.: New York, John Wiley and Sons, Inc., 834 p.
Pellas, P. (1954), Sur la formation de l'état métamicte dans le zircon: *Bull. Soc. franc. Minér. Crist.*, **LXXVII,** 447–460.
Pinto Coelho, A°. Vasconcelos (1954), O minerio de uranio de Mavudzi-Tete (Mocambique): *Garcia de Orta* (*Rev. junta missoes geogr. e invest. do Ultramar*) **2,** No. 2, 209–219. (See *Am. Mineral.* **41,** 164, 1956)
Pabst, A., and Thomssen, R. W. (1959), Davidite from the Quijotoa Mountains, Pima County, Arizona; *Bull. Geol. Soc. Am.* **70,** 1739. (abstract only)
Ramdohr, P., and Lawrence, L. J. (1958), Radioactive haloes in a davidite-ilmenite ore from Cloncurry, Queensland: *Journ. Geol. Soc. Australia*, **5,** 33–35.
Roso de Luna, Ismael, and Freitas, Fernando (1954), Geology and metallogeny of the uranium deposits of the Mavudzi valley, Tete (Portuguese East Africa): *Cong. Geol. Int. C. R. 19e Sess. Algiers, 1952, Fasc.* **XX,** 293–307.
Shawe, Daniel Reeves (1953), Heavy detrital minerals in stream sands of the eastern Sierra Nevada between Leevining and Independence, California: Ph.D. Dissertation, Stanford University, 190 p. abstracted in Dissertation Abstracts, **XIV,** 369–370, 1954.
Thomssen, R. W. (1961), Davidite from Pima County, Arizona: (in preparation).
Whittle, A. W. G. (1954), Radioactive minerals in South Australia: *Geol. Survey of South Australia, Bull. No.* **30,** 126–151.
Whittle, A. W. G. (1954), Radioactive minerals in South Australia: *Geol. Survey of South Australia, Bull. No.* **30,** 126–151.
——— (1955), The radioactive minerals of South Australia and their petrogenic significance: *Journ. Geol. Soc. Australia*, **2,** 21–45.
——— (1959), The nature of davidite: *Ec. Geol.* **54,** 64–81.

Supplementary Notes

(1) A few days after the completion of this paper an article by J. D. Jayton, entitled "The Constitution of Davidite," appeared in Economic Geology, 55, 1030–1038, August, 1960. Hayton records ten new analyses of davidite. With 5 of the new analyses densities from 4.41 to 4.50 are given. Using the cell dimensions given in the preliminary report by Pabst and Thomssen (1959) Hayton calculated the cell contents for all of the newly ana-

lyzed davidites and also for the Mozambique davidite, using Bannister and Horne's analysis 3, the same one used in this paper, Table 2 and 3.

In his table 7 Hayton has tabulated the calculated contents of the hexagonal cell in three different ways, varying in the grouping of cations. The oxygen count is of particular interest. His figures for this, divided by 3 to correspond to the rhombohedral cell content given in Table 3 of this paper, are:

	Anal. 8 (Maximum)	Anal. 5 (Minimum)	arithmetic mean	standard deviation
oxygen atoms per rh. cell	34.15	32.20	33.22	0.63

All of these figures are substantially below those reported in Table 3 of this paper.

Many factors contribute to the difference. Minor factors are:

1. Difference in the preliminary (10.36, 20.85) and revised (10.37, 20.87) cell dimensions.
2. Difference in the value taken for the weight of the unit of atomic weight. Hayton used 1.649×10^{-24} grs., which is the value, now obsolete, that would have been appropriate had dimensions been stated in kX units. I used 1.6604×10^{-24} grs., consistent with dimensions given in Ångstrom units.
3. Differences in atomic weight values used in calculation.
4. Differences in rounding of figures.

Factors 1 and 2 would tend respectively to raise and to lower the calculated oxygen content and hence tend to cancel each other. Factors 3 and 4 are negligible.

Major factors contributing to differences in the oxygen count are:

5. State of oxidation assumed for Fe. Hayton has taken all the Fe to be ferrous in every case. This reduces the oxygen count.
6. Departure of summation of analysis from 100% .

As seen from Hayton's sample calculation the atom counts obtained are only a proportion of the full cell content corresponding to the summation of the analysis used. There may be some doubt as to the propriety of adjusting an analysis to sum to 100% before starting the calculation but, in any case, using an analysis with a low total in the manner shown in Hayton's sample calculation necessarily leads to a low cell content. If the number of oxygens per hexagonal cell, 102.46, shown in Hayton's table 6, calculated from an analysis totalling 97.5% , is adjusted for a total of 100% it becomes 105.09, or 35.03 for the rhombohedral cell. If some of the iron were ferric the figure would be still higher.

Hayton considers three formulas, $AsB_{12}O_{33}$, $A_2B_{10}O_{33}$ and $A_2B_6C_{12}O_{33}$, corresponding to cation/oxygen ratios 0.606, 0.636 and 0.606. The ratio of his mean values is 61.54/99.65 or 0.618. The lower ratios suggested in Table 3 of this paper arise in part from the higher proportion of oxygen connected with the higher valence state of part of the iron as reported in the analyses used.

(2) Four months after this paper was submitted, an article "Contributions to the Mineralogy of Norway. No. 8. Davidite from Tuftan, Iveland," by Henrich Neumann and Thor L. Sverdrup, appeared in *Norsk Geologisk Tidsskrift*, **40**, 277–288, Dec. 1960. A chemical analysis, and density of 4.29 are reported for davidite. It seems highly probable that it corresponds to specimen No. 7 of this paper.

Manuscript received August 29, 1960.

THE AMERICAN MINERALOGIST, VOL. 46, MAY–JUNE, 1961

THE HYDROTHERMAL CONVERSION OF MUSCOVITE TO KALSILITE AND AN IRON-RICH MICA

Otto C. Kopp, *University of Tennessee, Knoxville, and Consultant, Metallurgy Division, Oak Ridge National Laboratory,* Lawrence A. Harris and G. Wayne Clark, *Metallurgy Division, Oak Ridge National Laboratory**.

Abstract

Attempts to grow large single crystals of muscovite using muscovite cleavage plates as seeds and shredded muscovite as nutrient produced an iron-rich mica and considerable quantities of the $KAlSiO_4$ polymorph called kalsilite. This result is of interest since kalsilite is not a common mineral in nature. Optical data and x-ray measurements are presented for both the iron-rich mica and the kalsilite.

Introduction

Attempts to grow single crystal muscovite using muscovite seeds and nutrient in a steel lined autoclave produced an iron-rich mica and comparatively large quantities of the mineral kalsilite, the hexagonal form of $KAlSiO_4$. Kalsilite is relatively rare, although it may be more common than supposed since it is rather difficult to identify with assurance in thin section. Kalsilite was discovered in volcanic rocks from S.W. Uganda by Holmes (1942) and described by Bannister and Hey (1942), and first prepared in the laboratory by Rigby and Richardson (1947). Since that time additional work (Smith and Tuttle, 1957; Sahama and Smith, 1957; Smith and Sahama, 1957; and Tuttle and Smith, 1958) has done much to clarify phase relations in the system nepheline-kalsilite and polymorphism in $KAlSiO_4$. These studies indicate that at least seven different crystallized materials are possible. These include tetrakalsilite, orthorhombic $KAlSiO_4$, kalsilite, kaliophilite, disordered kaliophilite, a second orthorhombic phase with a smaller unit cell, and a new polymorph named tri-kalsilite (Sahama and Smith, 1957). The studies of Tuttle and Smith (1958) seem to indicate that sodium must be present in all stable phases mentioned above except kalsilite and the orthorhombic form of $KAlSiO_4$. Tri-kalsilite (Sahama and Smith, 1957) is found in a kalsilite-nepheline microperthite and hence it is probable that this kalsilite contains some sodium.

The system described here contained no appreciable quantities of sodium. At the temperatures and pressures used in these experiments kalsilite would appear to be the stable phase in the absence of sodium. This agrees with the results of Tuttle and Smith (1958) but not with the earlier studies of Rigby and Richardson (1947) which seemed to indicate that kalsilite must contain at least 1.5% Na_2O.

* Operated for the Atomic Energy Commission by Union Carbide Corporation.

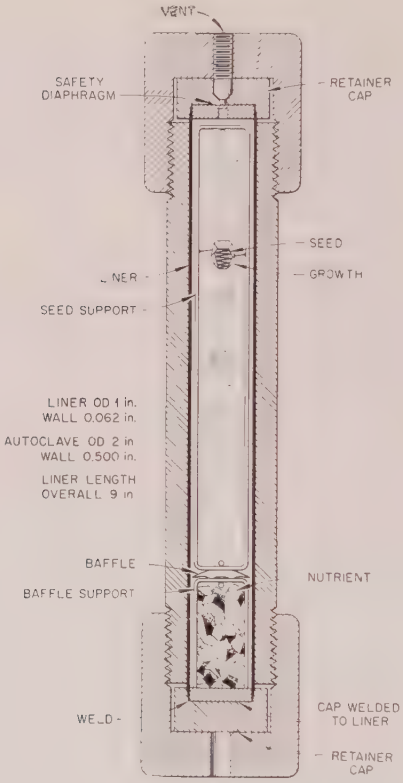

FIG. 1. Hydrothermal autoclave.

EXPERIMENTAL METHOD

Three hydrothermal runs were made using a one inch i.d. autoclave with a cold rolled steel liner. The autoclave was quite similar in design to those used by Bell Laboratories in their early quartz syntheses. (Fig. 1.) The following conditions were used:

Seeds and nutrient:	natural muscovite
Solvent:	KOH (1 N solution)
Partial fill:	70%
Temperatures:	
Seed area:	Approximately 410° C.
Nutrient area:	Approximately 425° C.
Estimated pressure:	1200 bars
Bomb liner:	Cold rolled low-carbon steel, 1″ o.d., $\frac{7}{8}$″ i.d.

Seeds were prepared from cleavage plates of natural muscovite, approximately $\frac{1}{2}$″ on an edge and 0.005″ thick. These plates were suspended in the upper portion of the liner, which during the run was the cooler

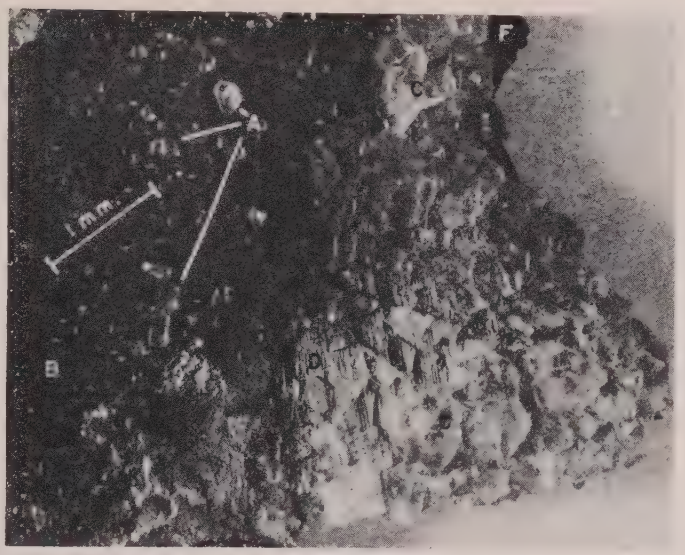

FIG. 2. Layered structure of converted muscovite seed plate.
A. Scattered crystals of kalsilite up to ½ mm. diameter.
B. Sheet of iron-rich mica.
C. Sheet of coalesced crystals of kalsilite; individuals up to 3.5 mm. diameter.
D. Thin layer of what appears to be partially digested muscovite at center of converted seed.
E. Sheet of coalesced crystals of kalsilite; individuals up to 3.5 mm. diameter.
F. Sheet of iron-rich mica.
G. Scattered crystals of kalsilite up to ½ mm. diameter.
(Note that layers E and G do not appear in this view.)

region of the system. Shredded pieces of muscovite were enclosed in a wire basket and placed at the base of the liner, which was the hotter region of the system. The seed and nutrient regions were separated by a perforated baffle placed convex upward and containing approximately 20% open space.

The ends of the liner were welded shut and a 70% partial fill of 1 N KOH solution added with a hypodermic syringe through a small hole drilled in one end cap. This fill hole was then easily welded shut. KOH was used as solvent rather than NaOH to reduce the number of components in the system, since the potassium mica was of interest. Runs were made lasting for twenty-one days, fourteen days, and twenty-nine days. A leak developed at some undetermined time during the first run of twenty-one days duration, probably rather early in the run since larger crystals of kalsilite were obtained in the second run of fourteen days. The final run of twenty-nine days duration was made to learn whether larger crystals of kalsilite could be grown. While this run pro-

duced more crystals of kalsilite, they were no larger than those produced in the preceding run.

Experimental Results

Several general observations could be made from these experiments:

1. The original muscovite of the seed plates was largely converted to two new crystalline phases: an iron-rich mica and the mineral kalsilite.

2. The converted seed plates contained seven distinct layers consisting of kalsilite, the iron-rich mica, and a minor amount of unconverted muscovite. The nature of this layering is shown in Fig. 2. (Note that only five of the seven layers appear in the photograph which shows a converted seed plate broken across the layers.) It appears that during the conversion process the two outer sheets of iron-rich mica were formed at an early time in the run, and that the conversion of the remaining muscovite to kalsilite proceeded more slowly. The smaller, scattered crystals of kalsilite on the outer surfaces of the converted seed material probably did not start to grow until after at least some of the muscovite between the two iron-rich mica layers had been converted to kalsilite. The surficial kalsilite crystals almost certainly did not appear until distinct outer layers of the iron-rich mica had been produced.

3. The nutrient material which appeared largely converted to kalsilite, showed less development of the iron-rich mica than noted in the converted seed plates.

4. The iron-rich mica and also numerous small crystals of magnetite (black, octahedral, magnetic crystals) appeared more abundantly in the upper, cooler region of the liner.

The conversion apparently resulted from two major factors. First, the KOH solution attacked the cold rolled steel liner readily, yielding a solution rich in Fe^{+2} and Fe^{+3} ions. Second, the iron-rich mica appeared to be more stable under these conditions than the muscovite. The solvent was effective in attacking the muscovite, replacing the aluminum in the octahedral site with iron to produce some iron-rich mica and digesting the bulk of the muscovite to yield aluminum ions and SiO_4^{-4} groups which could then recombine with the potassium of the solvent and that produced during the disintegration of the muscovite to form kalsilite. The iron-rich mica appears to vary somewhat in its optical properties which may indicate that the replacement of aluminum by iron is incomplete. This is discussed further in the section dealing with optical data. The crystals of kalsilite which occur in the two inner layers are oriented with their *a*-axes lying within the plane of the original sheet. Many of the smaller crystals growing on the outer surfaces exhibit the same orientation; however, some grew with an *a*-axis normal to the surface and some were inclined to the surface (Fig. 3). There is some evidence for an

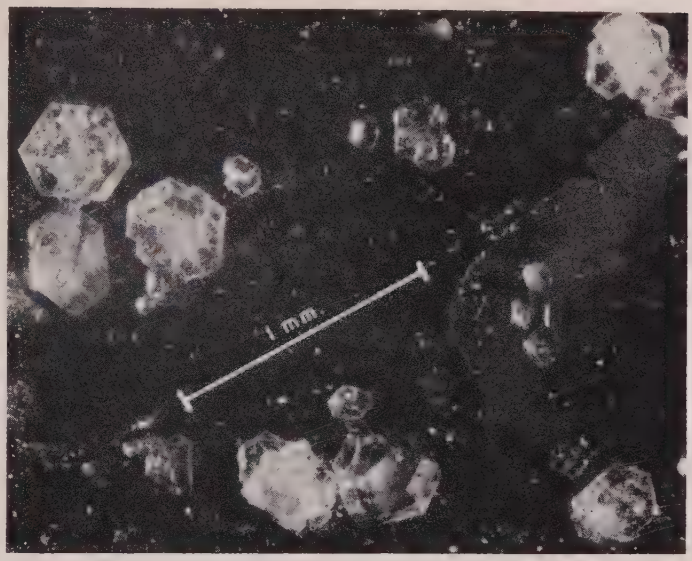

FIG. 3. Kalsilite crystals produced hydrothermally.

epitaxial relationship between the kalsilite and the mica. Crystals of kalsilite were also noted on the baffle plate, the upper end cap of the liner, and on the liner wall.

Numerous bubble inclusions are noted at the centers of most crystals, but the edges of the crystals are generally clear. Some of the bubbles are elongated or tubelike. Multiple growths are fairly common. In some cases, two or more individuals appear at distinct angles to each other. In other cases, a multiplicity of growth with only a slight angular divergence of axes results in tiny "rosette" shaped crystals.

The nature of the chemical reaction occurring during the synthesis of these materials may be expressed by a general chemical equation:

$$\underset{\text{(Muscovite)}}{KAl_2(Si_3Al)O_{10}(OH)_2} + Fe \xrightarrow[\text{(Temperature, Pressure)}]{\text{(KOH, } H_2O\text{)}}$$

$$\underset{\text{(Kalsilite)}}{KAlSiO_4} + \underset{\text{(Iron-rich mica)}}{K(Fe, Al)_2(Si_3Al)O_{10}(OH)_2} + \underset{\text{(Magnetite)}}{Fe_3O_4} + H_2$$

OPTICAL DATA

Optical data were determined for both the kalsilite and iron-rich mica formed during these runs. The kalsilite has the following optical properties:

Uniaxial negative	$\omega = 1.542 \pm 0.002$ $\epsilon = 1.538 \pm 0.002$	Colorless

These properties agree with those determined by Bannister and Hey (1942) in their original description of the mineral.

The iron-rich mica has the following optical properties:

Essentially uniaxial negative (Probably biaxial negative with 2V close to 0°)
$\alpha = 1.62 \pm 0.01$
$\beta = \gamma = 1.68 \pm 0.01$
Strongly colored and pleochroic. Black to greenish in macroscopic observation.
Pleochroism:
X = reddish brown
Y = Z = smoky green

Table 1 compares these values with reported indices of refraction for some other iron-bearing micas.

TABLE 1. COMPARISON OF INDICES OF REFRACTION FOR SEVERAL IRON-BEARING MICAS

Indices of Refraction	Iron-rich mica (±0.01)	Biotite	Lepidomelane	Annite
α	1.62	1.56–1.60	1.616–1.630	1.630
β	1.68	1.60–1.66	1.670–1.690	1.690
γ	1.68	1.60–1.66	1.670–1.690	1.690

The optical data on this material are somewhat variable, probably as a result of variations in the iron content. The determined value of α is uncertain because of the strong pleochroism and the plate-like nature of the material.

Physically, while this material retains the sheet structure of the original muscovite, it is considerably more brittle than muscovite or biotite. However, it still retains perfect basal cleavage and measurements of the value of α were made with difficulty. Also noted was the presence of variable quantities of an opaque material (probably magnetite) in intergrowth with the iron-rich mica.

KALSILITE CRYSTALLOGRAPHY

To the best of the authors' knowledge, well-developed crystals of kalsilite have not been found in nature nor produced in the laboratory previously. Hence, identification has been generally based on the optical and *x*-ray measurements which are possible on materials which are anhedral. The kalsilite crystals grown here (Fig. 3) were of sufficient size to make some interfacial angle measurements with the two-circle goniometer (Table 2). These values are believed to be accurate within ±2°. Greater accuracy would be desirable, but does not appear possible with

Table 2. Interfacial Angles for Hydrothermally Prepared Kalsilite

Form	Miller Indices	$\rho \pm 2°$	$\phi \pm 2°$
Basal pinacoid	{0001}	0°	—
Hexagonal prism	$\{10\bar{1}0\}$	90°	60° intervals
Hexagonal dipyramid	$\{10\bar{1}1\}$	61°	60° intervals
Hexagonal dipyramid	$\{20\bar{2}3\}$	46°	60° intervals

the materials available. The crystal faces generally show a slight curvature which tends to give a range of values. Several crystals were measured which show four distinct forms.

These measured values of interfacial angles compare favorably with the values for the $\{10\bar{1}1\}$ and $\{20\bar{2}3\}$ forms computed using the values a_0 (5.17 Å) and c_0 (8.67 Å) determined by Bannister and Hey (1942). The ρ angle for the $\{10\bar{1}1\}$ faces should be closer to 59°, and for the $\{20\bar{2}3\}$ faces closer to 48°. The hexagonal dipyramid assigned the $\{10\bar{1}1\}$ indices is rather well developed compared with the {2023} form which consists only of minute faces and which does not appear on all crystals.

The space group determined for kalsilite by Bannister and Hey (1942) is $P6_32$. The forms observed are possible forms in this crystal class.

X-ray data

X-ray data were determined for the iron-rich mica and kalsilite obtained in these runs. A comparison of basal plane reflections for the iron-rich mica formed in these experiments, lepidomelane, biotite, and

Table 3. Comparison of Basal Spacings for Several Micas

(hk·l)	Iron-rich mica[1]		Lepidomelane[2]		Biotite[3]		Muscovite[4]	
	d(Å)	I	d(Å)	I	d(Å)	I	d(Å)	I
00.1	10.04	100	10.1	100	10.1	100	10.0	100
00.2	5.06	50	5.04	20	4.58	20	5.0	60
00.3	3.37	100	3.36	100	3.36	100	3.34	80
00.4	2.51	95	2.51	40	2.51	40	2.48	40
00.5	2.033	45	2.01	80	2.00	80	2.00	70

[1] Copper radiation, Nickel filter, ($\lambda = 1.5418$ Å for K_α), diffractometer.

[2] ASTM *X*-ray Powder Data File, card number 2-0044, Molybdenum radiation, ($\lambda = 0.709$ Å), Nagelschmidt, 1937).

[3] ASTM *X*-ray Powder Data File, card number 2-0045, Molybdenum radiation, ($\lambda = 0.709$ Å), (Nagelschmidt, 1937).

[4] ASTM *X*-ray Powder Data File, card number 2-0055, Iron radiation, ($\lambda = 1.936$ Å), (British Museum).

muscovite is presented in Table 3. These results indicate that the iron-rich material is more similar to lepidomelane than to biotite. *X*-ray data for annite were not available. The recorded *x*-ray intensities were high for the even ordered reflections because a single plate of the iron-rich mica was mounted on a specimen holder to give only basal plane reflections, while the data shown for the other micas were taken from tabulations including all possible reflections.

Table 4 presents the *x*-ray powder photograph data for kalsilite. These results are very close to those of Smith and Tuttle (1957).

Smith and Sahama (1957) discussed order-disorder relations in kalsilite. The ordered form should either have a larger unit cell or be less

TABLE 4. *X*-RAY DIFFRACTION PATTERN FOR HYDROTHERMAL KALSITE
Debye-Scherrer camera, Copper radiation, Nickel filter, 12 hours

d(Å)	I	*d*(Å)	I
4.34	S	1.959	MW
3.97	VS	1.931	M
3.12	VS	1.770	M
2.582	VS	1.662	S
2.483	S	1.622	S
2.435	S	1.575	VS
2.219	S	1.560	M
2.175	VS	1.491	VS
1.992	M	1.459	M

symmetrical. Crystals of a kalsilite-nepheline microperthite from Kabfumu, (Belgian) Congo showed six additional diffuse reflections indicating that a new unit cell had to be taken at 30° to the usual cell. A rotation pattern about the *a*-axis of a single crystal specimen grown in these experiments was taken to determine whether the ordered or disordered form was present. Examination of the pattern showed no weak intermediate layer lines, indicating this sample to be of the disordered form.

CONCLUSIONS

Muscovite was readily converted under hydrothermal conditions to the $KAlSiO_4$ polymorph, kalsilite, and an iron-rich mica, very similar to lepidomelane in optical properties and x-ray diffraction pattern. *X*-ray and optical data indicate that the kalsilite described here corresponds closely to the natural kalsilite described by Bannister and Hey (1942) and the synthetic preparations of other workers. A single crystal rotation photograph indicates the kalsilite prepared in these experiments to be the disordered form.

It has been suggested that kalsilite may be more common in nature than is apparent. The apparent ease with which muscovite is converted to iron-rich mica and kalsilite suggests that additional occurrences of kalsilite in nature may be found where basic dikes intrude muscovite-bearing rocks.

References

Bannister, F. A. and Hey, M. H., 1942, Kalsilite, a polymorph of $KAlSiO_4$: *Mineral. Mag.*, **26,** 218–224.

Holmes, A. 1942, A suite of volcanic rocks from Southwest Uganda containing kalsilite (a polymorph of $KAlSiO_4$): *Mineral. Mag.*, **26,** 197–217.

Rigby, G. R. and Richardson, H. M., 1947, The occurrence of artificial kalsilite and allied potassium aluminum silicates in blast-furnace linings: *Mineral Mag.*, **28,** 75–87.

Sahama, Th. G. and Smith, J. V., 1957, Tri-kalsilite, a new mineral: *Am. Mineral.*, **42,** 286.

Smith, J. V. and Sahama, Th. G., 1957, Order-disorder in kalsilite: *Am. Mineral.*, **42,** 287–288.

Smith, J. V. and Tuttle, O. F., 1957, The nepheline-kalsilite system: I. *X*-ray data for the crystalline phases: *Amer. Jour. Sci.*, **255,** 282–305.

Tuttle, O. F. and Smith, J. V., 1958, The nepheline-kalsilite system: II. Phase relations: *Amer. Jour. Sci.*, **256,** 571–589.

Manuscript received August 29, 1960.

NOTES AND NEWS

ESTIMATION OF CHEMICAL COMPOSITION OF ROCKS

K. S. Heier
*Mineralogisk Museum, Oslo, Norway.**

Recently Friedman (1960) demonstrated how the chemical composition of rocks could be calculated from the mineralogical mode determined optically. The constituents which are fairly accurately computed are SiO_2, Al_2O_3, Fe_2O_3, FeO, MgO, CaO, Na_2O and K_2O. Each of these constituents calculated from the thin section analyses of the standard granite, G-1 (Fairbairn *et al.*, 1951), lies within the range reported by the chemists, and except for the alkalies, the computed concentrations of the elements are close to the arithmetic mean of G-1 rock analyses. Friedman (1960) also computed the chemical composition of a norite and obtained fair agreement with the chemical analysis of the same rock.

As calculation of chemical composition from the mineralogical mode and vice versa is, and has been, of great concern to petrologists some additional remarks seem appropriate. It is probably stating the obvious to say that the accuracy of these calculations depends upon at least two conditions:

(1) The mineral percentages computed from thin sections must be reliable.
(2) The optically determined composition of the minerals must be accurate.

If these two conditions are ideally satisfied, the chemical composition can be calculated with great accuracy. Rocks which for any reason, *e.g.*, grain size, secondary alteration, etc., do not allow these conditions to be satisfied are not amenable to this kind of treatment.

In general, granitic, or quartzo-feldspathic rocks show better agreement between analysed and calculated composition than rocks rich in ferro-magnesian minerals. This is because of the uncertainty and difficulty in deriving the exact chemical composition of ferro-magnesian minerals by optical means alone.

Friedman (1960) computed the chemical composition as weight per cent of the oxides. This demands a knowledge of the specific gravity of the minerals and the weight percentage of the various components in the pure mineral phases. There seems to be no reason why weight percentages of the elements must be used, inasmuch as unnecessary uncertainties and rather cumbersome calculations are introduced. The presence of elements in minerals and rocks is controlled by other factors than weight.

* Present address: Dept. of Geology, Rice University, Houston, Texas.

Of more direct use to the petrologist is the calculation of "equivalent molecular units" (Niggli, 1936), or even better, calculation of cation per cent. (For an explanation of this calculation, see Barth, 1952, pp. 76 82.)

Chemical analyses of G-1 and norite discussed by Friedman (1960) are calculated into cation per cent in Tables 1 and 2 respectively (columns I–IV).

Calculation of cation per cent of elements from mineral formulae is simple. Potassium feldspar $KAlSi_3O_8$ consists of 1 $KO_{1/2}$+1 $AlO_{1\ 1/2}$+3 SiO_2, together 5 units. 100% potassium feldspar contains 20 cat. % $KO_{1/2}$, 20 cat. % $AlO_{1\ 1/2}$, 60 cat. % SiO_2. Muscovite $KAl_2AlSi_3O_{10}(OH)_2$ consists of 1 $KO_{1/2}$+3 $AlO_{1\ 1/2}$+3 SiO_2+2 ($HO_{1/2}$), together 9 units, and 100% muscovite contains 100/9 cat. % $KO_{1/2}$, 3.100/9 cat. % $AlO_{1\ 1/2}$, 3·100/9 SiO_2, 2·100/9 $HO_{1/2}$.

Table 1. G-1—Granite

	I	II	III	IV	V
SiO_2	72.9	60	1214.0	68.1	68.2
$AlO_{1\frac{1}{2}}$	14.6	51	286.3	16.0	15.7
$FeO_{1\frac{1}{2}}$	0.9	80	11.3	0.6	0.8
FeO	1.0	72	13.9	0.8	
MgO	0.4	40	10.0	0.6	
MgO+FeO	1.4			1.4	1.4
CaO	1.4	56	25.0	1.4	1.4
$NaO_{\frac{1}{2}}$	3.3	31	106.4	6.0	4.9
$KO_{\frac{1}{2}}$	5.5	47	117.0	6.5	7.6
$NaO_{\frac{1}{2}}+KO_{\frac{1}{2}}$				12.5	12.5
			1783.9		

I. Arithmetic mean of rock analyses, weight per cent. Calculated to 100%.
II. Equivalent molecular weight.
III. Cation proportions×1000.
IV. Cation per cent from chemical analyses.
V. Cation per cent calculated from mineralogical mode using standard mineral formulae of Table 3.

The mineral content determined microscopically represents volume percentages. It can be shown that for common rocks the cation percentages calculated in this way from the volume of the minerals approximate the actual cation percentages of the total rock.

Table 3 lists the standard formulae of the modal minerals in G-1 and norite discussed by Friedman (1960). (With more detailed optical data for the minerals in the two rocks it is possible to express the mineral com-

Table 2. Norite

	I	II	III	IV	V
SiO_2	51.8	60	863.2	47.2	47.8
$AlO_{1\frac{1}{2}}$	19.8	51	388.3	21.2	22.1
$FeO_{1\frac{1}{2}}$	1.1	80	13.8	0.75	0.2
FeO	6.2	72	86.1	4.7	
MgO	8.9	40	222.5	12.2	
MgO+FeO				16.9	16.2
CaO	9.4	56	167.8	9.2	8.8
$NaO_{\frac{1}{2}}$	2.5	31	80.6	4.4	4.8
$KO_{\frac{1}{2}}$	0.3	47	6.4	0.35	0.1
$NaO_{\frac{1}{2}}+KO_{\frac{1}{2}}$				4.75	4.9
			1828.7		

I. Weight per cent of rock analysis calculated to 100%.
II. Equivalent molecular weight.
III. Cation proportions×1000.
IV. Cation per cent from chemical analysis.
V. Cation per cent calculated from mineralogical mode using standard mineral formulae of Table 3.

positions more exactly than in Table 3, but the standard formulae are close enough for the present considerations.)

In Tables 4 and 5 are the mineral modes of G-1 and norite respectively calculated into cation per cent. As water is not considered, the sum of the remaining constituents is recalculated to 100. These may be compared with the cation percentages calculated from the chemical analyses and for ease of comparison are set down as column V in Tables 1 and 2.

Comparisons between columns IV and V in Tables 1 and 2 show the same similarity between computed and analytically determined cation percentages as shown by Friedman (1960) for the weight percentages. In the first case no attempt was made to distinguish between MgO and FeO in the minerals. However, it is seen that the sum of these two elements is obtained with great accuracy. This is an advantage of calculat-

Table 3. Standard Formulae of Minerals

Quartz: SiO_2	Hornblende: $Ca_2(Mg, Fe)_3Al_2Si_6Al_2O_{22}(OH)_2$
Potassium feldspar: $KAlSi_3O_8$	Biotite: $K(Mg, Fe)_3AlSi_3O_{10}(OH)_2$
Albite: $NaAlSi_3O_8$	Muscovite: $KAl_2AlSi_3O_{10}(OH)_2$
Anorthite: $CaAl_2Si_2O_8$	Garnet: $Ca_3(Mg, Fe)_6Al_4Fe_2(SiO_4)_9$
Orthopyroxene: $(Mg, Fe)SiO_3$	Magnetite: $FeOFe_2O_3$
Clinopyroxene: $Ca(Mg, Fe)Si_2O_6$	

TABLE 4. CALCULATION OF CATION PER CENT OF THE ELEMENTS FROM THE MINERALOGICAL MODE OF G-1

	Mode Volume per cent	SiO_2	$KO_{\frac{1}{2}}$	$NaO_{\frac{1}{2}}$	$AlO_{1\frac{1}{2}}$	$FeO_{1\frac{1}{2}}$	CaO	MgO+FeO
Quartz	27.5	27.50						
K-feldspar	35.4	21.24	7.08		7.08			
(Plag. An_{23}	31.4)							
Albite	24.2	14.52		4.84	4.84			
Anorthite	7.2	2.88			2.88		1.44	
Muscovite	1.3	0.44	0.14		0.44			
Biotite	3.2	0.96	0.32		0.32			0.96
Magnetite	1.2					0.8		0.4
		67.54	7.54	4.84	15.56	0.8	1.44	1.36
Recalculated to 100%		68.2	7.6	4.9	15.7	0.8	1.4	1.4

ing the mineral mode into cation per cent; a direct calculation of the mode into weight per cent demands a knowledge of the MgO/FeO ratio in the minerals, for the atomic weights of the two elements differ.

Similarly the cation per cent sum of the alkalies is obtained with great

TABLE 5. CALCULATION OF CATION PER CENT OF THE ELEMENTS FROM THE MINERALOGICAL MODE OF NORITE

	Mode Volume per cent	SiO_2	$KO_{\frac{1}{2}}$	$NaO_{\frac{1}{2}}$	$AlO_{1\frac{1}{2}}$	CaO	$FeO_{1\frac{1}{2}}$	MgO+FeO
Quartz	0.1	0.10						
(Plag. An_{62}	63.2)							
Albite	24.0	14.40		4.80	4.80			
Anorthite	39.2	15.68			15.68		7.84	
Orthopy-roxene	28.7	14.35						14.35
Clinopy-roxene	1.0	0.50					0.25	0.25
Hornblende	4.8	1.68			1.12		0.56	0.84
Biotite	1.1	0.33	0.11		0.11			0.33
Garnet	1.0	0.37			0.17	0.08	0.12	0.25
Magnetite	0.1					0.07		0.03
		47.41	0.11	4.80	21.88	0.15	8.77	16.05
Recalculated to 100%		47.8	0.1	4.8	22.1	0.2	8.8	16.2

accuracy. The difference between computed and analysed cation per cent of sodium and potassium in G-1 is explained by the fact that all of the modal potassium feldspar was calculated as $KAlSi_3O_8$, thereby neglecting that a substantial amount of $NaAlSi_3O_8$ enters the same phase (as perthites). The ratio between $KAlSi_3O_8$ and $NaAlSi_3O_8$ in perthites cannot be determined optically. The failure to do so will not affect the sum of the cation percentages but will grossly affect the weight per cent calculations.

The computed concentration of ferric iron in the norite is seen to be unreliable. Though the analytical determination of ferric iron seems to be distinctly inferior to those of other constituents at the same concentrations (Ahrens, 1957), the reason for the great difference between computed and analytically determined cation per cent ferric iron in the norite is due to the fact that ferric iron is not included in the standard formulae of the ferro-magnesian minerals in Table 3. In these minerals ferric iron substitutes for Al in 6-coordination, and it should be noted that the computed cation per cent Al in the norite is higher than that determined analytically.

As the FeO, MgO, $NaO_{1/2}$, $KO_{1/2}$ concentrations and the FeO MgO and $NaO_{1/2}$ $KO_{1/2}$ ratios are of special value in petrological considerations, the difficulty in determining them optically is a serious deficiency. However, we need not consider optical methods alone and it will be shown how a combination of modal analyses with very simple analytical techniques may be applied.

A flame photometer for alkali determinations will soon be just as common in geological institutions as the polarizing microscope, and it can be used by everyone. Consider now the G-1 example. Based on thin section analyses the cation percentages listed in column V, Table 1 are obtained. Flame photometric alkali determinations give the concentrations of sodium and potassium listed in column I. As the sum of the cation percentages of $NaO_{1/2}$ and $KO_{1/2}$ may be computed accurately (compare columns IV and V) the cation per cent of $NaO_{1/2}$ and $KO_{1/2}$ may be found by the following relation:

$$\left(\frac{\text{wt. \% } Na_2O}{\text{mol. wt. } NaO_{\frac{1}{2}}} + \frac{\text{wt. \% } K_2O}{\text{mol. wt. } KO_{\frac{1}{2}}}\right)\cdot X = \text{sum of cat. \% } NaO_{\frac{1}{2}} + KO_{\frac{1}{2}}: \qquad 1.$$

$$\left(\frac{3.3}{31} + \frac{5.5}{47}\right)\cdot X = 12.5$$

$$X = 56$$

$$\text{cation per cent } NaO_{\frac{1}{2}} = \frac{3.3}{31}\cdot 56 = 6.0$$

$$\text{cation per cent } KO_{\frac{1}{2}} = \frac{5.5}{47}\cdot 56 = 6.5$$

(The factor X is the same as the conversion factor used in recalculating the cation proportions (column III) into cation per cent (column IV), or rather 1000 times this factor, *i.e.*,

$$X = \frac{100}{1783.9} \cdot 1000.)$$

In case of the norite X also equals 56, and the cation percentages are: $NaO_{1/2}$ 4.5, and $KO_{1/2}$ 0.4.

Similarly, the determination of ferrous iron by titration demands very little laboratory equipment and is done in one single determination on the bulk rock. Again, in the case of G-1, having determined the weight per cent of FeO as 1.0% (Table 1, column I), the cation per cent of FeO is found by the relation:

$$\frac{\text{wt. \% FeO}}{\text{mol. wt. FeO}} \cdot X = Y \qquad 2.$$

X is the same factor as in equation 1, i.e., 56, and Y is the cation per cent of FeO.

$$\frac{1.0}{72} \cdot 56 = Y$$

$Y = 0.8$ = cation per cent FeO.

cation per cent MgO = 1.4 − 0.8 = 0.6.

In case of the norite the cation per cent of FeO is found to be 4.8, and of MgO 11.4.

Having obtained the cation percentages of the elements through the combination of optical and chemical methods the weight per cent is, if for some reason this quantity should be desired, easily obtained by multiplying by the equivalent molecular weights and recalculating to a sum of 100.

References

Ahrens, L. H. (1957), A survey of the quality of the principal abundance data of geochemistry: *Physics and chemistry of the earth*, **2**, 30–45.

Barth, T. F. W. (1952), Theoretical petrology. John Wiley & Sons, Inc., New York, 387 p.

Fairbairn, H. W., Schlecht, W. G., Stevens, R. E., Dennen, W. H., Ahrens, L. H. and Chayes, F. (1951), A co-operative investigation of precision and accuracy in chemical, spectrochemical and modal analysis of silicate rocks: *U. S. Geol. Surv. Bull.*, **980**, 57 p.

Friedman, G. M. (1960), Chemical analyses of rocks with the petrographic microscope: *Am. Mineral.* **45**, 69–78.

Niggli, P. (1936), Über Molekularnormen zur Gesteinsberechnung: *Schweiz. mineral. petrog. Mitt.*, **16**, 295–317.

THE AMERICAN MINERALOGIST, VOL. 46, MAY-JUNE, 1961

GEDRITE FROM OXFORD COUNTY, MAINE*

DANIEL J. MILTON AND JUN ITO, *Harvard University, Cambridge, Mass.*

OCCURRENCE

Gedrite (aluminian anthophyllite) occurs in the metamorphosed Ammonoosuc volcanics at several localities in Grafton, Oxford County, Maine. The material chosen for study is from an elevation of about 1730 feet in the tributary entering Black Brook at about elevation 1650 near the west edge of the Old Speck Mountain 15′ quadrangle.

The estimated mode of the rock is:

40% quartz
45% albite
7% gedrite
5% garnet
1% biotite
1% chlorite
1% magnetite.

The pre-metamorphic nature of the rock is not definitely known, but it was probably a felsic tuff, perhaps considerably modified by sedimentary processes.

The gedrite forms dark green needles or platy prisms about one centimeter long, with some tendency to sheaf-like aggregation. It is partially altered to a brownish-yellow mineral of low birefringence that may be a serpentine or a chlorite.

SEPARATION

The rock was crushed and the 50 to 200 mesh fraction was used for separation. Gedrite was concentrated by means of heavy liquids and a Frantz isodynamic separator and remaining impurities were picked out by hand. Most of the altered gedrite was removed by floating in fresh methylene iodide. The product used for analysis is estimated to have contained less than 0.5% of the alteration product and less than 0.1% of other impurities.

CHEMICAL COMPOSITION

Table 1 gives the chemical composition and the atomic ratios calculated on the basis of 24 oxygen atoms, corresponding to the amphibole formula $AM_2M_5(Si,Al)_8O_{22}(OH)_2$. The assumption that there are 24

* Contribution from the Department of Mineralogy and Petrography, Harvard University.

oxygen atoms to the formula, or 96 to the unit cell, leads to a calculated density only 1% less than the measured density, well within the probable error of the various determinations. Six out of the seven anthophyllites studied by Rabbitt, however, also have higher measured than calculated densities. This suggests that the conclusion drawn by Francis (1956) for a particular anthophyllite, that there are more than 96 oxygen (plus fluorine) atoms per unit cell, may be frequently valid.

The amount of aluminum in the tetrahedral positions is the highest

Table 1. Composition of Gedrite

SiO_2	40.71	Si	5.99	8.00
TiO_2	0.29	Al^{iv}	2.01	
Al_2O_3	18.73	Al^{vi}	1.23	
Fe_2O_3	0.90	Mg	2.34	
FeO	24.39	Fe''	3.00	
MnO	0.14	Fe'''	.10	
MgO	10.66	Mn	.02	7.20
CaO	0.05	Ti	.03	
Na_2O	1.59	Ca	.01	
K_2O	0.06	Na	.46	
H_2O^+	2.75	K	.01	
H_2O^-	0.15	OH	2.70	
F	tr.			
Total	100.42			

Spectrographic determinations
V 0.0x
Ga 0.0x
Zn 0.0x
Co, Ag, Cu very weak
Jun Ito, analyst.

reported for any anthophyllite, within the limits of error equal to the two out of eight positions usually considered as the limit on the gedrite side of the anthophyllite series. The Fe/Mg ratio is higher than in any anthophyllite listed by Rabbitt, but recently Seki and Yamasaki (1957) have found an anthophyllite very near the ferrogedrite $Fe_5Al_2Si_6Al_2O_{22}(OH)_2$ end member. The sodium content is the highest reported for any anthophyllite. Calcium is even lower than usual, as might be expected from the association with albite. Potassium is, as usual, very low.

The sum of the cations in the formula (other than hydrogen and the silicon and aluminum required to fill the tetrahedral positions) is 7.20. The mean value for the complete analyses (with alkali determinations)

listed by Rabbitt is 7.13, significantly greater than the 7.00 indicated by the usual anthophyllite formula $M_7(Si,Al)_8O_{22}(OH)_2$. The excess cations are presumably housed in the mostly vacant A position, as was suggested for calcium by Whittaker (1960). The sum of the calcium, sodium, and potassium atoms in Rabbitt's analyses shows a small but definite positive correlation with the total number of non-tetrahedral cations. This suggests that there is a tendency for the larger minor cations to enter the A position, but that they are not restricted to it. In some anthophyllites the cation sum is less than 7.00, so that some of the M positions must be vacant, especially so if some of the A positions are occupied.

The H_2O content is high, but within the known range for anthophyllite. Francis has discussed an unusually hydrous anthophyllite, concluding that water molecules are present in the A or M positions or, less likely, that SiO_4 tetrahedra are replaced by $(OH)_4$ tetrahedra. For a number of anthophyllites listed by Rabbitt the sum of the silicon and aluminum atoms is less than 8, and in these the average H_2O content is significantly higher than in the others, suggesting that replacement of silicon tetrahedra by hydroxyl tetrahedra does occur.

Nomenclature

The anthophyllite series may be considered an incomplete solution between four end members: magnesioanthophyllite $Mg_7Si_8O_{22}(OH)_2$, fer-

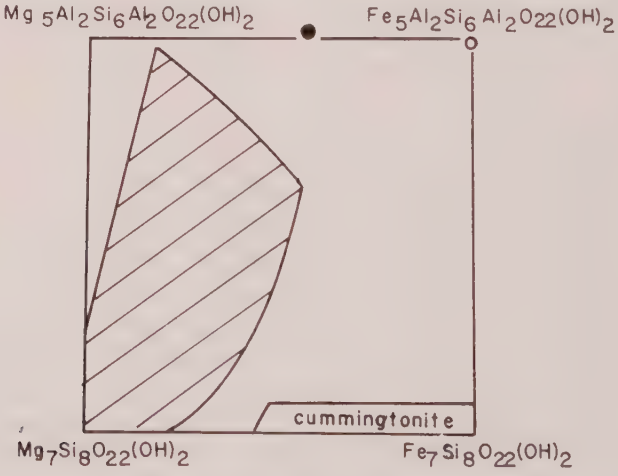

Fig. 1. Compositional field of anthophyllite. Closed circle is gedrite of this paper. Open circle is analyzed ferrogedrite of Seki and Yamasaki (1957). Hatched field encloses anthophyllite analyses compiled by Rabbitt (1948).

roanthophyllite $Fe_7Si_8O_{22}(OH)_2$, magnesiogedrite $Mg_5Al_2Si_6Al_2O_{22}(OH)_2$, and ferrogedrite $Fe_5Al_2Si_6Al_2O_{22}(OH)_2$ (Fig. 1). Seki and Yamasaki, who found a naturally occurring mineral very close to the last end member, preferred to call it aluminian ferroanthophyllite, since the ratio of tetrahedral aluminum to the silicon which it replaces is less than unity. Although there is no obvious reason why this replacement should be limited to two out of eight atoms, the known compositions suggest that this is a natural limit. The name gedrite is entrenched and, unlike most varietal names, is associated with a meaningful ideal formula. It would seem a proper name for the mineral here described.

Density

The density, as determined by suspension in Clerici solution, with the density of the liquid in turn determined by pycnometer, is 3.37. Calculation from the composition and the unit cell dimensions yields a density of 3.33_4.

Optical Properties

The optical properties are:

$\alpha = 1.671 \pm 0.002$	$X = a$	yellowish gray
$\beta = 1.681 \pm 0.002$	$Y = b$	greenish gray
$\gamma = 1.690 \pm 0.002$	$Z = c$	greenish gray
$(-)\ 2V_{meas} \sim 75°$		abs. $Z > Y > X$

Indices were determined by means of a spindle stage (Wilcox 1960) with the oils checked at the time of use by a Leitz-Jelley microrefractometer. The axial angle was determined by the method of Kamb (1958). Extinction positions were carefully observed in monochromatic light of various wave lengths, in an attempt to find dispersion of the bisectrices. None was found.

The regression equations of Hey yield indices for this composition of $\alpha = 1.6704 \pm 0.025$, $\beta = 1.6789 \pm 0.015$, $\gamma = 1.6911 \pm 0.0012$ which are satisfactorily close. Seki and Yamasaki's diagram gives $\alpha = 1.669$ and $\gamma = 1.696$, which are a somewhat poorer match.

X-ray Diffraction Data

Measurements of a powder photograph taken in Fe radiation are given in Table 2. Indexing of most reflections follows Johansson (1930) and Seki and Yamasaki (1957). The cell dimensions as calculated from the back reflections are:

a_0 18.59_4 Å b_0 17.89_0 Å c_0 5.30_4 Å

All reflections are consistent with the accepted space group *Pnma*.

Hey (1956) presented regression equations relating chemical composition and physical properties for the anthophyllite series. His equation indicates a b_0 of 18.005 ± 0.04 Å, so the measured value lies outside his probable range.

Association

From several optical tests the associated plagioclase is an albite with less than 5% an. The garnet has a refractive index of 1.806, a cell edge of

Table 2. *X*-Ray Powder Data for Gedrite

Fe/Mn radiation

I	d_{obs}	d_{calc}	*hkl*	I	d_{obs}	d_{calc}	*hkl*
5	8.97 Å	8.49 Å	020	3	1.997	1.991	661
8	8.27	8.25	210	2	1.976	1.979	751
2	5.06	5.02	230			1.972	602
2	4.93	4.91	111	2	1.876	1.877	702
2	4.66	4.65	400	2b	1.83	1.832	931
4	4.48	4.47	040	1	1.787		
3	4.14	4.13	420	1	1.774		
3	3.88	3.88	131	2b	1.745		
4	3.65	3.65	231	1b	1.667		
4	3.35		β610	1	1.629		
7	3.23	3.21	440	2	1.617		
10	3.06	3.05	610	2	1.601		
1	3.00			1b	1.579		
1	2.90	2.88	521	2	1.550	1.550	12·00
3	2.85	2.84	260	1	1.541		
3	2.82	2.83	251	3	1.511	1.512	10·61
3	2.75	2.75	630	1	1.500		
1	2.71			2	1.491	1.491	0·12·0
3	2.67	2.68	351	2	1.439		
2	2.57	2.57	161	1	1.425		
3	2.55	2.55	202	2	1.416		
4	2.50	2.50	451	2b	1.324		
3	2.44	2.44	302	2b	1.285	1.287	2·12·2
2	2.34	2.34	650	1	1.124		
3	2.32	2.32	551	2	1.028	1.031	16·80
2	2.23			1	1.015		
3	2.16	2.16	502	1	1.006		
3	2.13	2.13	561	1	0.999		
2	2.07			1	0.992		
2	2.015						

Camera radius 114.59 mm.
Corrected for film shrinkage
Low angle cutoff ≥ 15 Å
Intensities by visual estimate
b=line broadening.

11.521 Å, a density of 4.20, and a MnO content of 0.82. This fits a composition of about $al_{77}py_{18}gr_3sp_2$, according to the charts of Sriramadas (1957). The γ indices of the biotite and chlerite are 1.637 and 1.620, respectively. Assuming the usual degree of aluminum substitution (one third of the tetrahedral positions) these indicate Fe/Fe+Mg ratios of about 0.58 for the biotite and 0.43 for the chlorite.

The four ferromagnesian minerals are plotted on an AFM diagram in Fig. 2. The points are, within the limits of accuracy, collinear, with the gedrite and biotite having close to the same Fe/Mg ratio, intermediate between the more siderophile garnet and the more magnesiophile chlorite.

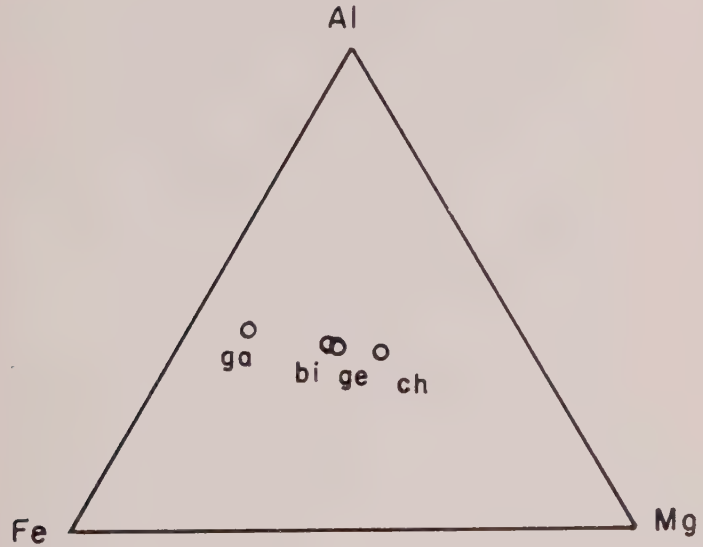

Fig. 2. Compositional relations of gedrite and associated garnet, biotite, and chlorite.

Biotite is, strictly speaking, projected onto the plane of the diagram from the K corner of a KAFM tetrahedron, so that the closeness of the biotite and gedrite points is not irregular. Gedrite, garnet, and chlorite, on the other hand, have all major, and presumably determining, components in common. A collinearity of these points would indicate less than the two degrees of freedom required by the mineralogical phase rule. Probably, were the compositions more accurately determined, there would be a narrow triangle between these three points. As less aluminous anthophyllite would be expected to be stable under the same physical conditions, the gedrite apex is most likely the bottom apex of the triangle, perhaps by virtue of the chlorite being more aluminous than was assumed.

Acknowledgments

Thanks are due to Professor C. S. Hurlbut, Jr. for a critical reading of this paper. Work was performed during the tenure of a National Science Foundation pre-doctoral fellowship by the senior author.

References

Francis, G. H., 1955, Gedrite from Glen Urquhart, Inverness-shire: *Mineral. Mag.*, **30,** 709–716.

Hey, M., 1956, On the correlation of physical properties with chemical composition in multivariate systems: *Mineral. Mag.*, **31,** 69–95.

Johansson, K., 1930, Vergleichende Untersuchungen an Anthophyllit, Grammatit und Cummingtonit: *Zeits. Krist.*, **73,** 31–51.

Kamb, W. B., 1958, Isogyres in interference figures: *Am. Mineral.*, **43,** 1029–1067.

Rabbitt, J. C., 1948, A new study of the anthophyllite series: *Am. Mineral.*, **33,** 263–323.

Seki, Y. and Yamasaki, M., 1957, Aluminian ferroanthophyllite from the Kitakami Mountainland, Northeastern Japan: *Am. Mineral.*, **42,** 506–520.

Sriramadas, A., 1957, Diagrams for the correlation of unit cell edges and refractive indices with the chemical compositions of garnets: *Am. Mineral.*, **42,** 294–299.

Whittaker, E. J. W., 1960, The crystal chemistry of the amphiboles: *Acta Cryst.*, **13,** 291–298.

Wilcox, R. E., 1959, Use of the spindle stage for determining refractive indices of crystal fragments: *Am. Mineral.*, **44,** 1272–1293.

THE AMERICAN MINERALOGIST, VOL. 46, MAY–JUNE, 1961

LAMELLAR STRUCTURE IN A TYPE I DIAMOND*

R. M. Denning, *Department of Mineralogy, University of Michigan*

A lamellar structure parallel to octahedron planes is not unusual in diamonds. Such structure becomes visible between crossed polars when the diamond is observed along a [110] direction.

A very pale-yellow diamond crystal, apparently free of birefringence, was selected for stress-optical study. A rectangular parallelopiped was cut in such a way as to be bounded by two dodecahedral planes and one cube plane. The excellence of the natural octahedral faces was such that the optical goniometer could be used to determine the orientation. The largest orientation error of any of the planes is 6 minutes of arc. The dimensions of the diamond sample are $2.6\times3.6\times4.6$ mm. After the diamond was cut, it was found to show very low double refraction.

Figure 1 shows three views of the crystal between crossed polars. In each view, the vibration directions of the polars are parallel to the edges of the crystal. The interference colors are all first order gray. The birefringence of the lamellae is about 2×10^{-5}. A central nucleus shows a

* Contribution No. 239 Dept. of Mineralogy, University of Michigan.

birefringence of 2.5×10^{-4}. The sharp edges of the nucleus are parallel to {111} planes or edge [112] or nearly parallel to {112} or edge [111] or nearly parallel to {221} or edge [114]. With careful adjustment of the illumination, a Becke line can just be detected at the {112} (or [111]) boundary. The lamellae are to a large extent alternately length slow and length fast. The vibration directions within the lamellae are parallel to {111} at midpoint, and in most of the lamellae they make an angle of

FIG. 1. Birefringence patterns in type I diamond. Crossed linear polars. Vibration directions are parallel to edges of crystal. A(001), B(110), C(110). The dimensions are 2.6×3.6×4.6 mm.

about 40° to the {111} planes at the extremities. Such a distribution of vibration directions gives rise to the broad extinction cross. Other extinction bands reveal a more complex distribution of vibration directions. The lamellae in adjacent sectors meet in sharply defined but rather irregular surfaces roughly parallel to cube planes. Some of the dark areas near the nucleus appear optically isotropic.

When the crystal is viewed normal to the cube facet (Fig. 1A), the birefringent areas are seen to be roughly divided into four sectors. Extinction bands are irregularly distributed. There is little if any evidence of lamellar structure in this orientation.

Twinning is practically absent. The grinding rate of the crystal as ob-

served during the preparation of the specimen gave no indication of twinning. The grinding behavior probably is the most sensitive test for twinning in diamond. Under favorable conditions, if 1% of the area being cut were twinned, the twinning could be easily detected. Theoretically if a tenth of a per cent of the cut surface were twinned, it should be possible to detect the twinning from the grinding behavior. No twinning was recognized.

As a further check, a number of Laue photographs were taken. While these failed to reveal twinning, it was noted that the scattering power for x-rays is not uniformly distributed over the volume of the crystal. It was possible to correlate the intensity of scattering with the strength of double refraction. The nucleus and the corners of the crystal show the greater scattering power. Microdensitometer traverses along the Laue spots show that the regions of greatest double refraction scatter x-rays about twice as strongly as the optically isotropic portions. An attempt was made to obtain an x-ray topograph from the (220) reflection with copper radiation, as described by Wooster (1945). The thickness of the crystal and other experimental factors did not permit the resolution of the desired features, so reliance had to be placed on the energy distribution in the Laue spots. Ultra-violet and infra-red absorption spectra were studied for the entire crystal as well as for selected areas of the crystal. The absorption characteristics of all parts of the crystal are typical of type I diamonds. The crystal is opaque for wavelengths below 315 mμ, and the absorption bands in the 7–9 μ region, characteristic of type II diamonds, are absent.

In ultra-violet radiation from a mercury lamp, no fluorescence can be visually detected. However, a rather weak blue fluorescence is excited by x-radiation from a copper tube. It can be demonstrated that the most strongly fluorescent portions of the crystal are the regions of strongest double refraction. The lamellar distribution of the fluorescence is not so well developed as is the lamellar birefringence. The fluorescence is always greatest on the side of the diamond nearest the x-ray source, because of the absorption of x-rays by the diamond. Photographs of the fluorescence were taken, but the low contrast makes half tone reproduction impractical.

It was noted that as the crystal was compressed on a cube plane, the lamellar birefringence tended to disappear, even at the fairly low stress of a few hundred kilograms/cm.^{2}. It may be that the increased optical homogeneity is more apparent than real. Both the x-ray diffraction and the fluorescence studies were repeated with the diamond under stresses up to nearly 1000 kg./cm.^{2}. No difference, either in the diffraction pattern or in the fluorescence, was detected. Another similar diamond

uncut) was stressed non-uniformly until it showed tenth order interference for sodium light. The local maximum stress was then 20,000 kg./cm.^{2} (280,000 lbs/inch^2), at which stress the diamond failed along a cleavage plane at an opaque inclusion. No change in either the x-ray pattern or the distribution of fluorescence was induced by such stress. No hysteresis effects, optical or otherwise, were noted after the stress was removed.

The correlation of birefringence, x-ray scattering and fluorescence in diamond has previously been observed by Raman and his colleagues (1944, 1949).

The data suggest that the diamond crystal used grew under periodically varying conditions which resulted in a cyclical variation of minor constituents. It seems reasonable that the variation in composition is due to the substitution of some element other than nitrogen, since no variation in ultra-violet or infra-red absorption of the kind recently correlated with nitrogen content by Kaiser and Bond (1959) has been observed for various regions of the crystal.

While the birefringence of the nucleus is too large to be explained by nitrogen substitution, the birefringence of the lamellae if due to nitrogen substitution would indicate a variation of nitrogen content in adjacent lamellae of at least 3.5×10^{20} atoms/cm.^{3}.

In order to explain fully the strain which gives rise to the birefringent lamellae, the accompanying crystal imperfection, the distribution of fluorescence, together with the uniformity of the ultra-violet and infra-red absorption, it is believed that other atoms than nitrogen must be present in different amounts in adjacent lamellae.

The diamond was furnished by Industrial Distributors (Sales) Ltd., and was cut by Dr. M. A. Conrad. The work was supported in part by the Office of Naval Research and the Atomic Energy Commission.

References

Wooster, N. and W. A. (1945), *Nature*, **155,** 786.

Kaiser, W. and Bond, W. L. (1959), Nitrogen, a major impurity in common Type I diamond: *Phys. Rev.*, **115,** No. 4, 857–863.

Raman, Sir L. V. and Rendall, G. R. (1944), Birefringence patterns in diamond: *Proc. Ind. Acad. Sci.*, **19,** Ser. A, No. 5, 265–273.

Ramachandran, G. N. (1949), *Ibid.*, **24,** Ser. A, No. 1, 65–79.

THE AMERICAN MINERALOGIST, VOL. 46, MAY-JUNE, 1961

THE DENSITY SEPARATION OF CLAY MINERALS IN THALLOUS FORMATE SOLUTIONS*

J. A. KITTRICK, *Agronomy Dept., Washington State University, Pullman, Washington.*

With the many recent improvements in identification of clay minerals by *x*-ray diffraction, the main problem in clay mineral analysis has become one of quantitative analysis. *X*-ray diffraction as a quantitative method is hindered by such sample variables as crystal perfection, orientation, particle size, and chemical composition. To obtain more reliable quantitative results, additional information, such as cation exchange capacity, sorption of polar liquids, elemental analysis, and differential thermal analysis are often considered. But even use of all of these methods will not necessarily give correct quantitative results, because percentage composition must be determined in terms of a set of of standard minerals with relatively ideal mineral properties. These standard minerals are seldom, if ever, identical to the clay minerals in the sample. On the relatively rare occasions when the *precision* of analyses has been determined, the data are frequently presented as representing *accuracy* when, in reality, the accuracy is almost always unknown in quantitative clay mineral analysis.

At present, the only way in which one could quantitatively analyze a natural mixture of clay minerals without involving tenuous assumptions as to some of their chemical or physical properties, would be to separate the individual mineral components and weigh them. To this end, differential starch precipitation (Beavers and Marshall, 1951) and retention by ion exchange resins (mentioned by Wiklander, 1951) did not show initial promise as clay mineral separation methods. Differential absorption in nitrobenzene-tetrabromethane and continuous flow electrophoresis showed only slight initial promise and were not extensively tested. Efforts were then concentrated on the one method which did show initial promise, the density separation of clay minerals in thallous formate solution.

MATERIALS AND METHODS

Kaolinite H-2, montmorillonites H-11, H-23, H-24, and H-26, and illite H-36 were obtained from Wards Natural Science Establishment;

* Scientific Paper No. 2036, Wash. Agr. Exp. Sta. Pullman. Project No. 1384. The author wishes to express his appreciation to Dr. H. W. Smith for his helpful criticism of the manuscript.

imilar materials have been extensively studied (API, 1951). Kaolinite 81 (England) and vermiculite 189 (Libby, Montana) were also obtained rom Wards and kaolinite 91 (Edgar, Florida) from the Edgar Plastic Kaolin Company.

In order to determine the apparent densities of clay minerals, approximately 0.1 gm. clay samples were added to about 10 ml. of thallous ormate solution of suitable density in 15 ml. culture tubes. Interaction etween the clay and thallous formate appeared to be complete after bout 30 minutes. Centrifuging at about 1000 rpm. for 5 minutes completed clay movement (either up or down). Tl^+ was removed from the xchange sites* by precipitating the Tl^+ as TlCl and then oxidizing the Tl^+ to Tl^{+++} with bromine. $TlCl_3$ is water soluble, and was removed by entrifuge washing. Densities of Tl^+ solutions were determined by eighing a known volume.

Density Separation in Thallous Formate Solution

This method is based on density variations acquired by clay minerals n concentrated thallous formate solutions. Several non-clay minerals re known to increase their densities in Clerici solution (thallium ormate-malonate mixture). Hutton (1950) also noted a tendency for he density of montmorillonite to increase. Rodda (1952) made practical se of this to separate a mixture of kaolinite from montmorillonite with lerici solution of specific gravity 3.55. At this specific gravity, the kaonite floated as anticipated, but the montmorillonite (normal specific ravity of about 2.6) sank anomalously, presumably owing to adsorption of the thallium.

Kaolinite—Montmorillonite Mixtures

The densities acquired by several layer silicates in thallous formate re shown in Table 1. Illite and vermiculite sank in solutions of specific ravity 3.00 and lower and floated in solutions of specific gravity 3.10 nd higher, whereas kaolinite floated and montmorillonite sank over the hole specific gravity range tested. The easiest separation in this group ppeared to be that of kaolinite from montmorillonite. To this end, qual amounts of three pairs of pure kaolinite and montmorillonite kaolinite H-2 and montmorillonite H-23, kaolinite 81 and montmorillonite H-24, kaolinite H-2 and montmorillonite H-11) were mixed *dry*. Approximately 0.1 gm. portions of the mixtures were added to thallous ormate solutions of 3.2 specific gravity. The mixtures were allowed to

* Necessary because it was found that Tl^+ saturation essentially eliminates the diagstic (001) peak of montmorillonite; the mechanism is to be discussed in another ublication.

Table 1. Densities Acquired by Layer Silicates in Thallous Formate Solution

Mineral	Float (+) or sink (−) in Tl^+ formate of specific gravity:				
	2.6	2.8	3.0	3.2	3.4
Kaolinite 91	+	+	+	+	+
Illite H-36	−	−	−	+	+
Vermiculite 189	−	−	−	+	+
Montmorillonite H-26	−	−	−	−	−

separate with no stirring. All three kaolinite-montmorillonite mixtures split into two roughly equal components, one of which sank and the other floated. Floating material was removed with a suction-tube device and excess thallous formate was removed from both components by centrifuge washing prior to *x*-ray diffraction analysis.

A rather good separation of kaolinite and montmorillonite was achieved as was indicated by the *x*-ray diffraction patterns (not shown). In some cases, small percentages of kaolinite or montmorillonite remained in the wrong fraction, but these presumably could be removed with further separations. Similar results were obtained at specific gravity 3.4 and neither solution pH nor previous ion saturation of the clay appeared to affect the separation.

Effect of Agitation

Agitation of any kind diminished the completeness of separation and a relatively prolonged or violent agitation frequently prevented any separation at all. The mineral particles would no longer move independently; instead the whole mass moved either up or down, depending on the solution density and the dominant mineral component. Apparently, agitation causes the montmorillonite component to create a network (perhaps like that shown by Kittrick, 1957) that completely envelopes the kaolinite component, resulting in the movement of kaolinite and montmorillonite as a unit. The same result was obtained when the montmorillonite and kaolinite were mixed *wet* prior to the separation attempt. No way was found by which this entrapment could be eliminated, so the method as it now stands appears to have no practical value for the separation of clay minerals.

References

American Petroleum Institute, (1951), Research project 49. Columbia University Press, New York.

Beavers, A. H. and Marshall, C. E. (1951), The cataphoresis of clay minerals and factors affecting their separation: *Soil Sci. Soc. Amer. Proc.*, **15,** 142–145.

Hutton, C. O. (1950), Studies of heavy detrital minerals: *Bull. Geol. Soc. Amer.*, **61,** 635–716.

Kittrick, J. A. (1957), Electron microscope observations on several freeze-dried macromolecular systems: *J. Polymer. Sci.*, **28,** 247–250.

Rodda, J. L. (1952), Anomalous behavior of montmorillonite clays in Clerici solution: *Am. Mineral.*, **37,** 117–119.

Wiklander, L. (1951), Saturation of colloids and soils by means of exchange resins; *Ann. Roy. Agr Coll. Sweden*, **18,** 154–162.

THE AMERICAN MINERALOGIST, VOL. 46, MAY–JUNE, 1961

A FAYALITE-BEARING PEGMATITE, BURNET COUNTY, TEXAS

Elbert A. King, Jr., *Austin, Texas.*

Fayalite has been reported from numerous localities throughout the world, and it is associated with quartz in some igneous rocks and in a few pegmatites (Shibata, 1937).

A fayalite-bearing pegmatite is located half a mile N. 78° W. from the north end of Buchanan Dam on the shore of Lake Buchanan, Burnet County, Texas. The pegmatite strikes N. 50° W., dips 50° to 80° NE., averages 4 to 6 feet wide, and is exposed for about 120 feet when the lake surface elevation is less than 1,010 feet above sea level. The country rock is pink Precambrian granite composed mostly of pink microcline, quartz, biotite, and hornblende.

There are two readily discernible zones in the pegmatite, an outer zone of perthitic pink microcline, in which there are microcline crystals up to 8 inches in diameter, and an inner zone or core of smoky quartz. The quartz and microcline are graphically intergrown at several places along the boundary between the two zones.

The fayalite occurs in anhedral masses and rough tabular crystals in the quartz core of the pegmatite. Crystals 6 inches long and weighing in excess of 2 pounds have been found, but the average size is about 2 inches long and the average weight between 3 and 4 ounces. On fresh surfaces the fayalite is lustrous black and on weathered surfaces dark brown.

X-ray diffraction with copper K_α radiation shows the following prominent peaks in decreasing order of intensity: 2.833, 2.502, 2.567, and 5.250 Å.

Properties are as follows:

Biaxial (−)
$r>v$ distinct
$\alpha=1.819$, $\beta=1.858$, $\gamma=1.868$
$\gamma-\alpha=0.049$
$2V=53°$
Specific gravity (28° C.) $=4.22\pm0.02$

The optical properties and x-ray data indicate that the fayalite is not pure Fe_2SiO_4 but probably contains small amounts of additional cations that have been admitted into the orthosilicate structure thereby slightly modifying the crystal structure and properties (Ford, 1935).

The fayalite is a very minor constituent of the pegmatite with only about 12 pounds of the mineral having been collected to date. The only other accessory mineral in the pegmatite is biotite, which occurs throughout both the microcline zone and the quartz core in plates and crystal sections up to 3 inches in diameter.

References

Ford, E. W. (1935), The crystal structure of fayalite: *Ohio State Univ. Abstracts of Doc. Dissert.*, **14**, 32–39.

Shibata, H. (1937), Fayalite in pegmatite from Sirawadani, province of Omi, Japan: *Geol. Soc. Japan, J.*, **46**, 553, 538 (Japanese).

THE AMERICAN MINERALOGIST, VOL. 46, MAY–JUNE, 1961

THE GROWTH OF SYNTHETIC CHRYSOTILE FIBER

Julie Chi-Sun Yang, *Basic Research Section, Johns-Manville Research Center, Manville, New Jersey.*

In the course of numerous studies on the formation of inorganic fibrous material, considerable attention has been drawn to the synthesis of chrysotile asbestos because of the desirable properties of this material in technological applications. Chrysotile has been synthesized under hydrothermal conditions by Jander, W. and Wuhrer, J., (1938) and many others, but the crystals formed were generally in matted fibrils, about 1μ in length, which could be recognized only by examination with the electron microscope. This investigation was undertaken in our laboratory as part of a research program on the ternary system MgO-SiO_2-H_2O to increase knowledge of the genesis and the crystal structure of serpentine materials (Yang, 1960).

It was found that synthetic chrysotile fiber growth can be promoted by employing proper mineralizers, trace elements and controlled pH mediums in the hydrothermal synthesis. Fiber bundles formed under these conditions average 100μ or more in length, but individual fibers are about 15–20μ. These consist mainly of clinochrysotile with trace amounts of platy lizardite.

Experimental

Optimum conditions for hydrothermal synthesis are tabulated as follows:

Starting Materials:

Magnesium oxide (c.p) and special bulky silicic acid mixtures of MgO/SiO_2 molar ratio 1.5, water/solid ratio 10

Temperature (C)	300–350
Pressure (psi)	1230–1800
Time (days)	5– 10
pH of the system	10.3 to 10.7 controlled by adding Na_2CO_3 or Na_2CO_3-$NaHCO_3$ buffer
Mineralizer	An amount of F^- equivalent to 1–2% by weight of the starting material in the form of 0.01N NH_4F solution.

From rate of formation studies, it was found that bundles of fibers of maximum length 50μ together with tightly matted crystal aggregates were formed at the end of 6 hours. No unreacted magnesia, magnesium hydroxide or silica was detected by x-ray diffraction, but these compounds were found in trace amounts under microscopic examination.

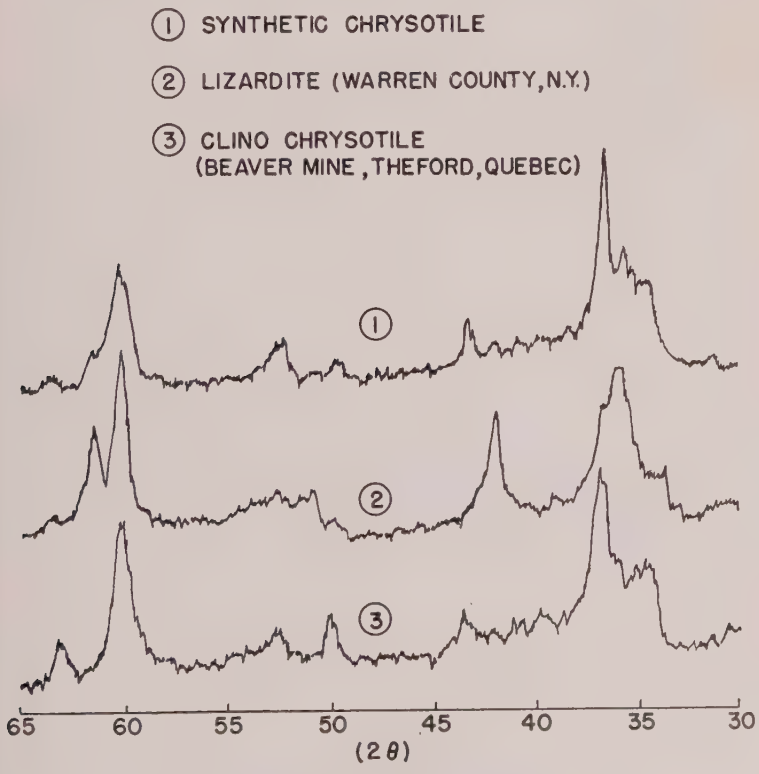

FIG. 1. X-ray diffraction patterns of synthetic clinochrysotile, lizardite and natural chrysotile.

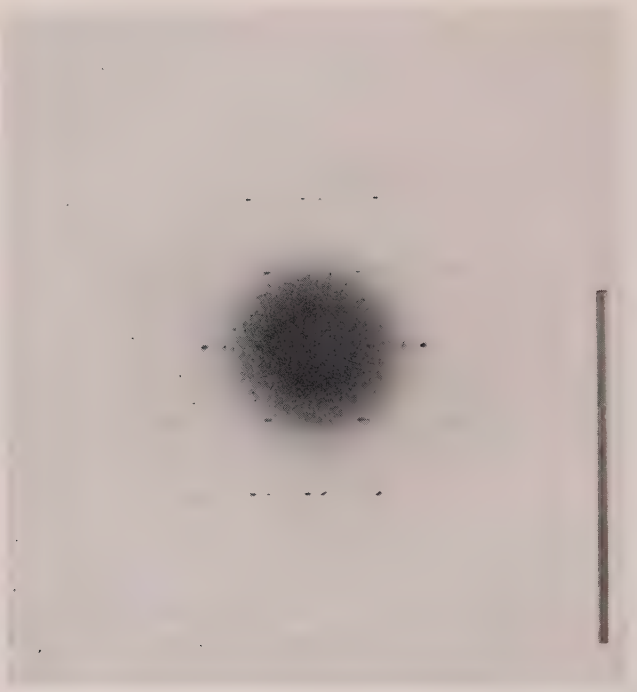

FIG. 2. Electron diffraction pattern of a single crystal of synthetic fiber of clinochrysotile.

The amount of crystal aggregates decreased as the reaction time was lengthened; eventually these aggregates converted entirely to fiber bundles.

CHARACTERIZATION

The synthetic chrysotile was subjected to chemical analysis, petrographic examination, *x*-ray diffraction, DTA and thermal dehydration studies. The chemical composition, crystal structure, and all its properties resemble those of natural chrysotile.

The fine resolution of the *x*-ray diffraction peak between diffracting angle 2θ 35–90° (Fig. 1) and the electron diffraction pattern of the single fiber crystal indicated the predominant species in the synthetic sample to be clinochrysotile (Fig. 2) as described by Whittaker, et al. (1956) and Zussman, et al. (1957). No antigorite was observed, but a trace amount of platy lizardite was also found to be present. Again, this frequently occurs as the major component in fibrous chrysotile, as is indicated in the findings of Whittaker and Zussman and from the observations made on samples from Bell mine, Thetford, Quebec and Jeffrey mine, Asbestos, Quebec.

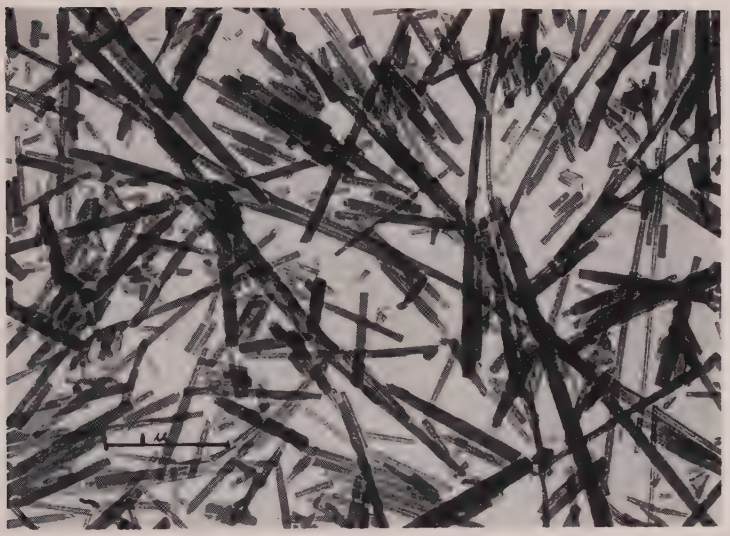

(*a*)

(*b*)

FIG. 3. Electron Micrographs of Synthetic Chrysotile. *a*. Opened Fibers ×16,000. *b*. Bundles of Fibers ×4000.

Electron micrographs of the synthetic substance showed that the fibers are extremely thin but have thick tube walls. The pronounced "cone-in-cone" effect often observed in synthetic chrysotile described in the literature was greatly reduced, and the individual fibers appeared to be more or less uniform in size (Fig. 3). The outside diameter of the

fiber was about 300–400 Å, and the inside diameter averaged 50 Å. The inner voids were partially filled with amorphous material as is true of natural chrysotile (Bates, 1958).

Chemical analysis of the pure synthetic material indicated that no foreign ions from the mineralizer had entered the structure.

Acknowledgment

The author wishes to express her appreciation to Mr. Morrow C. Miller, who prepared the electron micrographs and electron diffraction pattern and Dr. Jurg W. Meyer for helpful suggestions regarding the electron diffraction work in this study.

References

Bates, T. F., (1958), Selected electron micrographs of clays and other fine-grained minerals: Final report on the investigation of morphology origin and structure of fine-grained minerals. *Circular No. 51.* Mineral Industries Experimental Station, College of Mineral Industries, The Pennsylvania State University, 23.

Jander W. and Wuhrer, J., (1938). Hydrothermal reactions (I) Formation of magnesium hydrosilicates: *Zeit. anorg. u allgem. Chemie*, **235** 273–294.

Whittaker, E. J. W. and Zussman, J., (1956), Characterization of serpentine minerals by *x*-ray diffraction: *Min. Mag.*, **31,** 107.

Yang, J. C., (1960), The system MgO-SiO_2-H_2O below 300° C. (I) low temperature phases from 100 to 300° C. and their properties: *J. Am. Ceram. Soc.*, **43**(10), 542–549.

Zussman, J., Brindley, G. W., and Comer, J. J., (1957), Electron diffraction studies of serpentine minerals: *Am. Mineral.*, **42,** 133–53.

THE AMERICAN MINERALOGIST, VOL. 46, MAY–JUNE, 1961

QUICK IDENTIFICATION OF POTASH FELDSPAR, PLAGIOCLASE, AND QUARTZ FOR QUANTITATIVE THIN SECTION ANALYSIS

Olaf Anton Broch, *Geological Survey of Norway, Oslo, Norway.*

Describing his simple and useful point counter, Chayes (1949) rightly remarks (p. 9): "Only an operator whose bravery exceeds his wisdom will attempt analyses when he has reason to suspect that errors of identification will be more than a trifling component of the total precision error." He took a good step towards eliminating such errors when he simplified the procedure of staining potash feldspar with HF and cobaltinitrite (Chayes, 1952).

In this connection I want to describe a still simpler modification of the procedure, developed by several workers at the Geological Museum, Oslo, and successfully used by the present author and many others:

Pour a little HF into the bottom of a plastic coverglass box (such as

used by manufacturer for packing 50 pieces of 32×24 mm. coverglass). Place uncovered thin section face down on the box instead of lid for 2 minutes. Place thin section face up on table. Apply (with dropper or directly from bottle, test tube etc.) freshly prepared saturated watery solution of cobaltinitrite and let react for 5 minutes. Wash gently under tap. Avoid scratching. The entire procedure is carried out at room temperature. Covering with tape or some such material is unnecessary. (After use put lid on coverglass box, wrap it in plastic foil and keep it in your office if you like!)

Plagioclase and quartz. To distinguish at a glance plagioclase from quartz is sometimes difficult or impossible in thin section. Use the *uncovered* thin section treated as above. Use reflected light from a Monla lamp placed a little higher than the microscope table. Tilt lamp axis (beam of light) about 15°. Due to diffuse reflection the etched plagioclase appears grayish white, whereas quartz is noticeably darker (dark gray). (Potash feldspar is of course strongly greenish yellow and is still more easily seen than in the ordinary way of observing.) For confirmation when (rarely) desirable, arrange so that transmitted light can be switched on at will. (The author substituted the Leitz Microdialamp for the microscope mirror.) Plagioclase appears darker (faintly brownish) than quartz (white).

By this procedure the quantitative determination of quartz and both feldspars can be quickly and safely performed with the aid of the point counter. At the same time there can be determined one or more colored constituents. It is, however, necessary to make a separate determination of *apatite* which is not readily distinguished from quartz in uncovered thin sections. It may therefore be just as convenient to determine the percentages of colored components or most of them separately along with apatite after covering the thin section, either provisionally using glycerine, or permanently with canada balsam. This, when using the ordinary laboratory counter with only five keys, obviously implies no extra work.

The method described was developed for some granitic rocks (quartz, plagioclase, microcline, hornblende, biotite, apatite, titanite) with plagioclase almost free from impurities, often untwinned and, in ordinary covered thin section, having nearly the same relief as quartz.

References

Chayes, F. (1949), Simple point counter for thin-section analysis: *Am. Mineral.*, **34**, 1–11.

——— (1952) Staining of potash feldspar with sodium cobaltinitrite in thin section: *Am. Mineral.*, **37**, 337–340.

THE AMERICAN MINERALOGIST, VOL. 46, MAY–JUNE, 1961

DECOMPOSITION OF PYRITIZED CARBONACEOUS SHALE TO HALOTRICHITE AND MELANTERITE

CHARLES B. SCLAR, *Battelle Memorial Institute, Columbus, Ohio*

In April, 1959, the writer examined several polished sections of gold- and silver-bearing pyritic zinc ore from a locality in the Dominican Republic. Three sections, two composed dominantly of pyrite disseminated through carbonaceous illitic shale and the third composed dominantly of sphalerite with minor pyrite, were stored in a desk drawer. In August, 1959, the desk was moved into a centrally air conditioned area where the temperature is controlled during the summer months between 21° and 24° C. except for infrequent interruptions of short duration (<48 hours). The local dehumidification equipment is somewhat inefficient so that the relative humidity in the room is high and not unlike that in mines and caves. In August, 1960, the writer noticed a white efflorescence of acicular crystals on both the polished and the rough surfaces of the pyritized shale specimens; the sphalerite-rich specimen was unaffected.

The white efflorescence is water soluble and is composed dominantly of radial-fibrous aggregates of halotrichite [$Fe^{+2}(Fe^{+3}, Al)_2(SO_4)_4 \cdot 22H_2O$] and subordinately of lath-shaped to tabular-vermiform crystals of melanterite [$FeSO_4 \cdot 7H_2O$] (Fig. 1). These minerals are intimately associated and appear to be in equilibrium. X-ray powder diffraction data agree with those reported for halotrichite by Bauer and Sand (1957) and for melanterite on ASTM card 1-0255. A spectrographic analysis showed that the major cations are Fe and Al; trace amounts (<0.5%) of Ca, Mg, Zn and Cu are also present. The presence of SO_4 was confirmed by the $BaSO_4$ test.

The acicular crystals of halotrichite have $\gamma = 1.490 \pm 0.002$, $Z \wedge c = 38°$, and weak birefringence. The individual crystals have a maximum length of 1.5 mm. and range in thickness from about 1.5 to 5 microns. An aqueous solution of the efflorescence gave a positive reaction for iron with both potassium ferro- and ferricyanide and with ammonium hydroxide which suggests that this halotrichite contains some ferric iron proxying for aluminum and represents an intermediate composition in the halotrichite-bilinite $[Fe^{+2}Al_2(SO_4)_4 \cdot 22H_2O] - [Fe^{+2}Fe^{+3}(SO_4)_4 \cdot 22H_2O]$ series.

Abundant shale and unaltered brass-yellow pyrite fragments ranging in size from a few microns to 0.2 mm. in diameter are enclosed in the halotrichite aggregates. Many fragments have a specular facet which

shows that they were once part of the now disrupted and pitted polished surface.

In immersion mounts the tabular melanterite crystals appear as straight, hook-shaped, semicircular to almost annular and S-shaped forms. They have $\beta = 1.478 \pm 0.002$ and (+)2V large (~75°). Most of these crystals are oriented in immersion mounts and show slightly to moderately off center Bx_a and Bx_o interference figures. Such crystals have the optic plane transverse to the elongation, small extinction

FIG. 1. (Left) Photomicrograph of halotrichite crystals. Two melanterite crystals are labeled (m). Plane polarized light. ×80. (Right) Curved tabular crystals of melanterite. Crossed nicols. ×80.

angles (0°–12°), and positive and negative elongation for Bx_a and Bx_o sections, respectively.

Halotrichite and melanterite are fairly common weathering products of pyritic aluminous rocks and accumulate in protected cracks and re-entrants. They also coexist in efflorescences which form on the walls and timbers of underground workings, particularly those in pyritic coal seams and pyritic ore deposits. In a recent paper, Brant and Foster (1959) briefly described discrete occurrences of halotrichite and melanterite on the surface of a basement-stored pyritic coal core, and concluded that both minerals formed under similar conditions. This paper supports their viewpoint.

Where the relative humidity is high, pyrite decomposes rapidly, and

weakly acid sulfate solutions are released which attack aluminous minerals and bring aluminum into solution. Evaporation of films of these aqueous solutions results in crystallization of halotrichite and or melanterite. The halotrichite/melanterite ratio at any point is probably determined by the local concentration of clay minerals or other soluble aluminous minerals in the pyritic rock.

Occelshaw (1925; see Mellor, 1935, and Campbell and Smith, 1951) has shown that halotrichite is a congruently saturating compound which is in equilibrium at 25° C. with aqueous solutions containing between 4 and 10% of $FeSO_4$ and between 25 and 20% of $Al_2(SO_4)_3$, respectively, and that melanterite is in equilibrium at 25° C. with aqueous solutions containing higher concentrations of $FeSO_4$ and correspondingly lower concentrations of $Al_2(SO_4)_3$. His equilibrium diagram also shows that when alunogen [$Al_2(SO_4)_3 \cdot 16H_2O$] is not present in the crystallized product, the corresponding aqueous solutions contained at least 10% $FeSO_4$ and less than 20% $Al_2(SO_4)_3$ during crystallization or a minimum Fe/Al weight ratio of about 1.15. To obtain a solution with this minimum ratio would require the dissolution of about 3 grams of iron-free illite containing 25% Al_2O_3 for each gram of pyrite. These data support the hypothesis proposed above that local shifts in the Al^{+3} and Fe^{+2} concentration levels of the aqueous solutions are responsible for the variable halotrichite/melanterite ratio of the efflorescence and that the two minerals crystallize under the same physical conditions. The reduced state of the iron in these minerals is probably due to the combined effect of the low acidity of the parent solutions and the carbonaceous matter in the shale.

References

Bauer, G. S., and Sand, L. B. (1957), *X*-ray powder data for ulexite and halotrichite: *Am. Mineral.*, **42**, 676–678.

Brant, R. A., and Foster, W. R. (1959), Magnesian halotrichite from Vinton County: Ohio, *Ohio Jour. Sci.*, **59**, 187–192.

Campbell, A. N., and Smith, N. O. (1951), *The Phase Rule and Its Applications* by A. Findlay, Ninth Edition, Dover, New York, p. 350.

Mellor, J. W. (1935), A comprehensive treatise on inorganic and theoretical chemistry: Vol. 14, Longmans Green, London, pp. 299–300.

Occleshaw, V. J. (1925), The equilibrium in the systems aluminum sulfate copper sulfate-water and aluminum sulfate-ferrous sulfate-water at 25° C. *Jour. Chem. Soc.*, **127**, 2598–2602.

THE AMERICAN MINERALOGIST, VOL. 46, MAY-JUNE, 1961

THE BENFORD PLATE

D. B. Craig, *Geology Department, University of Wisconsin, Madison, Wisconsin.*

Mr. James Benford of Bausch and Lomb Incorporated, in cooperation with Dr. R. C. Emmons, Department of Geology, University of Wisconsin, has designed a substage mica plate to be used in conjunction with the conventional mica plate as an aid in the study of interference figures. The purpose is to eliminate the isogyres of a figure and to reduce the appearance of an optic axis to a dark spot of zero retardation. The color rings are unaffected.

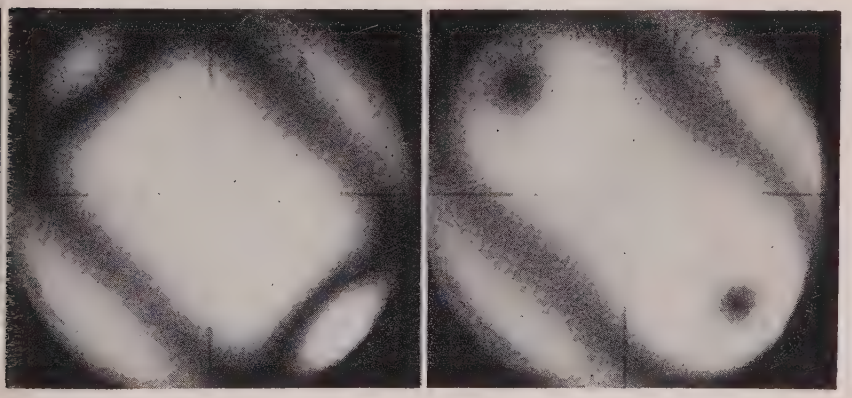

Fig. 1. Acute bisectrix figure of muscovite. (Left) Without Benford plate. (Right) With Benford plate and accessory mica plate inserted.

The lower mica plate is inserted at 90° to the upper mica plate, the two thereby cancelling each other. There can be no isogyres since they represent loci of extinction and such are destroyed by the lower plate. The color rings are shifted but are returned by the upper plate. The optic axes are spots in relation to the color rings rather than parts of isogyres. They represent points of zero retardation rather than part of an area of extinction.

In measuring 2V by the method of Horace Winchell (1939), which is outstandingly satisfactory, it is most convenient to measure 2D on the ocular scale. In measuring dispersion of an interference figure, the distribution of the color fringes is strikingly easily observed. The symmetry of the color ring distribution is also well revealed.

There is one precaution in application of the Benford plate which

should be specified and checked at the time of purchase—it is that the two plates (the usual accessory mica plate of 155 mμ retardation and the substage Benford plate) have equal retardation. The manufacturer must allow himself some tolerance from the stated 155 mμ value of the plates but can select pairs of matched plates for use with this method of interference figure analysis. The tolerance does not ordinarily come to the attention of the operator in routine work but it is quite noticeable in the use of the two plates and leads to two sources of error:

1. If the two plates are of slightly different retardation 2D is of different value when measured in two positions which are 90° apart obtained by rotating the micrometer ocular. Neither value is correct. This provides the simplest method to test the equipment for matching plates, using a muscovite mount (2V=44°) on the stage and a 4 mm. N.A. 0.85 objective. The absolute retardation of the plates is of no concern, merely that they are selected to agree.

2. When one is observing dispersion, this effect can modify the distribution of the color fringes, leading to an incorrect determination of the crystal system and orientation. If, however, the plates are well matched, observations of dispersions in interference figures is both more sensitive and more precise than is possible by the conventional method.

This technique has been in satisfactory classroom use for several years at the University of Wisconsin.

THE AMERICAN MINERALOGIST, VOL. 46, MAY–JUNE, 1961

THE CHALCOKYANITE SERIES

H. Strunz, *Berlin, Germany.*

Some important earlier results on the chalcokyanite series were not reported in the paper of Pistorius (1960). These additional results are:

Chalcokyanite	$CuSO_4$	*Pmnb* Z=4
Kokkoros and Rentzeperis (1958)		a_0=6.69 Å, b_0=8.39 Å, c_0=4.83 Å $a:b:c$=0.797:1:0.576
Zinkesite	$ZnSO_4$	*Pmnb* Z=4 a_0=6.74 Å, b_0=8.60 Å, c_0=4.77 Å $a:b:c$=0.784:1:0.555
Synthetic	$CoSO_4$	*Pmnb* Z=4 a_0=6.72 Å, b_0=8.47 Å, c_0=4.66 Å $a:b:c$=0.793:1:0.550

Full structure determinations for $CuSO_4$ and $ZnSO_4$ are given by Kokkoros and Rentzeperis (1958). The Cu, Zn and Co sulfates are

isotypic, and diadochic substitution of Cu, Zn and Co is possible. The $MgSO_4$ and $NiSO_4$ form another structure type (Dimaras, 1957, and Rentzeperis and Soldatos, 1958).

At the International Mineralogical Association meeting at Copenhagen in 1960, it was agreed to use the spelling "chalcokyanite." The crystallographic orientation is that of Scacchi (1873) with *a* halved.

References

Dimaras, P. I. (1957), *Acta Cryst.*, **10,** 313.
Hocart, R. and Serres, A. (1931), *C. R. Acad. Sci. Paris*, **193,** 1180.
Kokkoros, P. A. and Rentzeperis, P. J. (1958), *Acta Cryst.*, **11,** 361.
Pistorius, Carl W. F. T. (1960), *Am. Mineral.*, **45,** 744–746.
Rentzeperis, P. J. and Soldatos, C. T. (1958), *Acta Cryst.*, **11,** 686.
Scacchi (1873), *Acc. Napol. Att.*, **5,** 26.
Schiff, K. (1934), *Z. Krist.*, **87,** 379.

THE AMERICAN MINERALOGIST, VOL. 46, MAY–JUNE, 1961

THE OCCURRENCE OF CUSPIDINE IN PHOSPHORUS FURNACE SLAG

A. Wilson and J. K. Leary, *Oldbury, Birmingham.*

Cuspidine ($3CaO \cdot CaF_2 \cdot 2SiO_2$) is a rare natural mineral which was first described by Scacchi.[1] Since that time the mineral has been synthesized by solid state reaction,[2] from melts[3] and hydrothermally.[4] It has also been observed as a constituent of electric welding slags.[5]

In the present investigation, three types of slag which came from furnaces fed with fluorine containing phosphate rock were examined. The first type was one which had a normal silica/lime ratio of 0.85, the second type was one which had been cooled slowly (1300° C.—100° C. in 35 hours) and which had a low silica/lime ratio of 0.67, the third type was the same as type 2 but the cooling was carried out in six hours. On examination, all three types were found to contain up to 35% of cuspidine. Fig. 1 shows the spear shaped crystals which are characteristic of the compound.

Analysis

It was possible to pick out small quantities of cuspidine crystals from the crushed slags and these were examined optically and by means of x-rays.

X-Ray Examination

Cell dimensions and the space group were determined from a single crystal of cuspidine. The values obtained have been compared with those of Smirnova, Rumanova and Belov.[6]

FIG. 1. Slag with silica/lime ratio of 0.67. Cooled in six hours to give a glassy matrix with skeletal phenocrysts of cuspidine. Crossed nicols. ×35.

Powder photographs were also taken and the *d* values of the interplanar spacings were measured. These values check very closely with natural cuspidine and synthetic cuspidine.

OPTICAL PROPERTIES

Measurements were only made on material obtained from a normal slag with silica/lime = 0.85. The crystals are biaxial positive with the following values: $\alpha = 1.590$, $\beta = 1.593$, $\gamma = 1.602 \pm 0.002$, 2V (measured) = 58°, optical axial plane (010), twinning plane (001), extinction angle X/\a = 7°, cleavage plane (110) poor. The refractive indices and extinction angle agree with values given by Valkenburg and Rynders[4] but the 2V angle reported here is lower. However, their 2V angle is an estimated value and it is found that our results agree closely with those published elsewhere.[7]

TABLE 1. COMPARISON OF SINGLE CRYSTAL *X*-RAY DATA

	a_0(Å)	b_0(Å)	c_0(Å)	β	Z	ρ g/cm^{-3}
Present work	7.57	10.57	10.93	69°53′	3.98	2.95
Results from Ref. 6	7.54	10.43	10.85	69°56′	3.84	2.97–2.99

References

Scacchi, A. (1877), *Zeits. Krist.* **1,** 398.
Tilley, C. E. (1947), *Min. Mag.*, **28,** No. 197, 90.
McCaughey, Kautz and Wells (1948), *Am. Mineral.*, **33,** 200.
Van Valkenberg, A. and Rynders, G. F. (1958), *Am. Mineral.*, **43,** 1195.
Lapin, V. V. (1941), *Compt. Rend. Acad. Sci. URSS,* **31,** 694.
Smirnova, R. F., Rumanova, I. M., Belov, N. V. (1955), Zapiski Vsesoyuz. *Mineralog. Obshchestva,* **84,** 159.
United States Department of the Interior, *Geological Survey Bulletin* **848.**

THE AMERICAN MINERALOGIST, VOL. 46, MAY-JUNE, 1961

THE STABILITY OF THE ARSENIC TRIBROMIDE IMMERSION LIQUIDS DURING STORAGE*

Robert Meyrowitz and Harold Westley, *U. S. Geological Survey, Washington* 25, *D. C.*

It is now 10 years since the first complete series of immersion liquids of high index of refraction (1.74–2.00) suitable for routine use was proposed (Meyrowitz and Larsen, Jr., 1951). A set of the liquids, in clear glass bottles with ground-glass stoppers and ground-glass dust covers, has been stored in a dark cupboard continuously. During this 10-year interval, the bottles were opened only a few times either to determine the index of refraction of the contained liquid or to transfer the liquid to a new glass bottle after the liquid had been filtered.

The liquids were filtered twice: first, after their indices of refraction were measured when they were 6 months old, and second, before they measured when they were 10 years old. When the liquids were 6 months old, some of the liquids had developed a slight turbidity and crystals of sulfur were present in the 1.98, 1.99, and 2.00 liquids. The liquids containing methylene iodide, sulfur, and arsenic tribromide ($n = 1.74$–.81) were originally yellow amber and became slightly darker at the end of 6 months. Now, at the end of 10 years, they are purple brown. The liquids containing arsenic disulfide ($n = 1.82$–2.00) were originally yellow amber to dark amber and at the end of 10 years are slightly darker.

The liquids at the end of 10 years contained no large crystals. Some had a small amount of fine precipitate but the liquids were otherwise transparent and suitable for use. The inside surface of the glass bottles appeared to be cloudy as if they had been etched by the liquids or as if a fine deposit had formed on the inside surface of the bottle.

Table 1 gives the original indices of refraction of the liquids and their

* Publication authorized by the Director, U. S. Geological Survey.

Table 1. Changes in Refractive Indices of Arsenic Tribromide Liquids During Storage

25° C. n_{Na} (initial)	Δn (6 months)	Δn (9 months)	Δn (10 years)
1.741	−0.001	−0.001	+0.001
1.752	−0.001	−0.001	+0.001
1.762	0.000	−0.001	+0.001
1.771	0.000	−0.001	+0.001
1.781	0.000	−0.001	+0.001
1.791	−0.001	−0.001	+0.001
1.801	0.000	−0.001	+0.001
1.810	+0.001	+0.001	+0.001
1.819	0.000	0.000	0.000
1.830	−0.001	−0.001	0.000
1.840	−0.001	−0.001	0.000
1.848	+0.002	+0.001	+0.001
1.861	−0.002	−0.002	−0.001
1.870	−0.001	−0.002	−0.002
1.880	−0.001	−0.002	−0.001
1.891	−0.002	−0.003	−0.002
1.901	−0.002	−0.002	−0.002
1.910	−0.002	−0.002	−0.002
1.920	−0.003	−0.003	−0.002
1.932	−0.002	−0.003	−0.002
1.942	−0.002	−0.003	−0.002
1.951	−0.003	−0.004	−0.003
1.960	−0.003	−0.003	−0.002
1.969	−0.003	−0.004	−0.004
1.979	−0.003	−0.003	−0.002
1.988	−0.002	−0.002	−0.001
1.998	−0.003	−0.002	0.000

change at the end of 6 months, 9 months, and 10 years. Changes in the liquids under actual use, rather than during "dead" storage, will probably be much greater.

Reference

Meyrowitz, R. and Larsen, E. S., Jr. (1951), Immersion liquids of high refractive index: *Am. Mineral.*, **36**, 746–750.

THE AMERICAN MINERALOGIST, VOL. 46, MAY–JUNE, 1961

THE DIRECT DETERMINATION OF HEXAGONAL LATTICE PARAMETERS

LORIN HAWES, *Department of Chemistry, Australian National University, Canberra, Australia.*

In a previous article (Hawes, 1960) methods were derived for the determination of lattice parameters of cubic, tetragonal and orthorhombic crystals directly from "*d*" spacing data in the absence of systematic errors.

The general method may be readily extended to hexagonal (or suitably indexed rhombohedral) crystals as well; the derivation is similar to the tetragonal case, except that $\alpha = h^2 + hk + k^2$.

When observed Q values are treated in steps essentially the same as in the tetragonal case,

$$a_0 = \sqrt{4/3 \frac{D^*}{A\ D^*}} \quad \text{and} \quad c_0 = \sqrt{\frac{D^*}{C\ D^*}}$$

The terms in these equations are as defined previously.

REFERENCE

HAWES, L. L. (1960), A method for the direct determination of lattice parameters: *Am. Mineral.*, **45,** 1285–1287.

Erratum

On page 1095 in the September–October, 1960 issue of the *American Mineralogist*, the value of c_0 for PdHg at the bottom of Table 1, should read 3.702 instead of 3.072 A.

BOOK REVIEWS

LEAD ISOTOPES IN GEOLOGY, by R. D. Russell and R. M. Farquahar, 243 pages, Interscience Publishers, Inc. 250 Fifth Avenue, New York. Price $9.00.

As stated in the preface, the authors mention that this short monograph is concerned with isotopes of common lead, and interpretation of lead isotope abundances and their applications which would be of interest to the geologist. Accordingly, the book is divided into eight short chapters with subheadings, and 12 appendices of lead isotope abundance values given in 119 pages. The chapter titles include: Introduction, measurement of lead isotope ratios, the age of the Earth, dating of galenas by means of their isotopic constitutions, anomalous leads, case histories (three are given), extension of the Holmes-Houtermans model, and lead-uranium-thorium methods of age determinations.

The small book is well organized and each topic is clearly presented. When ideas of the authors are stated, they admit that other scientists may dispute them, especially as to the source of lead.

In conclusion, the book is well worth reading for those interested in interpretation of lead isotope methods and their applications to geology.

Eugene B. Gross
Department of Mineralogy
The University of Michigan
Ann Arbor, Michigan

TRAP ROCK MINERALS OF NEW JERSEY, by Brian H. Mason. 51 pages, 16 figures, and one foldout map. New Jersey Geological Survey Bulletin 64, 1960. $1.50.

The bulletin consists of a brief résumé of the geology, paragenesis, and localities of minerals occurring in the Triassic Trap Rock of New Jersey. The minerals were examined in a collection from the American Museum of Natural History, New York. A statement on the zeolite group is also included by the author. This is followed by a brief description of 60 minerals with optical properties given for non opaque ones. A list of discredited minerals and unconfirmed occurrences concludes this bulletin.

The publication is well illustrated with black and white geologic map showing mineral localities and many photographs of mineral specimens. Bulletin 64 is well suited for mineralogists interested in collecting from the Trap Rock deposits of New Jersey.

Eugene B. Gross
Department of Mineralogy
The University of Michigan
Ann Arbor, Michigan

ADVANCES IN *X*-RAY ANALYSIS, Vol. 4. Edited by William M. Mueller. Plenum Press Inc., 227 West 17th St., New York 11, N. Y. 576 pp., illustrated. $15.00.

This volume contains the complete texts of 38 reports presented at the Ninth Annual Conference on Applications of *X*-ray Analysis, held August 10–12, 1960, in Denver, Colorado, and sponsored by the University of Denver.

NEW MINERAL NAMES

Perite

Marianne Gillberg. Perite, a new oxyhalide mineral from Långban, Sweden. *Arkiv Mineral. Geol.*, **2,** No. 44, 565–570 (1960).

The mineral occurs in the Råmen drift (130 m. level) as sulfur-yellow plates about 0.5 mm. in size in fissures in a skarn of hausmannite, calcite, a ludwigite-like mineral, and a few crystals of a red unidentified mineral. Analysis by Alexander Parwel gave $PbCl_2$ 26.33, PbO 23.69, Bi_2O_3 45.74, MnO 0.46, CaO 1.44, MgO 0.07, CO_2 1.19, H_2O^- 0.04, H_2O^+ 0.10, insol. 1.00, sum 100.06%. After deducting calcite and hausmannite, the unit cell content is $Pb_{4.03}Bi_{3.94}O_{7.93}Cl_{3.80}(OH)_{0.22}$ or $PbBiO_2Cl$, the Bi analogue of nadorite. Easily soluble in dilute acids. The mineral is sulfur-yellow with adamantine luster. G. $8.00 \pm .01$, corrected for impurities 8.16. H. 3. Does not fluoresce in long- or short-wave ultraviolet radiation. Habit tabular. Cleavage relatively distinct perpendicular to the *c*-axis. The *n* could not be determined because the mineral reacts with S-Se melts, but is probably above 2.4.

Weissenberg and Guinier photographs gave for natural and synthetic perite, respectively, orthorhombic, *a* $5.627 \pm .05$, $5.593 \pm .002$; *b* $5.575 \pm .02$, $5.558 \pm .002$; *c* $12.425 \pm .09$, $12.428 \pm .008$ Å.; these are very close to the data for nadorite. Space group *Bmmb*. Indexed *x* ray powder data are given; the strongest lines for the mineral are 2.86 (10) (113), 1.620 (9) (133, 313), 3.77 (8) (111), 1.251 (420, 240).

The mineral was synthesized by fusing PbO and Bi_2O_3 with an excess of $BiCl_2$, and leaching the excess $PbCl_2$ with cool water.

The name is for Per Geijer, Swedish geologist.

Michael Fleischer

Freudenbergite

Gerhard Frenzel. Ein neues Mineral: Freudenbergit. ($Na_2Fe_2Ti_7O_{18}$) *Neues Jahrb. Mineral., Monatsh.* **1961,** No. 1, 12–22.

The mineral occurs in an apatite-rich alkali syenite from Michelsberg, Katzenbuckel, Odenwald, as small, mainly xenomorphic grains averaging 0.15 mm. long, 0.05 mm. thick. The rock contains sanidine 62 vol. %, diopside-aegirine pyroxene 15, apatite 11, amphibole 6, zeolitized feldspar 4, freudenbergite 2, plus traces of biotite, hematite, ilmenite, and sphene. Freudenbergite occasionally occurs in parallel intergrowths with hematite.

The mineral was purified by treatment with cold 40% HF for 4 days (the mineral was only slightly attacked) followed by separation with bromoform. Two analyses were made by Fresenius and Schneider, after dissolving by boiling repeatedly with $HF \cdot H_2SO_4$ and fusion with $KHSO_4$. Loss on ignition (thought to be high because of the presence of material decomposed by the HF treatment) and SiO_2 were determined on a separate portion. FeO was not determined and may have been present. Analyses gave Na_2O 6.90, 7.15; K_2O 1.33, 0.37; MnO 0.26, 0.14; MgO 0.47, n.d.; Fe_2O_3 18.94, 20.19; Al_2O_3 0.47, n.d.; TiO_2 63.62, 64.43; Nb_2O_5 2.73, 2.97; SiO_2 2.03, ign. loss 2.98, sum 99.73, 100.26%. These correspond closely to $Na_2Fe_2(Ti_{6.81}Nb_{0.19})O_{18}$. Spectrographic analysis showed traces of Cd, Cu, Ca, Sr, Ba, but no Ta.

Guinier photographs and powder data show freudenbergite to be hexagonal, *a* 9.62, *c* 22.40 Å, $c/a = 2.328$. With d. detd.$\sim$4.3, $Z = 5.89$ or 6, d. calcd.$= 4.38$. The unit cell is close to that of hoegbomite, but the *x*-ray powder data for the two minerals differ considerably. Indexed *x*-ray powder data are given for freudenbergite; the strongest lines are 3.627 (vs) ($11\bar{2}4$), 1.911 (s-vs) ($23\bar{5}0$), 5.81 (s) (0004), 3.101 (s) ($12\bar{3}1$), 3.015 (s) ($12\bar{3}2$), 2.731 (s) ($12\bar{3}4$), 2.712 (s) ($30\bar{3}2$), 2.069 (s) ($40\bar{4}1$), 2.049 (s) ($13\bar{4}5$), 1.596 (s) ($40\bar{4}9$). Cleavage basal and prismatic good.

Color blackish, rutile-like, olive- to steel-gray in fine powder, streak pale yellow-brown; under the microscope transparent, O dark brown, E yellow brown. Optically uniaxial, positive, *ns* (Li, in S-Se melts) $o \sim 2.37$, $e \sim 2.42$. Reflecting power in air R_o 16.5, R_e 17.2% in oil (n 1.515) R_o 4.8, R_e 5.3%. Yellow-brown internal reflections; weakly anisotropic under crossed nicols. The mineral polishes well; the abrasion hardness is less than that of hematite and diopside.

Freudenbergite is considered to be of late magmatic origin.

The name is for the late Professor Wilhelm Freudenberg, who studied the Katzenbuckel rocks.

Discussion.—Not clearly related to any known mineral, perhaps best placed with the multiple oxides near hoegbomite.

M. F.

Kennedyite, Karrooite

O. Von Knorring and K. G. Cox. Kennedyite, a new mineral of the pseudobrookite series: *Mineralog. Mag.*, **32,** 676–682 (1961).

The mineral occurs in a sill at the base of the Karroo volcanic succession, Mateke Hills, Southern Rhodesia, in lath-shaped crystals up to 2 mm. in length in a ground-mass of alkali feldspar. Phenocrysts of olivine and clinopyroxene are also present. Analysis of material purified by magnetic and heavy liquid separations gave (O. v. K., analyst): TiO_2 60.33, Al_2O_3 2.15, Fe_2O_3 28.77, Cr_2O_3 0.37, FeO 2.00, MnO 0.07, MgO 6.45, CaO trace, sum 100.14%. This corresponds to $Mg_{0.69}Fe^{+2}_{0.12}Fe^{+3}_{1.56}Al_{0.18}Cr_{0.03}Ti_{3.27}O_{10}$ or approximately $MgFe_2^{+3}Ti_3O_{10}$, *i.e.*, derived from pseudobrookite by the substitution of MgTi for $2Fe^{+3}$. Spectrographic analysis also showed traces of Si, Ca, V, Ni, Ga, and Zr.

Indexed *x*-ray powder data are given. The strongest lines of kennedyite are 3.485 (vs) (220, 101), 4.88 (s) (200), 2.743 (s) (230), 1.865 (s) (002), 2.450 (m) (301), 1.970 (m) (331), 1.544 (m). From the powder data, the unit cell has a 9.77, b 9.95, c 3.73 Å.

Kennedyite is black, in small grains dark brown, translucent. Luster metallic, brilliant. G. (suspension) 4.07. Extinction parallel. In polished section at high magnification, lamellar intergrowths (exsolved rutile?) were seen. Pleochroism not apparent. Under crossed nicols steel-gray to purplish-brown anisotropic effects were noted.

The name is for Professor W. Q. Kennedy of the University of Leeds. The name karrooite is suggested for the end member $MgTi_2O_5$, one of the major components of the mineral kennedyite.

Discussion.—The nomenclature of intermediate compounds is always difficult. Pseudobrookite, $Fe_4^{+3}Ti_2O_{10}$, is the only end-member of this group that occurs naturally; others that have been named are $Al_4Ti_2O_{10}$ (tieilite), $Ti_4Ti_2O_{10}$ (anosovite), and now karrooite ($Mg_2Ti_4O_{10}$); these have been synthesized and have also been found in Ti-rich furnace slags. None of these should have been given mineral names. There is no satisfactory way of naming the intermediate member of a heteromorphic substitution series, such as kennedyite is, and further new names should be avoided if possible, if additional intermediate members of slightly different composition are found.

M. F.

Nickelemelane, Cobaltomelane, Nickel-cobaltomelane, Cryptonickelmelane, Alumocobaltomelane, Buryktalskite

I. I. Ginzberg and I. A. Rukavishnikova. Minerals of the ancient crust of weathering in the Urals. Oxides and hydroxides of manganese: *Izdeltsvo Akad. Nauk S.S.S.R.*, **1951,** 92–130 (in Russian).

K. K. Nikitin. Manganese minerals of the crust of weathering of the Buryktal ultrabasic massif: *Kora Vyvetrivaniya*, **3**, 39–55 (1960) (in Russian).

I. I. Ginzburg. Nickele- and cobalto-melanes: *Kora Vyvetrivaniya*, **3**, 56–66 (1960) (in Russian).

These are studies of manganese oxides formed by the weathering of ultrabasic rocks in the Urals. Many new analyses were given, with *x*-ray powder data, optical study, and D.T.A. New names used are listed above; they are not specifically defined, but nickele-melanes contain NiO 3.68 to 15.50% with a max. of .0.45% CoO; nickel-cobaltomelane with Ni>Co, but with high (up to 5.6% CoO); cobaltomelanes with Co>Ni; alumo-cobaltomelanes with Co>Ni and a high content of Al_2O_3 (up to 11%); cryptonickelmelane, close in composition and *x*-ray powder diagram to cryptomelane, but containing much NiO (up to 4.8%) and CoO (up to 2.0%).

The analyses assigned these names differ greatly; so do the *x*-ray powder patterns. The authors recognize that the samples are mixtures; the *x*-ray patterns include lines of geothite, cryptomelane, and "elizavetinskite" (see below). Ginzburg subtracts these and defines as the pattern of the new mineral "buryktalskite" the lines at 4.88 (10), 4.66 (10), 4.61 (10), 1.482 (10), 9.17 (7), 3.09 (7), 1.834 (7), 1.689 (7).

Discussion.—These are obviously not names of minerals, but of complex mixtures. They undoubtedly do contain one or more new minerals, but what these are remains unknown. Many of the lines attributed to "buryktalskite" can be assigned to strong lines of pyrolusite, lithiophorite, or cryptomelane; others cannot be assigned with any confidence. The names are therefore, like limonite and asbolane, merely mineralogical waste baskets.

M. F.

Elizavetinskite

V. I. Mikheev. X-ray methods of determining minerals: *Gosgeoltekhizdat* **1957,** 868 pp. (p. 409) (in Russian).

I. I. Ginzburg. Nickele- and cobaltomelanes: *Kora Vyvetrivaniya*, **3,** 56–66 (in Russian).

The name is given to a black, powdery sample in clay from the Elizavetinsk deposit, Sverdlovsk region, for which *x*-ray powder data are given. The strongest lines are 4.75 (10), 2.350 (10), 1.872 (10), 1.442 (7), 9.68 (6), 1.380 (6), 1.235 (6). These are interpreted as giving an orthorhombic unit cell with *a* 3.725, *b* 12.38, *c* 9.455 Å. The formula is assumed to be (Mn, Co) O(OH). Mikheev states that the *x*-ray pattern is close to that of lithiophorite.

Ginzburg recognizes that some of his analyzed samples give *x*-ray patterns close to those of elizavetinskite and suggests that the formula should be (Mn, Co, Ni) O (OH).

Discussion.—The name has no standing. Every strong line of the *x*-ray pattern corresponds closely to the published data for lithiophorite, a mineral known to contain appreciable amounts of cobalt and nickel. Detailed discussion will be published elsewhere.

M. F.

Behierite

J. Behier. Travaux mineralogiques. *Rep. Malgache, Rapport Annual Serv. Geol.* **1960,** 181–199.

A preliminary note. Two small crystals in albite and associated with rubellite were found in the pegmatite at Manjaka, Madagascar, and were thought to be zircon or xenotime. *X*-ray study by Miss Mary E. Mrose of the U. S. Geological Survey indicates that

the mineral is a tantalum borate, presumably $TaBO_4$. The name is for Jean Behier, mineralogist of the Service geologique, Madagascar.

Discussion.—Names should not be published without data.

M. F.

Orthopinakiolite

Rein Randmets. Orthopinakiolite, a new modification of $Mg_3Mn^{+2}Mn^{+3}{}_2B_2O_{10}$ from Långban, Sweden. *Arkiv Mineral., Geol.*, **2**, No. 42, 551–555 (1960).

Bäckstrom (*Geol. Fören. Föhr.*, **17**, 257–259 (1895)) described orthorhombic pinakiolite from Långban; his analysis (No. 3, p. 325, Dana's System, 7th Ed., Vol. II) gave the same composition as for monoclinic pinakiolite. Re-examination of 150 samples of pinakiolite in the Swedish Museum of Natural History showed that 12 were orthorhombic, prismatic. Like the tabular monoclinic pinakiolite, they occur in granular dolomite with hausmannite and manganophyllite. The dimorphs were not found together, although Bäckstrom reports that they do occur together. Weissenberg photographs gave the unit cell as a 18.45±0.3, b 12.70±0.2, c 6.07±0.1 A., Z=8. G. 4.03. (3.935 Bäckstrom). The space group is *Pnn*2 or *Pnnm*. Indexed x-ray powder data are given; the strongest lines of orthopinakiolite are 2.59 (10) (710, 341); 5.17 (9) (111), 2.52 (9) (531, 621, 150); 2.03 (9) (821, 103); 2.20 (8) (721, 351, 142); 1.523 (8) (281, 12.0.0, 181).

The mineral is considered to be a member of the ludwigite-vonsenite group (erroneously given as ludwigite-paigeite group), but a and c of orthopinakiolite are approximately double a and c of the group.

M. F.

Strontioborite

V. V. Lobanova. A new borate—strontioborite: *Doklady Akad. Nauk S.S.S.R.*, **135**, 173–175 (1960).

The mineral was found in a study of the residue insoluble in water of the saline Kungur strata of the near-Caspian region (could this be the Inder region? M.F.). It occurs as small colorless plates, mostly 0.10–0.15 mm., but up to 2 mm. Biaxial with very large 2 V (about 85°), usually positive, but sometimes negative, elongation positive and negative, extinction inclined, so probably monoclinic; ns (all +0.002), α 1.470, β 1.510, γ 1.579 (these correspond to a positive mineral, with 2 V about 78°. M.F.). The mineral is very brittle.

Analysis by M. M. Vil'ner gave B_2O_3 57.85, CaO 4.15, SrO 21.66, MgO 5.75, H_2O 11 52, sum 100.93%, which corresponds closely to $4(Sr, Ca)O \cdot 2MgO \cdot 12B_2O_3 \cdot 9H_2O$, with Sr:Ca=3:1.

Unindexed x ray powder data by V. I. Appolonov are given (102 lines). The strongest lines are 7.33 (10), 4.09 (8), 3.50 (7), 3.32 (7), 3.06, (6) 2.033 (6) (not stated whether A or kX).

The mineral occurs in rock salt with fine lamellar structure due to the layered distribution of the fine grained borates boracite, strontioborite, and halurgite ("galurgit" - I can't identifiy this. M. F.). Anhydrite is also present.

Discussion. Requires verification. Some of the data could be construed as indicating a mixture of strontioginorite, boracite, and anhydrite.

M. F.

Unnamed

F. T. Ingham and E. F. Bradford, The geology and mineral resources of the Kinta Valley, Perak Federation of Malaya, *Geol. Survey District Mem. No.* **9**, 1–347 (1960) (see p. 105).

A yellow coating on cassiterite crystals from Sungei Lah section, Chenderiang, contained varlamoffite and another secondary mineral of the approximate composition "$CaO \cdot SnO \cdot SiO_2$." Analysis gave CaO 19.14, SnO_2 58.48, SiO_2 21.26, loss on ignition 0.50, sum 99.38%. (This corresponds to 0.95 $CaO \cdot 1.07\ SnO_2 \cdot 0.98\ SiO_2$. M.F.).

The mineral is pale yellow to colorless, translucent. G. 4.3 ± 0.2 (Berman balance), H. $3\frac{1}{2}$–4. Optically biaxial, negative, *ns* α 1.765, β 1.784, γ 1.799 (all $\pm .003$), 2V (Universal Stage) $85 \pm 2°$. From the optics, it is monoclinic or triclinic. The mineral fluoresces yellowish-green under short-wave UV light.

Thin-section study indicates that the mineral was formed by hydrothermal alteration of a cassiterite-quartz assemblage.

M. F.

Innelite

Yu. A. Balashov and N. V. Turanskaya. The lanthanum maximum of the rare earths in lamprophyllite. *Geokhimiya* **1960,** No. 7, p. 618–623 (in Russian).

Mention is made of a new barium silicate named innelite, to be described by S. M. Kravchenko. It is from pegmatite, Inagli massif, central Aldan, and contains BaO about 40%. Of the total rare earths, La is 64%, Ce 31%, and Nd 4.5%.

M. F.

NEW DATA

Dachiardite

Glauco Gottardi. Sul dimorfismo mordenite-dachiardite: *Periodico Mineralogia (Roma)*, **29,** p. 183–191 (1960).

A new analysis of dachiardite from Elba gave SiO_2 63.00, Al_2O_3 14.78, Fe_2O_3 trace, CaO 5.10, SrO trace, MgO 0.21, K_2O 1.77, Na_2O 1.81, H_2O^{110} 2.69, H_2O^{400} 8.87, H_2O^{900} 1.18, sum 99.41%. This corresponds to the formula

$$K_{0.67}Na_{1.05}Ca_{1.63}Mg_{0.10}(Al_{5.20}Si_{18.80}O_{48}) \cdot 12.68H_2O$$

or

$$(K_2, Na_2, Ca)_{2.5}(Al_5Si_{19}O_{48}) \cdot 14H_2O.$$

G. calcd. 2.138, measured 2.206. Dachiardite is therefore a dimorph of mordenite.

M. F.

Corrensite

J. L. Martin Vivaldi and D. M. C. MacEwan. Corrensite and swelling chlorite: *Clay Minerals Bull.*, **4,** 173–181 (1960).

A useful review is given of the various materials that have been described as corrensite. The suggestion is made that the name corrensite be restricted to a 1:1 regularly interstratified chlorite—"swelling chlorite." The nature of "swelling chlorite" is discussed; it appears to be distinct from vermiculite and the montmorillonites.

M. F.

DISCREDITED MINERALS

Namaqualite (=Kyanotrichite)

Brian Mason. The identity of namaqualite with cyanotrichite. *Mineralog. Mag.*, **32,** 737–738 (1961).

Optical and x-ray study of a sample labelled "namaqualite," that had been supplied by J. R. Gregory, who sent the type material to A. H. Church (1870), showed it to be kyanotrichite. The original analysis agrees with kyanotrichite except that SO_3 was not reported. The original analysis gave H_2O 32.38%; the formula of kyanotrichite requires H_2O 22.4, SO_3 12.4; probably in the original analysis, loss on ignition was determined.

M. F.

Ampangabeite (= Samarskite)

L. Van Wambeke. Etude comparative de l'ampangabeite et de la samarskite: *Bull. soc. franc, mineral. crist.*, **83,** 295–309 (1960).

Samples were examined of samarskites from 7 localities and of 6 amphangabeites from 4 localities, including the type locality. X-ray powder data (after ignition), D.T.A. curves, and x-ray fluorescence analyses are given. Ampangabeite is identical with samarskite. Weathered outer zones of the mineral show leaching of Y, U, Ca, and other rare earths and sometimes are enriched in Pb.

M. F.

ADULARIA WITH CHLORITE

These are truly magnificent specimens, the finest available in decades from the noted Val Cristallina locality in Switzerland. They include large sharp twinned crystals and groups of adularia more or less completely coated with attractive green chlorite, some with small apatite crystals. 2 x 2″, $5.00; 2 x 3″, $7.50, $10.00; 3 x 4″, $15.00; 4 x 5″, $17.50; 4 x 6″ to 7 x 8″, $30.00, $35.00.

OTHER RECENT ACQUISITIONS

Alvite. Norway. Brown massive piece with unusual gel structure 3 x 5″, $35.00

Davyne. Germany. Colorless crystals in nosean sanidinite 2 x 2″, $5.00

Dioptase. French Congo. Bright emerald green crystal groups 1 x 2″, $15.00; 2 x 2″, $30.00; 3 x 3″, $150.00

Gold. New Zealand. A polished slice of quartz rich in native gold 1¼ x 1⅝″, $45.00

Hibonite. Madagascar. Black crystalline with blue-gray corundum 4½ x 6″, $35.00; black crystals in rock 3 x 3½″, $35.00

Ilmenite. Norway. Very large crystals 2 x 2½″, $20.00; 3½ x 4″, $25.00; large crystals on rock 2 x 3″, $20.00; 3 x 4″, $27.50

Kasolite. New York (first reported occurrence in the state). Straw yellow pseudomorphs after small uraninite crystals in pegmatite with uranophane, allanite, etc. 3 x 4″, $10.00; 4 x 5″, $15.00

Nigerite. Nigeria. Minute crystals on rock 2 x 3″, $20.00

Miargyrite. Bolivia. Crystalline mass with native silver 2 x 2½″, $25.00 each

Spinel. Madagascar. Large octahedral crystals 2 x 2″, $15.00; crystal clusters with calcite 3 x 4″, $15.00

Spinel. Ferrian (Pleonaste). Queensland. Black waterworn nuggets averaging half inch. $12.00 per ounce.

Ullmannite. Arsenian (Corynite). Austria. Crystalline mass with siderite 2 x 3″, $10.00.

For a complete listing of recent acquisitions in mineral specimens write for Catalog FM 13.

WARD'S *NATURAL SCIENCE ESTABLISHMENT, INC.*
P.O. BOX 1712 ROCHESTER 3, N.Y.

GEORGE BANTA COMPANY, INC., MENASHA, WISCONSIN, U.S.A.